The role of 15-hydroxyprostaglandin dehydrogenase in breast cancer

Lisa Marie Allinson

Submitted in accordance with the requirements for the degree of

Doctor of Philosophy

The University of Leeds

Faculty of Medicine and Health

April 2019

The candidate confirms that the work submitted is her own and that appropriate credit has been given where reference has been made to the work of others.

The copy has been supplied on the understanding that it is copyright material and that no quotation from the thesis may be published without proper acknowledgement.

© 2019 The University of Leeds and Lisa Marie Allinson

Acknowledgements

First and foremost I would like to thank my supervisors, Dr Christine Diggle, Dr Ian Carr, Professor David Bonthron, Dr Rajgopal Achuthan and Sir Alex Markham for their wealth of knowledge and consistent support throughout my PhD. Without their expert guidance and encouragement this PhD would not have been possible.

I would also like to thank Mike Shires, Professor Andrew Hanby and Dr Laura Wastall for their immunohistochemistry advice. I would like to thank Morag Taylor, Ummey Hany and Dr Agne Antanaviciute for their support in the NGS facility and Dr Claire Taylor for her assistance with pyrosequencing.

I would like to thank all the members of Level 9 (Leeds Institute of Medical Research at St James's), I have loved working alongside such a fantastic group of people. In particular I would like to thank Caroline Berteau, Catriona Marshall, Diana Baxter and Robyn Broad for making all those hours in cell culture all the more enjoyable.

Finally, I would like to give a special thanks to my family and Luke for all of their support and reassurance throughout my PhD, I couldn't have done it without you.

Abstract

Breast cancer is the most common cancer in the UK, resulting in over 11,500 deaths in 2016 (Cancer Research UK, 2016), therefore improved therapies are needed. COX2 expression is often induced in breast cancer (Shim et al., 2003), resulting in increased prostaglandin production. Excess prostaglandin E_2 increases proliferation, migration, invasion and angiogenesis of cancer cells (Sobolewski et al., 2010; Lee, E.J. et al., 2007; Tomozawa et al., 2000; Hashemi Goradel et al., 2018). Inhibiting prostaglandin production with COX2 inhibitors has shown promising results in cancer treatment, yet some patients exhibit adverse side effects to the drugs.

15-hydroxyprostaglandin dehydrogenase (15-PGDH), encoded by the *HPGD* gene, is the key enzyme in prostaglandin metabolism and is an alternative target in the prostaglandin pathway. Up-regulation of 15-PGDH has shown encouraging results in colorectal and gastric cancer, however little research has been completed in breast cancer. This thesis aimed to assess 15-PGDH expression in breast cancer, how its transcription is regulated and determine the biological effects of 15-PGDH over-expression in breast cancer.

Expression of 15-PGDH was observed in only 4% of primary breast cancers, suggesting up-regulation of 15-PGDH may be a suitable treatment in most breast cancers. Treatment of MCF7 and MDA-MB-231 breast cell lines with demethylating agent decitabine and histone deacetylase inhibitor vorinostat showed a significant up-regulation of *HPGD* mRNA expression in MDA-MB-231 but not MCF7 cells. Methylation analysis revealed no significant change in methylation following epigenetic drug treatment, indicating 15-PGDH expression is indirectly regulated by methylation. Cistrome database analysis highlighted several transcription factors that bind to the 15-PGDH promoter, but no trend between transcription factor and 15-PGDH expression was observed.

Over-expression of 15-PGDH in MCF7 cells had no effect on proliferation or invasion, but significantly decreased migration and colony formation compared to matched controls. RNA sequencing indicated increased expression of genes involved in cell adhesion in the 15-PGDH over expressing clone, confirmed by increased mRNA and protein expression of protocadherin 7.

These results indicate that over-expression of 15-PGDH reduces metastasis and colony formation *in vitro*. Consequently, patients with aggressive breast cancer and high COX2 expression in particular may benefit from up-regulation of 15-PGDH expression.

Contents

List of Figures

List of Tables

Abbreviations

15-PGDH	15-hydroxyprostaglandin dehydrogenase (protein)
ACTB	β-actin (gene)
AML	Acute myeloid leukaemia
ANOVA	Analysis of variance
AP-1	Activating protein-1
APS	Adenosine 5′ phosphosulfate
AZA	5-aza-2′-deoxycytidine (decitabine)
AZURE	Adjuvant Zoledronic Acid to Reduce Recurrence
cDNA	complementary DNA
ChIP-Seq	Chromatin immunoprecipitation with DNA sequencing
COX	Cyclo-oxygenase
CpG	Cytosine-phosphate-guanine
cPGES	Cytosolic prostaglandin E_2 synthase
CRCLM	Colorectal cancer liver metastases
CREB	cAMP-responsive element-binding
CYP	Cytochrome P450
DAB	3,3′-Diaminobenzidine
dCTP	Deoxycytidine triphosphate
DEPC	Diethyl pyrocarbonate
dGTP	Deoxyguanosine triphosphate
dH_2O	Distilled water
DHA	Docosahexaenoic acid
DMBA	7,12-dimethylbenz[a]anthracene
DMEM	Dulbecco's Modified Eagle Medium
DMSO	Dimethyl sulphoxide
DNA	Deoxyribonucleic acid
DNMT	DNA methyltransferase
DNMT1	DNA methyltransferase 1
dNTP	Deoxyribonucleotide triphosphate
DPBS	Dulbecco's Phosphate-Buffered Saline

DTT	Dithiothreitol
dTTP	Deoxythymidine triphosphate
EDTA	Ethylenediaminetetraacetic acid
EEA1	Early endosomal antigen 1
EET	Epoxyeicosatrienoic acid
EGF	Epidermal growth factor
EGFR	Epidermal growth factor receptor
Egr-1	Early growth response factor-1
EMT	Epithelial-mesenchymal transition
ENCODE	Encyclopaedia of DNA Elements
EPA	Eicosapentaenoic acid
ER	Oestrogen receptor
Ets	E26 transformation-specific
FCS	Foetal calf serum
FDR	False discovery rate
FLAP	5-lipoxygenase activating protein
G418	Geneticin
GFP	Green fluorescent protein
GO	Gene ontology
GSTA1	Glutathione S-transferase A1 (gene)
HAT	Histone transacetylase
HDAC	Histone deacetylase
HER2	Human growth factor receptor 2
HETE	Hydroxyeicosatetraenoic acid
HNF3β	Hepatocyte nuclear factor 3β
HPETE	Hydroperoxyeicosatetraenoic acid
HPGD	15-hydroxyprostaglandin dehydrogenase (gene)
HPGD1	Atlas anti-15-PGDH antibody
HPGD2	Novus Biologicals anti-15-PGDH antibody
HPGD3	Cayman Chemical anti-15-PGDH antibody
HUVEC	Human umbilical vein endothelial cells

IFNγ	Interferon gamma
IHC	Immunohistochemistry
IL-4	Interleukin 4
IL-β	Interleukin-β
IPTG	Isopropyl β-D-1-thiogalactopyranoside
lncRNA	Long non-coding ribonucleic acid
LOX	Lipoxygenase
LPS	Lipopolysaccharide
LTA_4	Leukotriene A_4
LTC_4	Leukotriene C_4
LTD_4	Leukotriene D_4
LTE_4	Leukotriene E_4
MDS	Myelodysplastic syndrome
MGMT	O-6-Methylguanine-DNA Methyltransferase
miRNA	MicroRNA
MOPS	3-(N-morpholino)propanesulfonic acid
mPGES	microsomal prostaglandin E_2 synthase
mRNA	Messenger ribonucleic acid
MRP4	Multiple drug resistance-associated protein 4
NAD	Nicotinamide adenine dinucleotide
NSAID	Non-steroidal anti-inflammatory drug
NSCLC	Non-small cell lung cancer
ORF	Open reading frame
PBS	Phosphate buffered saline
PBS-T	Phosphate buffered saline with 0.1% Tween-20
PCA	Principle component analysis
PCDH7	Protocadherin-7
PCR	Polymerase chain reaction
PFA	Paraformaldehyde
PGD_2	Prostaglandin D_2
PGE_2	Prostaglandin E_2

PGE-M	PGE_2 metabolite
$PGF_{2\alpha}$	Prostaglandin $F_{2\alpha}$
PGI_2	Prostacyclin
PGIS	Prostacyclin synthase
PGT	Prostaglandin transporter
PHO	Primary hypertrophic osteoarthrophy
PLA_2	Phospholipase A_2
PP_i	Pyrophosphate
PR	Progesterone receptor
PR	Permanent red
PUFA	Polyunsaturated fatty acid
qRT-PCR	Quantitative reverse transcription polymerase chain reaction
RIN	RNA integrity number
REC	Research ethics committee
RNA	Ribonucleic acid
RNA-Seq	RNA sequencing
RPMI	Roswell Park Memorial Institute
rRNA	Ribosomal ribonucleic acid
RT-PCR	Reverse transcription polymerase chain reaction
SAHA	Suberoylanilide hydroxamic acid (vorinostat)
SDS	Sodium dodecyl sulfate
SNP	Single nucleotide polymorphism
SOC	Super Optimal broth with Catabolite repression
TAE	Tris-acetate-EDTA
TBS	Tris-buffered saline
TBS-T	Tris-buffered saline with 0.05% Tween-20
TCGA	The Cancer Genome Atlas
TMA	Tissue microarray
TNBC	Triple negative breast cancer
TNF-α	Tumour necrosis factor-α
tRNA	Transfer ribonucleic acid

TSA	Trichostatin A
TXA_2	Thromboxane A_2
VEGF	Vascular endothelial growth factor
XBP1	X box protein 1
Xgal	5-bromo-4-chloro-3-indolyl-β-D-galactopyranoside
αS-dATP	Deoxyadenosine alpha-thio triphosphate

Chapter 1 Introduction

1.1 Normal breast anatomy

The female breast is a complex tissue which undergoes changes during puberty, pregnancy, lactation and menopause (Hassiotou and Geddes, 2013). The major function of the breast is to produce and secrete milk, providing nutrition to the new born. The breast mainly composes of a network of ducts and glands (Figure 1.1). Terminal duct lobular units are the major functional unit of the breast and consist of the extra-lobular and intra-lobular terminal duct and lobule. Myoepithelial cells surround epithelial cells, all contained within a basement membrane to form lobules. Milk is secreted from epithelial acini cells into lactiferous ducts which facilitate transport of the milk to the nipple. Lymph nodes which carry lymph fluid and white blood cells are also present in the breast and armpit. The remaining breast consists of connective tissue and fatty tissue.

1.2 Breast Cancer

Cancer is the process in which cells acquire the ability to proliferate uncontrollably, resist cell death and have the potential to metastasise beyond the primary location (Hanahan and Weinberg, 2011). When this occurs in cells originating within the breast it is classed as breast cancer.

Breast cancer was the most common cancer in the UK in 2015, with almost 55,000 new cases every year (Cancer Research UK, 2016). The survival rate is 78% 10 years after diagnosis, yet there were still around 11,400 breast cancer related deaths in 2014-2016 (Cancer Research UK, 2016). Consequently, new and improved breast cancer therapies are needed.

1.2.1 Histological classification of breast cancer

As breast cancers are highly heterogeneous they are categorised using a range of criteria to help determine the best treatment regimen for each individual patient. Most breast cancers arise from epithelial cells in the milk ducts (ductal) or lobules (lobular). Subsequently, one method of characterising the highly heterogeneous population of breast cancers is by assessing histological features.

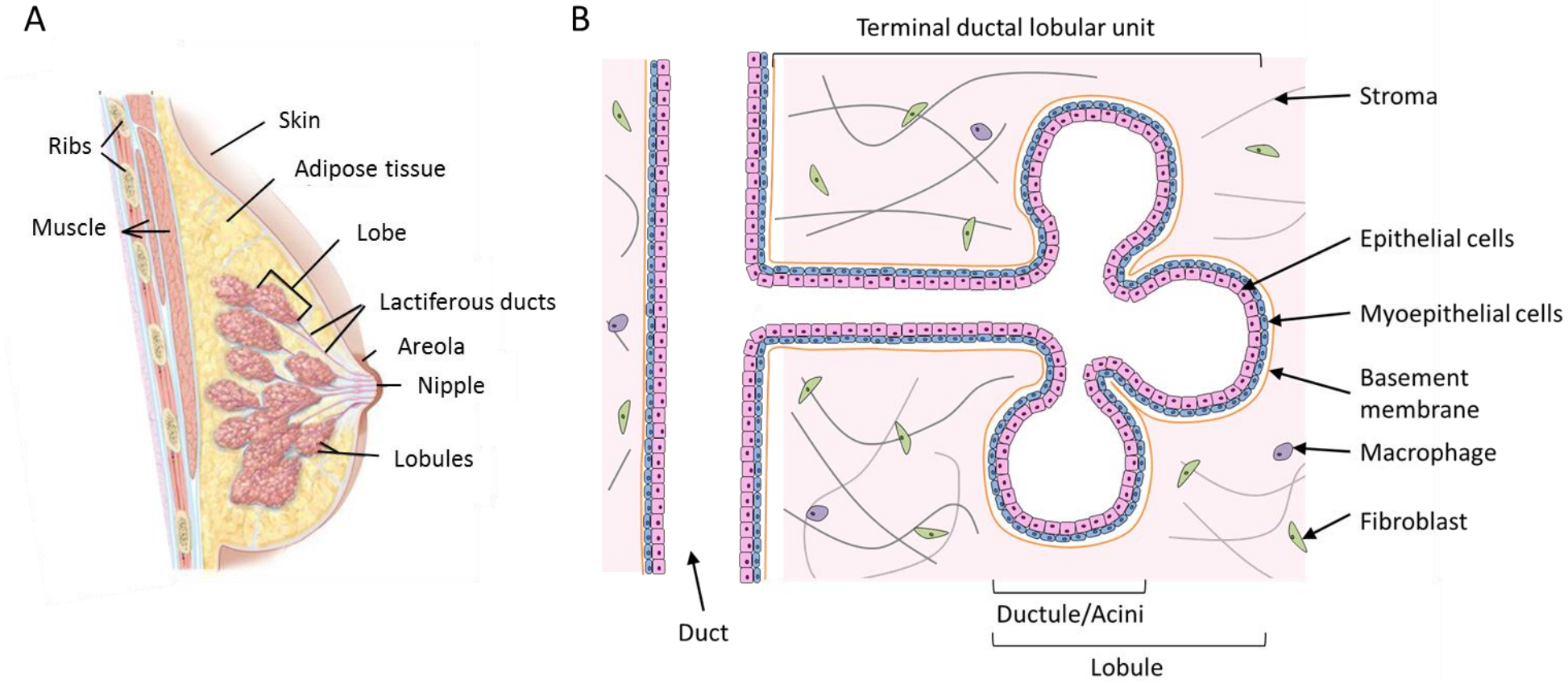

Figure 1.1 Diagrammatic representation of breast anatomy. (A) Anatomy of the healthy breast adapted from https://nbcf.org.au/about-national-breast-cancer-foundation/about-breast-cancer/what-you-need-to-know/breast-anatomy-cancer-starts/. (B) Schematic representation of a terminal ductal lobular unit, based on https://www.medscape.org/viewarticle/548921_2 and (Kumar et al., 2013).

Initially, it is determined whether the carcinoma is invasive or pre-invasive (*in situ*). Carcinomas are classed as invasive once the cancerous cells have penetrated the duct or lobule basement membrane into the stroma.

The stroma consists of connective tissue and cells that support the function of the parenchymal cells of the breast. Identification of a stromal gene expression signature associated with breast cancer clinical outcome highlights the importance of the stroma in breast cancer (Finak et al., 2008). In the presence of cancer, stromal cells including tumour associated macrophages and cancer associated fibroblasts acquire a modified phenotype (Durning et al., 1984; Su et al., 2014; Pollard, 2004). The presence of cancer associated fibroblasts and tumour associated macrophages in the tumour microenvironment has been linked to breast cancer progression and poor survival (Medrek et al., 2012; Karagiannis et al., 2012). It is believed that cancer associated fibroblasts and tumour associated macrophages influence epithelial cancer cell behaviour by promoting epithelial-mesenchymal transition (EMT) or increasing vascularisation of tumours via paracrine signalling (Leek et al., 1996; Su et al., 2014; Soon et al., 2013; Sewell-Loftin et al., 2017).

Over 7,900 new cases of breast carcinoma *in situ* were diagnosed in the UK in 2015, an 186% increase in incidence since the early 1990's (Cancer Research UK, 2016). *In situ* carcinomas can be stratified depending upon the origin of the cancer. Early stage carcinomas tend to be confined to the ducts and lobules; these are known as ductal carcinoma *in situ* and lobular carcinoma *in situ*. Ductal carcinoma *in situ* can be further classified into the architectural subtypes; cribriform, micropapillary, comedo, papillary or solid (Makki, 2015). These terms refer to morphological features observed under the microscope, some ductal carcinoma *in situ* carcinomas show a single pattern, although most show a combination of these morphological features.

Cribriform carcinoma is a rare form of breast cancer with favourable prognosis, accounting for 0.3-3.5% of breast cancers (Sinn and Kreipe, 2013; Cong et al., 2015). The term cribriform comes from the Latin word 'cribrum' meaning sieve (Branca et al., 2017) and relates to the histological appearance of well-defined sized spaces formed by arches of cells. Micropapillary carcinoma accounts for between 2-8% of breast cancers, exhibiting finger-like projections with a sponge-like appearance (Wu, Y. et al., 2017; Leonard and Swain, 2004). Comedo breast cancer is defined by intraluminal necrosis surrounded by a layer of large and more pleomorphic neoplastic cells (Shekhar et al., 2008; Leonard and Swain, 2004). Papillary carcinoma accounts for only 0.5% of newly diagnosed breast cancer cases (Pal et al., 2010) and is characterised by large papillations

with fibrovascular stalks (Leonard and Swain, 2004). Finally, carcinomas described as solid contain compact neoplastic cells (Leonard and Swain, 2004).

Invasive ductal carcinomas are the most common type of breast cancer and account for around 72-80% of all breast cancers (Arps et al., 2013). Invasive ductal carcinomas can be further divided into subgroups based on cell type, secretions, architecture and immunohistochemical profile. The subgroups include 'no special type', invasive tubular, cribriform, mucinous, medullary and papillary carcinoma. Other types of invasive breast carcinoma include invasive lobular carcinoma and the more rare forms such as inflammatory breast cancer, Paget's disease and apocrine carcinoma.

'No special type' carcinomas are those that do not have specific differentiating features and account for around 60% of invasive ductal carcinomas (Badowska-Kozakiewicz et al., 2017). The mucinous subtype refers to epithelial cells with mild atypical nuclei and abundant mucus (Makki, 2015). It is a rare subtype associated with improved disease free survival compared to 'no special type', but there is no difference in overall survival (Bae et al., 2011). Medullary breast carcinoma presents itself as a well-defined tumour mass with poorly differentiated morphology (Makki, 2015). Apocrine breast cancer epithelial cells have abundant granular cytoplasm with prominent nuclei, accounting for 1-4% of all breast cancer cases (Weigelt et al., 2010).

Once invasive breast cancer reaches the lymph nodes or blood stream, it has the potential spread to other parts of the body, becoming metastatic. Breast cancer most commonly migrates to the brain, liver, lungs or bone. Once the cancer has metastasised it becomes very difficult to treat, therefore preventing cancer cell migration is a key area in breast cancer research.

1.2.2 Breast cancer grading and staging systems

Grading and staging of breast cancer helps clinicians to determine prognosis and aid selection of a suitable treatment for each patient. There are several methods described in the literature for grading breast cancer, which assess the characteristics and spread of the individual carcinoma.

One of the common methods employed to categorise breast cancer staging is the TNM system. This method assesses tumour size, lymph node invasion and metastatic spread. The stage is graded 1-4 with subgroups for each grade. Generally speaking the lower grades present small tumours with few to no cancer cells in the lymph nodes and the highest grade shows any size

tumour with the presence of metastatic cancer in other parts of the body. The higher the stage of breast cancer the worse the prognosis.

A method recommended by various governing bodies including the World Health Organisation is the Bloom–Richardson–Elston grading system, more commonly known as the Nottingham Grading System (Rakha et al., 2010). This method assesses the following criteria:

- Tubule formation – Assesses what percentage of the tumour cells form normal duct structures. The more tubular structures the lower the score (score 1 = >75% tumour area, score 2 = 10-75% tumour area, score 3 = <10% tumour area).
- Nuclear pleomorphism – How uniform (normal) or large and irregular (pleomorphic) the nuclei appear. The more uniform the nuclei the lower the score.
- Mitotic count – The number of dividing cells present within 10 high power fields. The fewer dividing cells the lower the score (score 1 = <7 mitoses, score 2 = 8-14 mitoses, score 3 = >14 mitoses).

Each factor is given a score out of three and the three scores are added together to give a score out of nine. Those scoring 3-5 are grade 1, those scoring 6-7 are grade 2 and those scoring 8-9 are grade 3. The higher the overall grade the worse the patients' prognosis.

1.2.3 Molecular classification of breast cancer

Molecular classification of breast cancer has been developed to enable personalised treatment for patients based on the individual carcinoma molecular features. The first molecular classification was completed by Perou and Sorlie in 2000 (Perou et al., 2000). Breast cancer was initially divided into subgroups; Luminal (consisting of two or three further subgroups), basal and HER2 positive. A 'normal-like' group was also reported, but this subgroup consisted of samples with low cancer cell content. Subsequently, subgroups based on the expression prolife of three receptors, oestrogen receptor (ER), progesterone receptor (PR) and human epidermal growth factor receptor 2 (HER2), has become common practice (Table 1.1). Further stratification of these subgroups has also been reported, making the molecular classification of breast cancer increasingly more complex. Factors such as claudin, cytokeratin, Ki67, androgen receptor and E-cadherin expression, as well as epidermal growth factor receptor (EGFR) and p53 mutations are often taken into account (Eliyatkin et al., 2015; Perou et al., 2000).

Table 1.1. Definition of breast cancer molecular subtypes.
Definition of breast cancer molecular subtypes according to ER, PR and HER2 expression patterns, adapted from (Neve et al., 2006; Subik et al., 2010).

Molecular subtype	ER expression	PR expression	HER2 expression
Luminal A	+	+	−
Luminal B	+	+	+
HER2	−	−	+
Basal-like	−	−	−

Around 70-80% of breast cancers are ER-positive (Ali and Coombes, 2000; Onitilo et al., 2009). A large majority of ER-positive samples are also positive for the PR, with almost 60% of ER-positive breast cancers also expressing the PR (Onitilo et al., 2009). Only 1-4% of ER-negative samples show PR expression (Hefti et al., 2013). Furthermore, HER2 over-expression occurs in 15-20% of breast cancers and is linked to an aggressive phenotype (Godone et al., 2018). Overall, the known expression of these proteins by the cancer cells enables targeted therapeutic treatment resulting in a better prognosis.

Triple negative breast cancer (TNBC) (a type of basal-like breast cancer) accounts for 10-15% of breast cancers and is associated with an aggressive phenotype and is more common in younger women (Aysola et al., 2013; Dent et al., 2007). Due to a lack of targeted treatment, these patients have a poor prognosis and it is a subgroup of breast cancer that requires improved therapeutic options.

Both histological grade and the molecular profile of an individual cancer are used to determine the best treatment for each patient. The complexity of these grading systems is continually increasing thanks to improved understanding of the disease, leading to improved and more personalised treatment regimes.

1.2.4 Current treatment options

Current treatment takes into account the type of breast cancer, the size and grade of the cancer, whether the cancer has migrated and the hormone receptor status of the cancer cells. The optimal treatment regime is personalised for each patient to ensure the best possible response.

In most situations surgery is performed to remove the cancerous tissue. The amount of tissue removed depends upon the size and spread of the cancer. A small section of the breast containing the cancerous cells may be removed (lumpectomy) or a partial section of the breast may be removed (quadrantectomy). In more advanced cases the whole breast is removed

(mastectomy) or a radical mastectomy performed, which involves the removal of the breast, axillary lymph nodes and some underlying chest muscle. In most cases surgery is followed by a combination of radiotherapy, chemotherapy, endocrine therapy and targeted therapy.

Radiotherapy is usually given as an adjuvant therapy following a lumpectomy, with some patients receiving radiotherapy after a mastectomy. Radiation therapy involves gamma rays that are targeted to a tumour or site where the tumour has been removed to kill any residual cancer cells. Radiotherapy may be given alone or in combination with chemotherapy or endocrine therapy.

Chemotherapy can be used in a neoadjuvant or adjuvant setting, depending upon the individual case. Chemotherapy involves systemic administration of one or more cytotoxic agents which prevent DNA synthesis or cell division. This targets cells with a high turn-over rate, which includes but is not limited to cancer cells. Consequently, there are many adverse side effects to chemotherapy. Due to a lack of targetable receptors TNBC is usually treated with surgery followed by a combination of chemotherapy drugs such as fluorouracil, epirubicin and cyclophosphamide.

Endocrine therapy also known as hormone therapy is usually used in ER-positive patients. Treatment depends upon whether the patient is pre- or post-menopausal. Tamoxifen inhibits the activity of the ER and is typically given to pre-menopausal women. Whereas aromatase inhibitors (e.g. exemestane and anastrozole) are given to post-menopausal women to reduce conversion of androgens into oestrogens by the aromatase enzyme.

Targeted therapy such as trastuzumab (Herceptin) can be used in patients who over-express the HER2 protein. The monoclonal antibody blocks the activity of HER2, slowing the cancer cell growth.

Immunotherapy in breast cancer is a recent phenomenon and involves activation or suppression of the immune system. TNBC is thought to be more immunogenic than other breast cancer subtypes (Liu, Z. et al., 2018), therefore TNBC patients are ideal candidates for immunotherapy. Atezolizumab is an immunotherapy drug that blocks PD-L1 activity. Inhibiting PD-L1 activates tumour-specific T-cell immune responses and thus enhances anti-tumour activity (Salmaninejad et al., 2019). Consequently, atezolizumab has recently been approved by the FDA for treatment of locally advanced or metastatic TNBC patients in combination with chemotherapy drug nab-paclitaxel (Cortes et al., 2019). Prostaglandin E_2 (PGE_2), a physiologically active lipid compound, has immunosuppressive properties. PGE_2 moderates

chemokine production, inhibits attraction of pro-inflammatory cells and enhances the accumulation of immune suppressor cells (Wang, D. and DuBois, 2016; Kalinski, 2012). This suggests that reducing PGE_2 signalling may be beneficial in breast cancer, particularly in TNBC patients, by re-establishing the patient's immune system and increasing anti-tumour activity.

With improved breast cancer treatments and personalised patient treatments, the overall survival rate for breast cancer patients after one year increased by 14% to 96% between 1972 and 2011 (Cancer Research UK, 2016). This has been aided by improved diagnosis. The introduction of the mammogram in the mid 1990's for women aged 50-71 lead to earlier breast cancer detection. Although patient survival is relatively high for breast cancer compared to other cancer types, 11,563 people died of breast cancer in 2016 (Cancer Research UK, 2016), therefore improved treatments are still needed.

1.2.5 Risk factors

Many risk factors have been associated with breast cancer including family history, extended exposure to endogenous oestrogens indicated by early menarche and late menopause, hormone replacement therapy, and lifestyle factors such as diet, lack of exercise and alcohol consumption (Kaminska et al., 2015; Howell et al., 2014). It is believed that 23% of breast cancers are preventable (Cancer Research UK, 2016), therefore gaining a better understanding of the causes is advantageous.

1.2.5.1 Genetic mutations

It has long been recognised that mutations in the DNA sequence can lead to cancer. DNA mutations may be hereditary or acquired and it is believed that hereditary factors account for 25% of breast cancer risk (Cancer Research UK, 2016). Genetic mutations leading to cancer often occur in tumour suppressor genes or oncogenes.

A strong association between *BRCA1* and *BRCA2* mutations and breast cancer has been well-established. *BRCA1* and *BRCA2* are a tumour suppressor genes, involved in the DNA repair process, therefore individuals with a *BRCA1* and *BRCA2* germline (inherited) mutation are predisposed to ovarian and breast cancer (Paul and Paul, 2014). Women with a defective BRCA gene have a 45-65% chance of developing breast cancer before they are 70 years old (Antoniou et al., 2003). Furthermore, BRCA mutations are also important in sporadic breast cancer, where the patients' family do not have a history of breast cancer. As many as 17 out of 193 patients

with sporadic breast cancer exhibit deleterious germline *BRCA1* or *BRCA2* mutations, with *de novo* BRCA mutations being extremely rare (De Leeneer et al., 2012).

Extensive research is on-going into the genetic changes involved in breast cancer development. Many genes have been implicated in the pathogenesis of breast cancer such as *TP53*, *PTEN* and *PALB2* (Wesola and Jelen, 2017; Ngeow et al., 2017; Schon and Tischkowitz, 2018). Determining whether these mutations are driver mutations (drive cancer) or passenger mutations (play no role in cancer but accompany driver mutations) is challenging. Cancer cells acquire numerous somatic genetic changes, many of which are clonal and their interactions are not well understood. It is therefore essential to perform downstream functional studies to clarify their clinical significance.

Targeting genes regularly mutated in cancer offers a more personalised treatment and is receiving increasing interest in breast cancer research. Targeted gene therapy with *TP53* has been suggested in patients with TNBC, as *TP53* was the most mutated gene in TNBC, occurring in 62% of basal TNBC patients (Shah et al., 2012). Treating TNBC cell lines with PRIMA-1^{MET}, which reactivates the *TP53* gene, decreased cell proliferation and migration and induced apoptosis (Synnott et al., 2017). Despite significant data showing *TP53* therapy is valuable in cancer, not just TNBC, targeted *TP53* therapies are yet to be approved by the US Food and Drug Administration. This emphasises the complexity of personalised targeted gene therapy in the clinic.

1.2.5.2 Chronic inflammation

Acute inflammation occurs in response to harmful stimuli to protect and repair tissue damage, yet if inflammation is uncontrolled and becomes chronic it can lead to carcinogenesis (Landskron et al., 2014). Chronic inflammation has recently been described as a hallmark of cancer due to its role in proliferation, angiogenesis and metastasis (Colotta et al., 2009).

One mechanism involved in chronic inflammation is PGE_2 signalling via the EP2 receptor. Binding of PGE_2 to the EP2 receptor induces pro-inflammatory mediators including cytokines IL-23 and IL-17 (Sheibanie et al., 2007a; Sheibanie et al., 2007b), leading to inflammation. This indicates the importance of PGE_2 signalling and the prostaglandin pathway in cancer.

1.2.5.3 Lifestyle

Acquired genetic mutations may arise as the result of a spontaneous event. The regularity of these events is increased with exposure to specific mutagens such as tobacco. Evidence

suggests that there is small but significant increased risk of invasive breast cancer in individuals who have or still do smoke (Jones et al., 2017).

Other more prevalent factors in breast cancer include alcohol consumption and obesity, with each independently causing 8% of breast cancers in 2015 (Cancer Research UK, 2016). Despite these factors being preventable, the rate of obesity has tripled in the past 20 years as a result of the Western lifestyle, with over 155 million overweight or obese children worldwide (Hossain et al., 2007). Consequently, the percentage of cancers arising as a result of obesity is likely to increase in the future and the predicted decrease of breast cancer incidence may not be as great as anticipated. For these reasons there is still a challenge to understand the molecular and cellular basis of breast cancer progression, so that identification and treatment can be optimised.

1.3 Eicosanoids

Eicosanoids are biologically active lipids involved in various processes including inflammation, homeostatic biological functions and cancer (Funk, 2001; Wang, D. and Dubois, 2010). Eicosanoids are derived from metabolism of straight-chain polyunsaturated fatty acids (PUFAs). The name eicosanoids is derived from the Greek name for twenty, 'eicosa' (Funk, 2001), as eicosanoids are composed of twenty carbon atoms and two or more carbon-carbon double bonds. PUFAs are either oxidised, stored as triglycerides or stored in cell phospholipid membranes until further cellular processing (Fabian et al., 2015).

Fatty acids are often referred to as ω-3 and ω-6. This indicates the position of the first double bond from the methyl end within the chain, for example the first double bond in arachidonic acid is at carbon 6 and therefore it is an ω-6 fatty acid. Furthermore, the number of carbon atoms and double bonds within the fatty acid are referred to by lipid numbers, for instance arachidonic acid is a 20 chain carbon with 4 double bonds thus has a lipid number of 20:4 (Figure 1.2). The positioning of the double bonds can have a significant effect of the function of the product.

There are three ω-3 PUFAs involved in human physiology. Eicosapentaenoic acid (EPA) and docosahexaenoic acid (DHA) are both found in fish oils while α-linoleic acid comes from plant oils. There are many ω-6 PUFAs, yet arachidonic acid is the main precursor for eicosanoid biosynthesis in mammalian cells and one of the best studied ω-6 PUFAs.

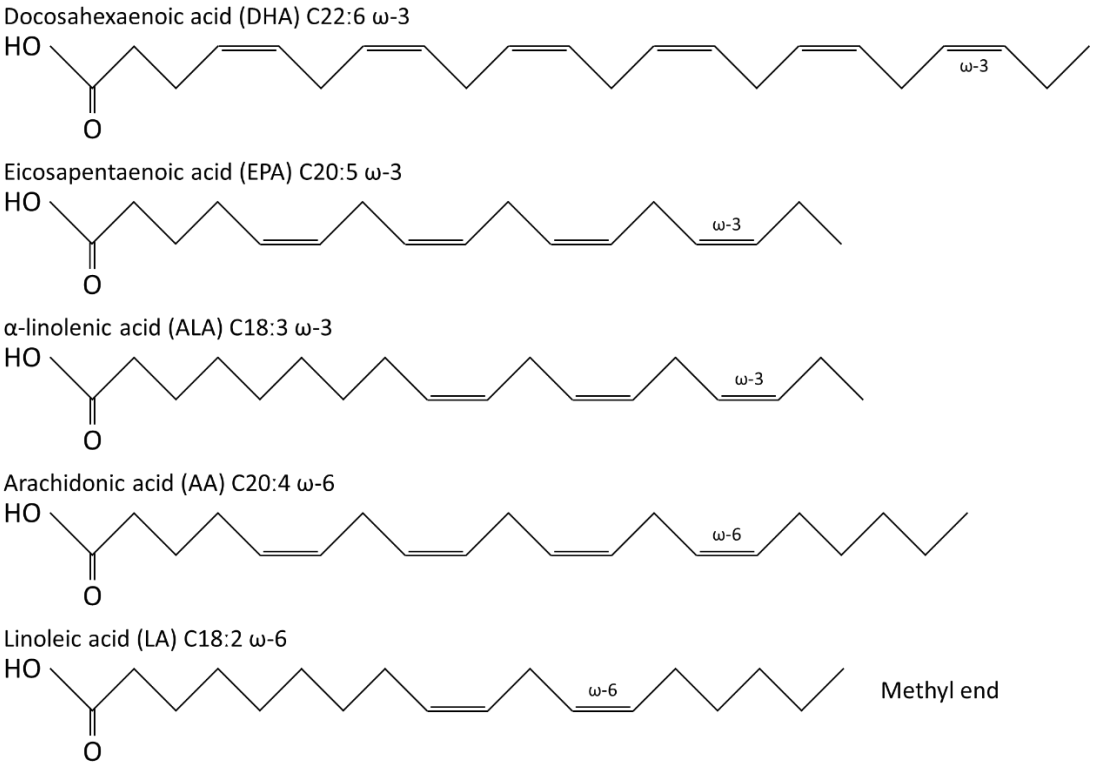

Figure 1.2 Polyunsaturated fatty acid structures. Left to right shows the carboxyl end to the methyl end of the structures. Ω (ω) label determined by the position of the carbon atom with the first double bond, carbons counted from the methyl end.

Arachidonic acid can be obtained from the diet, derived from linoleic acid, or in most cases released from the cellular membrane by phospholipase A2.

The intake ratio of ω-6/ω-3 fatty acids in the diet has dramatically changed since the introduction of processed foods and vegetable oils from 2:1 to 10:1 or more (Zanoaga et al., 2018). This increased intake of ω-6 fatty acids has been linked to obesity, diabetes and other chronic diseases such as cancer (Simopoulos, 2016; Simopoulos, 1999; Iyengar et al., 2013). Both ω-6/ω-3 fatty acids compete for the same enzyme binding sites, therefore it is believed that increasing the intake of ω-3 fatty acids may prevent cancer (Iyengar et al., 2013). Altering the ω-6/ω-3 fatty acid balance with fish oil supplements, including DHA and EPA, is currently being investigated in cancer prevention and improving patient outcome. There is a well-established link between ω-3 fatty acids and colorectal cancer (Cockbain et al., 2014; Camargo Cde et al., 2016; Tokudome et al., 2015), yet more research is required to demonstrate this link with breast cancer.

Combination therapy with DHA and chemotherapy in breast cancer patients with visceral metastases showed improved time to progression and overall survival in patients with the highest plasma DHA incorporation (Bougnoux et al., 2009). Therefore modulation of the eicosanoid pathway in breast cancer may be beneficial.

PUFAs are metabolised by several enzymes including cyclo-oxygenases, lipoxygenases and cytochrome P450 enzymes (Figure 1.3). The eicosanoid products include prostaglandins, thromboxanes, leukotrienes, lipoxins, resolvins, and eoxins. Eicosanoids act on local cells and have a relatively short half-life (seconds to minutes) (Wymann and Schneiter, 2008), this suggests the need to maintain a tight control on eicosanoid levels, as they can be generated as required in response to physiological need and quickly removed so that normal homeostasis can be maintained.

1.3.1 Lipoxygenase pathway

Lipoxygenases (LOX) are a group of enzymes that convert arachidonic acid into leukotrienes, hydroxyeicosatetraenoic acids (HETEs) and hydroperoxyeicosatetraenoic acids (HPETEs). Each of the products have diverse biological functions including transcription factor activation, regulation of apoptosis and influencing cell growth (Steele et al., 2000).

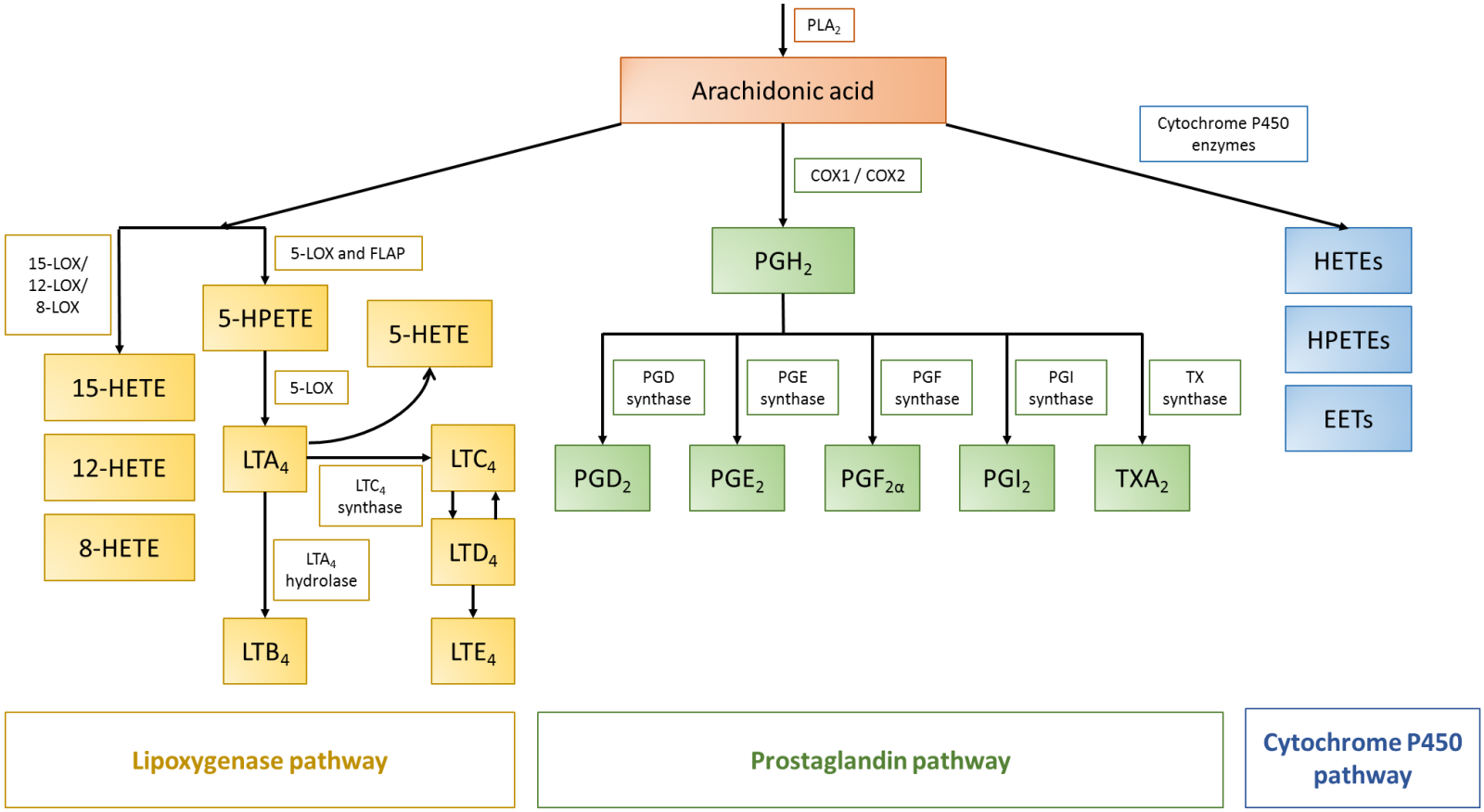

Figure 1.3 Arachidonic acid metabolism pathway. Adapted from (Wang, D. and Dubois, 2010). Yellow = lipoxygenase pathway. Green = Prostaglandin pathway. Blue = Cytochrome p450 pathway. PLA_2 = phospholipase A_2, PG = prostaglandin, LT = leukotriene, TX = thromboxane, HETE = hydroxyeicosatetraenoic acid, HPETE = hydroperoxyeicosatetraenoic acid, EET = epoxyeicosatrienoic acid, LOX = lipoxygenase, COX = cyclo-oxygenase, FLAP = 5-lipoxygenase activating protein.

LOX enzymes are named according to their ability to insert molecular oxygen at the specified carbon atom of arachidonic acid, for instance 5-LOX inserts oxygen at carbon five. 5-LOX, which requires the 5-lipoxygenase activating protein (FLAP) for activation, is the key enzyme in leukotriene production (Figure 1.3), while lipoxygenases, 12-LOX, 15-LOX-1 and 15-LOX-2 are required for the production of HETEs.

15-LOX-2 is believed to have anti-carcinogenic properties, whereas 5-LOX and 12-LOX have been linked to cancer development (Wang, D. and Dubois, 2010). Modulating the activity of some of these enzymes is of interest as a target for cancer therapy. 12-LOX inhibitors significantly inhibited MCF7 breast cell line proliferation (Natarajan and Nadler, 1998). Furthermore, inhibition of angiogenesis, inflammation, and induction of apoptosis has lead to the development of LOX and FLAP inhibitors as chemotherapeutic agents (Steele et al., 2000).

1.3.2 Cytochrome P450 pathway

Cytochrome P450 (CYP) enzymes are a large group of oxidative enzymes which contain heme as a cofactor and many are involved in drug metabolism. Furthermore, CYP enzymes are involved in the metabolism of selected pro-drugs used in cancer treatment, including tamoxifen, whose activity is increased following metabolism to α-hydroxytamoxifen (Boocock et al., 2002).

There are many different CYP enzymes involved in the metabolism of PUFAs to produce epoxyeicosatrienoic acids (EETs) and HETEs. Interestingly, EETs are associated with angiogenesis and proliferation as well as inflammation and pain (Spector and Kim, 2015); consequently CYP enzymes have been identified as a potential target in cancer treatment. As CYP enzymes have a diverse array of substrates, the downstream effects of altering CYP activity and expression may be complex and difficult to interpret.

1.3.3 Cyclooxygenase pathway (prostaglandin pathway)

There are two functional cyclo-oxygenase (COX) isoforms in humans, COX1 and COX2. The enzymes are mainly localised on the luminal side of the endoplasmic reticulum and nuclear envelope (Chandrasekharan and Simmons, 2004). COX1 is ubiquitously expressed under basal conditions, whereas COX2 is undetectable in most normal tissues and is notorious for being induced in various cancers including breast, colon, gastric, and lung cancer (Shim et al., 2003; Kim, H.S. et al., 2012; Hahm et al., 2002; Gupta and Dubois, 2001; Eberhart et al., 1994; Achiwa et al., 1999).

PUFA metabolism by COX1/2 produces intermediate prostaglandin H_2 (PGH_2). PGH_2 is further metabolised by several prostaglandin synthase enzymes or thromboxane A_2 synthase to generate prostaglandins and thromboxane A_2 (Figure 1.3). These lipid compounds are involved in an array of biological functions including hormone regulation, inflammation and regulation of blood clotting (summarised in Table 1.2) (Na et al., 2011; Mann, J.R. et al., 2006; Gomes et al., 2018).

1.3.3.1 COX2 and cancer

COX2 over-expression is associated with carcinogenesis through increased cellular proliferation, migration, invasion and metastasis as well as inhibition of apoptosis (Sobolewski et al., 2010; Lee, E.J. et al., 2007; Tomozawa et al., 2000; Hashemi Goradel et al., 2018). The majority of the carcinogenic effects are thought to result from increased prostaglandin production, in particular PGE_2 (summarised in Table 1.3).

COX2 over-expression was observed in 49% of early breast cancer patients (Kargi et al., 2013) and is a target in early breast cancer (Esbona et al., 2016; Half et al., 2002). Elevated COX2 expression was observed in 37.4% of invasive breast cancer and associated with poor distant disease-free survival (Ristimaki et al., 2002). Furthermore, over-expression of COX2 was observed in 72% of all breast cancers and correlated with large tumour size and advanced clinical status, highlighting COX2 as a possible identifier of an aggressive phenotype (Yan et al., 2004; Thill et al., 2010a). As a result COX2 expression is associated with poor prognosis, disease free survival and overall survival (Xu et al., 2017), emphasising the importance of the prostaglandin pathway as a target in breast cancer.

An *in vivo* mouse study with COX2 over-expressing MCF7 xenographs showed increased tumour size, angiogenesis and invasion of adjacent regional lymph nodes compared to the MCF7 control (Robertson et al., 2007). Furthermore, the onset of breast cancer was delayed in mice with COX2 knock-out mammary epithelial cells induced by immunosuppressor and carcinogen, 7,12-dimethylbenz[a]anthracene (DMBA), compared to wild-type mice (Markosyan et al., 2011). *In vivo* studies like these, alongside the clinical data, confirm the significance of COX2 expression in breast cancer and have fuelled the investigation of COX2 inhibitors in breast cancer.

There are two different types of COX inhibitors, non-selective and selective. Non-selective COX inhibitors inhibit both COX1 and COX2 isoforms, and include non-steroidal anti-inflammatory drugs (NSAIDs) such as aspirin and ibuprofen. Whereas selective COX2 inhibitors such as celecoxib, rofecoxib and etorcoxib, specifically target COX2.

Table 1.2 The biological functions of prostaglandins. Information compiled from the literature (Miller, 2006; Anderson, 2008; Narumiya and FitzGerald, 2001; Deshpande et al., 2018).

Ligand	Receptor	Functions
Prostaglandin D_2 (PGD_2)	DP	Anti-inflammatory Inhibition of platelet aggregation Vasodilation Bronchodilation Allergic mediator Relaxation of GIT and uterus Regulates sleep-wake cycle Regulates temperature and nociception
Prostaglandin E_2 (PGE_2)	EP1	Bronchoconstriction GI tract smooth muscle contraction Increased blood flow Pain perception
	EP2	Vasodilation Increased sodium and water excretion Bronchodilation GI tract smooth muscle relaxation Ovulation and fertilisation
	EP3	Decreased gastric acid secretion Increased mucus secretion Uterus contraction GI tract smooth muscle contraction Fever generation Kidney reabsorption Lipolysis inhibition Increased autonomic neurotransmitters Pain perception
	EP4	Uterus contraction GI tract smooth muscle contraction
	Not specified	Bone resorption and bone formation
Prostaglandin $F_{2\alpha}$ ($PGF_{2\alpha}$)	FP	Uterus contraction Smooth muscle contraction Fertilisation/Ovulation Bronchoconstriction Renal function Cardiac hypertrophy Regulation of intraocular pressure
Prostaglandin I_2 (PGI_2)	IP	Vasodilation Inhibition of platelet aggregation Renin release and sodium excretion Pain perception Smooth muscle relaxation Bronchodilation
Thromboxane A_2 (TXA_2)	TP	Vasoconstriction Increased of platelet aggregation Bronchoconstriction

Table 1.3 Summary of prostaglandin role in carcinogenesis

Adapted from (Wang, D. and Dubois, 2010). Grey background = receptor or pathway unknown.

Lipid	Receptor	Pathway	Function	Tumour type	*In vitro*	*In vivo*	References
PGE_2		Ras-Erk	Proliferation	Colorectal	✓	✓	(Wang, D. et al., 2005)
		Ras-Erk	Proliferation	NSCLC	✓	×	(Krysan et al., 2005)
	EP2	GSK3β-β-catenin	Proliferation	Colorectal	✓	×	(Castellone et al., 2005)
		PI3k-Akt-PPARδ	Survival	Colorectal	✓	✓	(Wang, D. et al., 2004)
		BCL-2	Survival	Colorectal	✓	×	(Sheng et al., 1998)
		NF-κB	Survival	Colorectal	✓	×	(Poligone and Baldwin, 2001)
	EP4	SRC-EGFR-PI3K-Akt	Migration and invasion	Colorectal	✓	✓	(Buchanan et al., 2003; Buchanan et al., 2006)
	EP1	SRC-EGFR	Migration and invasion	Hepatocellular	✓	×	(Han et al., 2006)
		Erk-ETS1	Migration and invasion	Pancreatic	✓	×	(Ito et al., 2004)
	EP2 and EP4	CCR7	Migration and invasion	Breast	✓	×	(Pan et al., 2008)
	EP4	PI3K-Akt	Migration and invasion	Lung and colorectal	✓	✓	(Yang, L. et al., 2006)
	EP4		Migration	Breast	✓	×	(Timoshenko et al., 2003)
	EP2		Angiogenesis	Breast	✓	×	(Chang et al., 2004) (Li, S. et al., 2015)
$PGF_{2\alpha}$	FP	Erk–FGF2–FGFR1–Erk	Proliferation	Endometrial	✓	×	(Sales et al., 2007)
	FP		Migration and invasion	Colorectal and endometrial	✓	×	(Qualtrough et al., 2007; Sales et al., 2008)
PGD_2	PPARδ		Proliferation inhibition	Prostate	✓	×	(Kim et al., 2005)
TXA_2	TP	RHOA	Migration	Prostate	✓	×	(Nie et al., 2008)

Prospective data collected by the Women's Health Initiative assessed the effects of regular NSAID use (two or more tablets/week) in postmenopausal women with no history of breast cancer in a large cohort.

Regular NSAID (including ibuprofen and aspirin) use for 5-9 years significantly reduced the risk of breast cancer by 21% which was increased to 28% after 10 or more years (Harris et al., 2003). Furthermore, regular use of aspirin decreased the risk of distant recurrence and breast cancer death in women who lived for more than one year after breast cancer diagnosis (Holmes et al., 2010). This data suggests that NSAIDs may be a suitable chemopreventative drug in breast cancer, but clinical trials are needed to confirm this data as the variation in dosage and compliance were not assessed in these studies.

Few clinical trials with NSAIDs have been completed in breast cancer, but with increasing evidence that aspirin reduces the recurrence of cancer, the Add-Aspirin trial is now on-going. The Add-Aspirin trial is a large phase III randomised clinical trial aimed to assess whether regular use of aspirin after treatment for early stage (non-metastatic) solid tumours can prevent cancer reoccurrence and death (Coyle et al., 2016). The study is focused on breast, colorectal, gastric and prostate cancers with patients receiving 100mg or 300mg aspirin or a placebo for 5 years. As the study is currently on-going no data is available to assess.

Pre-surgical treatment with celecoxib in breast cancer patients significantly decreased Ki67 expression (a measure of proliferation) compared to pre-treatment levels, but no significant reduction of Ki67 expression was observed compared to the untreated control group (Martin et al., 2010). Neoadjuvant celecoxib and exemestane combination treatment in locally advanced postmenopausal breast cancer patients showed comparable clinical response to patients treated with frontline treatments exemestane and letrozole alone, however three out of five patients showing complete clinical response were in the celecoxib and exemestane group (Chow et al., 2008). Despite no significant differences in these studies the findings are still interesting and therefore warrant further investigation. As both studies assessed used a small patient cohort increasing the number of subjects may improve the statistical power of the studies.

Although there is evidence COX inhibitors may be valuable in cancer treatment, the drugs are associated with adverse side effects such as gastrointestinal bleeding, nausea, abdominal pain and less common cardiovascular effects including myocardial infarction (Whitlock et al., 2015; Sostres et al., 2010; Hippisley-Cox and Coupland, 2005). COX1 inhibition, the key target of

aspirin, decreases levels of TXA_2 which is associated with blood clotting. Adverse effects of COX2 inhibition are thought to be primarily the result of decreased prostacyclin levels, which is a potent vasodilator that also inhibits platelet aggregation. Decreased blood clotting and reduced vasodilation as a result of COX inhibition along with altered PGI_2 and TXA_2 levels are therefore associated with cardiovascular events including myocardial infarction, stroke, hypertension and congestive heart failure.

By targeting the COX enzymes that function at the start of the prostaglandin synthesis pathway, prostaglandin production is halted. As each prostaglandin has specific but overlapping functions, COX inhibition can result in a range of unexpected side effects. Furthermore, COX inhibition leads to elevated COX substrate molecules, which are in turn are shunted through other pathways (e.g. the lipoxygenase pathway) creating a wider dysregulation of lipid based signalling. This alteration in the balance between different bioactive lipids is also thought to be another molecular mechanism for undesired and unexpected side effects of COX inhibition. Consequently, rather than the inhibition of COX, targeting of downstream steps that affect fewer prostaglandins may be give the same results, but with fewer side effects.

1.3.3.2 Other prostaglandins pathway components and cancer

Terminal prostaglandin synthases are the final enzymes involved in prostaglandin production (Figure 1.4), therefore targeting these enzymes may potentially result in fewer adverse side effects than seen with COX inhibition. As PGE_2 is thought to be the main prostaglandin involved in cancer progression the majority of the research in this area is focused on PGE_2 synthases. Development of microsomal prostaglandin E synthase 1 (mPGES-1) inhibitors has been reported, yet very few studies have focused on their role in carcinogenesis. Knock-out of the mPGES-1 gene led to decreased tumour formation and suppression of angiogenesis in a HER2 driven breast cancer mouse model (Howe et al., 2013). A recent study suggests that mPGES-1 inhibition also suppresses neuroblastoma xenograph growth (Kock et al., 2018).

Expression of prostacyclin synthase (PGIS) has also been implicated in breast cancer, with a significantly reduced 10-year survival in patients expressing PGIS and decreased cell death with PGIS over-expression *in vitro* when exposed to the NSAID sulindac (Klein et al., 2015). This study is the only known study focusing on PGIS in breast cancer, whereas other studies showed anti-carcinogenic effects with a colorectal knock-out mouse model and in a murine lung cell line over-expressing PGIS (Li, H.Y. et al., 2018; Sasaki, Y. et al., 2015).

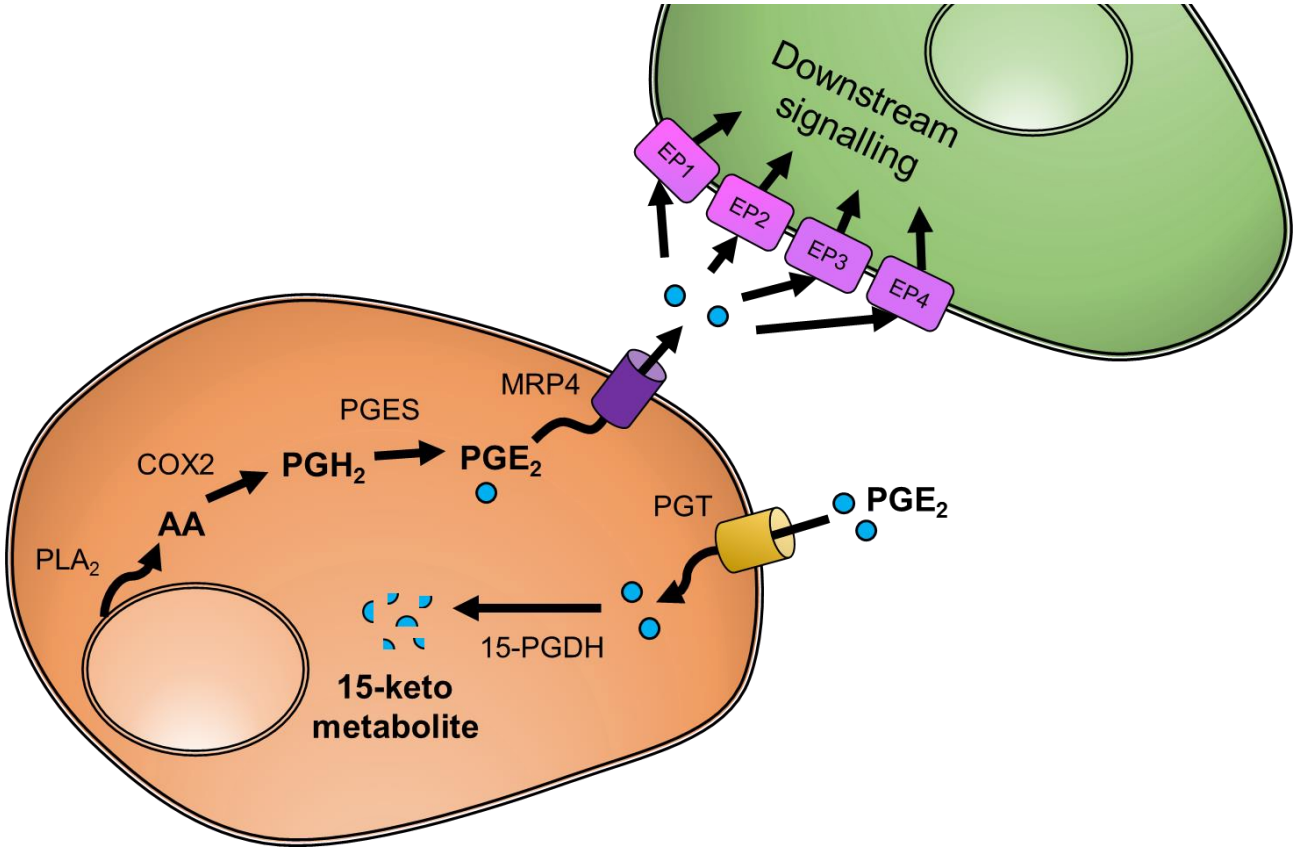

Figure 1.4 Prostaglandin E_2 synthesis, signalling and degradation pathway. PGES = prostaglandin E synthase. PLA_2 = phospholipase A_2. PGH_2 = prostaglandin H_2. AA = arachidonic acid. PGE_2 = prostaglandin E_2. PGT = prostaglandin transporter. MRP4 = multidrug resistance-associated protein 4 transporter. 15-PGDH = 15-hydroxyprostaglandin dehydrogenase. Adapted from (Tootle, 2013).

Consequently, PGIS expression may be deleterious in breast cancer, but as the breast cancer study used *in vitro* data, further assessment is required to determine whether this is also the case *in vivo*.

Multiple drug resistance-associated protein (MRP4), encoded by the *ABCC4* gene, is a member of the ATP-binding cassette family that exports prostaglandins from the cell, where they can bind to EP receptors on the cell surface membrane. As well as prostaglandins, MRP4 also exports a wide range of molecules including drugs such as methotrexate and cephalosporin's (Russel et al., 2008). Increased expression of the MRP4 transporter has been reported in prostate cancer, leading to a worse prognosis (Montani et al., 2013). Lowering the expression of MRP4 may reduce PGE_2 signalling, as PGE_2 would remain internalised, thus unable bind the EP receptors and is more likely to undergo degradation. MRP4 expression is elevated in basal-like breast cancer cell lines and therefore has been identified as a potential target in this subset of patients (Kochel et al., 2017).

PGE_2 is the key prostaglandin associated with cancer and exerts its effects through the G-protein couple receptors EP1-4. Each receptor initiates alternative downstream signalling and has been investigated in cancer pathogenesis. Decreased incidence of breast cancer has been reported following treatment with EP1 receptor agonist ONO-8711 in rats (Kawamori et al., 2001). EP2 knock-out models have also shown decreased lung, breast and skin tumour development (O'Callaghan and Houston, 2015). Additionally, inhibition of EP4 signalling inhibited breast cancer metastasis in mice, whereas no effect was observed following EP3 antagonism (Ma, X. et al., 2006). For these reasons targeting of the EP receptors have been proposed as possible therapeutic strategy, with less emphasis on the EP3 receptor.

The prostaglandin transporter (PGT), encoded by the *SLCO2A1* gene, is an organic anion-transporting polypeptide transporter that actively pumps prostaglandins into the cell. There is limited research on *SLCO2A1* in breast cancer, yet a few studies have shown that its expression is decreased in gastrointestinal cancer (Holla et al., 2008; Takeda et al., 2016). The presence of both the PGT and 15-PGDH is required for PGE_2 removal and inactivation, so their up-regulation could result in reduced activation of the EP receptors as a consequence of reduced levels of extracellular PGE_2 (Nomura et al., 2004). On the contrary, PGT expression has been shown to promote tumorigenesis in mice and *in vitro* suppression lead to reduced tube formation and wound healing in a colorectal cell line (Nakanishi, T. et al., 2017). *SLCO2A1* is up-regulated in malignant breast cell lines, as well as having higher expression in malignant compared to non-

malignant tissue in eight out of thirteen breast cancer samples (Wlcek et al., 2008). This suggests that targeting the PGT may not be as beneficial in breast cancer.

1.4 15-hydroxyprostaglandin dehydrogenase

15-hydroxyprostaglandin (15-PGDH) dehydrogenase is a key enzyme in prostaglandin and lipoxin metabolism. 15-PGDH is encoded by the *HPGD* gene which is located at chromosome 4q34-35. There are six *HPGD* reference sequence transcript variants (Figure 1.5), yet transcript 1 is the only transcript containing all seven exons and therefore producing functional 15-PGDH protein.

15-PGDH is an NAD+ dependent oxidoreductase, and catalyses reversible oxidation of the 15(S)-hydroxyl group, forming a 15-keto metabolite (Ensor and Tai, 1995). The 15-keto metabolite exhibits significantly reduced biological activity and can be further metabolised by 15-keto-prostaglandin-Δ(13)-reductase (Tai et al., 2002). 15-PGDH has affinity for PGE_2, $PGF_{2\alpha}$, and PGI_2 in the µM range, whereas its affinity for PGD_2 is significantly lower (Tai et al., 2002). Additionally, PGD_2 and TXA_2 can undergo non-enzymatic degradation (Schuligoi et al., 2007).

Loss of 15-PGDH activity has been found to cause the rare, recessively inherited disorder primary hypertrophic osteoarthrophy (PHO) (MIM: 259100), resulting in thickening of the skin, excessive bone formation and digital clubbing (Uppal et al., 2008). Patients with PHO show increased levels of PGE_2 and reduced levels of its breakdown product, PGE-M (Uppal et al., 2008). Genetic disruption of 15-PGDH expression in mice also blocked production of the urinary PGE_2 metabolite, PGE-M (Backlund et al., 2005).

Furthermore, single nucleotide polymorphisms (SNPs) in *HPGD* have been associated with cancer progression (Thompson et al., 2013; He, N. et al., 2014). A SNP in the 3' untranslated region of *HPGD* (rs8752) has been associated with increased risk of prostate cancer in Chinese patients (Qi et al., 2017). The same SNP is associated with a miR-485-5p binding site, and has been linked to increased risk of breast cancer (He, N. et al., 2014). Furthermore, a second SNP (rs2555639) has been linked to increased risk of colon cancer and decreased 15-PGDH expression (Thompson et al., 2013). Despite this no increased incidence of cancer has been noted in 15-PGDH null patients, indicating that loss of 15-PGDH alone is insufficient to cause cancer (Uppal et al., 2008).

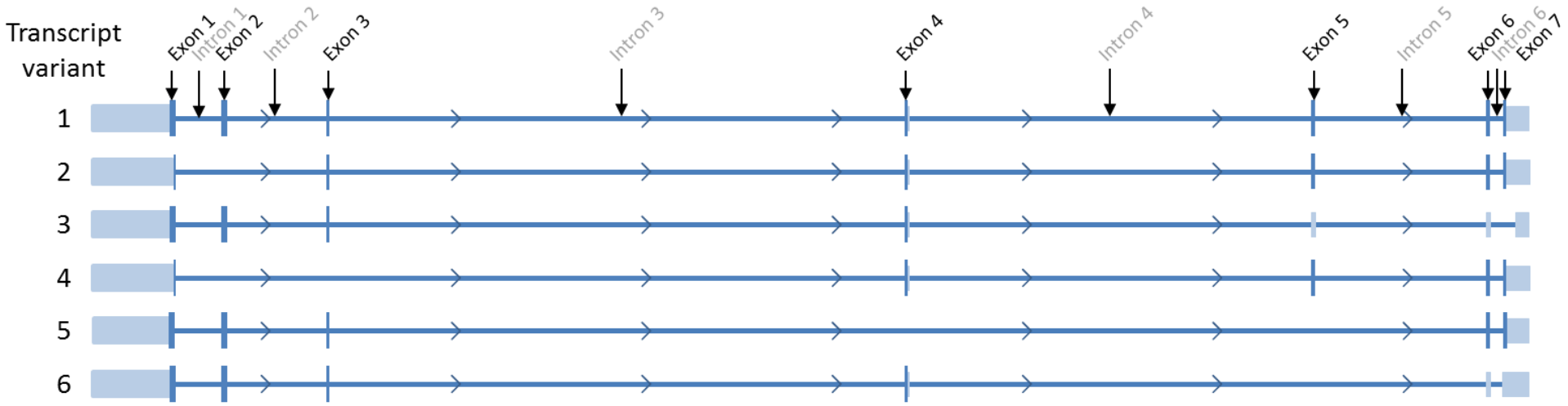

Figure 1.5 *HPGD* transcript variants. Dark blue = coding, pale blue = non-coding. Transcript 1 is the only transcript encoding functional 15-PGDH.

1.4.1 15-PGDH and cancer

Compared to COX2 little research has been published on 15-PGDH effect on cancer and on breast cancer in particular. The majority of the research suggests 15-PGDH has tumour suppressor activity, yet there are a few studies which suggest the contrary, emphasising that further research into 15-PGDH's function in breast cancer progression is required.

15-PGDH is ubiquitously expressed in mammalian tissues (Tai et al., 2002), but this is not always the case in cancer. Decreased 15-PGDH protein and mRNA levels were observed in malignant tissue in cancers including breast, gastric, colon, bladder, and lung cancer (Wolf et al., 2006; Liu, Z. et al., 2008; Seo, S.H. et al., 2015; Backlund et al., 2005; Li, Y. et al., 2014; Thiel et al., 2009; Tseng-Rogenski et al., 2010). Furthermore, *in silico* bioinformatics highlighted *HPGD* transcript levels were high in normal breast tissue, intermediate in luminal A and B subtypes of breast cancer and low in basal and HER2 positive breast cancer (Kochel et al., 2016). Decreased 15-PGDH expression in tumours may result in elevated PGE_2 in the tumour's microenvironment and thus increased PGE_2 signalling. As transcript levels do not directly translate to protein expression it would be interesting to see whether these observations are true at the protein level in breast cancer.

Despite the low expression of 15-PGDH reported above, 15-PGDH protein expression is up-regulated in the apocrine breast cancers (Celis et al., 2008). It has also been noted that increased 15-PGDH expression has been reported in malignant tissue compared to normal tissue (Thill et al., 2010a), although a small sample size was assessed which may have included more apocrine samples. Furthermore, the same group reported elevated levels of COX2 and 15-PGDH protein in ovarian cancer (Thill et al., 2010b). Although there is no overall consensus, these studies suggest 15-PGDH is generally reduced in most breast cancers, which could lead to increased levels of PGE_2 in the local microenvironment and contribute to cancer development and progression through changing a variety of cell behaviours.

Several studies have assessed the effect of 15-PGDH expression in cancer cell lines, with little focus on breast cancer. Increased 15-PGDH activity following treatment with NSAIDs led to significantly decreased proliferation both *in vitro* and *in vivo* in human medullary thyroid carcinoma (Quidville et al., 2006). The study also reported that 15-PGDH siRNA knock-down increased proliferation of a human medullary thyroid carcinoma cell line (Quidville et al., 2006). Additionally, siRNA or shRNA knock-down of 15-PGDH also increased colony formation in bladder and stomach carcinoma cell lines (Tseng-Rogenski et al., 2010; Thiel et al., 2009). Over-

expression of 15-PGDH in the MDA-MB-231 breast cell line resulted in significantly reduced colony formation and decreased colony size (Wolf et al., 2006). Similarly, adenoviral mediated over-expression decreased colony formation in both breast and colorectal cell lines (Kaliberova et al., 2009). Furthermore, down-regulation of 15-PGDH in the MCF7 cell line led to increased colony formation (Wolf et al., 2006). Over-expression of 15-PGDH *in vivo* in breast and colorectal xenographs has also been proven to delay tumour growth (Kaliberova et al., 2009; Yan et al., 2004; Wolf et al., 2006). Similarly, 15-PGDH knock-out induced a 7.6-fold increase in colon tumours and increased tumour growth in breast xenographs (Hahm et al., 2002; Wolf et al., 2006). These results indicate a strong link between 15-PGDH and cancer proliferation, but further attention to its role in breast cancer would be beneficial.

Little research has assessed the effect if 15-PGDH expression on apoptosis, but an increased number of apoptotic cells were reported in gastric cancer cells over-expressing 15-PGDH, alongside decreased expression of anti-apoptotic genes (Lou et al., 2012). Tai et al. also reported induced apoptosis in the A549 lung cell line following 15-PGDH over-expression, yet the data was not shown (Tai et al., 2007).

Increased 15-PGDH expression inhibited migration of HUVEC and colorectal cell lines (Kaliberova et al., 2009; Li, M. et al., 2008). Over-expression of 15-PGDH using a viral system enhanced the anti-tumour immune response and thus reduced development of pulmonary metastases in BALB/c mice with 4T1 tumours (Walker et al., 2011). Down-regulation of 15-PGDH expression also increased motility of bladder cancer cell lines (Tseng-Rogenski et al., 2010). On the other hand, a 15-PGDH over-expressing A549 lung carcinoma mouse xenograph induced EMT (Tai et al., 2007). Furthermore, increased migration was observed with the MDA-MB-231 breast cell line with increased 15-PGDH expression by Lehtinen *et al.* (Lehtinen et al., 2012), but the cell line was subjected to extensive *in vitro* culture leading to the increased 15-PGDH expression, therefore it is not clear whether the link is causative or associative.

Increased 15-PGDH expression in colorectal cell lines decreased the capacity of the cells to produce matrix metalloproteinase-2 and thus were less able to break down the Matrigel barrier, showing reduced invasion (Li, M. et al., 2008). Additionally, research into the effect of 15-PGDH expression on angiogenesis has shown that increased expression leads to decreased micro-vessel density in non-small-cell lung carcinoma (NSCLC) both *in vitro* and *in vivo* (Li, Y. et al., 2014; Huang, G. et al., 2008). No known data has been reported on whether 15-PGDH influences breast cancer invasion or angiogenesis.

Early loss of 15-PGDH expression has been reported in colon, gastric and bladder cancer (Myung et al., 2006; Park et al., 2018; Tseng-Rogenski et al., 2010), indicating that targeting 15-PGDH may improve patient prognosis. To date the loss of 15-PGDH in early breast cancer has not been assessed. Nevertheless, *HPGD* mRNA levels act as an independent predictor of breast cancer patient outcome with prolonged survival and increased levels are linked to improved relapse-free survival (Kochel et al., 2016). Equally, down-regulation of *HPGD* has been linked to poor over-all survival in gastric cancer and NSCLC (Seo, S.H. et al., 2015; Li, Y. et al., 2014).

Few studies have assessed the role of 15-PGDH expression in breast cancer progression, with the majority of research targeting lung and gastrointestinal cancer. Inadequate data on the effect of 15-PGDH expression on proliferation, migration, invasion and angiogenesis in breast cancer, and the limitations associated with the current studies suggests that further research is required to confirm these mechanisms in breast cancer.

1.4.2 15-PGDH regulation

There is current interest in understanding the regulation of 15-PGDH, not only how it is dysregulated during carcinogenesis, but also how it could be up-regulated as a potential therapeutic approach to help reduce PGE_2 production and signalling. The expression of 15-PGDH in various cancer types has been well examined, yet little research has aimed to assess the regulation of 15-PGDH expression. Evidence suggests that regulation of 15-PGDH may be a complex integration of several processes. A summary has been made below to assess proposed methods regarding the regulation of 15-PGDH expression.

1.4.2.1 Transcription factor regulation

Several transcription factors have been implicated in the transcriptional activation or repression of the *HPGD* gene through binding to regulation elements in its promoter. Binding sites for the E26 transformation-specific (Ets) family, activating protein-1 (AP-1) and cAMP-responsive element-binding proteins (CREB1 and CREB2) have been reported in the distal promoter element (Nandy et al., 2003). Conversely, Ets and AP-1 binding sequences have been identified in the proximal promoter region (summarised in Figure 1.6) (Nandy et al., 2003). The 15-PGDH promoter is induced by phorbol 12-myristate 13-acetate which activates AP-1 dependent transcription, and is in turn reversed by the co-expression of A-Fos which inhibits AP-1 (Greenland et al., 2000).

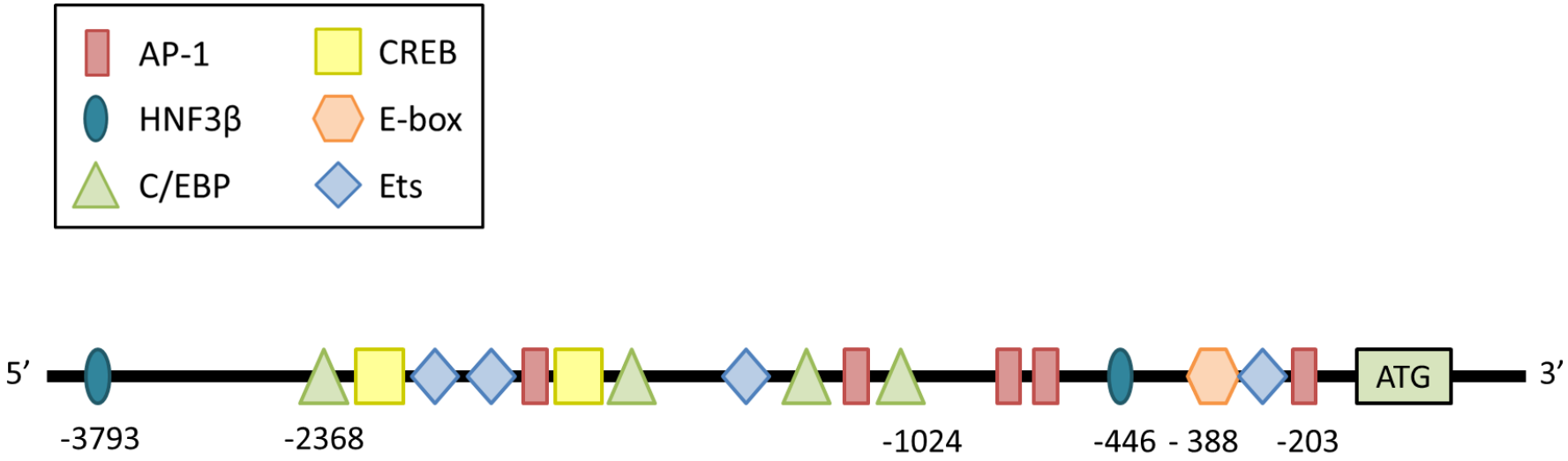

Figure 1.6 Known transcription binding sites in the *HPGD* gene promoter. Adapted from the literature (Na et al., 2011; Huang, G. et al., 2008)

The transcription factors Snail, Slug and Zeb bind to the E-box elements (Mann, J.R. et al., 2006). The interaction of Snail alongside histone deacetylase (HDAC) 2 and Slug but not Zeb1 has been found to repress 15-PGDH expression by binding to the 15-PGDH promoter in colon and NSCLC cells (Backlund et al., 2008; Yang, L. et al., 2007). Additionally, Snail and Slug are induced by EGFR signalling and epidermal growth factor (EGF) requires Snail and HDACs to repress 15-PGDH expression in colon cancer (Mann, J.R. et al., 2006). Exogenous EGF down-regulated 15-PGDH expression and enzyme activity in colorectal cell lines, while EGFR-specific tyrosine kinase inhibitor erlotinib, increased 15-PGDH expression by inhibiting EGFR activity (Backlund et al., 2005). Ultraviolet radiation also caused dose dependent suppression of 15-PGDH expression in human skin cells through induction of slug expression and silencing of slug blocked this down-regulation (Judson et al., 2010). This shows that there is an interplay between the expression of Slug and Snail as well as EGF/EGFR in the regulation of 15-PGDH.

Expression of the hepatocyte nuclear factor 3β (HNF3β) transcription factor induced 15-PGDH expression in lung cancer cells with HNF3β found to bind at two sites within the *HPGD* promoter (Huang, G. et al., 2008). Also implicating HNF3β in regulation of *HPGD* transcription, however this link has not been studied in breast cancer.

All together this data suggests that as part of its normal function *HPGD* expression is modulated by changes in the activity of a number of transcription factors. Targeting these transcription factors as a means to over-express 15-PGDH could prove a useful tool in cancer treatment. As none of these studies were performed with breast cell lines it would be beneficial to see whether these transcription factors also regulate 15-PGDH expression in the breast and whether they are dysregulated in breast cancer.

1.4.2.2 Reciprocal regulation of COX2 and 15-PGDH expression

Reciprocal regulation of COX2 and 15-PGDH has been reported in the A549 lung adenoma cell line (Tong et al., 2006b). Synergistic up-regulation of COX2 with pro-inflammatory cytokines interleukin β (IL-β) or tumour necrosis factor-α (TNF-α) in combination with phorbol 12-myristate 13-acetate treatment lead to down-regulation of 15-PGDH protein expression (Tong et al., 2006b). Adenoviral over-expression of COX2 but not COX1 also decreased 15-PGDH expression, emphasising the specificity of COX2 (Tong et al., 2006b). Similarly, gastric cancer cells over expressing COX2 showed decreased 15-PGDH expression and a negative correlation between 15-PGDH and COX2 was observed in gastric cancer tissue (Liu, Z. et al., 2008), but in this study the effect of 15-PGDH over-expression was not assessed.

This data indicates that 15-PGDH is down-regulated in COX2-driven lung and potentially gastric cancer, but no known link between COX2 and 15-PGDH expression has been reported in breast cancer.

1.4.2.3 Hypoxia link to expression

Certain stimuli have been shown to alter 15-PGDH expression in the tumour microenvironment including pro-inflammatory cytokines. Young et al. have shown that 15-PGDH protein levels can vary within a tumour with higher 15-PGDH in the centre of colorectal cancer liver metastases (CRCLM) than the periphery (Young et al., 2013). They also showed that this variation in expression may be due to hypoxia and using the human colon adenocarcinoma cell line HCA-7, showed that hypoxia induced 15-PGDH expression is reversible (Young et al., 2013). Furthermore, the group have shown that the activity of 15-PGDH was reduced in the centre of the CRCLM due to the hypoxic conditions limiting the availability of its cofactor NAD+ (Young et al., 2013).

The core of most solid tumours are hypoxic as a result of poor vascularisation with hypoxic gene signatures associated with poor prognosis in breast cancer, but these signatures vary greatly when comparing *in vitro* and *in vivo* data (Abu-Jamous et al., 2017). Given the interplay between hypoxia, 15-PGDH expression and prognosis in colorectal cancer (Young et al., 2013) it would be interesting to see whether this is also the case in breast cancer.

1.4.2.4 MicroRNA regulation

MicroRNAs (miRNAs) are non-coding RNA that bind mRNA leading to inhibition of translation and/or targeting mRNA for degradation (Huang, X. et al., 2015). Decreased expression of 15-PGDH has been linked to expression of several miRNA's.

The *HPGD* gene has been identified as a target for microRNA miR-620 and treatment with miR-620 compared to a mimic decreased 15-PGDH protein expression in the MDA-MB-231 breast and DU-145 prostate cancer cell lines (Huang, X. et al., 2015). miR-21 also targets the *HPGD* gene with over-expression of miR-21 shown to decrease levels of *HPGD* mRNA and thus protein levels in cholangiocarcinoma and gastric cells (Lu et al., 2014; Park et al., 2018). Interestingly, over-expression of COX2 and PGE_2 treatment also increased miR-21 expression in cholangiocarcinoma cells (Lu et al., 2014). Likewise, miR-21 inhibited the activity of 15-PGDH alongside miR-155 in breast cancer cells (Nikiforova et al., 2015), with both blocking 15-PGDH expression.

Together this shows that 15-PGDH expression is altered post-transcriptionally by means of mRNA degradation or translation inhibition. This alternative approach to 15-PGDH regulation warrants further investigation as a possible cancer treatment.

1.4.2.5 Epigenetic mechanisms

The role of epigenetic modifications in regulation of gene expression has received increasing levels of attention as a possible treatment for a range of cancers. Interestingly, epigenetic modifications can be both inherited and transient. These epigenetic changes may alter gene expression without changing the DNA sequence. Such epigenetic modifications include DNA methylation, histone modification, nucleosome remodelling and RNA mediated targeting (Dawson and Kouzarides, 2012).

1.4.2.5.1 DNA methylation

DNA methylation involves the addition of a methyl group to the fifth carbon of a cytosine residue to produce 5-methylcytosine, this usually occurs at cytosine-phosphate-guanine (CpG) dinucleotides and is catalysed by the DNA methyltransferase (DNMT) enzyme (Huang, T.H. et al., 1999). Around 70-80% of CpG sites within the human genome are methylated (Li, E. and Zhang, 2014). Methylation, particularly at gene promoters can inhibit transcription factor binding or result in recruitment of methyl-binding proteins which alter the chromatin structure (Auclair and Weber, 2012). DNA methylation is therefore often associated with decreased gene expression, including tumour suppressor genes.

Silencing of genes through methylation has led to the development of hypomethylating drugs such as azacitidine and 5-aza-2'-deoxycytidine. These drugs are analogues of the nucleotide cytidine, in which the carbon atom at position 5 in the pyrimidine ring has been replaced by a nitrogen atom as shown in Figure 1.7 (Diesch et al., 2016). While the presence of the nitrogen atom does not affect the analogues base pairing, it does mean that they cannot be methylated by DMNT. These drugs have been approved for treatment of myelodysplastic syndrome (MDS) and acute myeloid leukaemia (AML) (Malik and Cashen, 2014; Quintas-Cardama et al., 2010; Kaminskas et al., 2005; Saba, 2007).

5-aza-2'-deoxycytidine (AZA) also known as decitabine is converted into decitabine triphosphate, a deoxyribonucleotide, which can be incorporated into DNA in the place of cytosine.

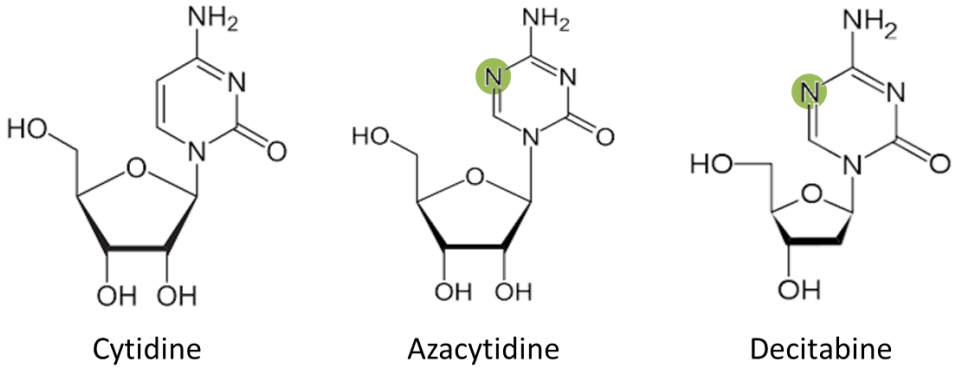

Figure 1.7 Chemical structure of cytidine (A), azacitidine (B) and decitabine (C). Figure adapted from Diesch et al. 2016 (Diesch et al., 2016). The 5th carbon atom has been replaced by a nitrogen atom in the pyrimidine ring (highlighted in green).

When DMNT1 attempts to methylate decitabine triphosphate it forms an irreversible complex which has to be removed by the host DNA repair machinery, resulting in a loss of methylation (Derissen et al., 2013). Through demethylation of CpG islands in gene promoter regions, demethylating agents can reactivate silenced genes (Figure 1.8). For instance treatment of the MDA-MB-231 cell line with decitabine increased *HPGD* mRNA expression (Wolf et al., 2006). Moreover, increased *HPGD* mRNA expression was observed with decitabine treatment in gastric carcinoma cell lines (Thiel et al., 2009), further implicating DNA methylation in 15-PGDH regulation.

1.4.2.5.2 Histone acetylation

In a cell, DNA is compacted into the chromatin through a complex organisational process which can either make a region of DNA accessible or inaccessible to the transcriptional machinery. The majority of DNA is wrapped around eight core histones to form nucleosomes which are further condensed to form closed chromatin. Chromatin is a highly dynamic complex and its structure around a gene can be rapidly modified through a wide range of mechanisms to change the accessibility of a gene's DNA to proteins, such as transcription factors and RNA polymerase II, altering its rate of transcription.

The lysine residues of the N-terminal tail of a histone core can be acetylated or de-acetylated by enzymes called histone transacetylases (HATs). Acetylation removes the positive charge of the histone reducing the strength of the interaction with negatively charged DNA (Lee, J. and Huang, 2013). This results in chromatin relaxation, increasing the access for transcription factors and RNA polymerase, leading to increased transcription (Figure **1.9**) (Lee, J. and Huang, 2013). Histone deacetylases (HDACs) on the other hand remove the acetyl groups and allow the histones to bind DNA more strongly (Lee, J. and Huang, 2013). Consequently the balance between HATs and HDACs determine the extent of chromatin relaxation and thus regulation of gene transcription.

As histone acetylation can regulate gene expression, it is not surprising that this has been exploited as mechanism of gene regulation via the use of HDAC inhibitors. Consequently, HDAC inhibitors have been identified as potential anti-cancer treatments through reactivation of silenced tumour suppressor genes (Quintas-Cardama et al., 2011) (Figure **1.9**).

There are three different classes of HDAC enzymes consisting of 18 different HDAC genes.

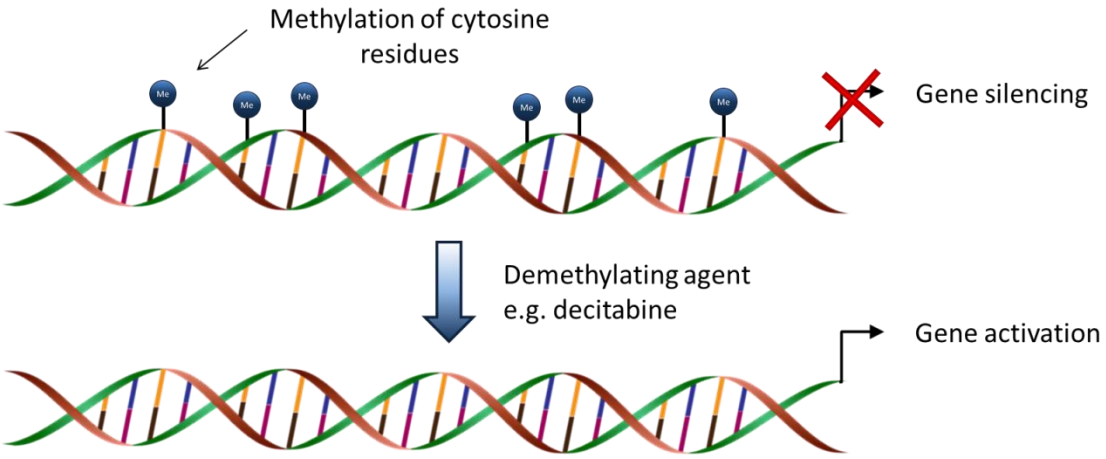

Figure 1.8 Mechanism of decitabine. Adapted from (Quintas-Cardama et al., 2010). Decitabine is converted into decitabine triphosphate which is incorporated into the DNA in place of cytosine. As a result DNMT1 can no longer methylate the DNA and methylation is lost.

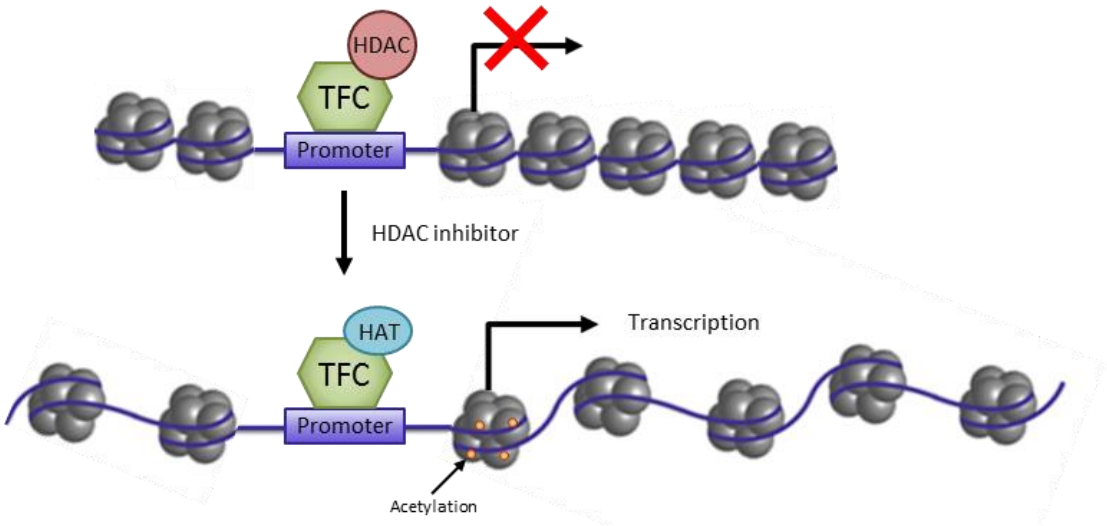

Figure 1.9 HDAC inhibitor mechanism. Adapted from (Marks and Dokmanovic, 2005). HDAC = histone deacetylase inhibitor, TFC = transcription factor complex, HAT = histone acetyltransferase. HDAC inhibition enables HATs to acetylate histones, relaxing the DNA and enabling transcription.

Suberoylanilide hydroxamic acid (SAHA), also known as vorinostat, is a broad range HDAC inhibitor that inhibits both class I (HDAC1, 2, 3, 6 and 8) and class II HDACs but not class III by binding the enzymes active site (Finnin et al., 1999) (Finnin et al., 1999; Marks and Dokmanovic, 2005; Newbold et al., 2013). Along with romidepsin, it has been approved in the treatment of T-cell lymphoma (Mann, B.S. et al., 2007; VanderMolen et al., 2011).

Increased *HPGD* mRNA expression has been noted in the breast cell line MDA-MB-231 after vorinostat treatment (Wolf et al., 2006), with similar observations in colorectal cell lines with HDAC inhibitors sodium butyrate and valproic acid (Backlund et al., 2008). Treatment of A549 and H1435 lung adenocarcinoma cell lines with sodium butyrate also showed an increase in 15-PGDH expression in a time and concentration dependent manner (Tong et al., 2006a).

Epigenetic gene regulation as a cancer treatment in general, is a relatively new concept, therefore little is known about the specificity and downstream effects of epigenetic drug treatment. Research suggests that modifying DNA methylation and histone acetylation may modify 15-PGDH expression *in vitro*, but limited research has addressed whether these drugs act directly at the *HPGD* gene locus. Epigenetic drugs have been clinically approved for the treatment of hematological malignancies (Lee, H.Z. et al., 2015; Mann, B.S. et al., 2007; Kaminskas et al., 2005; Malik and Cashen, 2014), therefore if 15-PGDH expression is epigenetically regulated, treatment with these drugs may also improve patient outcome in breast cancer.

1.5 Summary

Breast cancer was the fourth most common cause of cancer related deaths in the UK in 2016 (Cancer Research UK, 2016), consequently there is demand for new and improved treatments. The objective of this project is to assess the role of 15-PGDH in breast cancer, with the potential of exploiting 15-PGDH expression as a therapeutic option in the future.

Growing evidence shows that components of the prostaglandin pathway play a part in carcinogenesis. Adverse side effects resulting from a knock-on effect of COX inhibition has led to research into other components of the pathway as an alternative treatment approach. As 15-PGDH is the key enzyme in prostaglandin metabolism and the final step in the pathway, it may result in fewer adverse effects with comparable anti-carcinogenic effects.

In order to utilise 15-PGDH expression as a treatment in breast cancer it is important to elucidate the mechanisms involved in its regulation. Current research shows that a variety of mechanisms may alter 15-PGDH expression, including epigenetics. Furthermore, there is strong evidence that 15-PGDH expression is down-regulated in colorectal cancer and its expression is advantageous in patient prognosis. As less research has been completed with 15-PGDH in breast cancer, this study aims to assess the role of epigenetics in regulation of 15-PGDH expression and to study the effect of its over-expression in breast cancer.

1.6 Project aims

In summary, the main aims of the project are to complete the following;

- Assess the expression of 15-PGDH in breast cancer
- Determine how 15-PGDH expression is regulated in breast cancer
- Investigate the functional effects of 15-PGDH over-expression in breast cancer.

Chapter 2 Material and Methods

2.1 Cell culture

All cell lines were obtained in-house and authenticated via STR profiling completed by the CRUK genomics facility, University of Leeds (Table 2.1). Opened media was stored at 4°C for up to four weeks. Cells were passaged at 70-80% confluency and incubated at 37°C in 5% CO_2 (v/v) air. Cells were grown until passage 10-12 and discarded. The foetal calf serum (FCS) (Sigma) was heat inactivated by heating to 56°C for 30 minutes. Cells were regularly mycoplasma tested in-house. All cells were adherent except for the THP-1 cell line.

Table 2.1. Cell line culture media information. All media and supplements purchased from Gibco unless stated otherwise. Epidermal growth factor (EGF) (Peprotech), hydrocortisone (Sigma), insulin (Sigma) and cholera toxin (Sigma). DMEM = Dulbecco's Modified Eagle Medium. RPMI = Roswell Park Memorial Institute. BC = breast cancer.

Cell line	Origin	Cell type	Non-malignant/ malignant	BC Subtype	Culture media
A549	Lung	Epithelial	Malignant	N/A	DMEM GlutaMAX™10% FCS
CaCo-2	Colon	Epithelial	Malignant	N/A	DMEM GlutaMAX™10% FCS
HB2	Breast	Epithelial	Non-malignant	Unclassified	RPMI GlutaMAX™10% FCS
LoVo	Colon	Epithelial	Malignant	N/A	F12 nutrient mix GlutaMAX™ 10% FCS
MCF7	Breast	Epithelial	Malignant	Luminal A	DMEM GlutaMAX™10% FCS
MCF10A	Breast	Epithelial	Non-malignant	Basal	DMEM GlutaMAX™/F12 5% horse serum, EGF 20ng/ml, hydrocortisone 0.5 mg/ml, insulin 10µg/ml, cholera toxin 100ng/ml
MDA-MB-231	Breast	Epithelial	Malignant	Basal	DMEM GlutaMAX™ 10% FCS
MDA-MB-453	Breast	Epithelial	Malignant	Unclassified	RPMI GlutaMAX™ 5% FCS
SKRB3	Breast	Epithelial	Malignant	HER2	DMEM GlutaMAX™ 10% FCS
T47D	Breast	Epithelial	Malignant	Luminal A	DMEM GlutaMAX™ 10% FCS
THP-1	Blood	Monocyte	Malignant	N/A	RPMI GlutaMAX™5% FCS

2.1.1 Cell line passage

Adherent cells were grown in T75 vented cap cell culture flasks (Corning) until 70-80% confluent before passaging at a ratio of 1:6 (1:10 for the A549 cell line) twice a week. During passaging the cells were washed with Dulbecco's Phosphate-Buffered Saline (DPBS) (Gibco) and incubated

with 1x trypsin (Gibco) at room temperature for 3-5 minutes. The trypsin was inhibited by the addition of culture media and the cell suspension centrifuged for 5 minutes at 400 x g. The supernatant was discarded and the cell pellet resuspended in the appropriate amount of media.

Suspension cells were grown in T75 vented cap cell culture flasks and stored upright to increase cellular contact. The cells were grown until approximately 80% confluent by eye. The cells were then centrifuged and the pellet resuspended as described above.

2.1.2 Cell line cryopreservation

Frozen stocks of each cell line were prepared at the earliest possible time. Adherent cells were trypsinised and pelleted as described in Section 2.1.1 from a confluent T75 flask. The pellet was resuspended in culture media supplemented with additional FBS to a final of 20% FCS and 10% filter sterilised dimethyl sulphoxide (DMSO) (Sigma). Four cryovials (Nunc brand) per T75 flask were prepared with 1 ml of cell suspension per vial. The cells were slowly frozen overnight at −80°C before transferring the stocks to liquid nitrogen for long term storage.

2.1.3 Cell line resurrection

One cryovial of cells was resurrected into a T25 flask (Corning). Briefly, the cryovial was quickly thawed at 37°C and the cell suspension mixed with 10 ml of culture media. The cells were then pelleted and resuspended in culture media as described previously to remove the DMSO. The cells were then grown in a T25 flask overnight with the media changed the following day.

2.1.4 Polarisation of THP-1 cell line

THP-1 cells were grown in a T75 flask until ~80% confluent in 10 ml media. Half of the cell suspension was pelleted by centrifuging the cells at 400 x g for 5 minutes. The supernatant was discarded and the cells resuspended in 4 ml media supplemented with 5 ng/ml phorbol 12-myristate 13-acetate (PMA) (Sigma-Aldrich). 2 ml of cell suspension was plated per well of a 6 well plate and the cells left overnight to adhere. The supplemented media was removed and replaced with non-supplemented media for 72 hours.

The THP-1 cells were polarised to form M1 macrophages using media supplemented with 250 ng/ml lipopolysaccharide (LPS) (Peprotech) and 30 ng/ml interferon gamma (IFNγ) (Peprotech). M2 macrophages were produced from polarisation of the THP-1 cells using media supplemented with 30 ng/ml interleukin 4 (IL-4) (R&D Systems). The cells were incubated with the indicated supplements for 48 hours before RNA extraction.

2.1.5 Cell line epigenetic drug treatment

Epigenetic silencing of *HPGD* was investigated using DNMT inhibitor decitabine (Sigma) and histone deacetylase (HDAC) inhibitor vorinostat (Sigma). Decitabine and vorinostat were dissolved in DMSO to a 20 mM stock and stored in aliquots at −80°C. Cells were seeded at $5x10^4$ cells per well in a 6 well plate (Corning), and allowed to adhere overnight. For immunocytochemistry (ICC) the cells were seeded onto 70% ethanol sterilised glass coverslips. Cells were treated with 0.1% DMSO vehicle control, 1 µM vorinostat and/or 5 µM decitabine in 0.1% DMSO for 72 hours. Due to poor stability of both decitabine and vorinostat, cells were washed in media and the drug replaced each day. Cells were then harvested for DNA/RNA extraction or fixed for ICC with 4% paraformaldehyde (see Section 2.5.5 for more details).

2.1.6 Determining cell viability/metabolic activity using the MTS assay

Cell viability/mitochondrial metabolic activity was assessed using the CellTiter 96 AQueous One Solution Assay kit (Promega) according to manufacturer's instructions. The colorimetric reaction is outlined below with the quantity of formazan produced directly proportional to the number of active cells in culture:

MTS + NADH --> Formazan (Red)

20 µl of CellTiter 96 AQueous One Solution Reagent was added to 100 µl media in each well of a 96 well plate following the treatment time stated in the text (typically 24-72 hours). The samples were then incubated for 4 hours and the absorbance read at 490 nm using a Berthold Mithras LB 940 plate reader. As a small amount of spontaneous 490 nm absorption occurs in culture medium, the background absorbance from a media only control was deducted from the absorbance readings. The results were normalised to the DMSO or cell only control where appropriate.

2.1.7 Scratch wound assay

To assess the role of 15-PGDH in breast cancer, the ability of stable transfected clones to migrate was assessed using a scratch wound assay. The assay involves creating a wound in a cell monolayer and monitoring the wound closure. This assay is dependent upon cell proliferation as well as migration, therefore the 15-PGDH over-expressing clones were matched to control clones according to their proliferation rate in order to focus on the cells ability to migrate.

The cells were seeded at $2.25x10^4$ cells per well in a Corning 96-well plate in 10% or 1% FCS and allowed to adhere for 24 hours (approximately 90% confluent). The Essen IncuCyte WoundMaker was soaked in 45ml sterile water for 5 minutes followed by 70% ethanol for 5 minutes to sterilise the pins before being used to make a uniform 700-800 µm scratch wound in the cell monolayer. To do this the plate (with 100 µl media) was placed in the WoundMaker and the lid removed, the WoundMaker was carefully lowered into the 96 well plate and the lever gently depressed. Without releasing the lever the WoundMaker was removed and the plate lid replaced. The WoundMaker was cleaned in 45 ml 0.5% Alconox, 1% Virkon, sterile distilled water and 70% ethanol for 5 minutes each in turn. The cells were gently washed twice in 100 µl media and media containing 400 µg/ml G418 (Gibco) and the appropriate treatment were added to the plate. The plate was then placed in the Essen IncuCyte Zoom live cell imaging microscope. One or two wide images were taken per well every hour for 72 hours at x10 objective. The IncuCyte software was programmed to recognise the shape of the MCF7 cells and then determine the wound width and wound confluency over time.

2.1.8 Transwell invasion assays

A transwell invasion assay was performed with the MCF7 15-PGDH stable over-expressing and matched control clones to determine the effect of 15-PGDH expression on invasion. Transwell inserts with a Matrigel coating and 8 µm pore with Corning 24-well plates (Cat no. 354480) were selected to use alongside uncoated control inserts (Cat no. 354578). In order to pass through the pores of the transwell inserts the cells have to digest and invade the Matrigel coating. This process mimics *in vivo* invasion of tumour cells into healthy tissue. The control inserts act as a reference point for cell migration and the number of migrating cells is deducted from the final cell count.

Firstly, the cells were grown to 80% confluency prior to the assay. The Matrigel coated transwell inserts were then thawed at room temperature and 500 µl of serum-free DMEM was added to both the insert and the well for 2 hours and incubated at 37°C in 5% CO_2 (v/v) air to rehydrate the Matrigel inserts. DMEM with 10% FCS with or without 50 ng/ml EGF was added to the well (750 µl) to act as a chemoattractant and encourage the MCF7 clones to infiltrate the Matrigel and reach the serum rich media. The transwell insert was carefully lowered into the plate to ensure there were no air bubbles between the DMEM with 10% FCS and the membrane and $5x10^4$ cells in 500 µl was added to the insert and incubated at 37°C in 5% CO_2 (v/v) air for 48 hours to allow invasion. Control wells with no chemoattractant (DMEM with 1% FCS) with Matrigel inserts were used as well as control inserts (Figure 2.1).

At the end of the invasion assay, the media was removed from the cells and those remaining on the top of the insert were gently scraped away with a cotton swab. The cells that had successfully invaded the Matrigel and passed through the pores were fixed and stained using crystal violet working solution (150 ml methanol, 60 ml ethanol, 90 ml water, 90 ml 1% crystal violet solution). The transwell insert was submerged in crystal violet working solution for 1 minute and rinsed twice in distilled water before allowing to air-dry.

The membrane was carefully removed from the plastic insert using a scalpel and placed onto a drop of immersion oil on a slide. A drop of immersion oil was placed on top of the membrane and a coverslip carefully lowered on top to avoid air bubbles. Four images were then taken of the membrane at random locations using the Nikon Eclipse 1000 microscope camera at x10 objective. The number of invasive cells were counted and the percent invasion and invasion index calculated using the formulas below:

$$Percent\ invasion = \frac{\text{Mean \# of cells invading through Matrigel insert membrane}}{\text{Mean \# of cells invading through control insert membrane}} \text{x}100$$

$$Invasion\ index = \frac{\text{\% Invasion Test Cell}}{\text{\% Invasion Control Cell}}$$

2.1.9 Transwell migration assay

The ability of cells to migrate was assessed using the method described for transwell invasion assay, but only the data from the control cells inserts was assessed. Unlike the wound healing assay the cells had to pass through a physical barrier.

The number of migrating cells was assessed using the formula below and normalised to the control (X) clone with 1% FCS:

$$Migration = \text{Mean \# of cells migrating through control insert membrane}$$

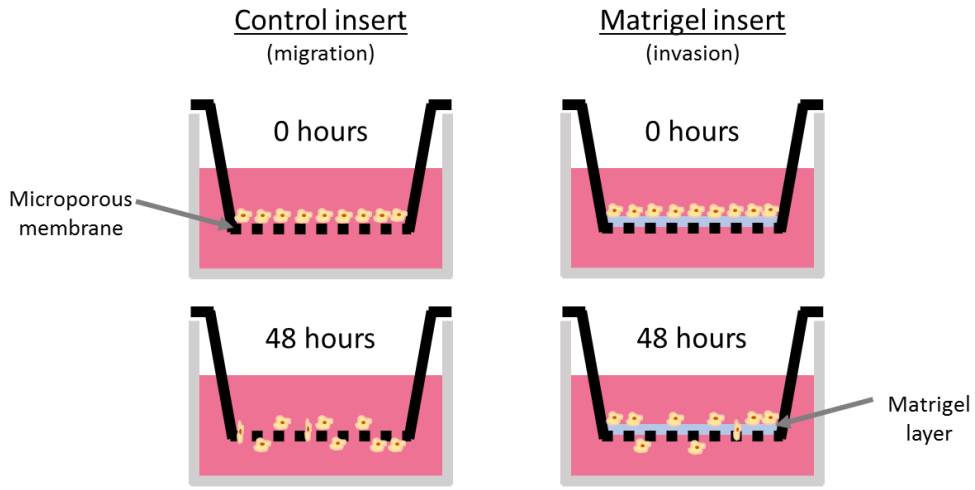

Figure 2.1 Transwell invasion assay experimental design. The invasive index of a cell is measured by the number of cells able to penetrate through the Matrigel layer in response to a chemoattractant.

2.1.10 Colony forming assays

Colony forming assays were performed to determine the ability of the stable transfected clones to form colonies from a single cell. The process mimics the formation of metastases by measuring the ability of a single cell *in vivo* to repopulate in a secondary site following migration from the primary tumour and invasion of a second tissue.

MCF7 clones were seeded at 500 cells per Corning 100 x 20 dish (55 cm^2) in 7 ml of DMEM 10% FCS and incubated for 14 days at 37°C in 5% CO_2 (v/v) air. Each experiment was performed in duplicate for each clone and each experiment repeated twice. Following the two week incubation period the media was gently removed from the cells and 2 ml of 5 mg/ml crystal violet working solution (Section 2.1.8) added to the petri dish for 1 minute to fix and stain the colonies. The solution was then removed and the plates washed twice with distilled water, before allowing the plates to air-dry. The number of colonies that had grown was recorded per treatment. Any colonies that were in contact were classed as a single colony and a 200 µm diameter minimum cut off size was used for counting.

2.1.11 Transient and stable transfections

2.1.11.1 Lipofectamine transfection

Cells were grown until 70-90% confluent in the appropriate cell culture vessel. The cell culture media was removed and replaced with fresh plating media. The amounts of the reagents used for each size of culture flask or well in a plate are shown in Table 2.2.

Table 2.2 Transfection reagent quantities

Cell culture vessel	Surface area	Plating medium	Opti-MEM	DNA	Lipofectamine 2000
24 well plate	2 cm^2	0.5 ml	2 x 50 µl	0.8 µg	2.5 µl
6 well plate	10 cm^2	2 ml	2 x 250 µl	4 µg	12.5 µl
T25 flask	25 cm^2	6 ml	2 x 625 µl	10 µg	31.25 µl
Corning 100x20 dish	55 cm^2	13 ml	2 x 1375 µl	22 µg	68.75 µl

Cells were grown until 70-90% confluent in the appropriate cell culture vessel. The cell culture media was removed and replaced with fresh plating media. For a 6 well plate 4 µg of the appropriate DNA was added to 250 µl of Opti-MEM (Gibco) and mixed using a wide bore pipette by pipetting up and down six times. 12.5 µl of lipofectamine 2000 was added to the other 250 µl Opti-MEM and mixed by pipetting up and down with a wide bore pipette. The solutions were left to stand for 5 minutes at room temperature before being mixed together by pipetting up

and down six times. The solution was left at room temperature for 20 minutes. 500 µl of the mix was then carefully pipetted drop by drop into the 6 well plate ensuring the entire of the well was covered. The plate was gently rocked back and forth ten times and incubated for 24 hours at 37°C before replacing the media or performing further experiments.

2.1.11.2 Geneticin treatment

The cytotoxic antibiotic geneticin (G418) is a neomycin sulphate analogue that functions by inhibiting protein synthesis. The gateway cloning destination vector contains a neomycin resistance gene, consequently, the cells that have successfully taken up the destination vector will be resistant to G418 treatment, while all other cells will undergo cell death.

The G418 (Gibco) concentration for stable transfected clone selection was optimised by completing a kill curve with MCF7 cells completed as follows: $8x10^4$ cells were seeded per well of a 24 well plate and allowed to adhere overnight. The following day the media was changed and G418 added at a range of 0-1000 µg/ml. Over the following 7 days, the media containing G418 was changed daily and the cells imaged at x10 objective using an Olympus CKK41 microscope with an Olympus Camedia C-7070 camera. Cell death was measured by assessing the confluency using ImageJ (Schneider et al., 2012).

The image files were opened in ImageJ and the background removed with the limitation of anything less than 15 pixels in size classed as background. The image was reformatted to an 8-bit image and the threshold level was adjusted in black and white mode. The brightness was set to 10 (light background). The dilate tool was used (settings: iterations = 2, count = 1) to fill in the gaps within the cells and the area % measured.

2.1.12 Isolation and growth of stable clones

The stable transfection protocol was performed as described in Section 2.1.11.1 in a Corning 100 x 20 dish. The cells were treated with 800 µg/ml G418 for two or more weeks, with the media changes every three to four days. Colonies of 10 or more cells were identified for isolation using a Nikon microscope. Nylon washers, sterilised in 70% ethanol were placed over the colony. Washer sizes M3 (diameter = 3.2 mm) and M4 (diameter = 4.3 mm) were selected depending upon the size of the colony and 10 or 20 µl of trypsin was added to the centre for M3 and M4 washers, respectively. The cells were incubated in the trypsin for 2-3 minutes and the cell suspension carefully transferred from the petri dish into 200 µl of media containing 800 µg/ml G418 in a 96 well plate. The clones were designated with an X followed by a number for

the control clones and H followed by a number for the 15-PGDH (or *HPGD*) over-expressing clones. They were numbered sequentially according to the order they were selected. The clones were then grown to the desired confluency, with the media replaced every 3-4 days.

When the cells were confluent in a 96 well plate they were trypsinised and transferred to a 24 well plate. When the cells reached confluency they were then transferred into a 6 well plate, then a T25 and eventually a T75 flask. Frozen stocks were created as master stocks once the cells were confluent in a T25 flask.

2.1.13 Hypoxic cell culture

Cells were seeded at $3x10^5$ cells per well of a 6 well plate and grown in standard conditions (37°C in 5% CO_2 and 20% O_2 (v/v) air) until 70-80% confluent. The cell culture media was replaced and the cells exposed to hypoxic conditions (37°C in 5% CO_2 and 5% O_2 (v/v) air) or normal conditions (control) for 24, 48 and 72 hours before harvesting RNA as described in Section 2.2.1. Each time point and treatment was performed in triplicate two times.

2.2 RNA methods

2.2.1 RNA extraction

RNA was extracted from cells to assess gene expression at a transcriptional level. RNA was extracted using TRIzol Reagent (Ambion) according to the manufacturer's instructions. RNase free pipette tips, plastic wear and Ambion nuclease-free water (Invitrogen) were used throughout the process. 1 ml of TRIzol was added per well of a 6 well plate or 7.5 ml per T75 flask and a cell scraper used to dislodge the lysed the cells, before the lysate was aliquoted into a microcentrifuge tube. 0.2ml of chloroform was added to the 1 ml TRIzol and shaken vigorously for 15 seconds. The sample was incubated at room temperature for 3 minutes and centrifuged at 12,000 x g for 15 minutes at 4°C. Two thirds of the aqueous (clear) phase was transferred to a fresh microcentrifuge tube and 0.5 ml of 100% isopropanol added to precipitate the RNA. The sample was inverted several times and incubated at room temperature for 10 minutes. The sample was then centrifuged at 12,000 x g for 10 minutes at 4°C. The majority of the supernatant was removed avoiding the pellet and 1 ml 70% ethanol in RNase free water added to wash the pellet. The sample was vortexed briefly and centrifuged at 7,600 x g for 5 minutes at 4°C. The supernatant was removed and the sample centrifuged again for 1 minute at 7,600 x g 4°C. All remaining ethanol was removed with a pipette and the pellet allowed to air-dry for 5-

10 minutes. Once the pellet became translucent it was resuspended in 12 µl of nuclease free water and stored at −80°C until required.

2.2.2 Nanodrop RNA quantification and quality assessment

The RNA was quantified and the quality assessed using the Nanodrop ND-1000 spectrophotometer (Thermo Scientific). 2 µl of RNA was loaded onto the spectrophotometer after blanking the equipment using water or the buffer used to resuspend the RNA. The absorbance at 260 nm and 280 nm was measured to determine the concentration and purity of RNA in regards to protein contamination. A ratio of 260/230 RNA was calculated to assess contamination by certain compounds e.g. TRIzol and chloroform carryover. A 260/230 ratio of ~2.0-2.2 was classed as pure RNA.

2.2.3 Qubit RNA quantification

RNA quantification was completed using the Qubit fluorometer and Qubit RNA assay kit (Thermo Fisher Scientific) when a more accurate concentration was required (e.g. RNA sequencing library preparation). When used to quantify RNA, the Qubit uses fluorescent dyes that specifically target RNA. The dye only emits light when bound to its target molecule, therefore the more RNA present the more light emitted. The fluorometer was calibrated using known standards for each set of samples. 1 µl sample RNA was added to 199 µl buffer while 10 µl of control RNA was added to 190 µl buffer. The solutions were mixed by vortexing for 2-3 seconds and incubated for 2 minutes before taking the measurement.

2.2.4 Formaldehyde gel RNA quality assessment

A formaldehyde gel was performed to confirm RNA integrity prior to cDNA synthesis. 1 µg RNA in 9 µl of RNA loading buffer (New England Biolabs) was denatured by heating to 65°C for 10 minutes. The sample was mixed by flicking and briefly centrifuged before placing on ice. All of the apparatus was soaked in 3% hydrogen peroxide (VWR) for 10 minutes and rinsed with diethyl pyrocarbonate (DPEC)-treated water to destroy and remove any residual nucleases. All consumables used were nuclease-free. A 1.3% formaldehyde agarose gel was prepared by adding 0.52 g agarose (Eurogentec) to 28.8 ml DEPC-treated water. The agarose was melted by heating the solution in a microwave and then cooled to 50°C. Next, 4 ml 10x 3-(N-morpholino)propanesulfonic acid (MOPS) buffer (Life Technologies), 7.2 ml formaldehyde (Sigma-Aldrich) and 1 µl 10 mg/ml ethidium bromide (Fisher-Scientific) were added to the solution and the volume topped up to 40 ml with DEPC-treated water. This was then poured

into a mould and allowed to set. Once the gel was set, it was submerged in the electrophoresis tank with 1x MOPS buffer and the denatured RNA samples loaded into the wells, followed by electrophoresis at 50 V for one hour. The gel was then visualised and images captured using a Bio-Rad Gel Doc (Bio-Rad). RNA was classed as being of good quality if two bands (28S and 18S ribosomal subunits) could be seen, with the 28S band approximately twice the intensity of the 18S band.

2.2.5 Agilent TapeStation RNA quality assessment

When necessary RNA quality was assessed using the Agilent 2200 TapeStation (Agilent). The TapeStation provides automated electrophoretic separation of total RNA and generates a RNA integrity number (RIN). A RIN is calculated using an algorithm that looks at the entire electropheric trace as well as the ribosomal 28S and 18S ratio in order to remove individual interpretation. A RIN of ≥8 was classed as high quality and therefore taken forward.

The broad range assay was used for RNA concentrations >25 ng/µl and the high sensitivity assay used for those with <25 ng/µl according to Nanodrop quantification. Firstly, for the broad range assay 1 µl of sample or ladder (Aligent Technologies) was added to 5 µl RNA sample buffer and vortexed for 1 minute. For the high sensitivity assay 2 µl RNA sample was added to 1 µl high sensitivity RNA sample buffer and vortexed for 1 minute. For both assays the samples were then heated to 72°C for 3 minutes to denature the RNA and placed on ice for 2 minutes before the samples were electrophoresed using the Agilent 2200 TapeStation.

2.2.6 DNase treatment

DNase treatment was completed using the Ambion DNA-free Kit (Ambion) according to manufacturer's instructions, to remove any DNA contamination in the RNA samples. The standard protocol was to DNase treat 10 µg RNA in a 50 µl reaction for 30 minutes with 1 µl DNase I at 37°C and 1x buffer and the reaction inhibited with 5 µl inactivation reagent with mixing for two minutes at room temperature. All of the samples were then centrifuged at 10,000 x g for 1.5 minutes and the supernatant recovered for cDNA synthesis or stored at −80°C until further processing.

For epigenetic drug-treated samples 144.8 ng of RNA was DNase-treated in a 9.5 µl volume due to a low RNA concentration. 0.95 µl 10x buffer and 0.55 µl DNase I was added. The sample was incubated at 37°C for 30 minutes and 2 µl of inactivation reagent added.

Stable transfection clone RNA required a vigorous DNase treatment to remove any remaining plasmid DNA. 5 µg RNA was treated in a 50 µl reaction (or otherwise scaled down). Half of the DNase enzyme was added for 30 minutes and the remaining enzyme added for an additional 30 minutes before inactivation (2 µl reagent) and collection as stated above.

2.2.7 First strand cDNA synthesis

First strand cDNA synthesis was completed using the Invitrogen SuperScript II Reverse Transcriptase kit according to manufacturer's instructions. 1 µg RNA for standard DNase-treated samples/66 ng epigenetic drug-treated samples/0.5 µg clone RNA in 10 µl final volume was added to 1 µl 10 mM dNTPs and 1 µl 500 ng/µl oligo(dT)24mer. The mix was heated to 65°C for 5 minutes and incubated on ice for 2 minutes. 4 µl of 5x first strand buffer was added, 2 µl 0.1 M DTT and 1 µl RNase OUT (RNase inhibitor) and the mix heated to 42°C for 2 minutes before addition of 1 µl of the Superscript enzyme. The sample was then heated 42°C for 50 minutes and 70°C for a further 15 minutes in a thermal cycler before storage at −20°C until required.

2.2.8 Reverse transcription polymerase chain reaction (RT-PCR) primer design

RT-PCR primers were designed using Primer3 or NCBI Primer-BLAST online software. The primers were designed to span two exons to eliminate genomic DNA amplification and where possible to meet the following criteria:

1. Primer length: 18–30 nucleotides
2. Melting temperature (Tm): 65-75°C and be within 5°C of each other
3. GC content: 40-60%, with the 3' of a primer ending in C or G to promote binding
4. Product size: 300-500 bp

Standard DNA oligonucleotides were ordered from Sigma-Aldrich. 0.0250 µM scale, desalted purification and dry primers were ordered. Once received the primers were resuspended in nuclease-free water to a 100 µM concentration.

A list of the primers used can be found in the appendix (Appendix 1, Appendix 2 and Appendix 3).

2.2.9 Standard RT-PCR

RT-PCR was performed to assess mRNA expression with a 20 µl reaction. Each reaction contained 4 µl GoTaq Green/Clear 5x Flexi buffer (Promega), 1.2 µl 25 mM $MgCl_2$ (Promega), 0.4 µl 10 mM dNTPs (Invitrogen), 0.4 µl 10 µM forward and reverse primer mix, 0.5µl cDNA, 0.3 µl Taq polymerase (made in-house), 13.2 µl distilled water (dH_2O). A master mix was prepared for multiple samples to minimise variation and limit the number of variables. A no template control (blank) and positive control was included in each run. Cycling conditions used are shown in Table 2.3 below. See appendix for annealing temperatures.

Table 2.3 Standard RT-PCR cycling conditions

Step	Temperature	Time	Number of cycles
Initial denaturation	95°C	3 minutes	x1
Denaturation	95°C	30 seconds	x35 (or otherwise stated)
Annealing	50-60°C	20 seconds	
Extension	72°C	30 seconds	
Refrigeration	4°C	Forever	x1

2.2.9.1 Hot start RT-PCR

For the primers where the in-house Taq polymerase was not suitable a hot start polymerase was used. The reaction was made up of the following reagents, 10 µl 2x HotShot Diamond PCR master mix (Client Life Science), 0.4 µl 10 µM F/R primers, 0.5 µl cDNA and 9.1 µl dH_2O. Hot start cycling conditions are shown in Table 2.4 below.

Table 2.4 Hot start RT-PCR cycling conditions

Step	Temperature	Time	Number of cycles
Initial denaturation	95°C	5 minutes	x1
Denaturation	95°C	30 seconds	x35 (or otherwise stated)
Annealing	50-60°C	20 seconds	
Extension	72°C	30 seconds	
Refrigeration	4°C	Forever	x1

2.2.9.2 Gradient RT-PCR

Gradient RT-PCR was performed to optimise new primer sets and ensure a single clean band was obtained where possible. To do this conventional RT-PCR was performed with a 6x master mix with 3 µl of positive control cDNA. RT-PCR was performed using the cycling conditions in Table 2.3, but a gradient of 50°C to 62°C across the heating block was used to determine the optimum annealing temperature. The annealing temperature generating the cleanest and strongest correct sized band was used for future experiments.

2.2.9.3 RT-PCR quantification

RT-PCR was quantified from an agarose gel using ImageLab software (Bio-Rad). The gel was performed as in Section 2.3.4 and imaged using a Bio-Rad Gel Doc. The resultant image (*.sc) file was opened in ImageLab and the lanes and bands for each sample were identified. Once these had been selected the analysis table was generated and exported into excel. The ImageLab software's Volume (Int) parameter was used to calculate the ratio between the *GAPDH* loading control and the gene of interest.

2.2.10 Quantitative RT-PCR (qRT-PCR)

mRNA expression for *HPGD* and β-actin (*ACTB* gene) (loading control) was assessed using the TaqMan expression assays. TaqMan assays were performed using primers from Qiagen (Hs01060665_g1 *ACTB* FAM-MGB and Hs00960587_m1 *HPGD* FAM-MGB). Each sample was run in triplicate with a reaction volume of 20 µl on the QuantStudio 5 Real-Time PCR System (Thermo Scientific). The sample was incubated at 50°C for 2 minutes, 95°C 10 minutes, 95°C 15 seconds, 60°C 60 seconds and cycled back to 95°C for 15 seconds for 40 cycles. Data was analysed using the QuantStudio Design & Analysis Software (Thermo Fisher).

A master mix was prepared for each of the samples and aliquoted into three wells to generate three replicates. One sample master mix comprised of 35 µl 2x TaqMan Universal Master Mix II (Applied Biosystems), 3.5 µl 20x primer mix, 3 µl cDNA and 28.5 µl nuclease free water.

A standard curve was included in every plate to assess the primer efficiency with A549 cDNA at a 4-fold dilution series. A negative no-template control was also included in each plate for each primer set to check for residual DNA contamination.

To assess mRNA expression fold-change was calculated by first normalising to the house-keeping gene and then calculating the change in expression using the formulas shown below:

ΔCt = Experimental gene Ct (*HPGD*) – Housekeeping gene Ct (*ACTB*)
ΔΔCt = Test sample ΔCt (treatment e.g. AZA) – Control sample ΔCt (control e.g. DMSO)
Expression fold-change = $2^{-\Delta\Delta Ct}$

2.2.11 RNA sequencing

2.2.11.1 Sample preparation

RNA sequencing (RNA-Seq) was completed to assess the downstream transcriptional effects of over-expressing 15-PGDH in MCF7 cells.

The highest 15-PGDH expressing MCF7 clone (H14), its matched control clone (X17) and non-transfected parent MCF7 cells were seeded at $4x10^5$ cells in 1% FCS media in 6 well plates for 24 hours. The cells were then treated with 0.1% DMSO or 1 µM prostaglandin E_2 (PGE_2) (Cayman Chemicals) in 0.1% DMSO for 6 hours. Each treatment was performed in triplicate.

Total RNA was extracted from the treated samples as described in Section 2.2.1 and the RNA quality was checked the Agilent TapeStation 2200 (Section 2.2.5). The RNA was then quantified using the Qubit fluorometer (Section 2.2.3) before proceeding with the library preparation.

2.2.11.2 Library preparation

mRNA libraries were prepared using the Illumina TruSeq Stranded mRNA kit with 1 µg of total RNA in 50 µl per sample. A no template control was also taken through the process to determine whether there was any contamination during the library preparation. The libraries were prepared according to the manufacturers guidelines (Figure 2.2). mRNA was selected by first denaturing the total RNA by heating to 65°C for 5 minutes and cooling to room temperature for 5 minutes in the presence of 50 µl RNA purification beads (oligo dT linked magnetic beads). The beads were removed from suspension in the presence of a magnetic field allowing the aqueous solution containing unbound RNAs such as rRNA, tRNA and lncRNA to be removed. The beads were washed with 200 µl of bead washing buffer before the mRNA was dissociated from the polyT oligo by heating the sample to 80°C for 2 minutes with 50 µl elution buffer. The poly(A) mRNA was allowed to re-anneal to the beads at room temperature and further washes in 50 µl bead binding buffer and 200 µl bead wash buffer were performed to remove residual rRNA and other contaminants. 19.5 µl Fragment, Prime, Finish mix containing random hexamers was added to the bound RNA prior to the sample been heated to 94°C for 8 minutes to elute, fragment and bind the random hexamer primers to the RNA. 17 µl of the supernatant was transferred to a new well. First strand cDNA synthesis was then performed using 8 µl SuperScript II with First Strand Synthesis Act D Mix (1 µl to 9 µl ratio, respectively). The samples were incubated at 25°C for 10 minutes followed by heating to 42°C for 15 minutes before terminating the reaction at 70°C for 15 minutes. Second strand cDNA synthesis was performed

in 5 µl Resuspension buffer and 20 µl Second Strand Master Mix containing DNA polymerase I and RNase H at 16°C for 1 hour. Strand specificity is achieved by replacing dTTP with dUTP within the master mix. The cDNA was purified and size selected for fragments of approximately 300 bp using 90 µl AMPure XP beads (Beckman Couter) and 135 µl supernatant discarded. The beads were gently washed with 200 µl 80% ethanol twice and air-dried. The samples were resuspended in 20 µl Resuspension buffer and 15 µl transferred to a new well and stored at −20°C overnight. Adenylation of 3' ends was performed by adding 12.5 µl A-Tailing Mix and incubating the samples at 37°C for 30 minutes and terminated by heating to 70°C for 5 minutes. 2.5 µl Resuspension buffer was added to each sample. Next the samples were indexed by ligating 2.5 µl indexed Illumina sequencing compatible adapters to each sample in the presence of 2.5 µl Ligation Mix by heating of 30°C for 10 minutes. 5 µl of Stop Ligation buffer was added to each well to stop the ligation process.

The samples were purified using 42 µl AMPure XP Beads and washing twice with 80% ethanol and allowing to air-dry. The samples were resuspended in 52.5 µl Resuspension buffer and 50 µl transferred to a new well. The AMPure XP Bead clean-up was then repeated a second time with 50 µl of beads and resuspended in 22.5 µl of Resuspension buffer and 20 µl transferred to a new tube. The libraries were then amplified by PCR using 5 µl PCR Primer Cocktail and 25 µl PCR Master Mix with 15 cycles of: 98°C 10 seconds, 60°C 30 seconds, 72°C 30 seconds with a final extension time of 72°C for 5 minutes. Finally, the cDNA libraries were purified and size selected to remove adaptor dimers and unincorporated adaptors using 50 µl AMPure XP beads as described above and resuspended in 32.5 µl Resuspension buffer and 30 µl transferred to a new well.

The library quality, size range and sequencing adaptor dimer contamination was validated using the Agilent TapeStation 2200 with the DNA broad range kit (as described for RNA in Section 2.2.52.3.3). Excess sequencing adaptor dimer if present was removed by AMPure XP bead mediated size selection. The mRNA libraries were then quantified by measuring fluorescence with the Qubit dsDNA assay kit and Qubit fluorometer (Life Technologies) (Section 2.3.3) before creating an equimolar pool of the libraries.

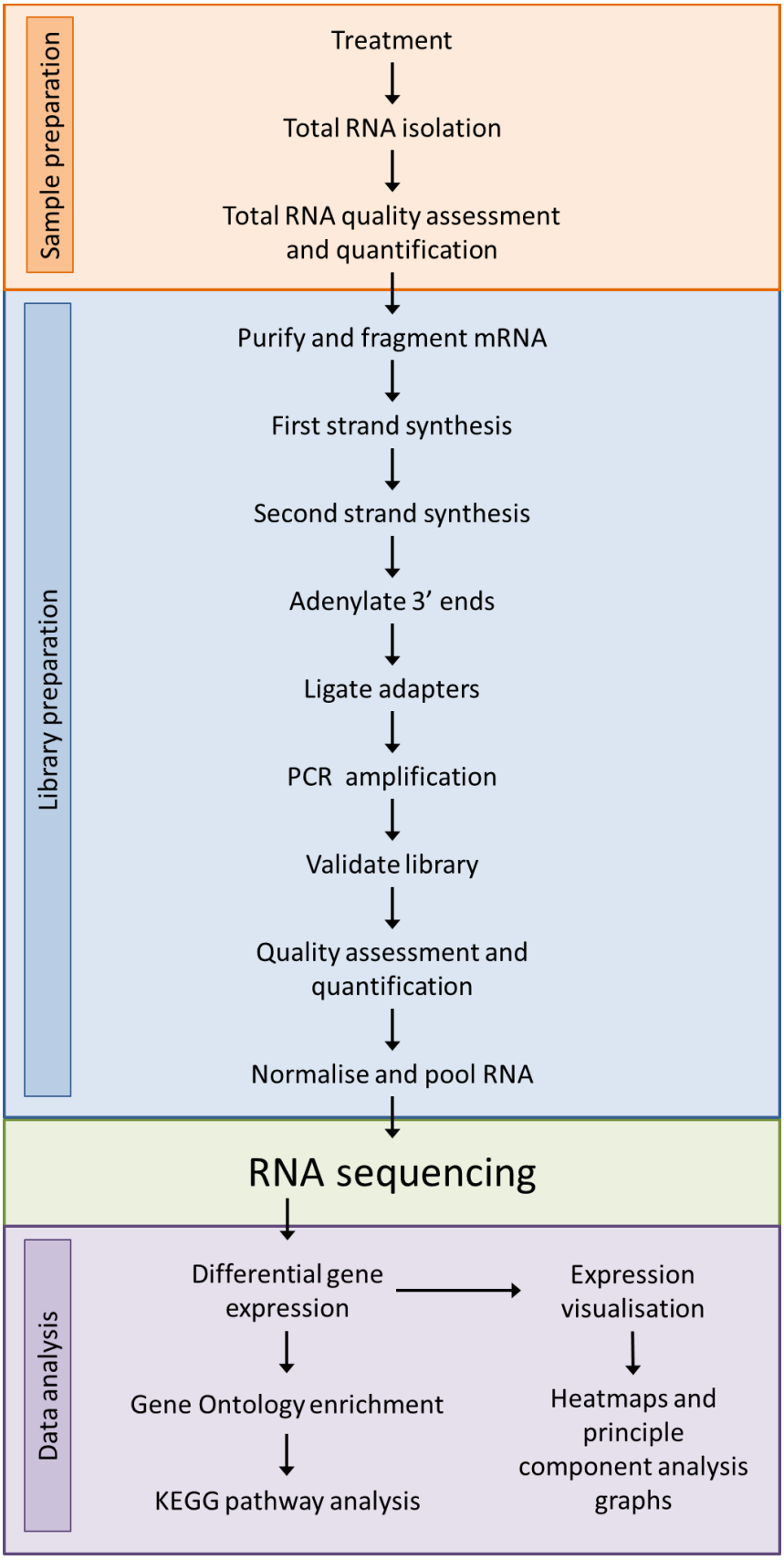

Figure 2.2 RNA sequencing workflow

The RNA libraries were sequenced by the University of Leeds's, Next Generation Sequencing Facility using the Illumina NextSeq 500 (Illumina) with a single end 75bp length read.

2.2.11.3 Data analysis

2.2.11.3.1 Differential gene expression

Differential gene expression analysis was performed in the R environment using the DeSeq2 and EdgeR packages as follows. Read count data from the complete RNA-Seq experiment for each transcript was determined using R package rSubRead and imported into R as a data matrix of integer values. Data relating to each specific pairwise analysis was then sub-setted with transcripts containing less than 3 reads in more than 2 samples removed from the data set. A dataframe containing the experimental design of each pairwise analysis (sample name, sample condition and which condition was the reference condition) and the read count matrix was entered in to either DeSeq2 or EdgeR. Once the differential analysis was completed, significantly differentially expressed transcripts with a p value, adjusted for multiple testing, of 0.01 or less were retained from the DeSeq2 based analysis or with a false discovery rate of less than 0.01 for the EdgeR analysis.

2.2.11.3.2 Expression visualisation

2.2.12.3.2.1 Heatmaps

Normalised read count data was exported from DeSeq2 following normalisation using the standard 'normTransform' function and filtered to remove data linked to transcripts not differentially expressed. The normalised read count data was used to create heat maps of gene expression between the two conditions using the pheatmap R package. To highlight the differences in expression of each transcript between samples, the colour scaling of each transcript was set to 'row' such that the colour range for each transcript was dependant solely expression range of the transcript and not the global expression range of all transcripts. To generate a clearer distinction between the different conditions in the pairwise analysis the transcripts were clustered by expression profile. Similarly, to determine how consistent the expression profile of samples in each condition was, the column we re also clustered, such that the samples with the most similar expression profile were placed together.

2.2.12.3.2.2 Principle component analysis graphs

The normalised read count data from the DeSeq2 analysis was used to create principle component analysis (PCA) graphs using the pcaData R package such that the variation within the set of samples was condensed in to two components which were then displayed on a XY graph.

2.2.12.3.3 Gene Ontology enrichment analysis

Gene ontology (GO) term enrichment for biological processes was performed using significantly differential expressed transcripts as identified by EdgeR. The normalised read counts were generated by EdgeR using the "Trimmed Mean of M-values" (TMM) method and filtered to remove transcripts found not to be significantly differentially expressed. Since the transcripts used were annotated as part of the RefSeq human data set, the transcript IDs were converted to non-redundant list of gene Entrez IDs using the org.Hs.eg.db, GOstats and GO.db R packages and datasets. A second list of non-redundant gene Entrez IDs consisting of all genes in the human gene was also generated. The reference gene list and list of differentially expressed genes were then used to generate a lists of GO terms linked to each gene list, which was then filtered for GO terms significantly (p value <0.01) over represented in the differentially expressed genes.

2.2.12.3.4 KEGG pathway analysis

As with the GO term enrichment a list of significantly (false discovery rate (FDR) <0.01) differentially expressed genes was generated using EgdeR. The RefSeq transcripts ID were converted to a non-redundant list of gene Entrez IDs, with each entrez ID linked to the greatest fold change for a transcript linked to each entrez gene. A list of KEGG pathway IDs was extracted from the KEGG Pathways web page and sequentially supplied to the pathway function of the 'Pathway' R package along with the gene ID list and linked fold change in expression values and species value (human = 'hsa'). This generated an image of each selected pathway in which up-regulated genes where highlighted in green and down-regulated genes in red.

2.3 DNA methods

2.3.1 DNA extraction

DNA was extracted from mammalian cell lines using the GenElute Mammalian Genomic DNA Miniprep kit (Sigma-Aldrich). Briefly, cultured cells were trypsinised and pelleted in a

microcentrifuge tube as described in Section 2.1.1. The supernatant was then discarded and the pellet stored at −80°C until required for DNA preparation. The pellet was thawed at room temperature and resuspended in 200 µl of Resuspension Solution. 20 µl of RNase Solution was added and the sample incubated at room temperature for 2 minutes to remove any contaminating RNA. The cells were lysed with 20 µl of Proteinase K and 200 µl of Lysis Solution C, with 15 seconds of vortexing and incubation at 70°C for 10 minutes. Meanwhile, the GenElute Miniprep Binding Column was prepared by adding 500 µl of Column Preparation Solution, centrifuging the column for 1 minute at 12,000 x g and discarding the flow-through. The sample was prepared for binding to the column by adding 200 µl of 100% ethanol to the sample lysate and mixing thoroughly by vortexing for 10 seconds. The lysate was then transferred to the column, centrifuged for 1 minute at 6,600 x g and the flow-through discarded, leaving the DNA bound to the column. The bound DNA was then washed twice using 500 µl Wash Solution. For the first wash the sample was centrifuged for 1 minute at 6,600 x g and the flow-through was discarded. On the second wash the column was placed in a fresh collection tube and centrifuged for 3 minutes at maximum speed 16,100 x g to remove any residual ethanol. The column was then placed in a new collection tube and 100 µl of Elution Solution placed in the centre of the binding column and incubated for 5 minutes at room temperature. The sample was eluted by centrifuging at 6,600 x g for 1 minute. An additional second elution was performed to maximise the recovery and pooled together. The DNA was stored at −80°C until required.

2.3.2 Nanodrop DNA quantification and quality assessment

DNA was quantified and the quality assessed using the Nanodrop ND-1000 spectrophotometer as described in Section 2.2.2. However, a 260/230 ratio of ~1.8 was classed as pure DNA.

2.3.3 Qubit DNA quantification

Qubit DNA quantification was completed using the Qubit fluorometer and Quant-iT dsDNA Broad-Range Assay Kit (Thermo Fisher Scientific). As with the RNA quantification the instrument measures a fluorescent signal emitted from the dye binding the DNA. Eight standards (0-100 ng/µl) were included on each run to create a calibration curve. Qubit working solution was prepared with BR (broad range) reagent and BR buffer at a 1:200 dilution. 10 µl of the control standard was added to 190 µl working solution and 2 µl sample DNA added to 198 µl working solution. The samples were mixed by vortexing for 5 seconds and incubated at room temperature for 2 minutes. The fluorescence was measured using the Qubit fluorometer at

485/520 nm for each of the standards and samples. The DNA content of each sample was calculated using the standards to generate a standard curve.

2.3.4 Agarose gel

Gel electrophoresis was performed with a 1% (w/v) agarose gel to confirm the product size and band intensity. Firstly, a 1% (w/v) agarose gel was prepared by dissolving agarose in 1x Tris-acetate-EDTA (TAE) buffer (1mM EDTA, 40mM Tris-base, 20mM glacial/acetic acid) by heating in a microwave. Once the agarose had dissolved the solution was cooled to 50°C before the addition of ethidium bromide (Fisher-Scientific) (final concentration of 0.2 µg/ml) and mixed by swirling. The gel was then poured into a mould and any bubbles removed before adding a comb with the desired size and number of wells. The gel was allowed to set for at least 30 minutes before placing in a gel electrophoresis tank. The gel was submerged in 1x TAE buffer and the samples loaded alongside a size marker. A Lambda HindIII marker prepared with orange G loading dye (Thermo Scientific) was used for larger DNA samples, whereas a 100 bp plus ladder (Thermo Scientific) was used for smaller samples. The 100 bp plus ladder was diluted by adding 5 µl ladder DNA and 10 µl 6x blue loading dye (Thermo Scientific) to 35 µl sterile water. Once the samples and ladder were loaded, gel electrophoresis was performed at 120 V for 60 minutes (large gels) or 60 V for 60 minutes (small gels) unless otherwise stated. The gel was then visualised using the Bio-Rad Gel Doc (Bio-Rad) and ultra-violet (UV) light.

2.3.5 Crystal violet gel

When a PCR product was required for downstream sequencing following gel electrophoresis a crystal violet gel was performed to prevent DNA damage from UV exposure. A 40 ml 0.8% (w/v) agarose gel with 10 mg/ml crystal violet (1:000) was prepared. A Lambda DNA/HindIII marker in orange G (Thermo Scientific) was used to enable visualisation of the marker in the gel and the product for assessment diluted with 10x orange G (Sigma) and loaded onto the gel. Samples were run in a 1:1000 crystal violet in 1x TAE running buffer at 50 V for 120 mins. The bands were visualised using a UVP dual intensity transilluminator (low).

2.3.6 PCR clean-up methods

ExoSAP-IT PCR Product Clean-up Reagent (Applied Biosystems) was used in most cases to clean-up PCR products prior to Sanger sequencing, when a single strong band was observed on a gel. 5 µl of PCR product and 2 µl ExoSAP-IT were incubated at 37°C for 15 minutes to degrade

remaining primers and nucleotides. The mixture was heated to 80°C for a further 15 minutes to inactivate the ExoSAP-IT enzyme.

Alternatively, when a larger volume of clean PCR product was required, purification was completed using the QIAquick PCR purification kit (Qiagen). Briefly, 5x the PCR reaction's volume of Buffer PBI was added to the PCR product and mixed by pipetting up and down. The mixture was then placed in a spin column and centrifuged at 16,100 x g for 60 seconds to allow binding of the PCR product to the membrane. The flow-through containing unused primers and nucleotides was discarded and the PCR product bound to the matrix was washed with 0.75ml of buffer PE (containing ethanol). The column was then transferred to a clean centrifuge tube and the PCR product eluted in 20 µl of sterilised water.

If two bands were amplified by a PCR, the desired product was excised from a 0.8% (w/v) agarose gel and visualised with a crystal violet gel (Section 2.3) and purified using the QIAquick gel extraction kit (Qiagen) as follows: The band(s) were carefully excised from the gel using a scalpel and placed in a microcentrifuge tube. The gel was then weighed and three volumes of Buffer QG added to each tube (100 mg = 100 µl buffer). The tube was then incubated at 50°C for 10 minutes with vortexing every 2-3 minutes to help dissolve the gel. When dissolved, one gel volume of isopropanol was added to the sample and mixed. The sample was then placed in a QIAquick spin column and centrifuged for 1 minute at 16,100 x g to bind the PCR product to the column. The flow-through was discarded and the sample washed in 0.5 ml Buffer QG by centrifugation for 1 minute at 16,100 x g to remove any residual agarose. 0.75 ml of Buffer PE was added to the column and incubated at room temperature for 3 minutes before centrifugation as before and the flow-through discarded. The column was spun for an additional 1 minute at 16,100 x g to remove all residual ethanol. The column was transferred to a clean microcentrifuge tube and the column incubated with 20 µl nuclease-free water for 1 minute at room temperature before eluting the DNA by centrifugation. To ensure purification of the single product was successful an aliquot of the sample was run on a 1% (w/v) agarose gel.

2.3.7 Bacterial Colony PCR

The colony selected for PCR was gently scraped off the LB agar plate using a 20 µl pipette tip and spread onto a new LB agar plate. The plate was incubated overnight at 37°C to allow the colony to grow for future experiments.

The same tip was immediately place in 50 µl of distilled water and the water pipetted up and down to resuspend the remaining cells. The sample was then heated to 100°C for 10 minutes

to liberate DNA from the bacterial capsule and the sample briefly centrifuged. Conventional PCR was then performed with the DNA in water used as template as described in Section 2.2.9.

2.3.8 Sanger Sequencing

Sanger sequencing is used to sequence DNA. The process involves the generation of DNA fragments of varying length terminating with a labelled dideoxynucleotide. This is achieved by performing the elongation step with a mixture of nucleotides and dideoxynucleotides, elongation can no longer occur when a dideoxynucleotide is incorporated. The DNA products are then separated by size using capillary gel electrophoresis. As the shorter fragments migrate faster they are detected first. A laser excites the label on the dideoxynucleotide terminating each strand. As each base is tagged with a different label the signal generated can be used to determine the nucleotide incorporated at that position. This generates a chromatogram with the fluorescent peak for each nucleotide, enabling accurate DNA sequencing.

Sanger sequencing was completed using the BigDye Terminator v3.1 Cycle Sequencing Kit (Applied Biosystems). Each sequencing reaction was made up of 1 µl BigDye 3.1, 1.5 µl BigDye buffer, 5.5 µl autoclaved distilled water, 1 µl sample and 1 µl 1.6 µM primer (forward or reverse). Both forward and reverse reactions were run to allow comparison where necessary. The PCR conditions were as shown in Table 2.5.

Table 2.5 Sanger sequencing cycling conditions

Temperature	Time	Cycles
96°C (Ramp 1°C/sec to 96°C)	1 minute	x1
96°C (Ramp 1°C/sec to 96°C)	10 seconds	x25
50°C (Ramp 1°C/sec to 50°C)	5 seconds	
60°C (Ramp 1°C/sec to 60°C)	4 minutes	
4°C (Ramp 1°C/sec to 4°C)	Forever	x1

The resulting DNA products were precipitated by adding 5 µl 125 mM EDTA and 60 µl 100% ethanol per well, the solutions were mixed and centrifuged at 3,000 x g for 30 minutes at 22°C. The plate was then inverted over tissue paper and centrifuged at 8 x g for 1 minute to remove the solution. The pellet was washed with 60 µl 70% ethanol and centrifuged at 8 x g at 4°C for 15 minutes. The plate was inverted again and centrifuged for a further 1 minute at 8 x g before allowing the pellet to air-dry in the dark for one hour. The plate was frozen until sequencing at which point the pellet was resuspended in 10 µl HiDi formamide (Applied Biosystems), and sequenced on an Applied Biosystems 3130*xl* system.

Base calling was performed using the Sequencing Analysis software v5.2 (Applied Biosystems) and the peak height ratios checked for each sample. The chromatogram traces were visualised and the sequence extracted using GeneScreen (Carr et al., 2011). The resulting sequence and expected sequence were aligned using the NCBI nucleotide BLAST database.

2.3.9 DNA bisulphite treatment

Bisulphite treatment of DNA converts unmethylated cytosines in the DNA to uracil, leaving methylated cytosine's unchanged. Bisulphite treatment was performed using the EpiTect Bisulphite Kit (Qiagen). Briefly, DNA was diluted to give 0.5-1.5 µg in 20 µl or up to 500 ng in 40 µl (sample concentration dependent) and added to 85 µl bisulphite mix and 35 µl or 15 µl DNA protect buffer (respectively). The sample was then briefly mixed and bisulphite DNA conversion completed using the PCR program in Table 2.6:

Table 2.6 Bisulphite conversion thermocycler conditions

Step	Time	Temperature
Denaturation	5 mins	95°C
Incubation	25 mins	60°C
Denaturation	5 mins	95°C
Incubation	1 hour 25 mins	60°C
Denaturation	5 mins	95°C
Incubation	2 hours 55 mins	60°C
Hold	Indefinite	20°C

The bisulphite converted DNA was transferred to a microcentrifuge tube and 560 µl Buffer BL added. The sample was briefly vortexed and the mixture transferred to an EpiTect spin column. The column was centrifuged at 16,100 x g for one minute and the flow-through was discarded. 500 µl Buffer BW was added to the column to remove residual sodium bisulphate, the column was centrifuged at 16,100 x g and the flow-through discarded. 500 µl Buffer BD was added to the spin column and incubated for 15 minutes at room temperature to desulphonate the samples. The columns were then centrifuged for 1 minute at 16,100 x g and the flow-through discarded. The DNA was washed twice by adding 500 µl Buffer BW, centrifuging at 16,100 x g and discarding the flow-through. The columns were centrifuged for a further one minute and then heated to 56°C for 5 minutes to evaporate any residual buffer. The spin columns were placed in a new collection tube and 20 µl Buffer EB placed into the centre of the membrane and incubated for one minute at room temperature. The DNA was eluted in the buffer by centrifuging for 1 minute at 15,000 x g. The elution step was repeated to maximise the recovery of bisulphite converted DNA. The DNA was then stored at −20°C until further processing.

2.3.10 Pyrosequencing

Pyrosequencing is a DNA sequencing technique that can used to assess DNA methylation in bisulphite-treated DNA samples. The method is based on a chain of enzymatic reactions in which nucleotide incorporation generates light, which in turn can be quantified. Methylation analysis enables identification of bisulphite converted cytosines in a known DNA sequence.

Single stranded DNA is sequenced by synthesising its complementary strand. Sequential addition of one deoxynucleotide triphosphate (dNTP) at a time enables identification of which nucleotide is incorporated. The dNTP is incorporated into the DNA sequence using Klenow fragment DNA polymerase I, which releases pyrophosphate (PP_i). ATP sulfurylase then converts PP_i and adenosine 5' phosphosulfate (APS) into ATP which is a substrate for luciferase, which produces light by converting luciferin to oxyluciferin. The intensity of the light signal is directly proportional to the amount of the nucleotide incorporated in to the DNA strand. Unincorporated dNTPs and ATP are then degraded by the addition of apyrase. The reaction then starts again with the next dNTP. This process is illustrated in Figure 2.3. Pyrosequencing was performed to assess changes in the DNA methylation status of cell lines before and after treatment. SNPs in the target sequence were identified using Sanger sequencing and the dNTP dispensation order adapted as required.

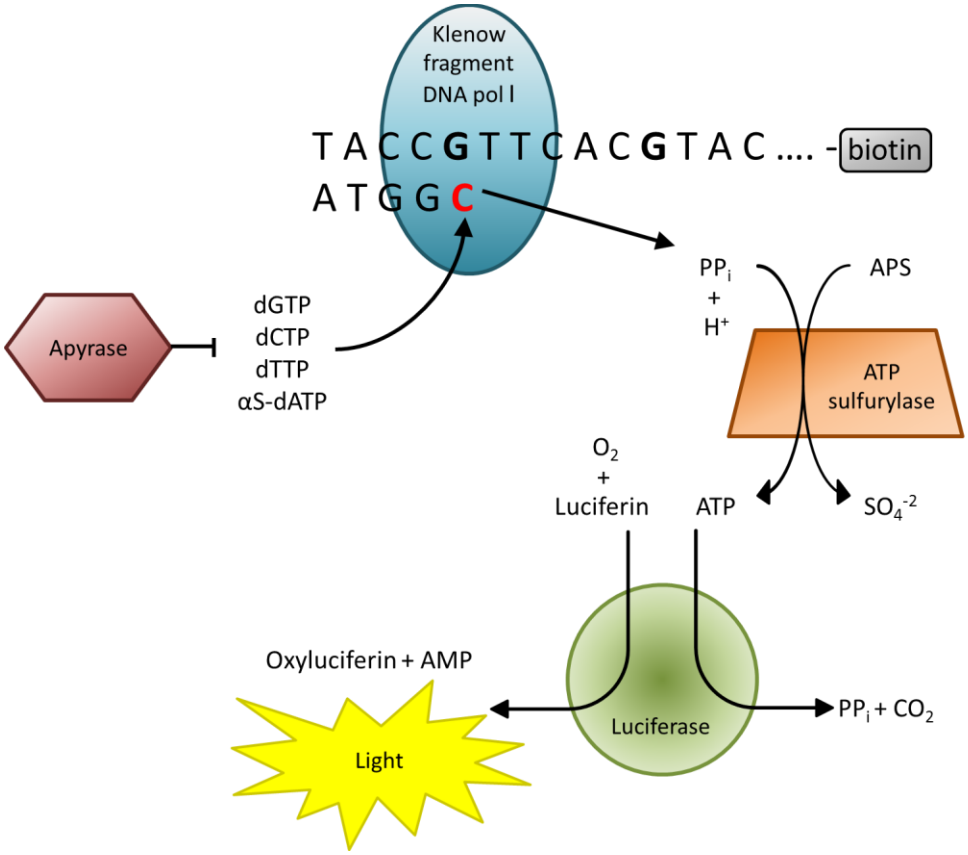

Figure 2.3 Pyrosequencing reaction. dGTP = deoxyguanosine triphosphate, dCTP = deoxycytidine triphosphate, dTTP = deoxythymidine triphosphate, and αS-dATP = deoxyadenosine alpha-thio triphosphate, are nucleotides used in the reaction. As dATP is too similar to ATP, αS-dATP was used to prevent false signalling. PP_i = pyrophosphate, APS = adenosine 5' phosphosulfate, SO_4^{-2} = sulphate, AMP = adenosine monophosphate.

2.3.10.1 Pyrosequencing PCR

DNA was extracted from the drug-treated and untreated control cells as described in Section 2.3 and bisulphite converted as described in Section 2.3.9. The bisulphite converted DNA was re-quantified using the Nanodrop before performing the pyrosequencing PCR amplification in which one primer was biotinylated to allow selection and subsequent sequencing of a single strand. A list of the pyrosequencing primers can be found in the appendix (Appendix 4). Pyrosequencing PCR was performed using the master mix described in Table 2.7 using the PCR settings shown in Table 2.7 Pyrosequencing sequencing PCR components:

Table 2.7 Pyrosequencing sequencing PCR components

Reagent	Volume (µl)	
	MGMT primers	*HPGD* primers
5x GoTaq Green Flexi Buffer	5	5
10 µM F/R pyrosequencing PCR primer	0.5	0.5
GoTaq Hot Start Polymerase (5 U/µl)	0.4	0.4
10 mM dNTP mix	1	1
25 mM $MgCl_2$	1.6	2.5
Nuclease free water	14.5	13.6
Bisulphite converted DNA (10 ng/µl)	2	2
Total	**25**	**25**

Table 2.8 Pyrosequencing sequencing PCR cycling conditions

Step	Temperature	Time	Cycles
Initial denaturation	95°C	15 minutes	x1
Denaturation	95°C	3 minutes	x50
Annealing	__°C	30 seconds	
Extension	72°C	10 seconds	
Refrigeration	4°C	Forever	x1

5 µl of each sample was run on a 2% (w/v) agarose gel (Section 2.3.4) to confirm the presence of a single strong band. Additional controls were included for each assay, with control methylated bisulphite-converted DNA, unmethylated bisulphite-converted DNA, unmethylated non-converted DNA (Qiagen) and a water no template control performed for each set of pyrosequencing PCR primers. A well-established assay for O-6-Methylguanine-DNA Methyltransferase (MGMT) was also used alongside the *HPGD* assays using *MGMT* primers to act as an experimental control.

2.3.10.2 Template preparation

Initially, 20 µl of a biotinylated PCR product was transferred to a PCR plate and diluted with 20 µl nuclease-free water. 0.4 µM sequencing primers (Appendix 5) were prepared by diluting 1.6

µl 10 µM sequencing primer in 40 µl annealing buffer (Qiagen) and placed in the relevant wells of a flat-bottomed 96-well pyrosequencing plate (Qiagen).

Streptavidin sepharose high-performance beads 34 µm (GE Healthcare) were fully resuspended before adding 3 µl to 40 µl binding buffer (Qiagen) and 40 µl added to the PCR plate containing the PCR products. The plate was sealed with a plate sealer and immediately placed on a shaker for 5 minutes to allow the biotinylated PCR products to bind to the streptavidin beads.

The plate was then placed onto a vacuum workstation (Biotage) and the PCR product solution aspirated using the vacuum pump for 20 seconds, leaving the beads and bound PCR products attached to the filter. The vacuum tool was then placed in 70% ethanol, allowing the solution to flow-through the filter and pump for 20 seconds to wash the PCR product. Next, the vacuum pump head was placed in denaturation solution for 20 seconds (Qiagen) to denature the DNA leaving only the biotin labelled PCR strand attached to the filter and draining away any remaining DNA. A final wash was completed with the wash solution (Qiagen) for 20 seconds. The vacuum pump was turned off and the head with the attached biotin labelled single stranded DNA was placed into the pyrosequencing plate containing the sequencing primers and heated to 80°C for 2 minutes to allow the sequencing primers to anneal.

2.3.10.3 Equipment set up

The bisulphite-treated sequence to analyse along with the nucleotide dispensation order details (Appendix 6, Appendix 7 and Appendix 8,) were loaded into the Pyro Q-CpG software (Biotage), which in turn calculated the volume of each nucleotide, enzyme and substrate required. Each dispensation order contains an additional G or C nucleotide to act as a bisulphite control, to confirm that all of the DNA had been successfully bisulphite converted. The suggested volume of each nucleotide, enzyme and substrate was rounded up to the nearest 5 µl and loaded into the pyrosequencing cartridge (Qiagen). Finally, the cartridge and pyrosequencing plate were placed in the Pyromark ID pyrosequencer (Biotage) and the sequencing performed.

2.3.10.4 Cleaning of the cartridge

As each cartridge can be reused several times, following the experiment the cartridge is cleaned with distilled water. To do this the cartridge is filled with distilled water and pressure applied to each compartment of the cartridge to flush water out of each needle. The remaining water is then poured out of the cartridge and the cartridge allowed to air-dry upside down to avoid dust entering the cartridge.

2.3.11 Cloned Bisulphite DNA sequencing

To validate the pyrosequencing results, pyrosequencing PCR was completed as described above for *HPGD* CpG island 1 product 2 (206 bp) using LoVo untreated and decitabine-treated bisulphite converted DNA samples. The remaining product was cloned in to pGEM-T easy vector and transformed into XL-1 blue cells (Section 2.4.4). Twenty white colonies per treatment were selected for sequencing as described in Section 2.4.4. The DNA from each colony was amplified using colony PCR (Section 2.3.7) with the amplicon from ten distinct colonies selected for Sanger sequencing.

Sanger sequencing was performed using the relevant pyrosequencing PCR primers as described in Section 2.3.8. The methylation status was assessed by loading the UCSC gene sequence and resulting bisulphite-treated DNA sequence into the CpGviewer software (Carr et al., 2007). The results were also confirmed manually using GeneScreen to view the electropherograms.

2.4 Microbiology methods

2.4.1 Mini-prep

DNA extraction and plasmid DNA purification when small quantities were required was completed using the GenElute Plasmid Miniprep Kit (Sigma). The cells were pelleted at 2,000 x g for 5 minutes and the supernatant discarded. The pellet was resuspended in 200 µl of resuspension solution (containing RNase A). The sample was transferred to a microfuge tube and an additional 200 µl of lysis solution added. The sample was mixed immediately by inverting 6-8 times and allowed to sit at room temperature for 5 minutes. 350 µl of neutralising/binding solution was then added and the sample mixed by inverting a further 6-8 times, before the sample was centrifuged at 12,000 x g for 10 minutes. The column was prepared by adding 500 µl of column preparation solution and centrifuging at 12,000 x g for 1 minute. The flow-through was discarded and the supernatant from the sample transferred to the column which was then centrifuged at 12,000 x g for 1 minute and the flow-through discarded. The column was washed with 500 µl of the optional wash solution and centrifuged again for 1 minute at 12,000 x g. The wash solution was discarded and 750 µl wash solution added and centrifuged again for 1 minute at 12,000 x g to remove salts and contaminants. The sample was then eluted in a fresh tube in 100 µl of elution solution at 12,000 x g for 1 minute. The purified plasmid containing the *HPGD* insert was stored at −20°C until required.

2.4.2 Maxi-prep

Larger quantities of plasmid DNA were prepared using a Qiagen Maxi-prep endotoxin free kit (12362) as follows: A 5 ml starter culture was prepared by inoculating 5 ml of LB broth containing the appropriate antibiotic (when required), with the colony of choice and incubated for 8 hours at 37°C with gentle rotation. 100 µl or 200 µl of the broth was added to 100 ml LB broth with appropriate antibiotic. The cells were cultured overnight at 37°C in a shaking incubator at 200 rpm. The cells were pelleted at 3,000 x g for 20 minutes at 4°C and resuspended in 10 ml of Buffer P1 containing RNase A. 10 ml Buffer P2 was added and the mix was inverted vigorously 4-6 times and incubated at room temperature for 5 minutes. 10 ml chilled Buffer P3 was added to the lysate and mixed by inverting 4-6 times. The sample was then placed in the QIAfilter cartridge for 10 minutes at room temperature to allow the protein precipitates to form a layer on the top of the solution. The plunger was then inserted into the cartridge and the solution filtered into a 50 ml falcon tube to which 2.5 ml Buffer ER was added and mixed by inverting 10 times before incubating on ice for 30 minutes. Meanwhile the QIAGEN-tip 500 was prepared by allowing 10 ml Buffer QBT to drain through the tip under gravity. The lysate was then added to the tip and allow to drain through the tip under gravity and the tip was washed twice with 30 ml of Buffer QC. The DNA was eluted in 15 ml Buffer QN into an endotoxin-free falcon tube and the DNA was precipitated by adding 10.5 ml isopropanol and pelleted by centrifuging at 15,000 x g for 30 minutes at 4°C. The pellet was washed with 5 ml of endotoxin-free 70% ethanol and centrifuged at 15,000 x g for 10 minutes. The supernatant was discarded and the pellet air-dried for 5-10 minutes before being resuspended in 170 µl TE Buffer.

2.4.3 LB broth and agar plate preparation

LB broth was prepared with 8 g of LB broth (Sigma) powder in 400 ml dH_2O, while 6 g of agar (Merck) was added to LB broth to make LB agar plates. The solutions were sterilised by autoclaving at 15 psi for 15 minutes. The LB broth was allowed cool to room temperature before use. LB agar was cooled to 50°C in a water bath for 30 minutes before 25 ml was added to a sterile plate and allowed to set. If required, the appropriate antibiotic was added to the LB agar (ampicillin (Sigma) 100 µg/ml or kanamycin (Sigma) 50 µg/ml) immediately before they were poured, while it was added to LB broth just before to use. Plates were wrapped in parafilm and stored at 4°C for up to one month.

LB agar/Amp/Xgal/IPTG plates were prepared as described above with the addition of 0.5 mM Isopropyl β-D-1-thiogalactopyranoside (IPTG) and 80 µg/ml 5-bromo-4-chloro-3-indolyl-β-D-

galactopyranoside (Xgal) alongside ampicillin. Due to the light sensitivity of Xgal the plates were wrapped in foil for storage.

2.4.4 pGEM-T easy vector and PCR product ligation for bisulphite sequencing

The selected PCR product was ligated into the pGEM-T easy vector (Appendix 9) using the following reaction: 1x rapid ligation buffer, 50 ng pGEM-T easy vector (Promega), 5 ng PCR product, 1 µl T4 DNA ligase (New England Biolabs) and made up to 10 µl with nuclease-free water. The mix was incubated at 4°C overnight to enable ligation of the PCR product to the vector. Successful recombination will result in the PCR product inserting within the *lac*Z gene, which encodes β-galactosidase, and disrupting the enzymes function.

XL1 blue cells (Aligent Technologies) were transformed with the pGEM-T easy vector containing the insert. XL1 blue cells allow blue-white colour screening of recombinant plasmids. 2 µl of the ligation reaction or 1 µl of a pUC19 control (Thermo Scientific) were added to 50 µl of cells and incubated on ice for 30 minutes. The cells were heat shocked at 42°C for 45 seconds and placed on ice for 2 minutes followed by the addition of 950 µl Super Optimal broth with Catabolite repression (SOC) media (Invitrogen) and incubation for 1 hour at 37°C 200 rpm. 100 µl of the cell suspension was spread onto an LB agar/Amp/Xgal/IPTG plate (Section 2.4.3). The remaining cells were centrifuged at 3,000 x g for 1 minute and resuspended in 50 µl and spread on a second agar plate. The plates were incubated overnight at 37°C.

Xgal is metabolised to a blue compound by the *LacZ* protein, which is induced by IPTG. Consequently, colonies containing the pGEM-T Easy vector without an insert should turn blue, while those with an insert remain white, allowing colonies with inserts to be easily selected. Therefore twenty white colonies were selected for colony PCR (Section 2.3.7) using M13 F-20 and M13 R primers and standard PCR reaction conditions with primer annealing at 55°C. Each colony was also plated onto a new LB agar/Amp/Xgal/IPTG plate.

PCR products from ten inserts for each treatment were Sanger sequenced with CpG1 P2 forward and reverse primers after purification using GenElute PCR clean up columns (Section 2.3.6, Section 2.3.7). The results were analysed manually and then processed using the CpG Viewer software.

2.4.5 Gateway cloning

Invitrogen's Gateway recombination cloning system enables simple and efficient transfer of DNA fragments between plasmids using site-specific recombination. Briefly, the sequence of interest is amplified using PCR primers containing forming *att*B1 and *att*B2 sequences flanking the gene. The DNA fragment is inserted into the Entry clone (pDONR201) (Appendix 10) by sequence directed recombination between the *att*P1 and *att*P2 sites in the vector and primer sequences, mediated by the BP Clonase II enzyme (BR reaction). This generates plasmids in which the insert is flanked by *att*L1 and *att*L2 sites. The insert can then be swapped for the *ccdB* sequence, a selectable marker, in a Destination vector (e.g. pDEST510 which is based on pDEST47 (Appendix 11)) containing *att*R1 and *att*R2 sites using the LR Clonase enzyme mix (LR reaction) (summarised in Figure 2.4).

2.4.6 Preparation of 15-PGDH expressing *E.coli* control cells

DE3 cells transformed with the pET-15b HPGD vector, producing wild-type 15-PGDH were provided by Dr Christine Diggle (Uppal et al., 2008). The DE3 control (non-transformed) and DE3 pET-15b HPGD (transformed) cells were grown on an LB agar plate without, and with ampicillin, respectively (Section 2.4.3). A single colony was used to generate a 5 ml starter culture in LB broth +/− ampicillin and grown at 37°C overnight. Half of the starter cultures were placed into two separate conical flasks containing 25 ml of LB broth. Ampicillin (100 µg/ml) was added to the flask containing transformed DE3 cells. The cells were grown at 37°C for minutes until the number of cells had doubled (measured using a spectrophotometer). 25 µl 1M IPTG was added to one of duplicate flasks to stimulate 15-PGDH production. The flasks were grown for a further 6 hours at 37 °C with gentle rotation. 1 ml of cells was aliquoted into microcentrifuge tubes and pelleted at 16,100 x g for 1 minute. The supernatant was discarded and the cell pellets snap-frozen and stored at −80°C until required.

The IPTG-stimulated DE3 pET-15b HPGD cells were used as a positive control for Western blots and the 15-PGDH activity assay. To release the protein the cells were lysed in 100 µl electrophoresis loading sample buffer (60 mM Tris pH 6.8, 10% glycerol, 4% SDS, 100 mM DTT) and further diluted where necessary.

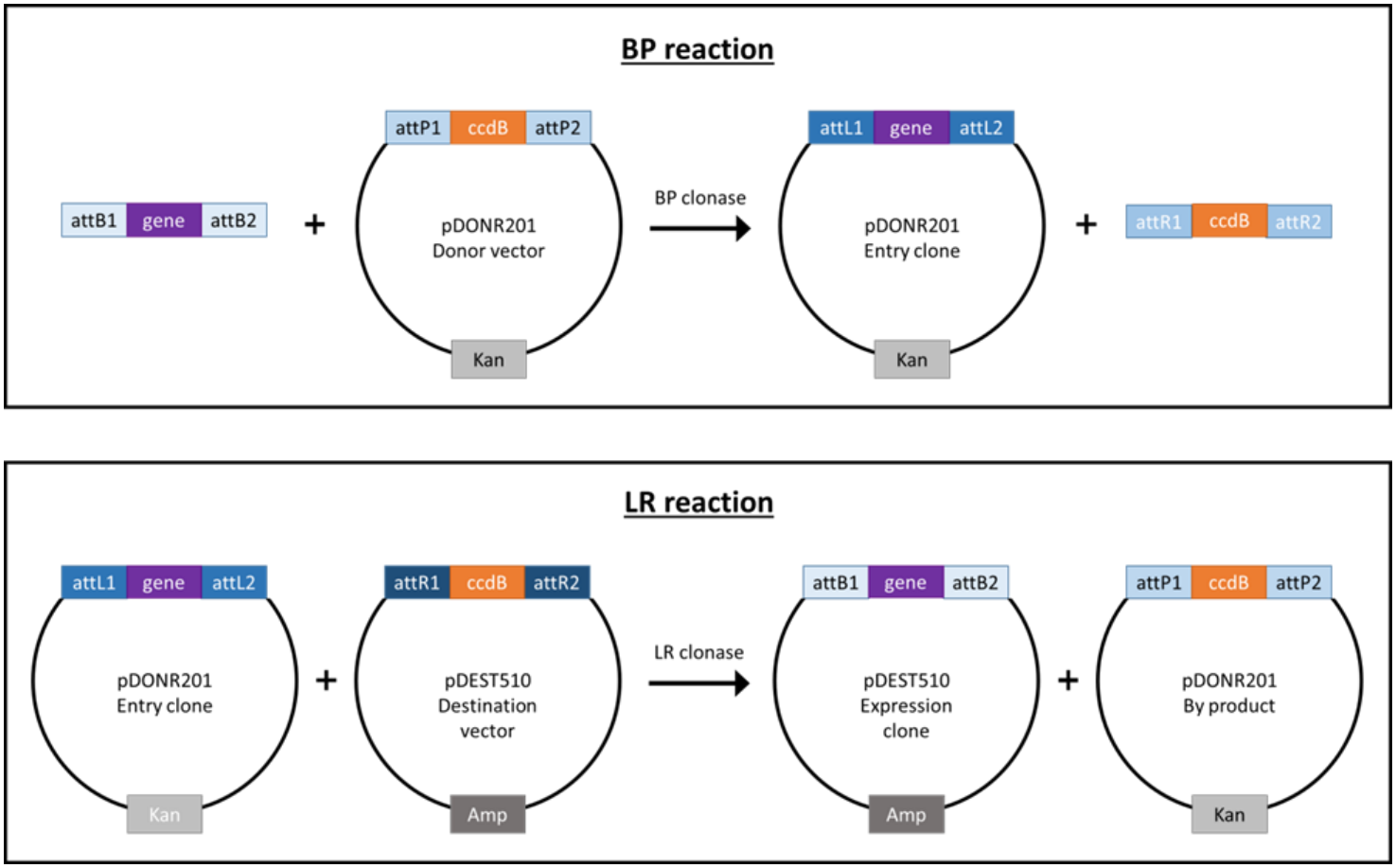

Figure 2.4 Gateway cloning BP and LR reaction. Sequential insertion of a given gene sequence into a donor and destination vector to generate an expression clone. Kan = kanamycin resistance gene, Amp = ampicillin resistance gene, att = recombination sequences, *ccdB* = *ccdB* gene.

2.5 Protein methods

2.5.1 Cell line protein extraction

Cells were grown in a T75 flask until 80% confluent. The media was then removed and the cells washed in ice cold PBS. Cells were lysed by the addition of 1 ml lysis buffer and incubation on ice for 10 minutes. Lysis buffer comprises of 10 ml RIPA buffer (0.1% SDS, 1 mM EDTA, 50 mM Tris-HCl pH 8.0, 150 mM sodium chloride, 1% NP-40, 0.5% sodium deoxycholate), 500 µl PhosStop phosphatase inhibitor (Roche, Basel, Switzerland), 100 µl P8340-protease inhibitor (Sigma) and 10 µl 0.1 M DTT. The cell lysates were scraped from the flask and transferred to a 1.5 ml microcentrifuge tube and centrifuged at 16,100 x g for 20 minutes at 4°C. The supernatant containing the proteins was transferred to a fresh microcentrifuge tube and stored at −80°C until required.

2.5.2 Protein quantification

Cell line protein extracts were quantified in duplicate using the Pierce BCA protein assay kit (Thermo Scientific). The colorimetric assay uses the Biuret reaction, where the reduction of Cu^{+3} to Cu^{+2} by proteins in an alkaline solution produces a purple product. The protein concentration is directly proportional to the colour intensity of the resulting solution. Briefly, 25 µl of sample or bovine serum albumin (BSA) protein standard (0-2000 ng) was added to two wells of a 96-well plate (Corning). Controls containing only the relevant buffer e.g. RIPA buffer, were added to account for background absorption. The BCA working solution was prepared (200 µl BCA reagent A and 4 µl BCA reagent B per sample) and 204 µl added per well. The samples were incubated at 37°C for 30 minutes and the absorbance measured at 540 nm using a Mithras LB 940 plate reader (Berthold).

2.5.3 Western blotting

Protein samples were prepared and quantified as described in Sections 2.5.1 and 2.5.2. The samples were then diluted to contain 20-25 µg total cell line lysate in 20 µl. *E.coli* control samples were generated as described in Section 2.4.6 and diluted to the appropriate concentration in 20 µl. 5 µl of 4x NuPAGE loading buffer (Invitrogen) was added to all samples, and then heated to 100°C for 5 minutes to denature the proteins. They were immediately placed on ice for 5 minutes and briefly centrifuged to collect the condensation.

A Novex 4-12% NuPAGE Bis-Tris polyacrylamide gel (Invitrogen) was prepared by removing the comb and plastic strip and rinsing the wells with water to remove any residual salts or gel. The electrophoresis tank was set up with 1x NuPAGE MOPS SDS running buffer (Invitrogen). 25 µl of sample was loaded into each well alongside 10 µl of SeeBlue Plus2 (Thermo Fisher) or Precision Plus protein ladder (Bio-Rad). The gels were run for 60 minutes at 180 V or until the loading dye had reached the bottom of the gel.

Meanwhile, the Amersham Hybond P Western blotting PVDF membrane (0.45 µm pore) was pre-activated by soaking for 10 seconds in methanol then washed twice in dH_2O for 5 minutes and then soaked in transfer buffer (1x NuPAGE transfer buffer (Invitrogen), 10% methanol in water) for 20 minutes. The SDS gel was then removed from the cassette and the proteins were transferred onto an Amersham Hybond P Western blotting PVDF membrane in NuPAGE transfer buffer (Invitrogen) using an XCell II blot module (Invitrogen) for 90 minutes at 30 V. Once the proteins had transferred, the membrane was stored in PBS at 4°C for up to two weeks.

The membrane was blocked in 5% non-fat milk (Marvel) in PBS for 1 hour at room temperature with gentle rocking. The primary antibody was diluted in 3 ml of 1% non-fat milk in PBS to the concentration stated in Table 2.9 below. The membrane was transferred to a 30 ml falcon tube and incubated with the diluted primary antibody for one hour at room temperature with constant rotation. The membrane was then washed three times in PBS with 0.1% Tween-20 (PBS-T) for 5 minutes with gently rocking. The HRP-conjugated secondary antibody was diluted in 3 ml 1% non-fat milk and incubated with the membrane for 1 hour at room temperature with rotation (Table 2.9). A further three washes in PBS-T for 5 minutes were completed before visualisation by chemiluminescent detection.

The membrane was developed using either SuperSignal West Pico or Femto Chemiluminescent Substrate (Thermo Scientific) (Table 2.9). Images were taken of the membrane using a Bio-Rad ChemiDoc MP imaging system with exposures between 1 second to 20 minutes depending upon the signal intensity. The detected bands were quantified using the Image Lab software as described in Section 2.5.3.1.

Due to low expression of 15-PGDH a more sensitive detection method was performed with the SuperSignal West Femto Chemiluminescent Substrate and Amersham Hyperfilm ECL (G E Healthcare). The film was exposed to the membrane for 60 seconds to 90 minutes depending upon the strength of the signal and developed using a Konica SRX-101A cold water film processor.

Table 2.9 Antibodies used for Western blotting

1°/2° antibody	Antibody	Catalogue number	Stock concⁿ	Working dilution	Chemiluminescent kit
1°	HPGD	HPA005679 (Atlas)	0.1mg/ml	1:50	Femto
1°	PCDH7	TA505452S (Origene)	1mg/ml	1:2000	Femto
1°	B-actin	E4156 (Sigma)	1mg/ml	1:1000	Pico
2°	Donkey anti-rabbit	A21207 (Thermo Scientific)	2mg/ml	1:500	
2°	Rabbit anti-mouse	A11029 (Thermo Scientific)	2mg/ml	1:500	

2.5.3.1 Western blot quantification

Western blot images taken on the ChemiDoc were quantified using the ImageLab software. The image file was opened in ImageLab and the lanes and bands for each sample were identified. Once these had been selected the analysis table was generated and exported into excel. The ImageLab software's Volume (Int) parameter was used to calculate the ratio between the β-actin loading control and the gene of interest.

2.5.4 Coomassie Blue protein gel

A Novex 4-12% NuPAGE Bis-Tris polyacrylamide gel was run as described in Section 2.5.3. The gel was then removed from the cassette and submerged in Coomassie Blue working solution (0.2% Coomassie Blue R-250 (Fisher Scientific), 10% glacial acetic acid and 45% methanol in water). The gel was incubated for 30 minutes at room temperature whilst gently shaking. The blue dye was then removed and replaced with a de-stain solution (5% methanol and 7.5% acetic acid in water) overnight. The de-stain was replaced with fresh solution for one hour, before imaging the gel using the Bio-Rad Gel Doc.

2.5.5 Immunocytochemistry

Cells were seeded onto 22 mm x 22 mm cover slips sterilised with 70% ethanol in 6 well plates (Corning) at $2x10^5$ cells/well and left to adhere overnight. Cells analysed after epigenetic drug treatment were seeded as described in the cell line epigenetic drug treatment section (Section 2.1.5) and treated for the described time period. Cells were fixed in 4% paraformaldehyde for 10 minutes, washed three times in PBS and stored in PBS at 4°C for up to two weeks.

Antigen retrieval was performed by incubating the cover slips with 1 ml 0.1% Triton X100 for 4 minutes. The cells was washed twice in PBS to remove any remaining detergent and blocked in

1% non-fat milk (Marvel) in PBS for 45 minutes to prevent non-specific binding. The blocking reagent was removed and 50 µl of the appropriate primary antibody dilution in 1% non-fat milk placed in the centre of the cover slip (see Table 2.10 below). A no primary control was included in all experiments. The cover slip was overlaid with parafilm to avoid the coverslips drying out and incubated at room temperature for 1 hour. The parafilm and primary antibody were removed and the cells washed three times in PBS. 50 µl of the appropriate secondary antibody dilution in 1% non-fat milk (see Table 2.10 below) was placed in the centre of the cover slip, covered with parafilm and incubated at room temperature for one hour. Fluorescently labelled antibodies were incubated in the dark. The secondary antibody solution was removed and the cells washed three times in PBS. For slides that were dual labelled a primary antibody mix was prepared and added as stated above before labelling with an appropriate secondary antibody mixture.

The cover slips were mounted onto Superfrost slides using two drops or Pro-Long Anti-fade mountant with DAPI and left to dry overnight in the dark at room temperature. The coverslips were sealed with nail varnish before imaging with the Zeiss microscope. For long term storage the slides were stored at 4°C in the dark.

Table 2.10 Antibodies used in immunocytochemistry

1°/2° antibody	Antibody	Target	Catalogue number	Stock concⁿ	Recommended dilution (ICC)	Working dilution
1°	HPGD1	15-PGDH	HPA005679 (Atlas)	0.1mg/ml	1:25-1:100	1:50
1°	FLAG-tag	FLAG protein	MAI-91878 (Thermo Sci)	1mg/ml	1:200-1:500	1:200
1°	EEA1	Early endosomal antigen 1	E4156 (Sigma)	1mg/ml	1:100-1:200	1:1000
2°	Donkey anti-rabbit (R)	Rabbit Ab	A21207 (Thermo Sci)	2mg/ml	1:200-1:2000	1:500
2°	Goat anti-mouse (G)	Mouse Ab	A11029 (Thermo Sci)	2mg/ml	1:200-1:2000	1:500

Optimisation was also performed with methanol fixation. The cells were incubated for 10 minutes in ice cold methanol and rinsed three times with PBS. An EEA1 control was performed alongside optimisation experiments as an additional positive control.

2.5.6 Haematoxylin and eosin staining

Paraffin/formalin fixed tissue blocks were sectioned at 5 µm thickness and placed on Superfrost Plus slides. The sections were then baked at 37°C overnight and overlaid with wax where necessary. Tissue sections were dewaxed with xylene for 3x 5 minutes (with an extra 5 minutes

on the first dewax if overlaid with wax), rehydrated in 100% ethanol 3x 1 minute and placed under running water for 5 minutes.

The sections were placed in Mayer's Haematoxylin (Solmedia) for 2 minutes before being rinsed under running water for 1 minute and placed in Scott's tap water (20 g sodium bicarbonate, 3.5 g magnesium sulphate in 1 L dH_2O) to blue the slides for 1 minute. The slides were then rinsed again for 1 minute with running water and counterstained with 1% aqueous eosin (Solmedia) for 1 minute. Following a further 1 minute under running water, the slides were dehydrated in 100% ethanol for 3x 2 minutes and xylene 3x 2 minutes. The sections were mounted using xylene based mountant, DePex (Merck).

2.5.7 Immunohistochemistry

The slides were prepared, dewaxed and rehydrated as described in the haematoxylin and eosin section (Section 2.5.6). Antigen retrieval was performed by microwaving the slides in pre-heated antigen retrieval buffer (10 mM trisodium citrate pH 6.0 with citric acid) for 10 minutes on high power before being allowed to cool for 20 minutes. The antigen retrieval buffer was displaced under running water for 5 minutes.

An endogenous peroxidase block was completed by immersing the slides in 1.2% (v/v) hydrogen peroxidase in methanol for 20 minutes at room temperature. The slides were placed in running water for 5 minutes and washed with PBS for 5 minutes. The slides were further blocked using 1x casein in Invitrogen antibody diluent for 20 minutes at room temperature.

The primary antibody was prepared at the concentrations stated in Table 2.11 below using antibody diluent. 100µl of antibody or diluent only control was pipetted onto each slide and incubated at the temperature and time stated in Table 2.9 in a humidity chamber to avoid the slides from drying out. The slides were washed 3x 5 minutes in PBS-T and 1x 5minutes in PBS.

The slides were then incubated for 40 minutes at room temperature with a HRP conjugated polymer (secondary) from the rabbit or mouse Envision kit (Dako). The slides were washed as described above and the slides stained with 100 µl 3,3'-Diaminobenzidine (DAB) working solution (20 µl DAB in 1 ml DAB substrate) at room temperature for 15 minutes. The slides were washed in running tap water for 5 minutes and stained with Mayer's Haematoxylin as described in the H and E Section. The slides were then dehydrated in three ethanol baths for 2 minutes each, and three xylene baths for 2 minutes each before mounting as described earlier.

Table 2.11 Antibodies used in immunohistochemistry

Antibody	Target	Type	Catalogue number	Stock conc^{n}	Working dilution	Incubation length (hrs)	Incubation temp.
HPGD1	15-PGDH	Rabbit polyclonal	HPA005679 (Atlas)	0.1mg/ml	1:50	17	4°C
FLAG-tag	FLAG protein	Mouse monoclonal	MAI-91878 (Thermo Sci)	1mg/ml	1:200	1	RT
CD68	CD68 macrophage marker	Mouse monoclonal	M0814 (Dako)	0.185mg/ml	1:3000	1	RT
IgG control	N/A	Rabbit polyclonal	AB-105-c	1mg/ml			

2.5.8 Immunohistochemistry dual staining

Dual stain immunohistochemistry was performed with the HPGD1 antibody and a macrophage marker (CD68) to assess whether the isolated cell staining with HPGD1 was in macrophages. Dual staining was completed using the Dako EnVision G|2 Doublestain System - Rabbit/Mouse DAB+/Permanent Red kit (K5361).

The primary breast tissue sections were dewaxed and rehydrated and microwave antigen retrieval performed as described in the standard immunohistochemistry section. Endogenous alkaline phosphatase, peroxidase, and pseudoperoxidase activity was blocked by adding 100 µl of the kits dual endogenous enzyme block for 5 minutes at room temperature. The slides were washed in tris-buffered saline (TBS) for 5 minutes and non-specific protein binding was blocked using the casein blocked as described in the standard IHC section (Section 2.5.7).

The CD68 macrophage marker primary antibody (M0814) was diluted 1:3000 in antibody diluent and 100 µl added to the slides for 1 hour at room temperature. The slides were washed three times in tris-buffered saline with 0.05% Tween-20 (TBS-T) for 5 minutes and TBS for 5 minutes at room temperature. Next they were incubated for 10 minutes at room temperature with the Polymer/HRP reagent that binds to both mouse and rabbit antibodies, after which they were washed as described earlier. The samples were incubated with DAB+ working solution (20 µl DAB to 1 ml DAB substrate) secondary for the HPGD1 antibody for 15 minutes at room temperature and the slides rinsed in running tap water for 5 minutes. Next the slides were incubated with 100 µl Doublestain Block for 3 minutes at room temperature and washed with TBS-T and TBS as described earlier.

15-PGDH antibody was prepared in antibody diluent and 100 µl of 1:50 dilution added per slide for 17 hours at 4°C in a humidify chamber. The slides were washed as described previously and incubated with 100 µl of Rabbit/Mouse LINK for 10 minutes at room temperature. The samples

were washed as stated earlier and incubated with 100 µl of Polymer/AP for 10 minutes at room temperature and rinsed again. The secondary Permanent Red working solution was prepared and 100 µl added for 25 minutes at room temperature, followed by 5 minutes of rinsing until running tap water.

The slides were counterstained with haematoxylin as described in the standard immunohistochemistry section and due to fading of the permanent red stain dehydrated by heating to 70°C for 20 minutes on a hot block. The slides were then immersed in xylene and mounted as described previously with DePex.

2.5.9 15-hydroxyprostaglandin dehydrogenase activity assay

15-PGDH catalyses the metabolism of prostaglandins through oxidation of the 15(S)-hydroxyl group to form their 15-keto metabolite:

$$PGE_2 + NAD(+) \xrightarrow{\text{15-PGDH}} \text{15-keto-}PGE_2 + NADH + H^+$$

The activity of 15-PGDH in MCF7 stable over-expressing clones was assessed by measuring the rate of NADH formation at 340nm with a 1-cm light path using a Beckman Coulter DU800 spectrophotometer. The assay was adapted from Uppal et al. 2008.

Firstly, cells were grown to 80% confluency, the media removed and the cells washed twice in PBS. The cells were lysed in 300 µl lysis buffer (50 mM Tris-HCl pH8, 5 mM EDTA, 0.1% Triton-X100, 1 mM DTT, 1 mM PMSF and 1:100 P3480 protease inhibitor) and transferred to a microfuge tube. The cell lysate was sonicated for 5 seconds, and the debris pelleted by centrifugation at 16,100 x g for 10 minutes at 4°C. The supernatant from the protein lysate was used in the following assay.

The assay reaction mixture contained 600 µl assay buffer (50 mM Tris-HCl pH 7.5, 1 mM DTT), 60 µl total protein lysate, 12 µl NAD(+) (Sigma) and 0.6 µl 100 mM PGE_2 or DMSO as a control was created by sequentially adding each component and measuring the solutions absorbance for several minutes or until the absorbance reading had levelled off before adding the next component and finally adding the PGE_2 after which the absorbance was read every minute up to 60 minutes.

The Beer Lambert Law was used to calculate the average concentration of NADH produced per minute over a 20 minute interval using the formula below:

$$Concentration\ (mol/L) = \frac{Absorbance\ change\ at\ 340nm\ (A)}{Molar\ absorptivity\ extinction\ coefficient\ (l\ mol^{-1}\ cm^{-1})\ \times Path\ length\ (cm)}$$

NADH molecular absorptivity extinction coefficient = 6220 l mol^{-1} cm^{-1}. Path length = 1 cm.

The data was then normalised to β-actin protein concentration from the Western blot

2.6 Statistical analysis

All statistical analysis was performed using the GraphPad Prism software (Graph Pad Software). One-way analysis of variance (ANOVA) was performed to assess individual differences between group means. In the case of the proliferation assays a two-way ANOVA was performed to assess the significance between the two clones. The Tukey Test was used to calculate the significant difference between the groups (p value). Chi squared tests were performed to compare observed and expected frequencies of receptor expression and metastatic frequency with the TMA clinical data. When comparing the outcome for two groups a two-tailed Fishers exact test was performed.

Chapter 3 Expression of 15-PGDH in breast cancer

3.1 Introduction

15-PGDH is an important enzyme in prostaglandin metabolism. Decreased expression of 15-PGDH has been observed in several cancers (Backlund et al., 2005; Liu, Z. et al., 2008; Li, Y. et al., 2014; Seo, S.H. et al., 2015; Thiel et al., 2009), yet little focus has been placed on breast cancer and few studies have assessed 15-PGDH protein expression in breast cancer. While little evidence has been published connecting breast cancer progression to enzymes in the prostaglandin pathway, such as 15-PGDH and COX2 at the protein level, if the link does exist it may have important implications for advances in future treatment options. Before it is possible to test for a relationship between breast cancer and 15-PGDH expression the expression profile of the protein in normal and breast cancer tissue must be determined.

3.1.1 Aims

The aim of this chapter was to gain a better understanding of 15-PGDH expression in breast cancer in order to assess the potential of increasing 15-PGDH expression as a treatment option. The objectives were as follows:

1. Determine the level of expression on 15-PGDH in primary breast cancer tissue samples and breast cancer cell lines
2. Assess whether there are any links between 15-PGDH expression and other clinical features such as cancer type
3. Determine the expression of other components of the prostaglandin pathway in breast cancer

3.2 Methods

3.2.1 RT-PCR

Conventional RT-PCR was performed to determine the *HPGD* mRNA expression and other components of the prostaglandin pathway in a selection of breast cancer cell lines as described in Section 2.2.9.

3.2.2 qRT-PCR

HPGD mRNA expression was also assessed by qRT-PCR for selected cell lines as described in Section 2.2.10.

3.2.3 Western blotting

Optimisation of the 15-PGDH antibody to be used for immunohistochemistry, immunocytochemistry and Western blotting was initially done by Western blotting. Three antibodies raised to different 15-PGDH peptide sequences were tested to determine their specificity. The antibodies were given the name HPGD1-3 (Table 3.1). Western blotting was performed as described in Section 2.5.3 using a 15-PGDH expressing *E.coli* clone and A549 as positive controls alongside the breast MCF7 cell line lysate.

3.2.4 Haematoxylin and eosin staining

Breast tissue sections showing 15-PGDH expression were stained with haematoxylin and eosin for structural visualisation and pathological analysis. This was performed by Angie Berwick on behalf of the Breast Cancer Now Tissue Bank.

3.2.5 Immunohistochemistry

3.2.5.1 Tissue Microarray (TMA)

Primary breast cancer tissue microarrays were labelled with 15-PGDH antibody to determine the 15-PGDH expression levels. Immunohistochemistry was performed as described in Section 2.5.7 using the antibodies listed in Table 3.2.

TMA1 was generated for the Adjuvant Zoledronic Acid to Reduce Recurrence (AZURE) clinical trial. The AZURE clinical trial aimed to assess whether adjuvant zoledronic acid reduced the recurrence in patients with high risk localised breast cancer (Coleman, R.E. et al., 2011; Coleman, R. et al., 2011). The TMA contains patient samples with stage II or III early-stage breast cancer, although it is not known whether the samples were collected prior to or after treatment.

TMA1 was solely used for optimisation of the 15-PGDH antibodies. It was stained with both HPGD1 and HPGD2 antibodies to determine the most reliable antibody for immunohistochemistry. HPGD1 and HPGD2 staining intensity was scored between 0-3 (0 being no staining, 3 being strong staining), and the percentage of breast cancer cells stained recorded. The percentage of cells and the staining intensity were then multiplied together to give a score out of 300. Scoring criteria was established in collaboration with pathologist Dr Laura Wastall.

Table 3.1 15-PGDH Western blot antibodies

Antibody	Company	Catalogue number	Stock conc^{n}	Working dilution	Immunising peptide sequences
Rabbit anti-15-PGDH (HPGD1)	Atlas	HPA005679	0.1mg/ml	1:250	LAANLMNSGVRLNAICPGFVNTAILESIEKEENMGQYIEYKDHIKDMIKYYGI
Rabbit anti-15-PGDH (HPGD2)	Novus Biologicals	NBP1-87062	0.05mg/ml	1:250	VDWNLEAGVQCKAALDEQFEPQKTLFIQCDVADQQQLRDTFRKVVDHFGRLDILVNNAGVNNEKNWEKTLQINLVSVISGTYLGLDYMSKQNGGEGGIIINMSSLAGLMPVAQQPV
Rabbit anti-15-PGDH (HPGD3)	Cayman Chemical	160615	1µg/µl	1:200	AGVNNEKNWEKTLQ
Mouse anti-β-actin	Abgent	A0125a	Unknown	1:1000	Not available
Swine anti-rabbit HRP conjugated	Dako	P0217	1.3g/L	1:130000	
Goat anti-rabbit HRP conjugated	Dako	P0448	0.25g/L	1:25000	
Rabbit anti-mouse HRP conjugated	Dako	P0260	1.3g/L	1:2500	

Table 3.2 Immunohistochemistry antibodies

Antibody	Company	Catalogue number	Stock conc^{n}	Working dilution	Immunising peptide sequences
HPGD1	Atlas	HPA005679	0.1 mg/ml	1:50	LAANLMNSGVRLNAICPGFVNTAILESIEKEENMGQYIEYKDHIKDMIKYYGI
CD68	Dako	M0814	185mg/L	1:3000	Unknown
COX2	Cayman Chemical	160126	1 mg/ml	1:50	Unknown
HIF-1α	Novus Biologicals	NB100-105	1 mg/ml	1:20	Unknown

A comparison was completed between 75 matched cores on the HPGD1 and HPGD2 labelled TMA1 slides. Following optimisation of the 15-PGDH antibodies the HPGD1 antibody was taken forward for future immunohistochemistry experiments.

15-PGDH expression in primary breast cancer was assessed using six graded TMA slides. The TMAs used were generated for general research purposes and consisted of two grade one, two grade two and two grade three primary breast cancer TMA slides. As TMAs were generated in the 1990's, limited clinical data was available for the samples. Where possible, data regarding patient age at diagnosis, hormone receptor status, metastasis and breast cancer related death was recorded. A total of 64 grade one, 109 grade two and 80 grade three patient samples were assessed. 15-PGDH labelling was scored by categorising them into the following groups; strong staining, intermediate staining, individual cell staining and no staining. Each patient sample consisted of three cores, therefore the strongest staining pattern observed out of the three cores was taken as the overall staining. Scoring was double checked by consultant pathologist, Professor Andrew Hanby.

3.2.5.2 Large breast tissue samples

Immunohistochemistry was performed with larger primary breast cancer tissue samples selected from the graded TMA slides. The samples were stained with 15-PGDH (HPGD1), CD68, COX2 and HIF-1α antibodies in Table 3.2 to assess the protein expression as described in Section 2.5.3. Samples were graded according to the Nottingham histological staging system (Rakha et al., 2010) by consultant pathologist, Professor Andrew Hanby.

3.2.5.3 Dual labelling immunohistochemistry with 15-PGDH and CD68 antibodies

To assess whether 15-PGDH isolated cell staining was in macrophages, immunohistochemistry dual staining was performed as described in Section 2.5.8 with macrophage marker CD68 and 15-PGDH (HPGD1) antibodies.

3.2.6 Immunocytochemistry

15-PGDH antibody optimisation for immunocytochemistry was performed using HPGD1 and HPGD2 antibodies with both 4% PFA and methanol fixation steps as described in Section 2.5.5. Further immunocytochemistry experiments were completed using HPGD1 antibody with 4% PFA fixation.

3.2.7 Coomassie gel

A 15-PGDH positive *E.coli* control generated as described by Uppal et al. (Uppal et al., 2008) was used in the Western blot experiments. A Coomassie stained SDS polyacrylamide gel was performed as described in Section 2.5.4 to confirm successful over-expression of 15-PGDH.

3.2.8 Pathological analysis

Haematoxylin and eosin stained primary breast cancer tissue was assessed by Professor Andrew Hanby and the samples graded using the Nottingham histologic grading system (Rakha et al., 2010).

3.2.9 Tissue ethics approval

All of the human tissue samples used in the project were ethically approved. The breast tissue was obtained from the Leeds Breast Tissue bank and ethical approval was granted from Leeds East research ethics committee (REC) (09/H1306/108), or provided by Professor Andrew Hanby under Leeds East REC (06/Q1206/180). The normal human colon used to optimise the antibody provided by Professor Philip Quirke had Local Ethical Approval (08/H1313/84).

Kidney tissue used for antibody optimisation was a totally anonymised sample obtained from pathology for quality assurance. The sample was originally obtained from the Leeds GIFT Research Tissue project.

3.2.10 Clinical data analysis

Statistical analysis was performed using GraphPad software. Chi squared tests were performed to compare observed and expected frequencies of receptor expression and metastatic frequency. When comparing the outcome for two groups a two-tailed Fishers exact test was performed.

3.2.11 15-PGDH positive control cell line

RNA and protein extracted from A549, a lung cancer cell line, that is known to express high levels of 15-PGDH was used as a positive control for a number of RNA and protein based expression assays.

3.3 Results

3.3.1 *HPGD* mRNA expression in breast cell lines

Conventional RT-PCR was performed on total RNA extracted from a panel of breast cell lines to determine approximate 15-PGDH expression levels (Figure 3.1). RNA from the A549 lung carcinoma cell line was used as the positive control.

Low levels of 15-PGDH were seen in all of the breast cancer cell lines, with a faint band in MDA-MB-231, SKBR3 and MCF7 cancer cell lines as well as non-malignant breast cell line MCF10A. No trend was observed between the non-malignant cell lines (MCF10A and HB2) and the cancerous cell lines.

qRT-PCR using mRNA extracted from lung, colorectal and breast cell lines show the low level of 15-PGDH expression in breast cell lines. A ~300 fold difference in expression is observed between the A549 lung cell line in comparison to the MCF7 and MDA-MB-231 breast cell lines. A ~7 and ~70 fold difference is seen in the colorectal cell lines.

3.3.2 Optimisation of 15-PGDH antibody

Three different 15-PGDH antibodies were assessed for use in immunohistochemistry. While each antibody binds to a different 15-PGDH epitope, the epitopes of HPGD2 and HPGD3 antibodies overlapped (Table 3.1 and Figure 3.2). Initially, for antibody validation, the antibody specificity was assessed by Western blotting using the three 15-PGDH antibodies with A549 used as the positive control (Figure 3.3).

A strong band was seen at 29-31 kDa in the A549 cell line for the HPGD1 Atlas antibody after 10 minutes exposure and a weaker band seen with HPGD2 labelling. A large amount of background was seen with the HPGD3 antibody and a second band at ~52 kDa was seen with the HPGD2 antibody in the cell line lysates. A faint band was also observed in the no primary control around 35 kDa. Although no 15-PGDH specific band was detected in the MCF7 breast cancer cell lines, the HPGD1 antibody showed the most specific binding and was more sensitive compared to the other antibodies tested.

Optimisation of the antibodies for immunocytochemistry was also performed by titrating the antibody and comparing two fixation methods with methanol (Figure 3.4 and Figure 3.5) or 4% PFA (Figure 3.6 and Figure 3.7). An early endosomal antigen 1 (EEA1) positive control, also a rabbit polyclonal antibody, was also used.

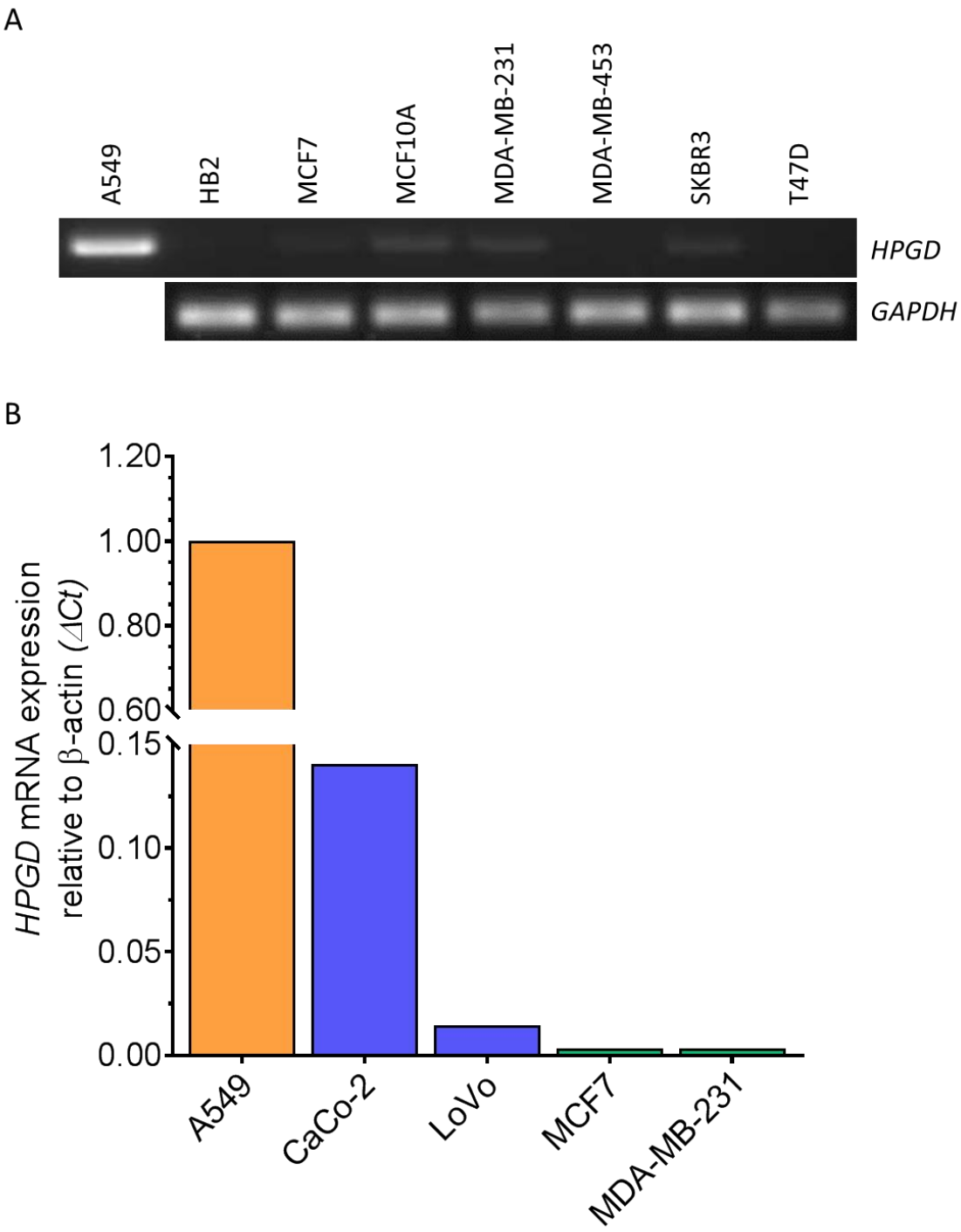

Figure 3.1 *HPGD* mRNA expression using conventional RT-PCR and qRT-PCR in cell lines. (A) *HPGD* and *GAPDH* mRNA expression in breast cell lines using conventional RT-PCR. *HPGD* = 38 cycles, *GAPDH* = 28 cycles. (B) *HPGD* mRNA expression normalised to β-actin endogenous control with qRT-PCR. Orange = lung cell lines, blue = colorectal cell lines, green = breast cancer cell lines. Low expression of *HPGD* mRNA seen in breast cell lines compared to both lung and colorectal cancer cell lines.

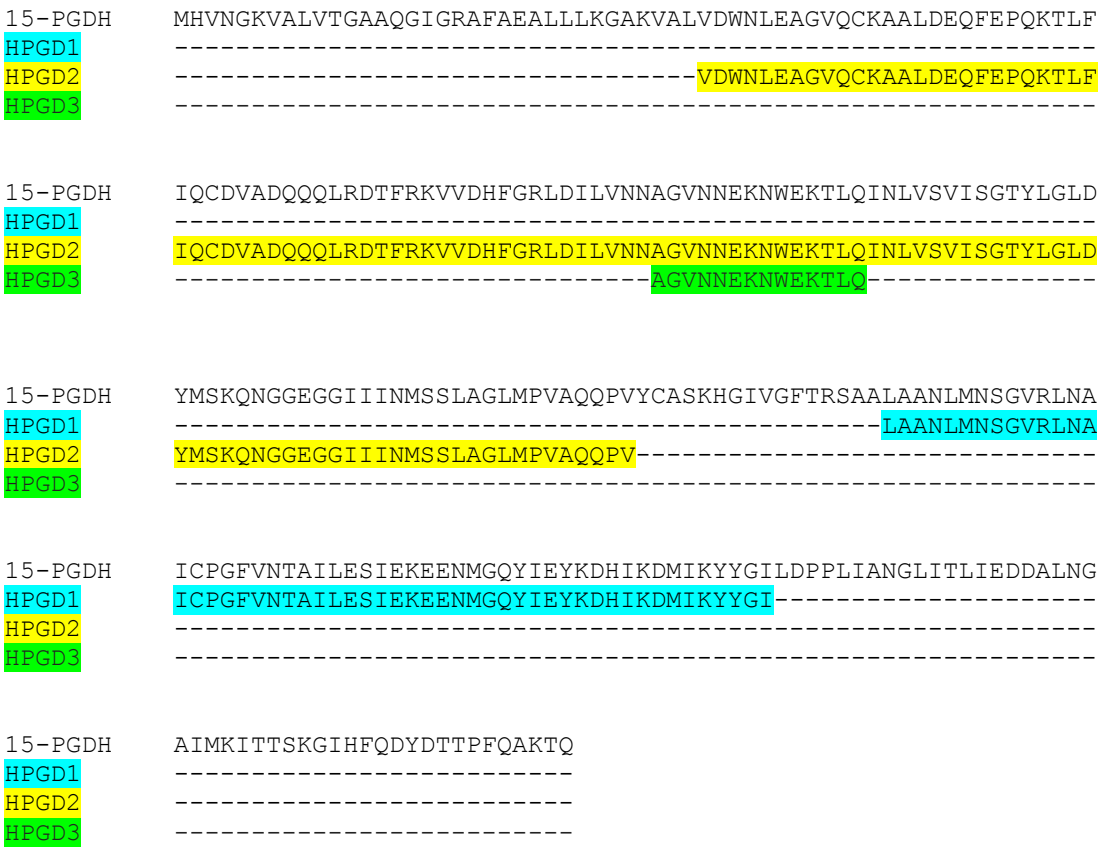

Figure 3.2 15-PGDH antibody immunising peptide sequences. A comparison of the immunising peptide sequence for the three 15-PGDH antibodies tested in this study. Line 1 = 15-PGDH amino acid sequence. Line 2 = HPGD1 (blue) Atlas anti-15-PGDH antibody immunising peptide sequence. Line 3 = HPGD2 (yellow) Novus biological anti-15-PGDH antibody immunising peptide sequence. Line 4 = HPGD3 (green) Cayman Chemical anti-15-PGDH antibody immunising peptide sequence.

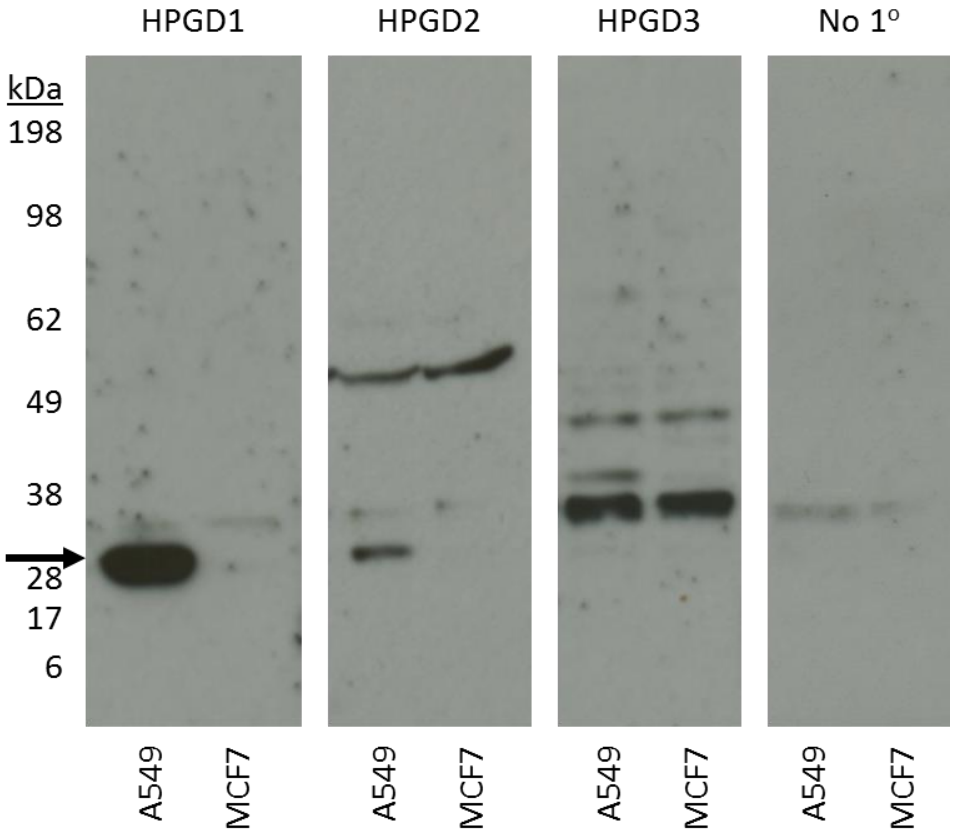

Figure 3.3 Western blot 15-PGDH antibody optimisation. A comparison of 15-PGDH labelling with the three different antibodies using Western blotting following. Results shown after 10 minutes exposure. HPGD1 = Atlas antibody, HPGD2 = Novus biologicals antibody, HPGD3 = Cayman Chemical antibody. 15-PGDH predicted band size = ~29-31 kDa. HPGD1 shows the most specific labelling with only one band at the correct size in the A549 positive control

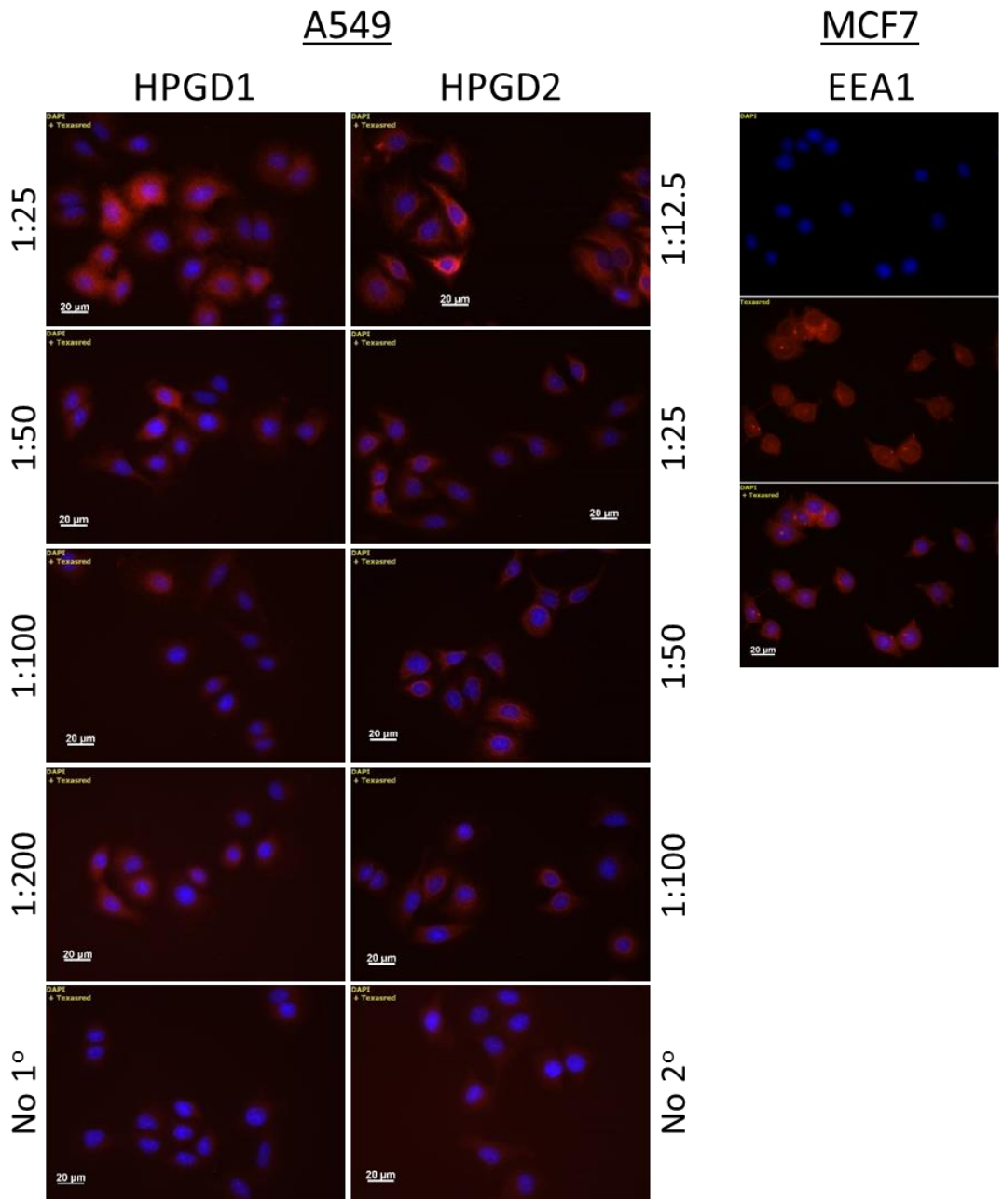

Figure 3.4 Immunocytochemistry optimisation with A549 cell line using methanol fixation. Stronger labelling with HPGD1 at 1:25 concentration. Blue = DAPI nuclear stain, red = 15-PGDH labelling with HPGD1 or HPGD2 antibodies, or the positive control early endosome antigen 1 (EEA1) labelling (centre). Additional controls were the no 1° where the primary antibody was omitted but the secondary antibody was present, and the no 2°, where both the primary and secondary antibodies were absent. The scale bar represents 20 µm. Exposure times were as follows: HPGD1 DAPI = 9 ms, Texas Red = 899 ms, HPGD2 DAPI = 6 ms Texas Red = 503 ms and EEA1 DAPI = 7 ms Texas Red = 894 ms. The exposure was kept consistent between images for the same antibody.

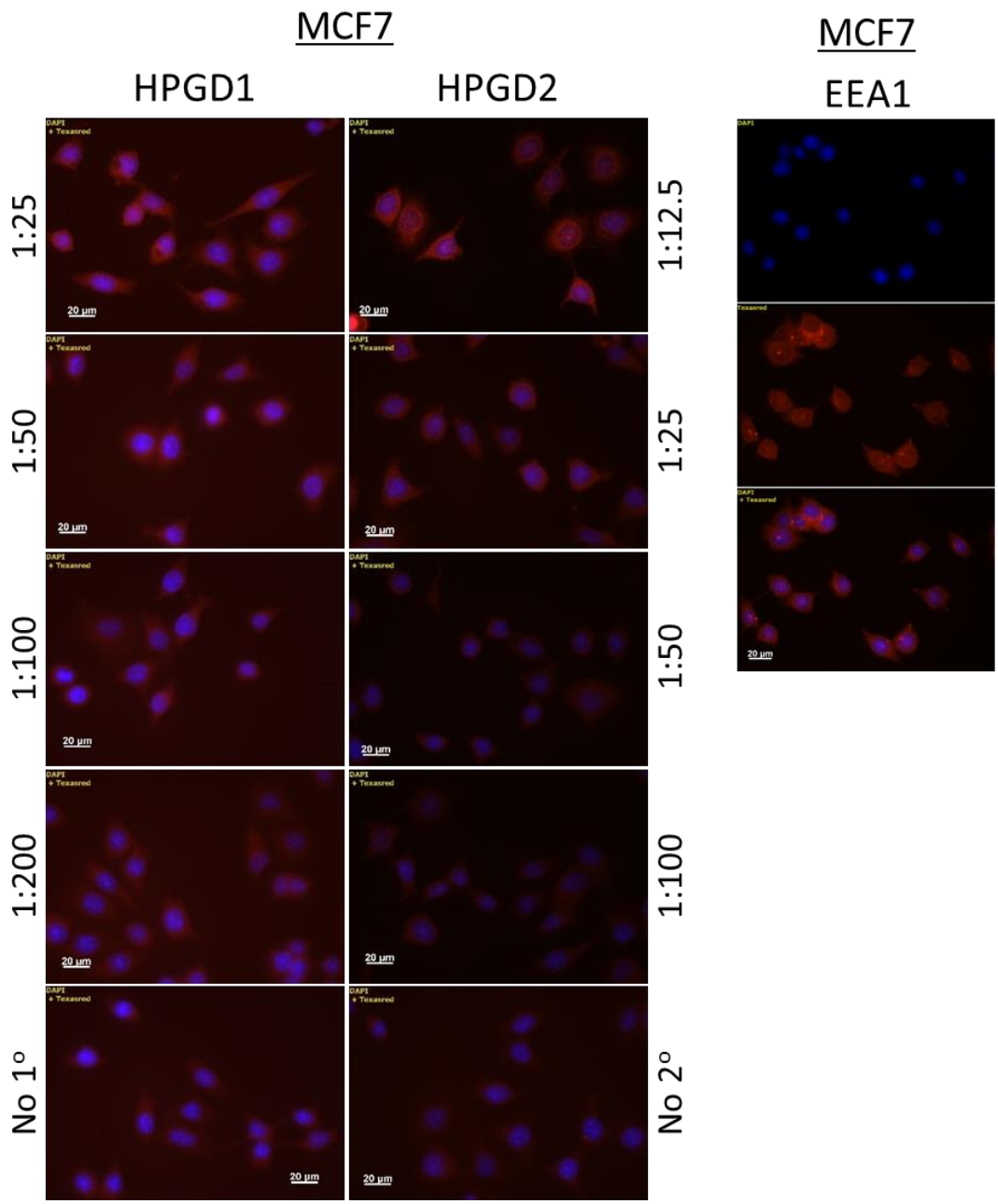

Figure 3.5 Immunocytochemistry optimisation with MCF7 cell line using methanol fixation. Background 15-PGDH labelling with both HPGD1 and HPGD2 antibodies. Blue = DAPI nuclear stain, red = 15-PGDH labelling with HPGD1 or HPGD2 antibodies, or the positive control early endosome antigen 1 (EEA1) labelling (centre). Additional controls were the no 1° where the primary antibody was omitted but the secondary antibody was present, and the no 2°, where both the primary and secondary antibodies were absent. The scale bar represents 20 µm. Exposure times were as follows: HPGD1 DAPI = 9 ms, Texas Red = 899 ms, HPGD2 DAPI = 6 ms Texas Red = 503 ms and EEA1 DAPI = 7 ms Texas Red = 894 ms. The exposure was kept consistent between images for the same antibody.

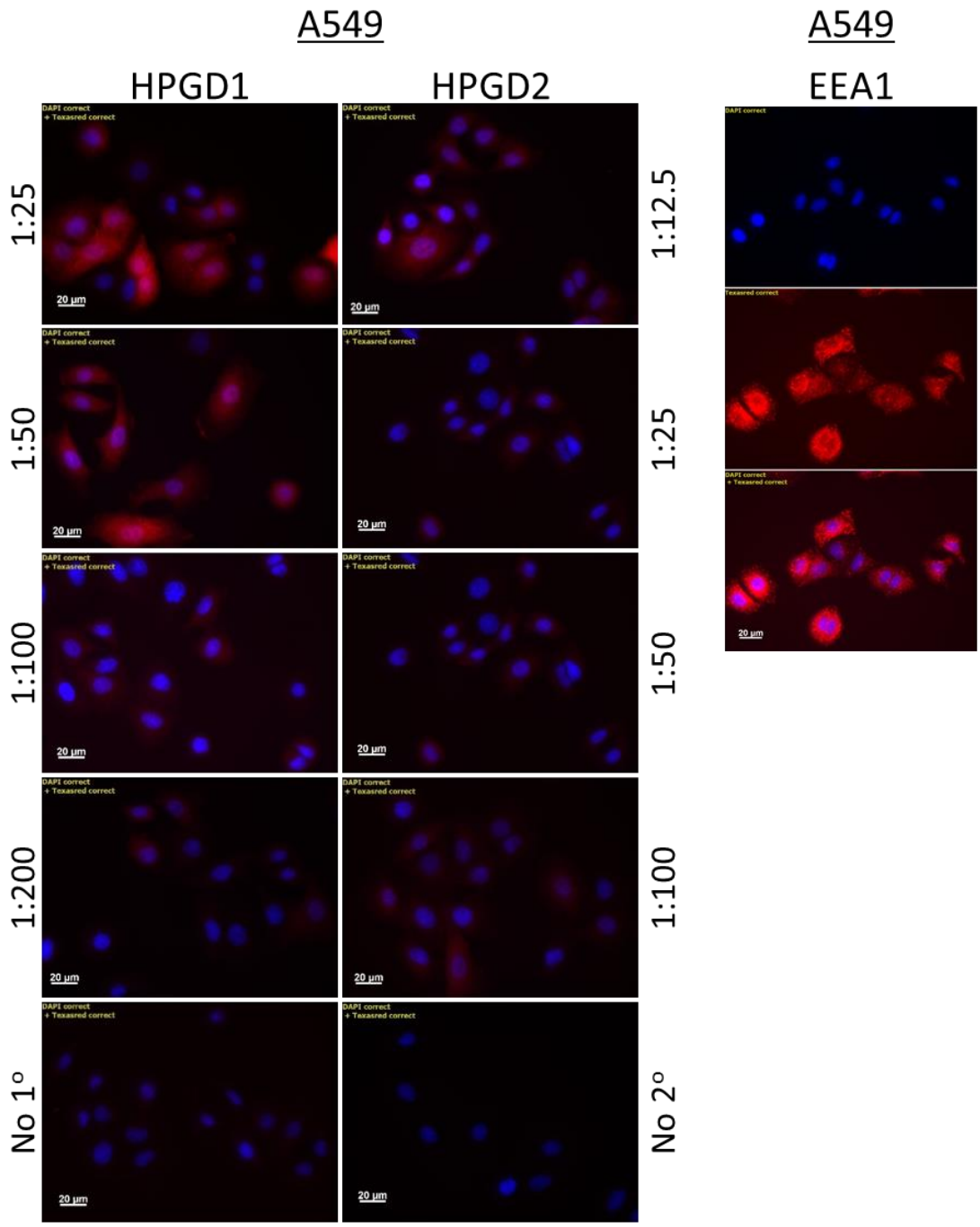

Figure 3.6 Immunocytochemistry optimisation with A549 cell line using 4% PFA fixation. Strong positive labelling in with HPGD1 compared to HPGD2. Blue = DAPI nuclear stain, red = 15-PGDH labelling with HPGD1 or HPGD2 antibodies, or control early endosome antigen 1 (EEA1) labelling (centre) (x40 obj). Additional controls were the no 1° where the primary antibody was omitted but the secondary antibody was present, and the no 2°, where both the primary and secondary antibodies were absent. The scale bar represents 20 µm. Exposure times were as follows: HPGD1 DAPI = 11 ms, Texas Red = 337 ms, HPGD2 DAPI = 10ms Texas Red = 429 ms and EEA1 DAPI = 14 ms Texas Red = 663 ms. The exposure was kept consistent between images for the same antibody.

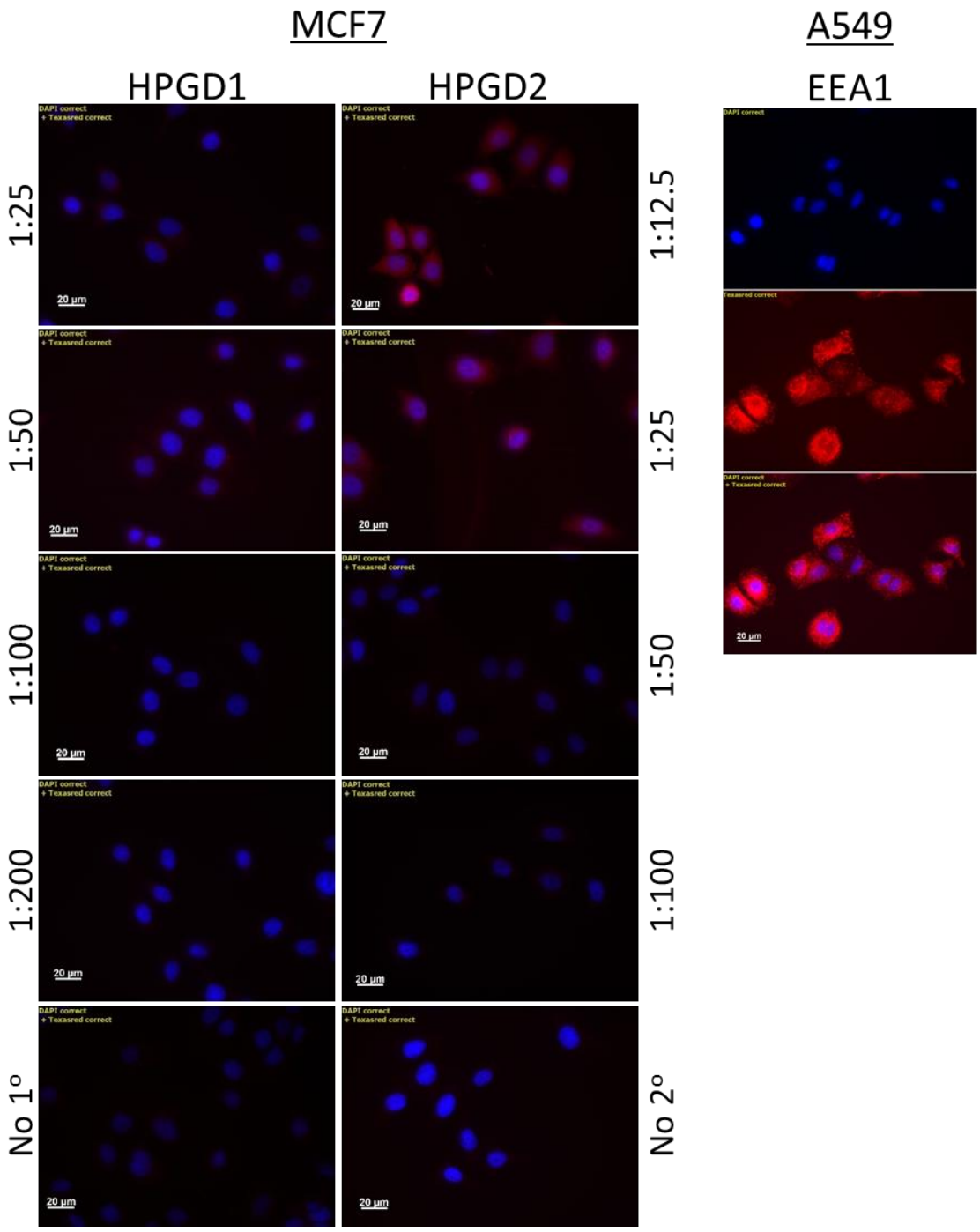

Figure 3.7 Immunocytochemistry optimisation with MCF7 cell line using 4% PFA fixation. Unexpected labelling with HPGD2, no labelling as anticipated with HGPD1. Blue = DAPI nuclear stain, red = 15-PGDH labelling with HPGD1 or HPGD2 antibodies, or control early endosome antigen 1 (EEA1) labelling (centre) (x40 obj). Additional controls were the no 1° where the primary antibody was omitted but the secondary antibody was present, and the no 2°, where both the primary and secondary antibodies were absent. The scale bar represents 20 µm. Exposure times were as follows: HPGD1 DAPI = 11 ms, Texas Red = 337 ms, HPGD2 DAPI = 10ms Texas Red = 429 ms and EEA1 DAPI = 14 ms Texas Red = 663 ms. The exposure was kept consistent between images for the same antibody.

EEA1 generated the expected localisation pattern in MCF7 cells, with cytoplasmic punctate labelling (Geninatti Crich et al., 2015), although this was clearer in the PFA fixed cells.

15-PGDH labelling was mainly cytoplasmic with some nuclear labelling. 15-PGDH labelling was observed in both A549 and MCF7 cell lines with the HPGD2 antibody with both fixation methods at the higher antibody concentrations. In comparison, strong background staining was observed with HPGD1 in the MCF7 cell line with methanol fixation but no labelling was observed with the 4% PFA fixation method. Also, strong 15-PGDH labelling was seen with the A549 cell line with 4% PFA fixation at the higher antibody concentrations tested. Where specific labelling was present the expression level between cells was not always uniform, as some cells within the population had much higher 15-PGDH protein than others. HPGD1 with 4% PFA fixation appeared to show the most specific labelling of 15-PGDH, matching the RT-PCR expression data, therefore these conditions were used in further immunocytochemistry experiments.

IHC was performed with the HPGD1 antibody on a breast cancer and normal breast tissue sample (Figure 3.8). Normal human colon was used as a positive control. Some non-specific staining was observed in the colon control, but the positive staining matched the expected pattern with 15-PGDH localised to the terminaly differentiated epithelial cells of the crypts (Yan et al., 2004). Isolated stromal cell staining was observed with the breast cancer sample with no expression in the epithelial cells.

To gain further information on the expression of 15-PGDH in breast cancer, immunohistochemistry was performed using the 15-PGDH antibodies HPGD1 and HPGD2 on a primary breast cancer TMA slide (Figure 3.9). Each of the antibodies used were IgG isotype, therefore an IgG isotype control was performed to differentiate non-specific background signal from specific antibody binding. Samples G11 and D10 (labelled by position on the TMA) were randomly selected to show the difference in 15-PGDH labelling.

A brown wash was seen in epithelial cells with the majority of the HPGD2 cores, wherease no background staining was seen with HPGD1 antibody. Many of the cores showed positive labelling with the HPGD2 antibody and a score of >150 was seen in 42.67% of TMA cores. On the other hand only 2.67% of the total cores scored >150 with the HPGD1 antibody. Isolated cell staining was observed in both HPGD1 and HPGD2 labelling for sample G11. Positive staining of isolated cell by the HPGD1 antibody was recorded in 36/152 (23.7%) samples.

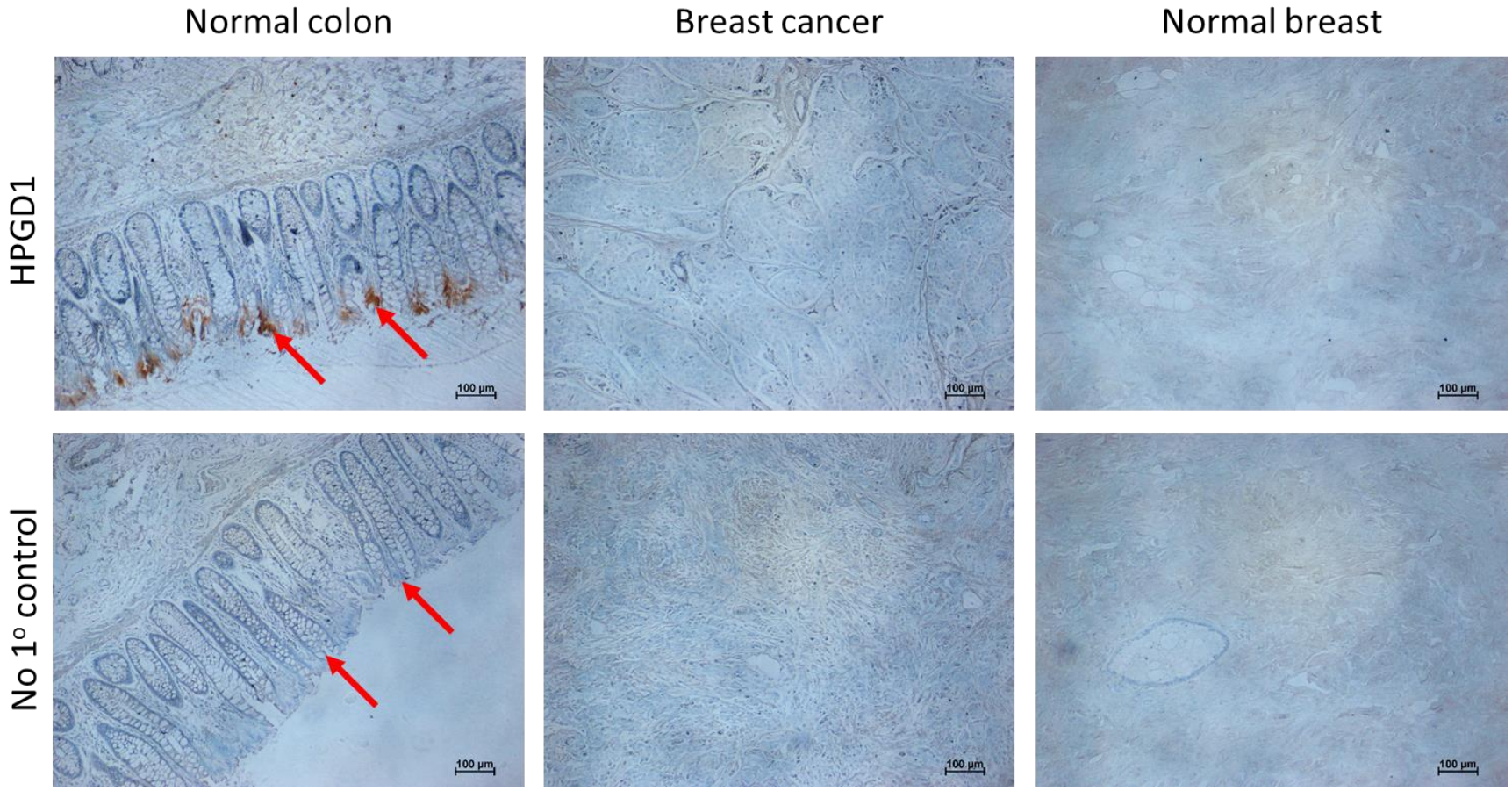

Figure 3.8 IHC with 15-PGDH antibody in malignant and non-malignant breast tissue. HPGD1 (1:100) staining in normal colorectal tissue, breast cancer and normal breast tissue. Scale bar represents 100 µm. Red arrows indicate terminally differentiated cells.

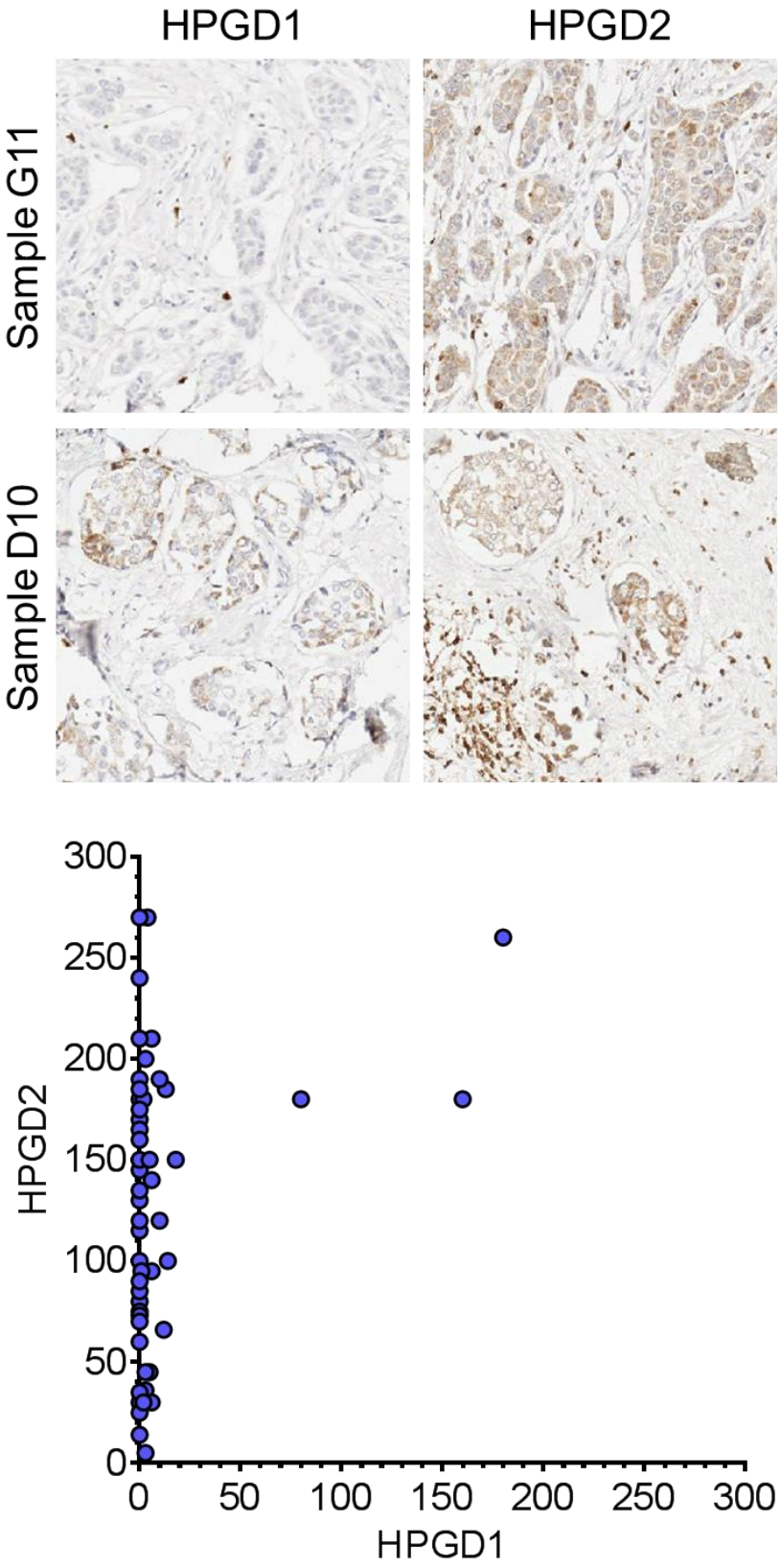

Figure 3.9 15-PGDH expression in primary breast cancer samples using HPGD1 and HPGD2 antibodies. (Top) HPGD1 and HPGD2 antibody staining pattern for the same samples (G11 and D10). (Bottom) Immunohistochemistry staining scores with HPGD1 and HPGD2 primary breast cancer samples. Background labelling seen with HPGD2 which is not seen with HPGD1.

In summary, having assessed three different 15-PGDH antibodies, HPGD1 was identified as the most specific antibody for all three applications by Western blotting, immunocytochemistry and immunohistochemistry. HPGD1 showed strong and specfic labelling for 15-PGDH, matching the expected labelling patterns with the positive controls. For these reasons HPGD1 was used in subsequent experiments.

3.3.3 15-PGDH protein expression in breast cell lines

15-PGDH protein expression was assessed in a selection of breast cancer cell lines using immunocytochemistry and Western blotting. Immunocytochemistry was performed with A549 cells as the positive control and the MCF7 cell line (Figure 3.6). Strong 15-PGDH expression was observed in the lung cell line, whereas no staining was observed with the MCF7 breast cell line.

An additional *E.coli* clone that expresses 15-PGDH was included in the Western blot as a positive control. 15-PGDH over-expression by the *E.coli* clone was induced using IPTG and was confirmed using a Coomassie stained gel (Figure 3.10A). A strong band was observed at ~29-31 kDa in the IPTG induced sample compared to the controls.

A Western blot was performed with the *E.coli* positive control and A549 and MCF7 total protein lysates (Figure 3.10B). Two bands were seen with the *E.coli* positive control samples, one at the expected size and one slightly larger band. The larger band may be the result of the presence of a polyhistidine-tag which was added for easy purification. As before, a strong band was seen in the A549 lung carcinoma positive control, yet no band was seen for the MCF7 cell line. Further assessment of other breast cell lines gave similar results with no bands seen in the MCF7, MDA-MB-231 and T47D cell lines.

3.3.4 15-PGDH expression in primary breast tissue

Following optimisation of the 15-PGDH antibody, the HPGD1 antibody was used to examine 15-PGDH protein expression in normal breast tissue sections and primary breast cancer using graded tissue microarray sections.

Four normal breast tissue samples were labelled with the 15-PGDH antibody (Figure 3.11). No 15-PGDH labelling was observed in the epithelial cells, with some isolated cells showing 15-PGDH expression.

Two sets of TMA slides (Set A or B) each consisting of 3 slides containing breast cancer samples graded 1, 2 or 3 were stained with the HPGD1 antibody.

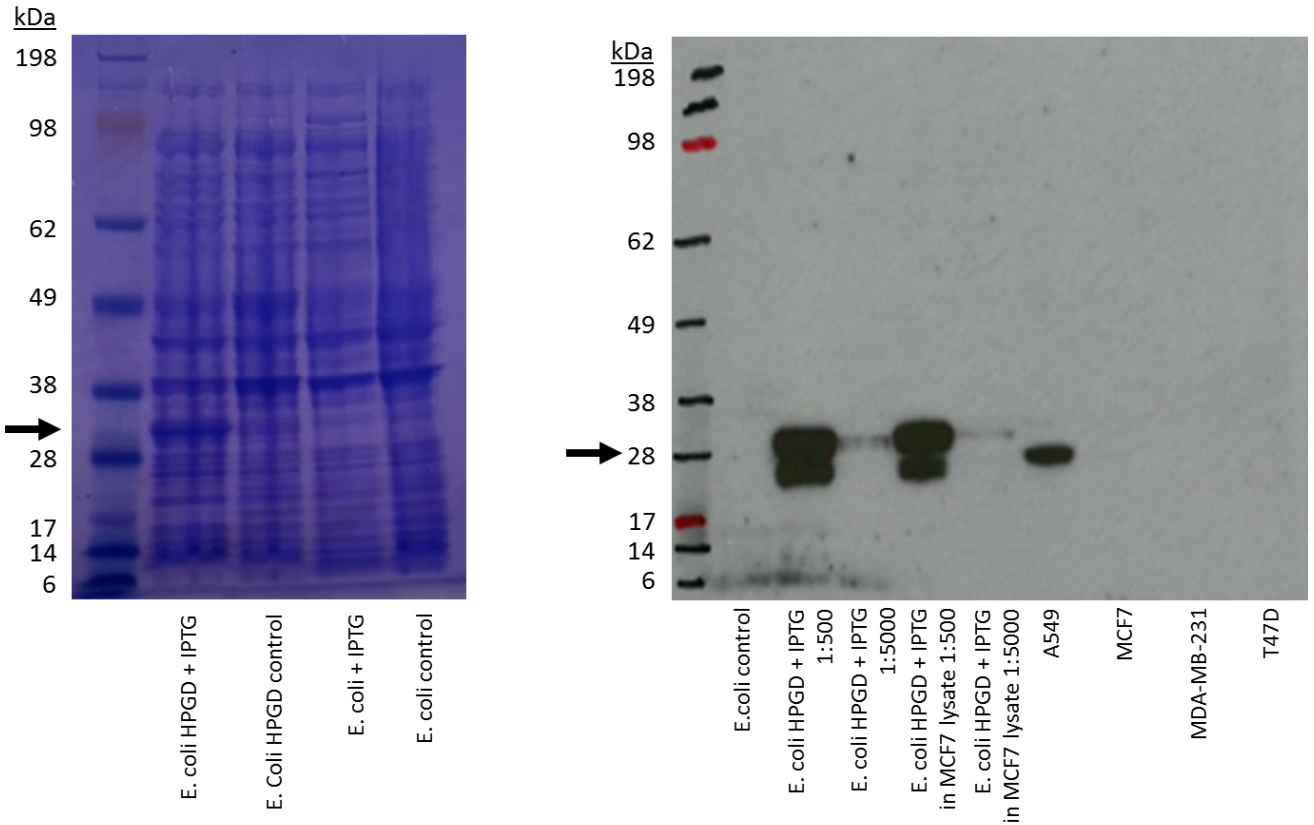

Figure 3.10 *E.coli* 15-PGDH positive control Coomassie gel and 15-PGDH expression in breast cancer cell lines using the Western blotting technique. Left = Coomassie gel with DE3 *E.coli* positive control with pET-15b HPGD vector. Treatment with IPTG stimulated 15-PGDH production. Right = Western blot wit E. coli positive controls and breast cell line lysates. Black arrows indicated 15-PGDH ~29kDa. A single strong band seen with the A549 positive control, no labelling in the breast cancer cell lines.

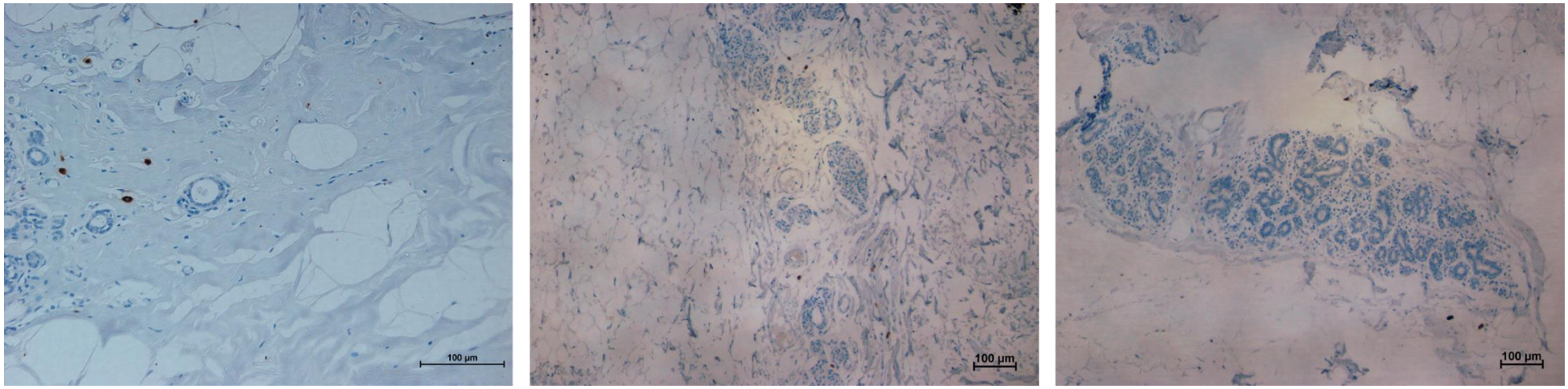

Figure 3.11 15-PGDH labelling in normal breast tissue. No 15-PGDH epithelial labelling was seen in normal breast tissue. Isolated cell staining was observed in the limited samples assessed.

Strong, intermediate or isolated cell staining was observed in the cores as shown in Figure 3.12. The percentage of cores with each category of staining was calculated (Figure 3.13). No trend was observed between the different breast cancer grades, with similar percentages of each staining category seen for each grade.

A total of 8 (~3%) out of the 253 samples on the six TMA slides showed strong 15-PGDH staining, 3 (~1%) showed intermediate staining and 104 (41%) showed isolated cell staining.

Different staining patterns were observed between the three cores of the same sample (Figure 3.14), therefore a decision was made to look at larger tissue sections of the 15-PGDH positive samples to gain a better understanding of 15-PGDH expression.

Twenty samples were requested, including all of the strong and intermediate staining sections alongside a selection of samples of various grades that displayed staining of isolated cells. Thirteen of the twenty sample blocks were obtainable and therefore used for further analysis. When screened for 15-PGDH expression six displayed strong staining, two intermediate staining and five presented with staining of just isolated cells.

Haematoxylin and eosin staining was performed on the selected large breast cancer sections. Figure 3.15 and Figure 3.16 identifies the different histological features identified by haematoxylin and eosin staining. This enabled Nottingham histological grading (Table 3.3) and the cancer subtype to be determined for the samples.

The tumour grade was assessed according to the Nottingham histological scoring system by scoring three individual components: tubular differentiation, nuclear pleomorphism and mitotic count. Although the tubular differentiation and mitotic count varied between the samples, grade 3 pleomorphic nuclei were observed in all of the 15-PGDH positive samples (not including the benign samples) (Figure 3.16). When considering 52% of breast cancer samples usually exhibit grade 3 pleomorphic nuclei (Dunne and Going, 2001), using a Chi squared test this was statistically significant ($p = 0.0014$).

Two of the thirteen samples fitted the morphological apocrine criteria (Figure 3.17), with three showing apocrine features. As apocrine breast cancer is relatively rare and only observed in 1-4% of cases (Weigelt et al., 2010), it was assessed whether a statistically significant number of the 15-PGDH samples were apocrine.

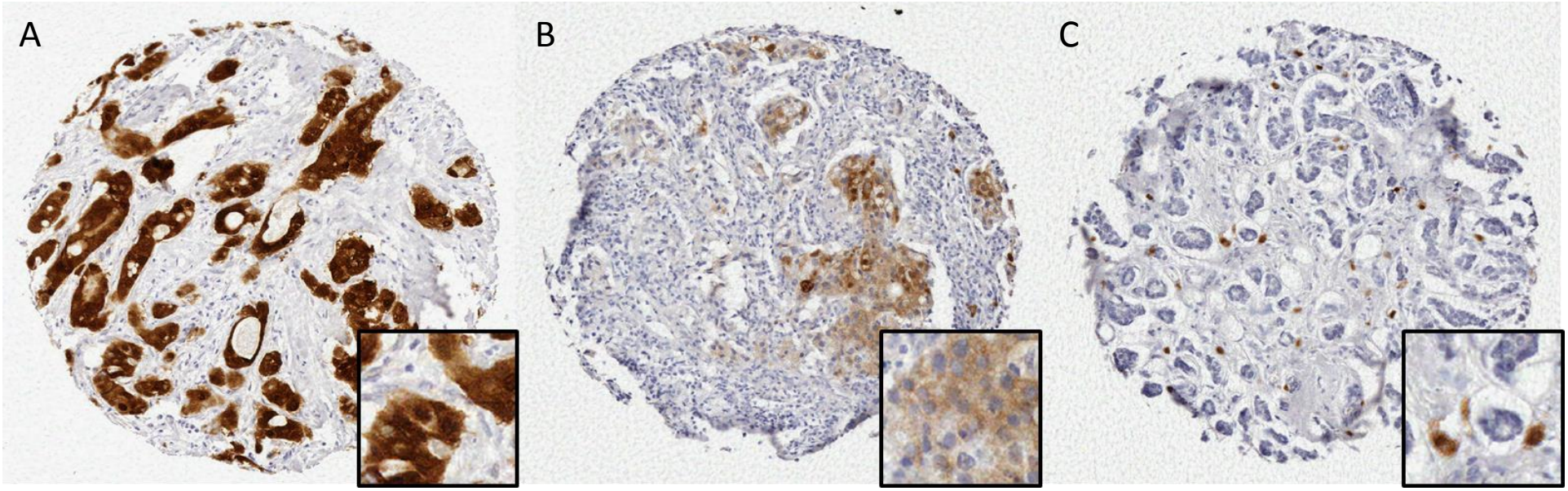

Figure 3.12 Graded primary breast cancer TMA immunohistochemistry staining patterns for 15-PGDH with HPGD1 antibody. (A) = strong 15-PGDH staining, (B) = intermediate staining, (C) = isolated cell staining.

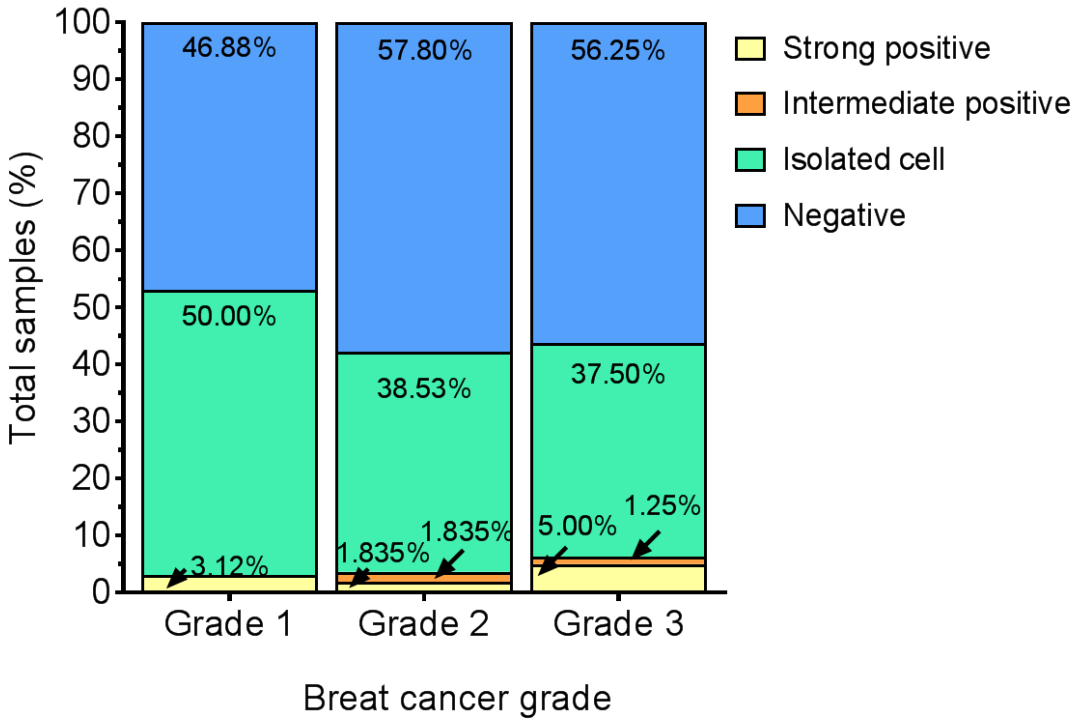

Figure 3.13 Immunohistochemistry 15-PGDH staining pattern analysis in graded primary breast cancer TMA slides. Percentage of total samples with strong, intermediate, isolated cell staining or no staining for each breast cancer grade. Grade 1 = 64 samples, grade 2 = 109 samples, grade 3 = 80 samples. Total = 253 samples.

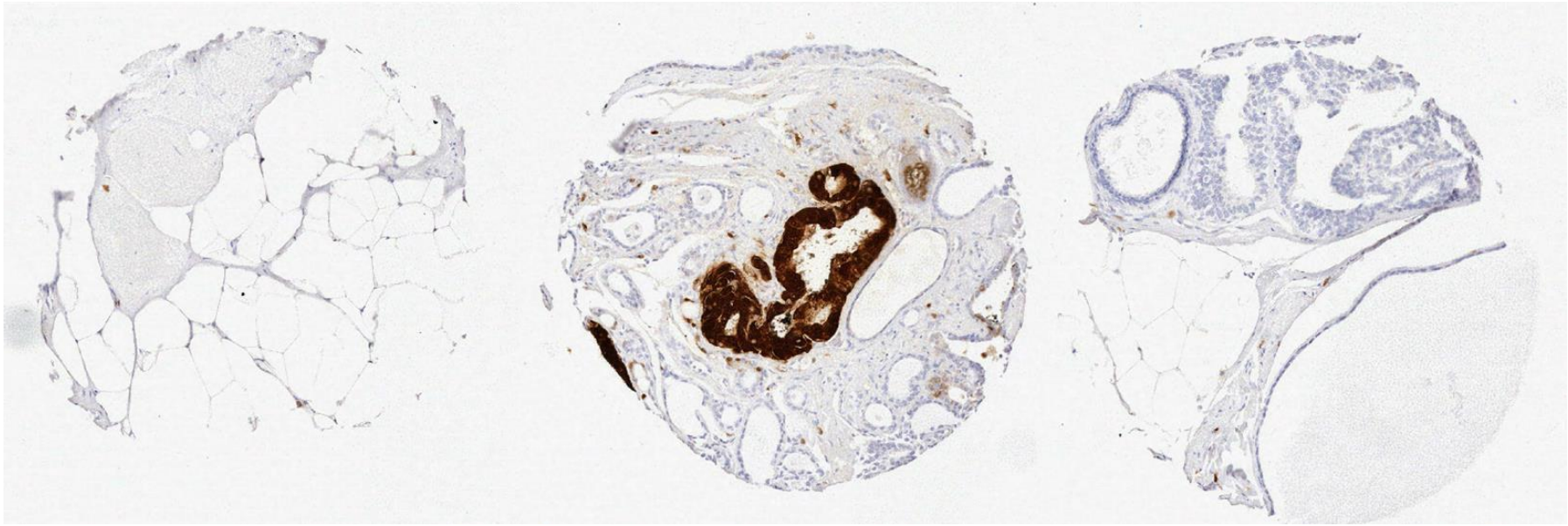

Figure 3.14 Varied 15-PGDH protein labelling in TMA immunohistochemistry samples. Varied 15-PGDH staining patterns between three TMA cores for one patient. Blue = haematoxylin labelling, brown = 15-PGDH labelling.

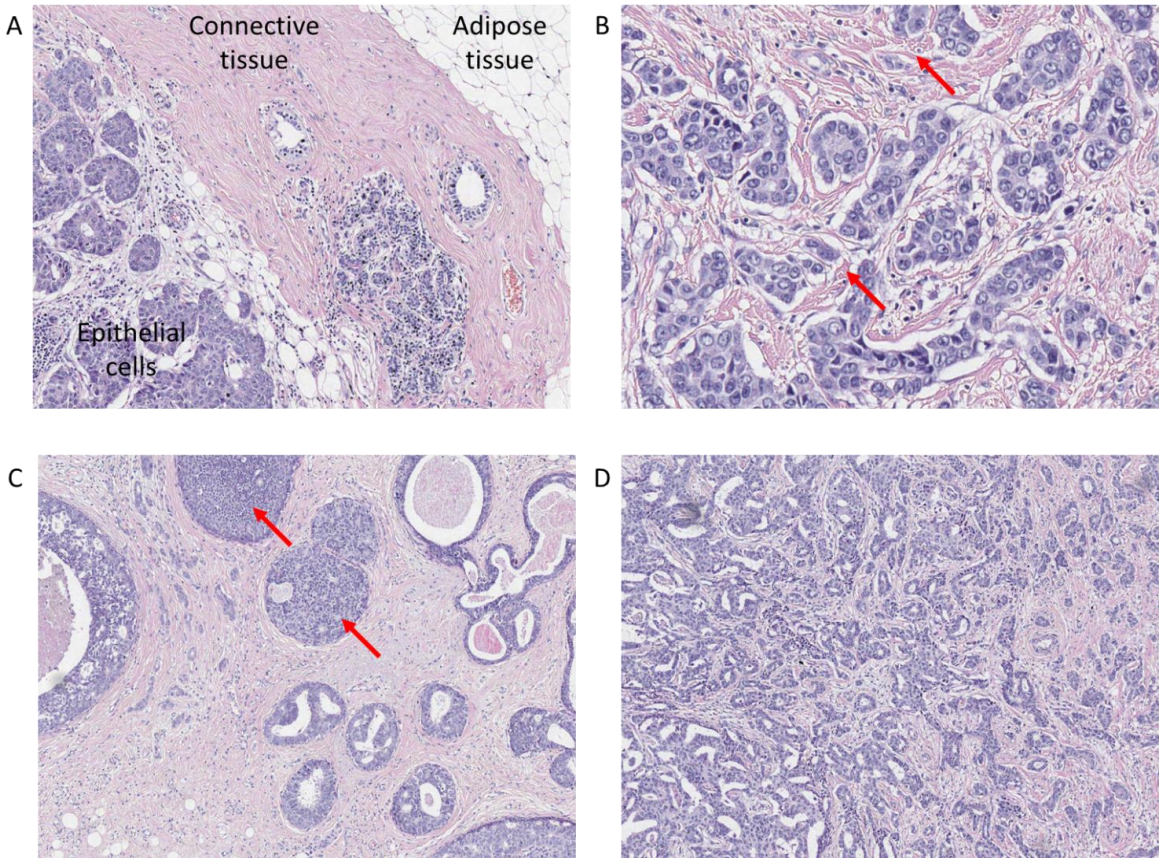

Figure 3.15 Breast tissue histology. (A) Three distinct regions of breast tissue – epithelial cells, connective tissue and adipose tissue. (B) Stroma – connective tissue (indicated by the red arrows). (C) Breast carcinoma *in situ* – cancerous epithelial cells develop in ducts and lobules without invading nearby tissue (indicated by the red arrows). (D) Invasive breast carcinoma – cancerous cells have invaded the breast tissue.

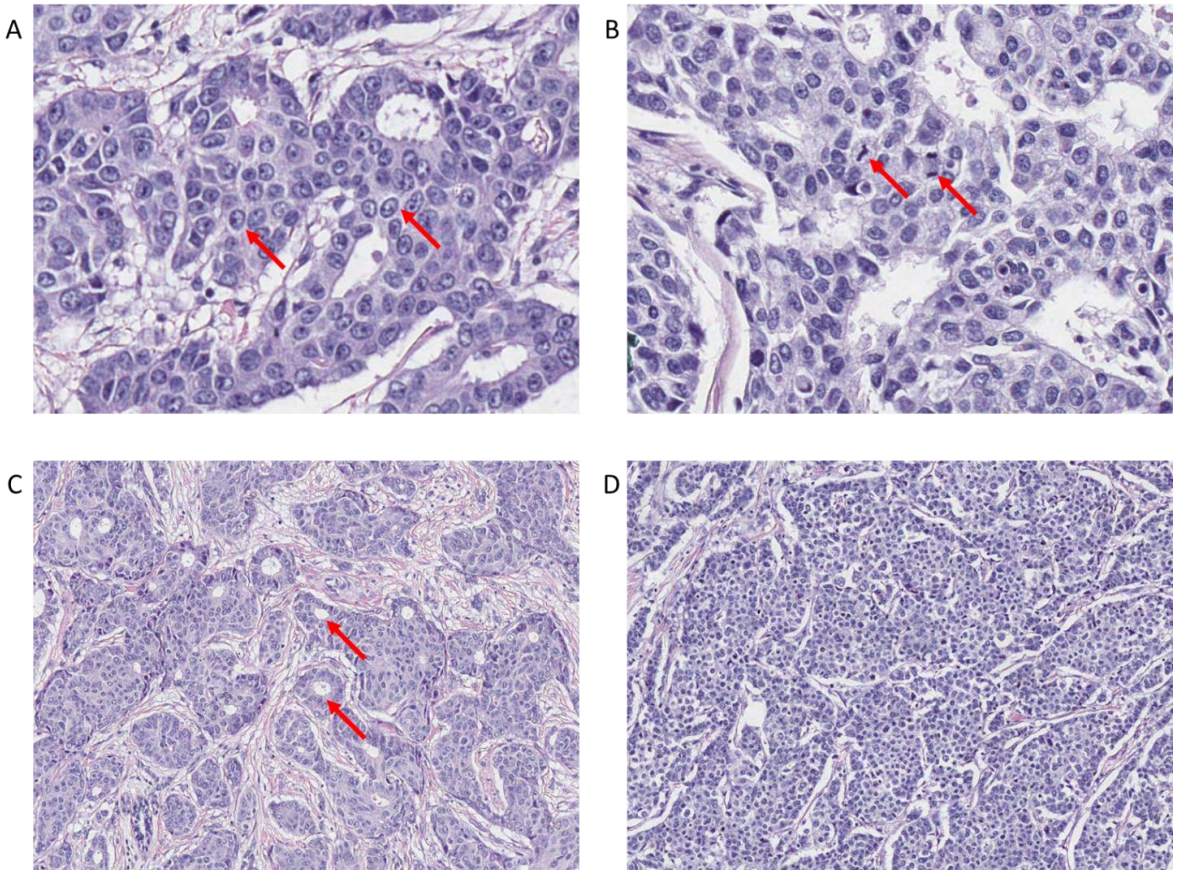

Figure 3.16 Summary of Nottingham histological grading. (A) Pleomorphic nuclei - marked variation in size and shape of nuclei (x30 obj) (indicated by the red arrows). (B) Mitotic count - the number of tumour cells actively dividing (x30 obj) (indicated by the red arrows). (C+D) Tubular differentiation - showing gland formation (x10 obj). (C) High gland formation (indicated by the red arrows), low score, (D) low gland formation, high score.

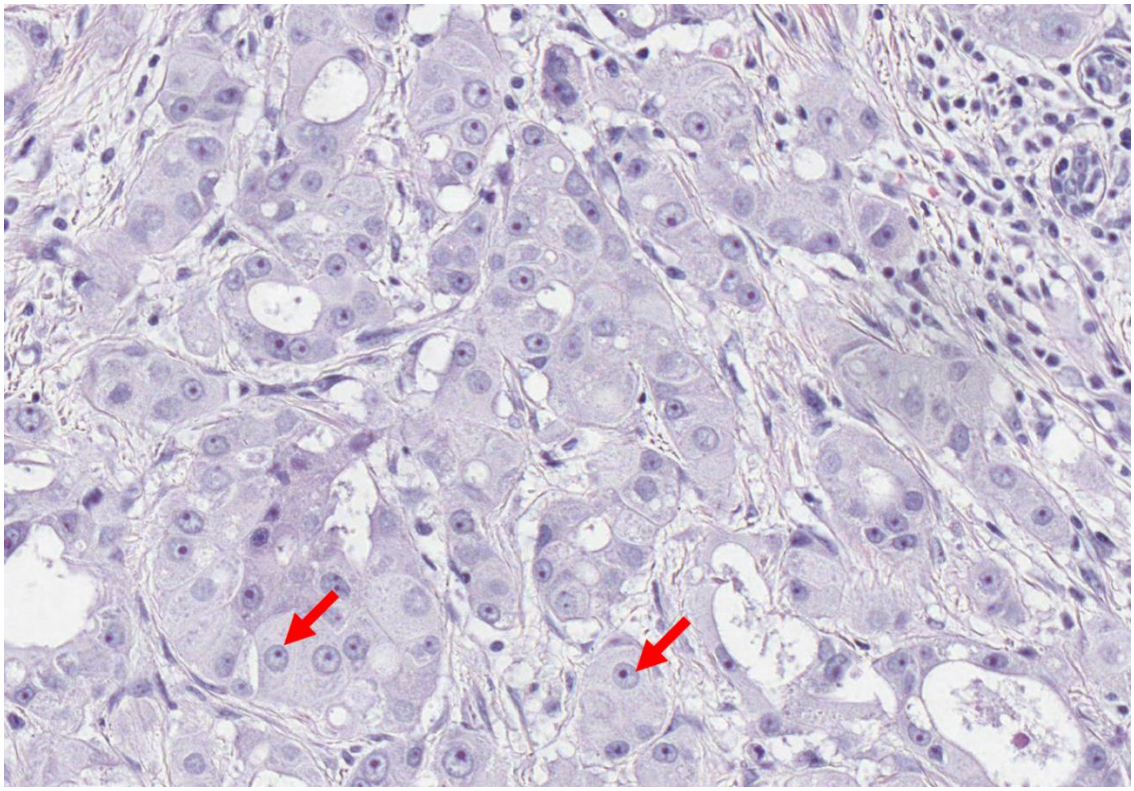

Figure 3.17 Apocrine breast cancer. Haematoxylin and eosin histological stain of an apocrine breast cancer (x20 obj). Red arrows indicate prominent large round nuclei with abundant, eosinophilic, granular and sharp-bordered cytoplasm.

Table 3.3 Nottingham histological staging of selected primary breast cancer samples

The tubular differentiation, nuclear pleomorphism and mitotic count can all be scored at a maximum of 3, with a potential total of 9. Grade 1 = score of 3-5, grade 2: 6-7, grade 3: 8-9. Samples labelled benign as part of the normal tissue was provided on the tissue section. The tissue block was different to that used for the TMA.

		Nottingham histologic grading				
15-PGDH staining	Sample	Tubular differentiation	Nuclear pleomorphism	Mitotic count	Total	Grade
Strong	1	1	3	1	5	1
	2	1	3	1	5	1
	3	2	3	1	6	2
	4	Benign				
	5	3	3	1	7	2
	6	1	3	3	7	2
Intermediate	7	1	3	1	5	1
	8	3	3	1	7	2
Isolated cell	9	Benign				
	10	Benign				
	11	1	3	2	6	2
	12	2	3	1	6	2
	13	3	3	2	8	3

Using the Chi squared statistical test and assuming two of the samples were truly apocrine and 4% of breast cancers were the apocrine subtype, a p value of 0.0164 was observed. If the five apocrine like samples were considered a p value of 0.0001 was obtained.

As apocrine is a rare form of breast cancer, steps were taken to identify a suitable apocrine cell line model (Appendix 12). Unfortunately none of the cell lines assessed fitted the apocrine profile taken from the literature, therefore it was not possible to follow up on the significance of 15-PGDH expression in apocrine breast cancer.

15-PGDH expression was confirmed in the selected primary breast cancer samples (Figure 3.18), but the sections available for three of the samples only contained benign tissue. The human colorectal tissue positive control showed labelling in the glandular cells on the mucosa surface epithelium as expected suggesting that the staining had worked for other slides in the experiment.

Clinical data was available for only 37 of the 64 grade 1 samples assessed in this study (Table 3.5). Due to the lack of samples showing intermediate 15-PGDH staining in grade 1 samples, compounded by clinical data for only one of the two strongly labelling samples, no statistical analysis could be performed on these datasets.

All of the samples with isolated cell staining for 15-PGDH were PR positive, HER2 negative, and all but one out of the fifteen samples were ER positive. This suggests a link between labelling of 15-PGDH in isolated cells and a luminal A molecular profile. An even distribution of histological types was observed for those samples with no 15-PGDH labelling, whereas the majority of those with staining of isolated cells were ductal carcinomas.

Given that ~80% of breast cancers are ER positive (Ali and Coombes, 2000; Onitilo et al., 2009), no statistical difference was observed between samples that are ER positive and those with 15-PGDH labelling of isolated cells ($p = 0.1967$) nor ER status and no 15-PGDH labelling ($p = 0.2207$). As 60% of those that are ER positive are usually associated with PR expression (Onitilo et al., 2009), no significant difference was observed in the samples with isolated cell group ($p = 0.5403$). Twenty percent of breast cancers are HER2 positive and all of the isolated cell group were negative, therefore there was no significant difference in HER expression ($p = 0.3173$). This data shows that 15-PGDH expression does not significantly alter or correspond to ER, PR or HER2 expression in this data set. If a larger cohort was tested a link may be found, but it would not likely be a strong association.

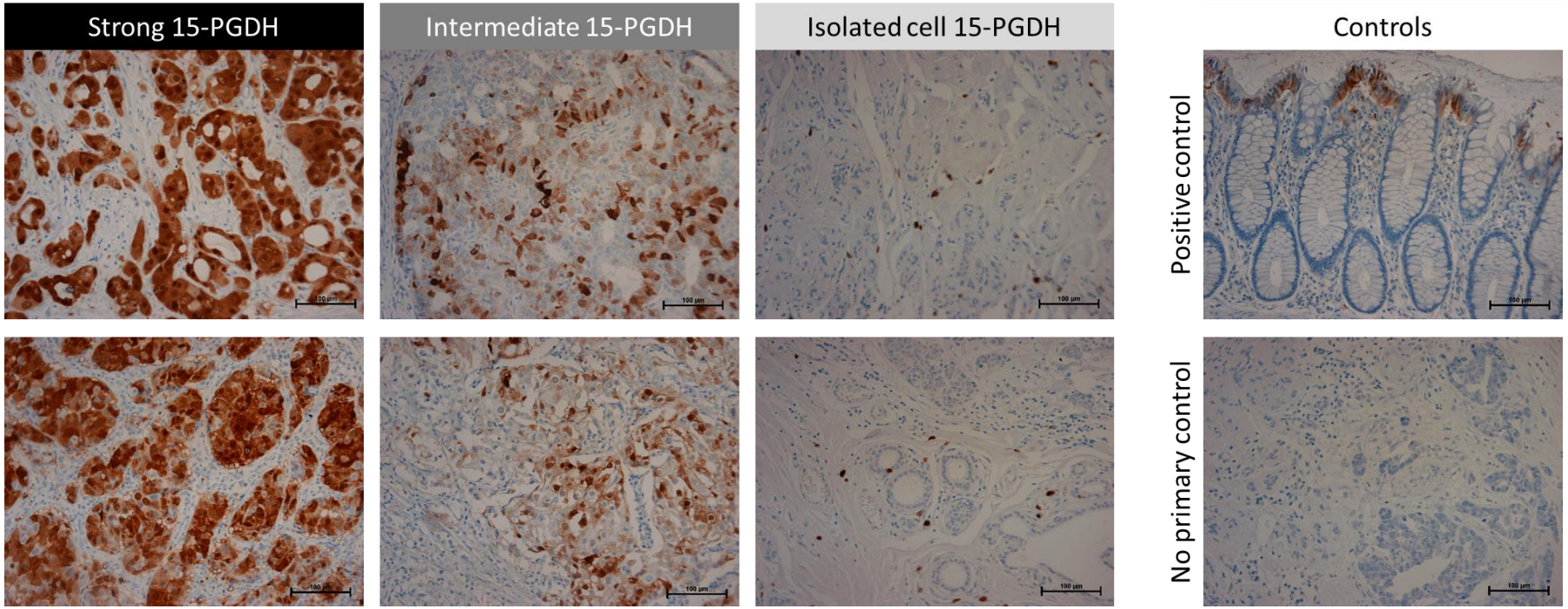

Figure 3.18 15-PGDH expression in selected primary breast cancer samples. Images show two different samples with strong, intermediate and isolated cell 15-PGDH labelling. Positive control = human normal colorectal tissue. Scale bar = 100 µM.

Table 3.4 Clinical and expression data for selected primary breast cancer samples

	Tissue block					TMA	Clinical data								
Sample	Grade	Description	15-PGDH staining	COX-2 staining	HIF-1α staining	Grade	Grade	Nodes	ER	Her 2	NPI	Chemo	Endocrine therapy	Metastatic disease	Breast cancer related death
1	1	Apocrine	High	Intermediate cytoplasmic	Negative	1	1	Positive	Negative		4.13	No	Yes	No	No
2	1	Apocrine	High	Intermediate cytoplasmic areas	Negative	2									No
3	2	Apocrine features	High	Very weak cytoplasmic	Negative	2									
4	N/A	Benign	High	Negative	Negative	3	3	Positive	Positive			Yes	Yes	No	N/A
5	2	NST	High	Intermediate cytoplasmic areas	Negative	3	3	Positive	Positive		5.04	Yes	Yes	No	N/A
6	2	NST	High	Negative	Negative	3									
7	1	NST	Intermediate	Weak cytoplasmic	Negative	2		Positive	Positive			Yes	Yes	No	N/A
8	2	Apocrine features	Intermediate	Strong rare cell, very weak cytoplasmic	Negative	3			Positive			No	Yes	No	No
9	N/A	Benign	Isolated cell	Strong rare cell	Negative	1			Positive				Yes	Yes	No
10	N/A	Benign	Isolated cell	Negative	Negative	2	3	Negative	Positive	Positive	4.26	No	Yes	No	N/A
11	2	Apocrine features	Isolated cell	Very weak cytoplasmic	Negative	2	2	Negative	Positive	Negative	3.44	No	Yes	No	N/A
12	2	NST	Isolated cell	Selected strong rare cells	Negative	3	3	Positive			6.2	Yes		No	N/A
13	3	NST	Isolated cell	Very weak cytoplasmic, Selected strong rare	Patch	3	3	Positive	Positive	Negative	5.36	Yes	Yes	No	No

Table 3.5 Summary of grade 1 primary breast cancer clinical data

	15-PGDH labelling			
	Strong	Intermediate	Isolated cell	None
Patient age (years) (n)				
≤ 50	0	0	1	1
> 50	1	0	21	13
Mean	(72)	(0)	(57.8)	(63.7)
Histological type (n)				
Ductal	1	0	13	4
Lobular	0	0	2	4
Others	0	0	4	3
Unknown	0	0	3	3
Hormone receptor status (n)				
ER positive	0	0	14	6
ER negative	1	0	1	0
Unknown ER	0	0	7	8
PR positive	0	0	4	0
PR negative	0	0	0	0
Unknown PR	1	0	18	14
HER2 positive	0	0	0	0
HER2 negative	0	0	4	1
Unknown HER2	1	0	14	13
Metastatsis (n)				
Yes	0	0	5	0
No	1	0	15	13
Unknown	0	0	2	1
Breast cancer related death (n)				
Yes	0	0	1	0
No	1	0	7	9
N/A	0	0	9	3
Unknown	0	0	5	2
Total samples	1	0	22	14

Thirty percent of women with early stage breast cancer will develop metastatic disease (Early Breast Cancer Trialists' Collaborative, 2005). This corresponded to the number of patients with metastatic disease and the 15-PGDH isolated cell labelling group ($p = 0.6256$), but no metastatic disease was reported in the samples with no 15-PGDH labelling ($p = 0.0183$). Regardless of this, when comparing the two groups there was no significant difference ($p = 0.1310$).

3.3.4.1 Isolated cell identification

The isolated cells staining positively for 15-PGDH expression exhibit macrophage morphology with a fried egg appearance (pathologist confirmed). Comparison of CD68 and 15-PGDH staining in tissue from the same region of one sample showed more positive 15-PGDH cells than CD68 (Figure 3.19). Some CD68 positive macrophages were identified at the lumen of a duct alongside detection of 15-PGDH expression, but no positive CD68 cells were seen scattered throughout the tissue, which was observed with 15-PGDH.

Macrophages are up to 20 µm in diameter, therefore staining 5 µm thick serial sections would not allow accurate classification of the single cells in each section. Therefore, to correctly identify whether 15-PGDH positive isolated cells were macrophages, dual immunohistochemical staining was performed with a 15-PGDH antibody and pan macrophage marker CD68. Nuance software was used to distinguish between the 15-PGDH permanent red (red/pink) and CD68 DAB (brown) staining.

Initially, optimisation of the assay was performed to improve the detection of the single cell macrophages in breast tissue. The secondary antibody staining was reversed to help identify co-localisation as the permanent red stain was not as prominent as the DAB and posed a technical challenge in the detection of single cells (Figure 3.20). When the single stains were performed with the breast tissue sections more CD68 macrophage labelling was detected than 15-PGDH labelling.

Using the optimised assay, clear single cell staining for 15-PGDH was observed in samples 1 and 4 in the epithelial cells, and sample 12 in the stromal cells. The CD68 labelling was most clear in samples 11 and 13 (Figure 3.21). No 15-PGDH staining was observed in the dual stain for sample 11, which showed strong isolated cell staining in the 15-PGDH single staining. Little to no co-localisation of the two antibodies was detected in any of the samples using the Nuance software.

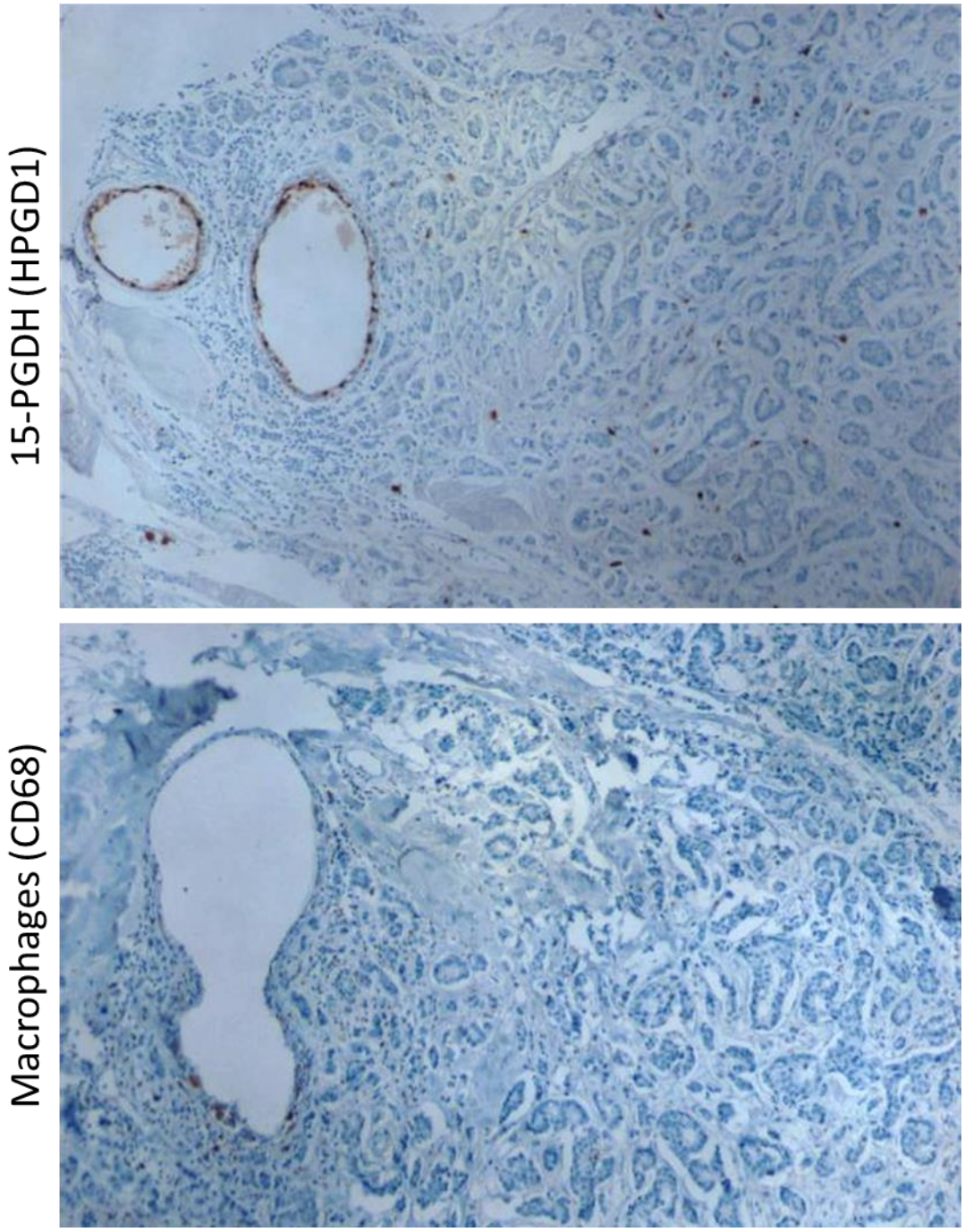

Figure 3.19 15-PGDH and CD68 immunohistochemistry images. Images of IHC with HPGD1 and CD68 macrophage marker antibodies in an aligned sample (x10 obj).

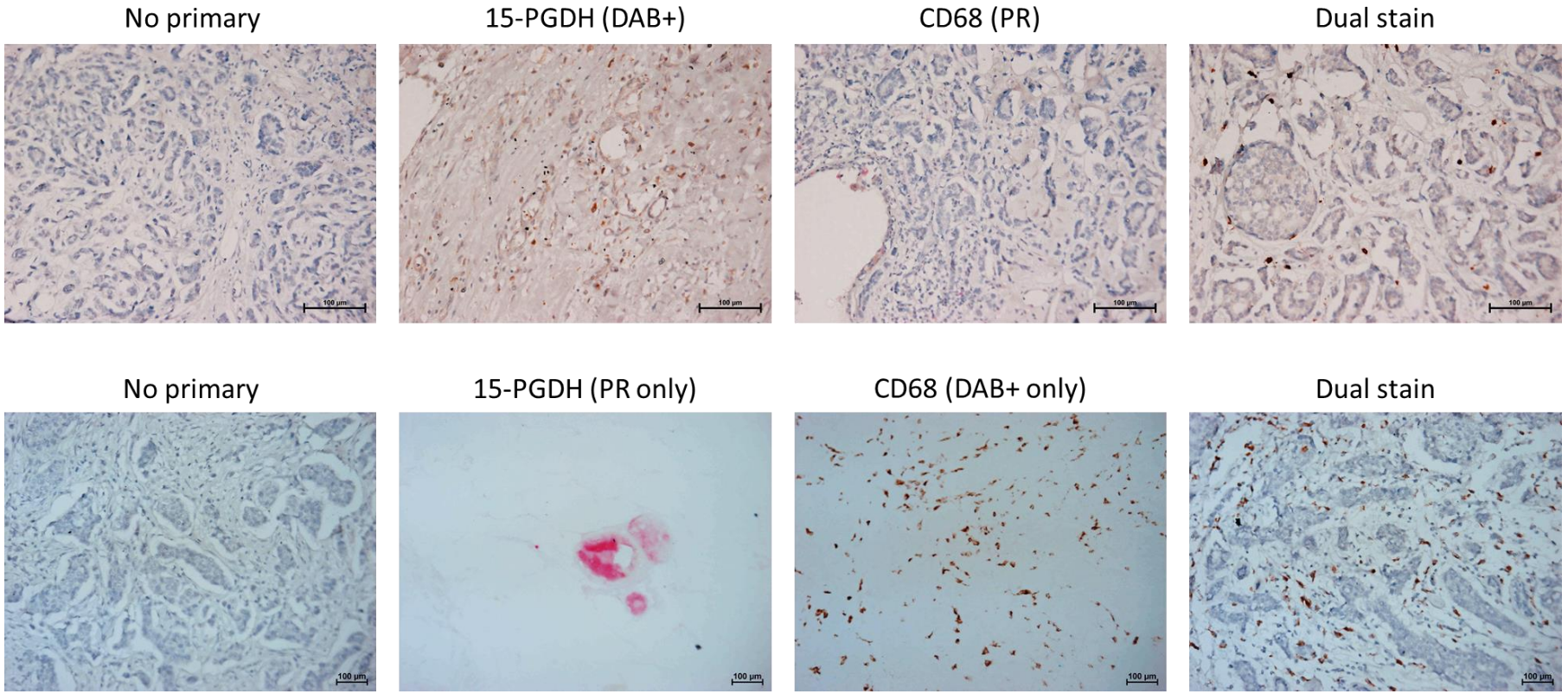

Figure 3.20 Dual stain IHC optimisation with 15-PGDH and CD68 antibodies. Row 1 = Samples counterstained with haematoxylin, 15-PGDH DAB+ secondary (brown) and CD68 permanent red (PR) secondary (red/pink). Row 2 = Samples not counterstained for easier staining identification, 15-PGDH permanent red secondary, CD68 DAB+ secondary. Scale bar represents 100 µm.

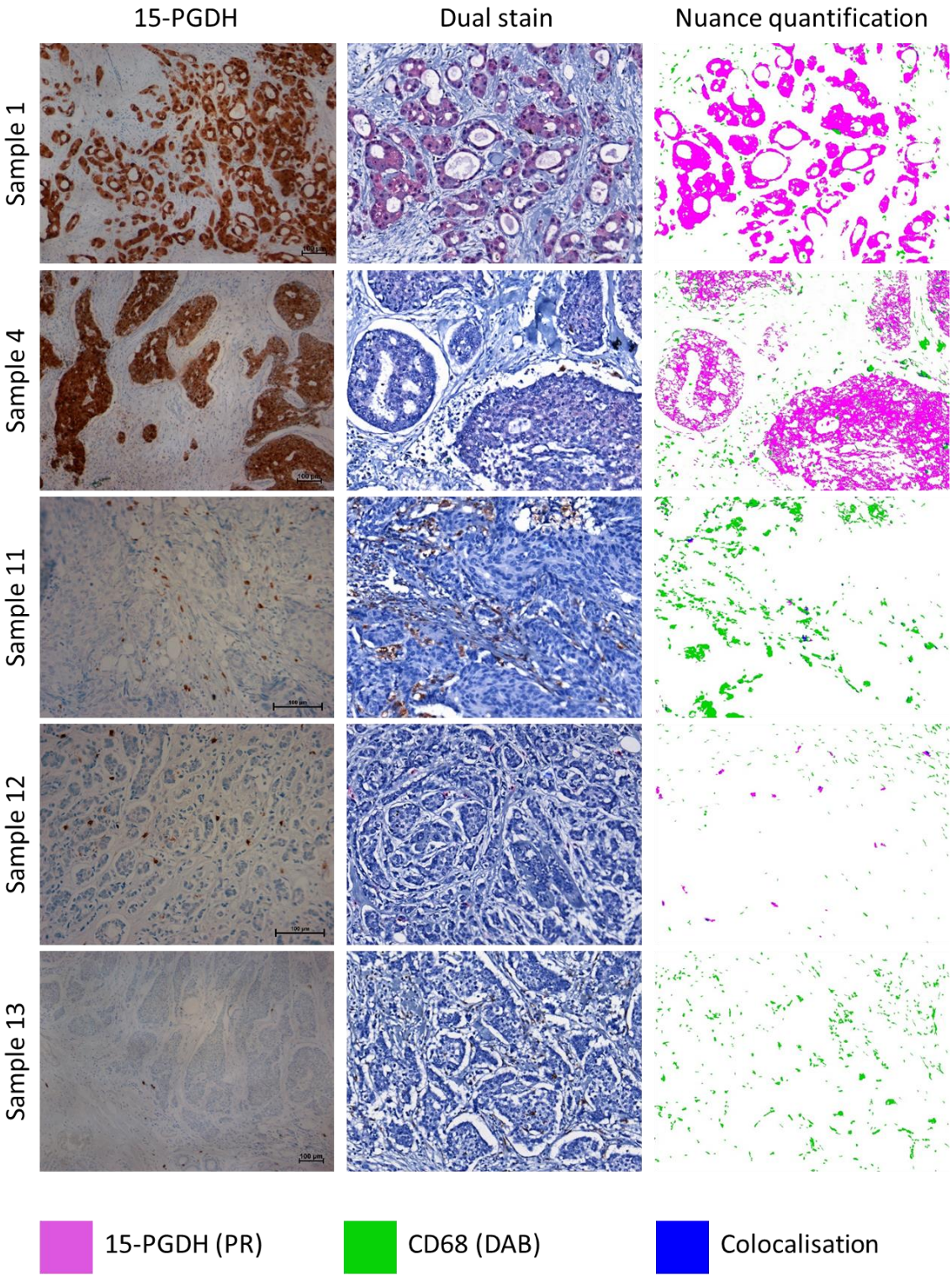

Figure 3.21 Immunohistochemistry dual staining for 15-PGDH and CD68 (macrophage marker) in selected primary breast cancer samples. (Left) 15-PGDH expression with DAB staining (brown). (Centre) Dual staining with 15-PGDH expression with permanent red secondary (red/pink) and CD68 expression with DAB secondary (brown). (Right), Nuance software antibody binding detection. Pink = 15-PGDH (permanent red), green = CD68 (DAB), blue = co-localisation of antibody binding. Limited co-localisation of 15-PGDH and CD68 observed.

Immunocytochemistry using fluorescent secondary antibodies was performed as an alternative method to detect cells staining for both CD68 and 15-PGDH. Due to PFA fixation of the tissue substantial background fluorescence was detected making it impossible to accurately detect specific labelling (data not shown).

To further assess whether 15-PGDH is expressed in macrophages, the human monocytic cell line, THP-1, was differentiated into M1 and M2 macrophages. RT-PCR was performed with the macrophage RNA, which showed no expression of 15-PGDH in the undifferentiated THP-1 parent cell line or the polarised macrophage cells (Figure 3.22). Nested PCR was also performed to detect whether very low levels of RNA transcripts were present, nevertheless there was still no expression of 15-PGDH observed (data not shown).

In addition, RNA-Seq data generated by Dr Nikki Re analysing THP-1, M0, M1, M2A and M2B polarised cells RNA profiles, was evaluated for 15-PGDH expression. No transcripts were detected in any of the samples assessed.

3.3.5 COX2 expression in the selected primary breast cancer samples

COX2 is a key enzyme in prostaglandin production and is frequently up-regulated in breast cancer (Shim et al., 2003; Kim, H.S. et al., 2012). It has also been suggested that 15-PGDH and COX2 can be inversely co-regulated (Tong et al., 2006b). Therefore COX2 expression was assessed in the selected primary breast cancer samples to see if there was a link between COX2 and 15-PGDH expression in breast cancer (Figure 3.23). A summary of both COX2 and 15-PGDH expression in the samples can be seen in Table 3.4. Cytoplasmic staining was observed in the mouse xenograph positive control slide, most strongly in immune cells but also in epithelial cells, while no staining was seen in the no primary control.

Intermediate cytoplasmic COX2 expression was observed in three of the selected breast cancer samples which also showed strong 15-PGDH staining, two of which were apocrine breast cancer. Weak cytoplasmic staining was also observed in one of the intermediate 15-PGDH samples and very weak cytoplasmic staining in two 15-PGDH expressing samples and two isolated 15-PGDH positive samples. Strong staining was observed in small regions of globules within the cytoplasm of luminal cells, which is thought to be non-specific. Labelling in rare isolated immune cells was seen in four of the selected primary breast cancer samples.

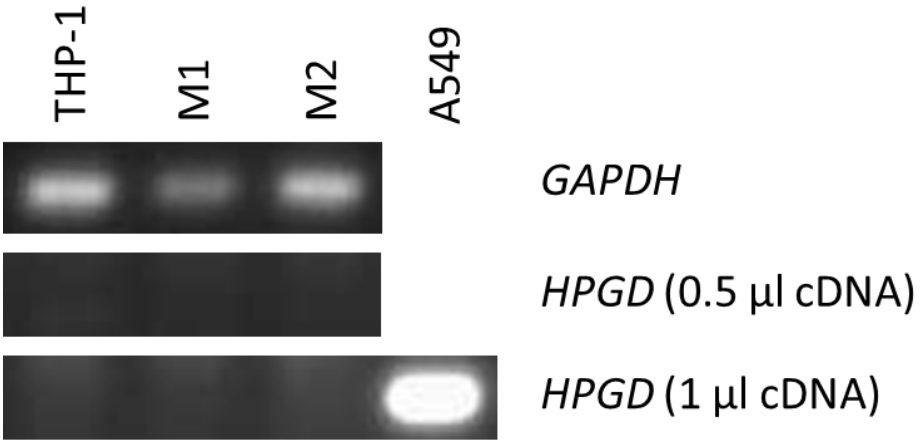

Figure 3.22 *HPGD* mRNA expression in polarised THP-1 macrophage cells. RT-PCR images for *GAPDH* and *HPGD* expression in THP-1, M1 and M2 macrophages. An A549 positive *HPGD* control was included. RT-PCR was completed with 0.5 and 1 µl cDNA for the primary PCR.

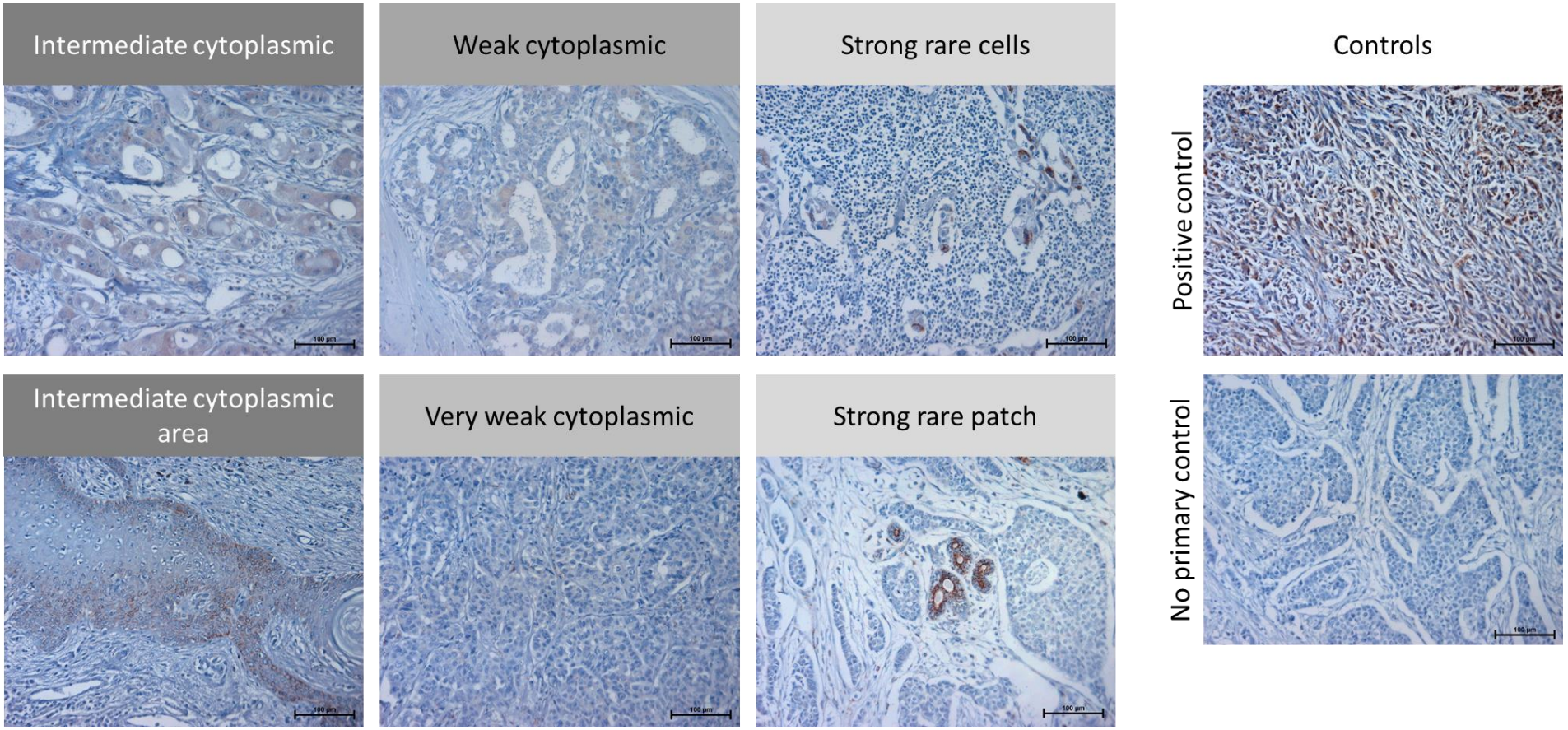

Figure 3.23 Immunohistochemistry with selected breast cancer samples and COX2 antibody. Samples stained with COX2 antibody and counterstained with haematoxylin (x20 objective). Scale bar represents 100 µm. Positive control xenograph sample kindly provided by Dr Milène Vol

3.3.6 HIF-1α expression in selected primary breast cancer samples

It has been found that hypoxia, demonstrated by the presence of the hypoxia marker HIF-1α, has a significant influence on gene expression (Maxwell et al., 1997). It was therefore hypothesised that hypoxia may alter 15-PGDH expression within a sample, possibly explaining the varied 15-PGDH expression within the three cores assessed for the TMA. The selected 15-PGDH expressing breast cancer samples were therefore assessed by immunohistochemistry for expression of the hypoxia marker HIF-1α (Figure 3.24).

Intermediate punctate staining was observed in the kidney positive control in cortex proximal tubule cells, yet no staining was observed in the primary breast cancer tissue samples with the exception of one sample. HIF-1α labelling in the cytoplasm of luminal cells was observed in a small number of localised sections in of one of the samples that showed isolated cell staining for 15-PGDH.

3.3.7 Prostaglandin pathway component expression in breast cell lines

Expression of other components of the prostaglandin pathway were assessed by conventional RT-PCR in breast cell lines (Figure 3.25). Multidrug resistance binding protein 4 (MRP4), encoded by *ABCC4*, is involved in the exportation of prostaglandins out of the cell, including PGE_2. HB2 and MDA-MB-231 cell lines exhibit the highest expression of *ABCC4*, with SKBR3 showing the lowest level of expression.

PTGS, PTGS2, PTGS3 encode different isozymes of the prostaglandin E synthase enzyme involved in the production of PGE_2. Both *PTGES* and *PTGES2* are microsomal, whereas *PTGES3* is located in the cytosol. Variation was seen between cell lines for each of the genes expression. One noticeable observation was that of MDA-MB-453 did not express *PTGES*, while it is relatively highly expressed in the other cell lines.

COX2 encoded by the *PGTS2* gene is involved in arachidonic acid metabolism, producing the prostaglandin precursor, PGH_2. *PTGS2* levels varied between cell lines, where four had little to no expression and three had moderate expression levels.

The *SLCO2A1* gene encodes the prostaglandin transporter, which actively pumps prostaglandins into the cell where they can then be metabolised by 15-PGDH. *SLCO2A1* expression varies considerably between breast cell lines. There was a high level of expression seen in MDA-MB-453, intermediate in MCF10A and T47D cells, whereas there was little to no expression seen in HB2, MCF7, MDA-MB-231 and SKBR3 cell lines.

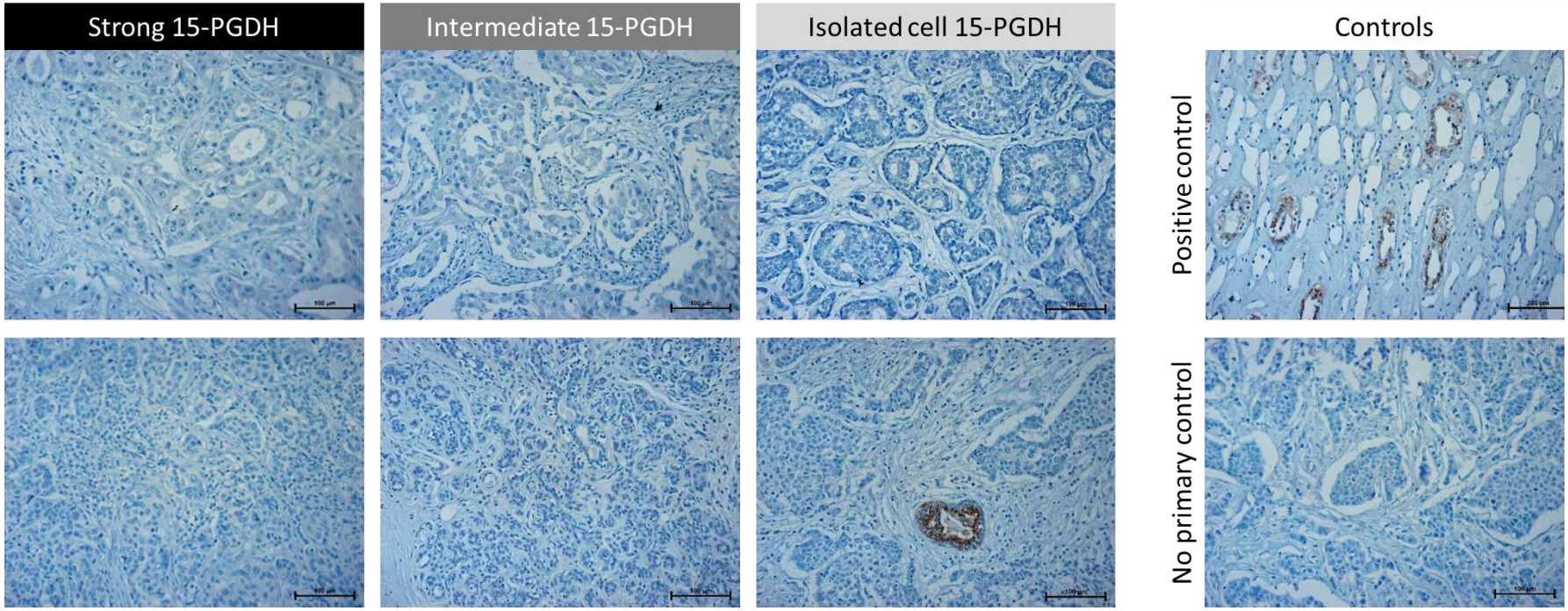

Figure 3.24 HIF-1α expression in selected primary breast cancer tissue samples. Two images per 15-PGDH staining pattern and positive and no primary control images. Samples stained with HIF-1α antibody and counterstained with haematoxylin (x20 objective). Scale bar represents 100 µm. The positive control was a normal human kidney tissue.

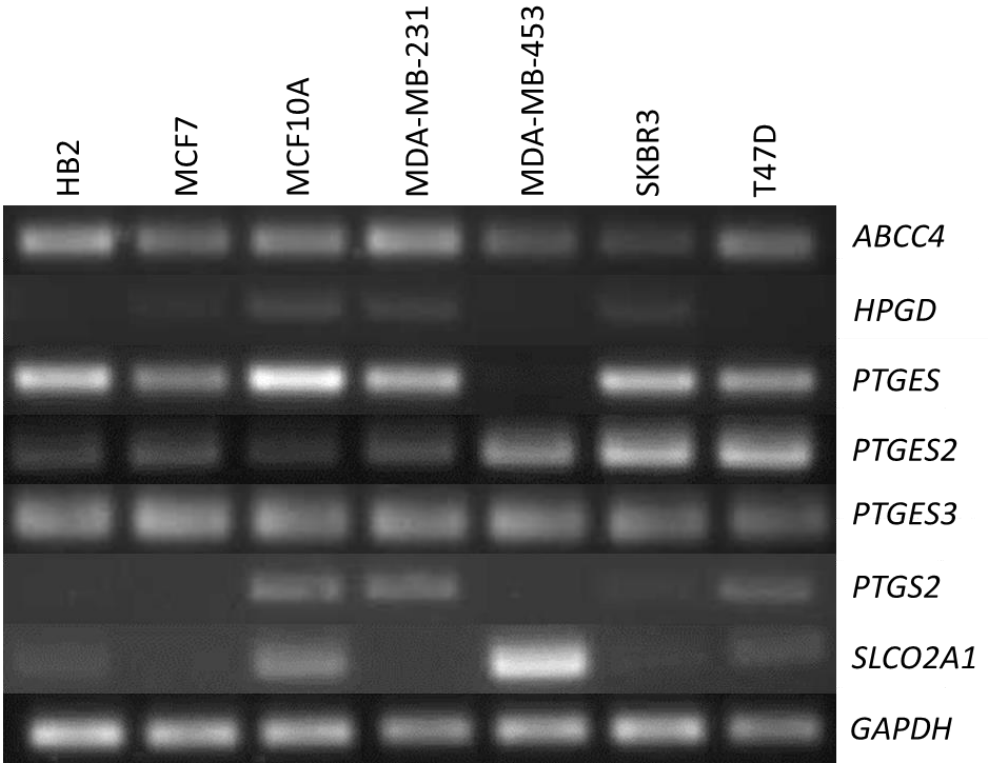

Figure 3.25 Prostaglandin pathway component mRNA expression using conventional RT-PCR. RT-PCR completed with 35 cycles with the exception of *HPGD* (38 cycles) and GAPDH (28 cycles). *ABCC4* = multidrug resistance binding protein 4 (MRP4), *HPGD* = 15-PGDH, *PTGES* = prostaglandin E synthase, *PTGES2* = prostaglandin E synthase 2, *PTGES3* = prostaglandin E synthase 3, *PTGS2* = cyclooxygenase-2 (COX2), *SLCO2A1* = prostaglandin transporter, *GAPDH* = glyceraldehyde 3-phosphate dehydrogenase.

3.4 Discussion

To determine if 15-PGDH is a potential treatment target in breast cancer it is important to define its expression profile in normal and cancerous breast tissue. Low expression of *HPGD* mRNA was observed in breast cancer cell lines in comparison to colorectal and lung cell lines. Heterogeneous expression of *HPGD* mRNA has been reported between different tissues, with the highest expression observed in the large intestine, followed by the lung, liver and small intestine (Backlund et al., 2005). This closely matches the qRT-PCR results for the colorectal and lung cell lines. Furthermore, an *in silico* bioinformatics study using TCGA data found that *HPGD* mRNA expression was lower in breast cancer than normal breast tissue (Kochel et al., 2016). This data suggests that up-regulation of 15-PGDH expression in breast cancer may be beneficial. It is important to note that it is difficult to interpret transcriptional data in breast cancer as the cell type content varies greatly to normal breast tissue, which mainly comprises of adipocytes compared to a larger proportion of epithelial cells in malignant tissue.

Extensive antibody optimisation was performed using three different 15-PGDH antibodies to facilitate the generation of reliable protein expression data. The three antibodies are raised to different epitopes with overlap for the HPGD2 and HPGD3 antibodies. Ideally using antibodies with non-overlapping epitopes that reveal the same labelling pattern would provide validation for the specificity towards the target protein. This was not the case with these antibodies, but with only one band in the Western blot and producing the expected labelling pattern and cellular localisation in IHC and immunocytochemistry, HPGD1 appears to be the most specific antibody.

Using HPGD1, 15-PGDH localisation was found to be mainly cytoplasmic with some nuclear staining, similar to that reported in the literature (Lehtinen et al., 2012). Functionally 15-PGDH is expected to be located in the cytosol, and the function of any nuclear localisation is not currently known. There is no evidence to suggest it can act to regulate transcription by interacting with transcription factor complexes, but its translocation to the nucleus may be a mechanism to add further control of PGE_2 degradation by removal of enzyme from the cytoplasm.

15-PGDH protein expression in breast cell lines was assessed by immunocytochemistry and Western blotting. The results show that 15-PGDH expression levels are below the limit of the technique's sensitivity in the assessed breast cancer cell lines. 15-PGDH protein expression has

been detected in the MDA-MB-231 cell line by Western blotting in which 50-150 µg of total protein extracts were loaded onto the gel and labelled using an antibody made for another study (Wolf et al., 2006). The antibody used was not available for this study and so the results could not be confirmed. In comparison, when 25 µg of MDA-MB-231 total protein lysate was loaded onto the Western blot and screened with a commercial antibody in this thesis no 15-PGDH expression was detected above background levels.

No 15-PGDH expression was observed in the normal breast tissue examined by immunohistochemistry labelling. Similarly, the Human Protein Atlas indicates no 15-PGDH protein expression was detected in breast tissue compared to high expression in the stomach and medium in the lung and colon (Uhlen et al., 2015). Conversely, decreased 15-PGDH protein expression has been reported in malignant tissue compared to matched normal tissue in a range of human cancers including breast, lung and colon (Backlund et al., 2005; Wu, R. et al., 2017). Yet 15-PGDH has also been reported to be up-regulated in breast cancer compared to normal tissue (Thill et al., 2010a). A small cohort was assessed in both studies (<22 samples), therefore the samples may not be a true representation of breast cancer as a whole. This data suggests that 15-PGDH expression is typically very low in breast cancer, therefore up-regulation of 15-PGDH may be advantageous in preventing breast cancer development as its expression even at modest levels may have a pronounced effect on local PGE_2 levels compared to tissue with no expression.

In a panel of 253 primary breast cancer samples of varying grades only 11 (~4%) labelled positively for 15-PGDH epithelial staining. Another study found 21% of 295 primary samples were positive for 15-PGDH protein expression (Lehtinen et al., 2012). The antibody used in the study was the HPGD2 Cayman Chemical antibody, which showed positive staining (score >150) in 42.67% of TMA cores in this study compared to 2.67% with HPGD1, therefore the data in the Lehtinen study may be unreliable in providing a true reflection of 15-PGDH expression.

Increased 15-PGDH protein expression has been reported in invasive apocrine carcinoma, with 14/21 (67%) samples exhibiting positive 15-PGDH expression and as a result has been implicated as an apocrine marker (Celis et al., 2008). In the 15-PGDH positive cohort used in this study, two samples were identified as apocrine by their histology and showed strong 15-PGDH staining. A further three demonstrated apocrine features, one with strong, one with intermediate and one with isolated 15-PGDH labelling. As apocrine breast cancer is extremely rare this suggests that 15-PGDH may be a good indicator of apocrine breast cancer. Whether

15-PGDH is simply an apocrine biomarker, or contributes to the development of the apocrine phenotype is not known.

Single isolated cell labelling was observed with both the HPGD1 and HPGD2 antibodies, which was more pronounced in the HPGD1 antibody. This suggests that it may be a true reflection of 15-PGDH expression. Similar labelling was observed on the Protein Atlas using the same HPGD1 antibody (Uhlen et al., 2017). Expression of 15-PGDH in isolated cells may influence the surrounding cells, as PGE_2 and other substrates of 15-PGDH produced in one cell may be taken up and metabolised in another cell in the same vicinity and so modulating PGE_2 within the cancer's microenvironment.

Morphological features suggest that the 15-PGDH isolated cell staining is labelling macrophages, but no convincing co-localisation was observed in the CD68 and 15-PGDH dual labelling experiments. This was possibly down to technical limitations of single cell staining due to overlapping spectra of the permanent red and DAB chromogen brown stain, making it difficult for the Nuance software to distinguish between the two signals. Also, due to the auto florescence caused by PFA during fixation it was not possible to determine dual expression of CD68 and 15-PGDH using fluorescent secondary antibodies. Future work could overcome this by using an alternative fixing method that causes less auto-fluorescence.

Furthermore, the THP-1 monocytic cell line did not show any 15-PGDH expression in its un-differentiated or differentiated states as judged by RT-PCR and RNA-Seq. As THP-1 cells are an immortalised cell line grown in tissue culture, they may not accurately reflect the behaviour of macrophages within breast cancer samples. Further examination of the isolated cells staining for 15-PGDH by a pathologist has led to the theory that the single stained cells may be mast cells, due to their granular cytoplasm. Additional research is required to test this hypothesisand ultimately identify the 15-PGDH positive isolated cells' cell type.

15-PGDH expression has been associated with leukocytes using a pan leukocyte marker, CD45, in abdominal aortic aneurysms (Sola-Villa et al., 2015). Furthermore, co-localisation of 15-PGDH expression with macrophage, T-cell and B-cell markers (CD68, CD3 and CD20 respectively) were assessed in the abdominal aortic aneurysm samples. Significant expression of 15-PGDH was linked to CD68, but this was not as significant as the pan-leukocyte marker and co-localisation was seen with CD20 and CD3 (Sola-Villa et al., 2015). This fits with the reduced CD68 expression compared to 15-PGDH. Consequently, isolated cells expressing 15-PGDH may be leukocytes, consisting of a selection of macrophages, B-cells and T-cells.

Limited clinical data was associated with the graded TMAs used in this study as the samples were collated in the early 1990's. Data was obtained for a selection of the grade 1 samples, which allowed some statistical analysis. Due to the small sample number and data collection bias the statistical analysis performed may not accurately represent the full dataset, but the resulting observations may help to generate new hypotheses.

Tumour associated macrophages have been well characterised and have been linked to poor prognosis (Yang, M. et al., 2018; Gyorki and Lindeman, 2008; Ward et al., 2015; Mahmoud et al., 2012). No statistical significance was seen between the 15-PGDH expression and metastasis in the isolated cell and no 15-PGDH groups in the grade 1 cohort. Five patients with metastasis were nevertheless found in the isolated cell group, which corresponds to the observation of poor prognosis with tumour associated macrophage infiltration in the literature. Only one patient out of the grade one primary breast cancer cohort died as a direct result of breast cancer, this patient demonstrated 15-PGDH isolated cell staining. No analysis could be performed between 15-PGDH expression and mortality due to a lack of data. The increased incidence of metastasis and breast cancer related deaths in the 15-PGDH labelled isolated cell group suggests that 15-PGDH expression in these isolated cells does not improve patient outcome. This would need to be confirmed by accurately identifying the isolated cells and assessing their presence in each of the samples.

A novel observation in the haematoxylin and eosin staining was that all of the 15-PGDH postive samples were grade three (high) for pleomorphic nuclei. Pleomorphic nuclei is a trait linked to genetic instability, which in turn leads to carcinogenesis (Bignold, 2003). This suggests that patient prognosis would be poor in the cohort assessed. Poor prognosis has been reported in patients with high *HPGD* mRNA expression (Lehtinen et al., 2012), yet only 20 samples presented high 15-PGDH expression, therefore the conclusions may not be reliable.

COX2 has been identified as a biomarker for apocrine breast cancer, alongside 15-PGDH (Celis et al., 2006). COX2 expression was observed in 36% of primary breast cancers, while only 4% of primary breast cancers are apocrine (Denkert et al., 2003; Weigelt et al., 2010). In the selected primary breast cancer samples the two apocrine samples showed intermediate COX2 expression and all of the samples that exhibited apocrine features presented weak COX2 cytoplasmic expression. This suggests that COX2 is a suitable biomarker for apocrine carcinoma. Reciprocal regulation of 15-PGDH and COX2 expression has been reported in the literature (Tong et al., 2006b; Tai et al., 2007) and decreased 15-PGDH expression and increased COX2

expression in breast cancer (Tong et al., 2006b), yet this does not appear to be the case in the samples in our cohort.

Hypoxia is often found in tumours, for example in breast cancer 63% of 261 tumours showed strong HIF-1α expression, these tumours comprised of 88% invasive carcinoma of no special type, 59% of which were grade 3 (Nalwoga et al., 2016). HIF-1a expression has also been linked to HER2 negative and ER positive samples (Bos et al., 2001). Two known HER2 negative and seven ER positive samples are in the selected breast cancer samples, therefore it would be predicted that some HIF-1α expression would be found in the selected breast cancer samples. HIF-1α expression has been described as cytoplasmic focal expression adjacent to necrotic tissue, intense expression distal to blood vessels or diffuse expression independent of the proximity to blood vessels in high risk breast cancer (Gruber et al., 2004). No HIF-1α expression was detected in the 15-PGDH positive primary breast cancer cohort, with the exception of one sample. A small patch of luminal cells showed strong HIF-1α expression, but this is not the expected observation. This suggests that the selected samples is a non-random selection, suggesting 15-PGDH expression is associated with low levels of HIF-1α. Immunohistochemistry with an alternative HIF-1α antibody would enable confirmation of the results.

As a result of the statistical analysis of the TMA's clinical data it would be interesting to assess the progesterone, HER2, and androgen receptor expression in the selected breast cancer samples. Furthermore, it would be beneficial to look at the expression of other components of the prostaglandin pathway. MRP4 (*ABBC4*) is involved in efflux of leukotrienes and prostanoids, such as PGE_2, in the low micromolar range, out of the cell (Russel et al., 2008). Over expression of MRP4 has been reported in cancers and this has been linked to multidrug resistance as MRP4 actively pumps drugs out of the cell, preventing cytotoxicity and inferring resistance in cancer (Zhang, G. et al., 2015; Norris et al., 2005; He, Z. et al., 2015; Kochel and Fulton, 2015; Holla et al., 2008). Furthermore, *ABCC4* knock down restored fluorouracil sensitivity to fluorouracil resistant cancer cells (Zhang, G. et al., 2015). High expression or MRP4 was found in MDA-MB-231 cells and intermediate in the MCF7 cell line compared to the panel of breast cells lines tested. This suggests that the MDA-MB-231 cell line would be less susceptible to substrates that exert their effects once internalised, but it would not make the cells resistant to those that bind to receptors on the cell surface membrane such as PGE_2.

PTGES3 encoding the cytosolic isoform of prostaglandin E synthase (cPGES), was expressed ubiquitously in the panel of breast cell lines assessed, which was also observed in colorectal cancer (Seo, T. et al., 2009). Expression of *PTGES* (mPGES-1) and *PTGES2* (mPGES-2), both

located in the cell membrane, differed between the cell lines tested, this has also been observed in colorectal cancer (Seo, T. et al., 2009). On the contrary, constitutive expression of mPGES-2 has been suggested in various cancers (Nakanishi, M. et al., 2010) and it has been demonstrated that mPGES-2 is not required for PGE_2 production in mice (Jania et al., 2009). mPGES-1 is over-expressed in a variety of cancers, it has been implicated in carcinogenesis and thus been labelled as a target for cancer suppression (Seo, T. et al., 2009; Isono et al., 2011; Nakanishi, M. et al., 2010).

Varied mRNA expression of COX2 (*PTGS2*) was observed in the panel of breast cancer samples assessed, with MCF10A, MDA-MB-231 and T47D cells also showing COX2 expression. Strong protein expression has been described in T47D, low expression in MDA-MB-231 cells and no expression in MCF7 cells, but no expression was also seen in the MCF10A cell line (Kochel et al., 2017).

Over-expression of PGT has been linked to increased invasion and apoptosis, while PGT suppression reduced tube formation and wound healing (Zhu et al., 2015; Nakanishi, T. et al., 2017). Lower PGT expression was observed in luminal B or basal breast cancer compared to normal breast tissue (Kochel et al., 2016). This was not the case for the breast cell lines assessed. The non-malignant breast cell line MCF10A showed intermediate expression and the HB2 cell line low expression. Whereas the basal cancer cell line MDA-MB-231 showed high expression levels of PGT. The trend was also observed by Kochel et al., yet there was a large variation between the individual samples (Kochel et al., 2016). The PGT transports PGE_2 into the cell, where it is metabolised by 15-PGDH, therefore it is predicted that the highest PGT expressing cell line (MDA-MB-453) has reduced PGE_2 signalling. The balance between the different components of the prostaglandin pathway is likely to be important in controlling the amount of PGE_2 available.

In conclusion, a loss of 15-PGDH expression and activity has been reported in various cancers (Backlund et al., 2005; Lee, J.J. et al., 2010). This data confirms that 15-PGDH mRNA and protein expression is low in normal tissue and breast cancer in general and since research suggests 15-PGDH may have tumour suppressor properties (Backlund et al., 2005; Liu, Z. et al., 2008; Yan et al., 2004; Wolf et al., 2006; Myung et al., 2006) up-regulation of 15-PGDH or exogenous 15-PGDH may be beneficial in breast cancer treatment. Additionally, where 15-PGDH is over-expressed in tumour cells these appear to be associated with the rare apocrine subtype.

Chapter 4 Regulation of 15-PGDH expression in breast cancer *in vitro*

4.1 Introduction

15-PGDH has been implicated as a tumour suppressor in many cancer types, including colorectal, lung and breast cancer (Wolf et al., 2006; Myung et al., 2006; Tai et al., 2007). Yet patients with inherited deficiency of 15-PGDH do not exhibit a higher incidence of cancer, so that 15-PGDH does not meet the classical criteria of a tumour suppressor (Uppal et al., 2008). Although *HPGD* mRNA expression is low in breast tissue relative to other normal tissues (refer to Chapter 3), 15-PGDH expression may be further reduced in breast cancer compared to normal breast; it has therefore been hypothesised that up-regulation of 15-PGDH may be beneficial. For this reason it is important that the underlying mechanisms involved in the regulation of 15-PGDH expression are elucidated, with the goal of exploiting these mechanisms for therapeutic purposes.

The conditions under which 15-PGDH expression can be altered are not well known, though changes in the local environment, due to inflammation and hypoxia have been suggested (Mitchell et al., 2000; Tai et al., 2011; Young et al., 2013). Several processes have been implicated in the regulation of 15-PGDH expression in different cancer types, including regulation at a transcriptional level, reciprocal regulation with COX2 expression and DNA modifications (summarised in Chapter 1).

DNA modifications, reflecting epigenetic regulation of 15-PGDH expression have been a suggested mechanism for expression control. This work builds upon an observation by Wolf et al., who demonstrated that treatment of the MDA-MB-231 breast cell line with decitabine (DNMT inhibitor) and vorinostat (HDAC inhibitor), significantly increased *HPGD* mRNA expression (Wolf et al., 2006). Further analysis is required to determine if this is a major means of transcriptional and subsequent protein expression control commonly found in breast cancer.

4.1.1 Aims

As mentioned above, the regulation of 15-PGDH expression has been studied in various malignancies, but few studies have focused on breast cancer; moreover, conflicting results within and between cancer types indicate that the regulatory mechanisms may vary depending upon the cancers origin. This study aims to fill a gap in the literature and assess various

mechanisms potentially involved in the regulation of 15-PGDH expression in breast cancer. In order to do this, this chapters objectives are to evaluate the following:

1. The involvement of DNA methylation in *HPGD* regulation
2. The involvement of histone acetylation in *HPGD* regulation
3. The role of transcription factors in regulation of *HPGD*
4. The effect of hypoxia on 15-PGDH expression

4.2 Material and methods

4.2.1 Cell treatment

MCF7 and MDA-MB-231 cells were treated with DNA methyltransferase inhibitor decitabine and/or histone deacetylase inhibitor vorinostat for 72 hours, as described in Section 2.1.5, to determine whether methylation or histone acetylation alters *HPGD* transcription. Optimisation of the decitabine and vorinostat treatment was completed to determine the concentration that produced the largest change in *HPGD* mRNA expression with minimal cytotoxicity. 5µM decitabine and 1µM vorinostat met this criteria and are also regularly used in the literature for epigenetic experiments (Wolf et al., 2006; Hesson et al., 2013; Lim et al., 2012; Dolskiy et al., 2017). Consequently, these concentrations were taken forward in future experiments.

MCF7 cells were exposed to normoxic (20% O_2, 5% CO_2), and hypoxic (5% O_2, 5% CO_2) conditions, as described in Section 2.1.13. The standard DNase treatment of RNA was performed as described in Section 2.2.6. cDNA synthesis and RT-PCR were performed to assess *HPGD* mRNA expression (Sections 2.2.7 2.2.9).

4.2.2 Pyrosequencing

Pyrosequencing was used to assess the methylation status of *HPGD* with and without treatment with epigenetic drugs decitabine and/or vorinostat (Section 2.3.10). CpG-rich regions, known as CpG islands, were selected for methylation sequencing since they allow analysis of a larger number of densely-packed CpG sites within a small region, and because CpG islands are believed to be the main locations of regulatory changes in DNA methylation.

A CpG island is defined by the following specifications (Fazzari and Greally, 2004):

1. More than 200 bp in size but usually between 300-3000 bp
2. Base composition of over 50% GC

3. Observed/expected ratio of CpG dinucleotides >0.6

HPGD has three such CpG islands (Figure 4.1, Table 4.1), the first of which is centred over the first exon-intron boundary. This CpG island covers part of the promoter region and ATG translation start site of the gene. The second and third CpG islands are located within introns 3 and 4 respectively. A total of 97 CpG sites were assayed over the three CpG islands.

Each assay was designed to meet the following criteria (Tost and Gut, 2007) and the primer design criteria mentioned in Section 2.2.8 where possible:

1. Pyrosequencing PCR primers
    a. Contain at least 4 non-CpG C residues (and therefore only complementary to completely converted DNA)
    b. No CpG sites within the primer region (to avoid preferential amplification)
    c. PCR product should be no more than 350 bp
2. Sequence <150 nucleotides, due to a limited read length in pyrosequencing from dilution effects and incomplete incorporated dispensed nucleotides

To meet the above criteria, each CpG island was divided into two or three PCR amplicons and sequenced with up to three sequencing primers. Pyrosequencing was performed in the reverse complement direction due to addition of the biotin on the forward PCR primers.

4.2.3 Cistrome ChIP-Seq data analysis

The Cistrome database is an archive of chromatin immunoprecipitation with DNA sequencing (ChIP-Seq) and chromatin accessibility data from gene expression omnibus, Encyclopaedia of DNA Elements (ENCODE) and Roadmap Epigenomics, which is based on 13,366 human samples (Mei et al., 2017).

ChIP-Seq enables the identification of DNA binding sites of specific proteins. The method involves cross-linking of protein to the DNA, after which the chromatin is sheared and precipitated using an antibody to a target protein. The precipitated protein is then uncoupled from the DNA and the DNA sequenced. In this case, as the target protein is unknown, the Cistrome database enables the analysis of data collected for over 800 transcription factors and 80 histone marks (Mei et al., 2017).

The region of binding that was assessed was chr4:174,522,254-174,523,564 (GRCh38), which covers the first CpG island (chr4:174,522,256-174,522,686) and 1000 bp upstream of the transcription start site.

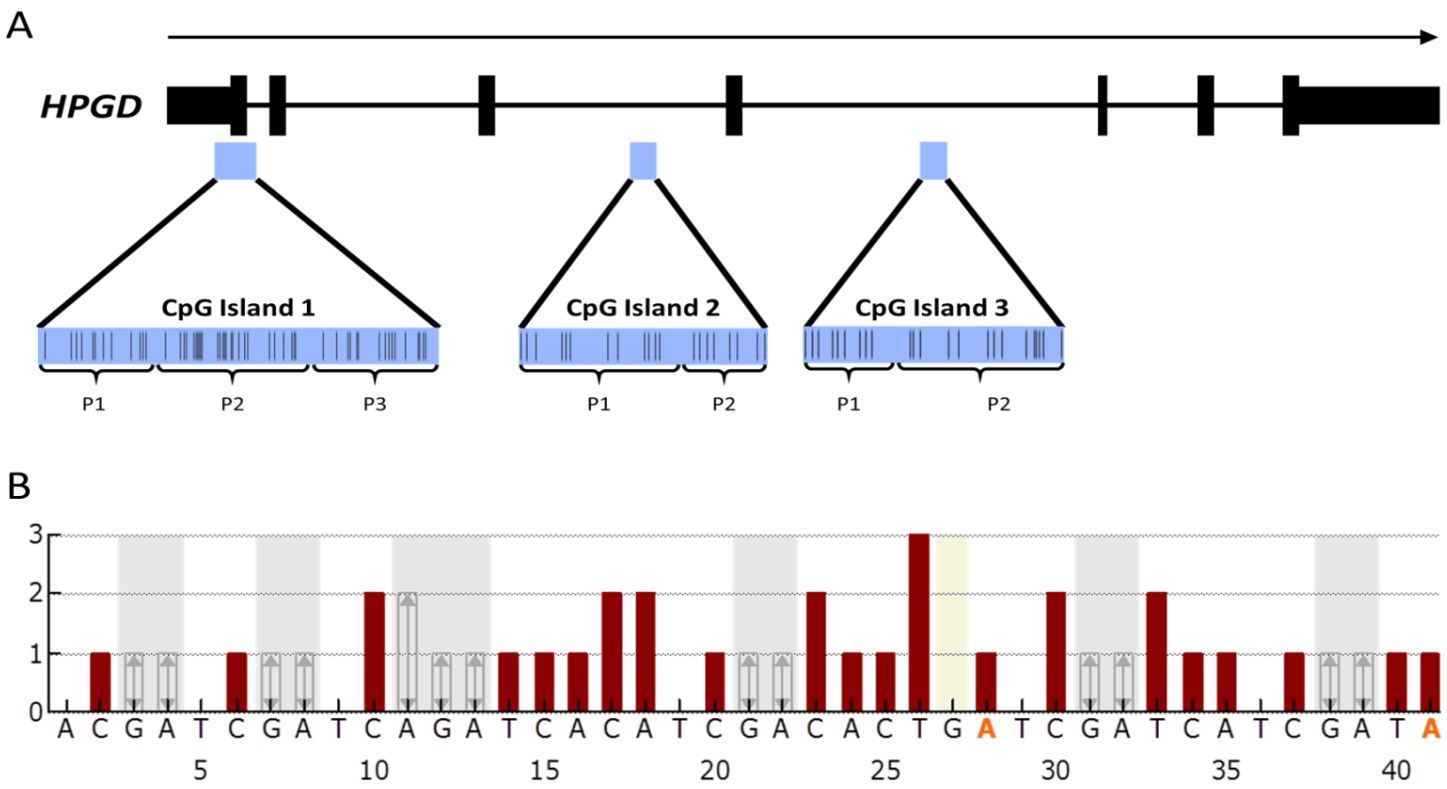

Figure 4.1 *HPGD* pyrosequencing assay design. (A) A schematic of the *HPGD* gene and its three CpG islands. Arrow indicates the direction of transcription. Gene coordinates = chr4:174,490,177-174,522,898 (GRCh38). CpG island 1 contains 54 CpGs in 431 bp, CpG island 2 contains 20 CpGs in 266 bp and CpG island 3 contains 22 CpGs in 278 bp. P1-3 show the PCR products generated for pyrosequencing. (B) Expected histogram of CpG island 1, product 2 (P2), sequencing primer set 2 (S2). The x-axis indicates the nucleotide dispensed, the y-axis the number of incorporated nucleotides. Red bar = incorporation of the indicated nucleotide, grey block = CpG site, grey arrows = variation on peak height and number of nucleotides incorporated depending upon methylation status of CpG, pale green = bisulphite control G nucleotide (should be no nucleotide incorporation).

Table 4.1 *HPGD* CpG island information

HPGD CpG island	Genomic cordinates	Location	Size (bp)	CpG count	Percentage CpG (%)	GC content (%)	Observed/expected CpG ratio
1	chr4:174522256-174522686	Exon 1 - Intron 1	431	53	24.6	71.7	0.96
2	chr4:174511677-174511942	Intron 3	266	20	15	59.4	0.86
3	chr4:174502396-174502673	Intron 4	278	22	15.8	61.5	0.85

4.3 Results

4.3.1 Optimisation of epigenetic drug concentration

MCF7 and MDA-MB-231 cells were treated with a range of doses of decitabine (0-20 µM) and vorinostat (0-10 µM) to assess their cytotoxicity. The "Genomics of Drug Sensitivity in Cancer" resource, which is a compilation of drug sensitivities in cancer cell lines, calculated the IC_{50} (the concentration at which the cells exhibit 50% loss of viability) for vorinostat in 881 cancer cell lines using a screening range 0.0391 to 10 µM, and determined a mean of 2.67 µM (Yang, W. et al., 2013). Furthermore, the IC_{50} values reported in solid tumour cells, including breast cancer cell lines, ranged from 0.013 µM to 1.3 µM after 48 or 96 hours exposure (Karahoca and Momparler, 2013). The concentration ranges selected cover the IC_{50} values indicated in the literature. Cell viability was measured at 0, 24, 48 and 72 hours after drug treatment.

A higher dose of decitabine than vorinostat was tolerated by both MCF7 and MDA-MB-231 cells (Figure 4.2). An IC_{50} for MCF7 cells after 72 hours was ~18 µM of decitabine, but decitabine did not kill more than 50% of the MDA-MB-231 cells, therefore an IC_{50} could not be determined. MCF7 cells were slightly more resistant to vorinostat compared to MDA-MB-231 cells, with an IC_{50} of ~1.1 µM and ~0.8 µM, respectively.

Interestingly, an increase in proliferation was observed in both MCF7 and MDA-MB-231 cells following 24 hours exposure to most concentrations of decitabine, though this trend was lost by 48 hours. In contrast, toxicity was observed at 24 hours with vorinostat. Increased toxicity for both decitabine and vorinostat was seen with 48 and 72 hours' treatment, which was confirmed visually through cell death and cell debris compared to the DMSO control (Figure 4.3). All further experiments were completed following 72 hours' treatment. This exposure time was considered the most clinically relevant, as decitabine has been FDA-approved for treatment of myelodysplastic syndromes with a dosing regimen of 15 mg/m^2 over 3 hours every 8 hours, for 3 days every 6 weeks (Saba, 2007).

The aim of these *in vitro* drug treatment experiments was to assess the role of epigenetic mechanisms in 15-PGDH expression. The mRNA expression of *HPGD* was therefore assessed following 72 hours' drug treatment with decitabine or vorinostat alone, to determine the concentration at which the largest up-regulation of *HPGD* was observed (Figure 4.4).

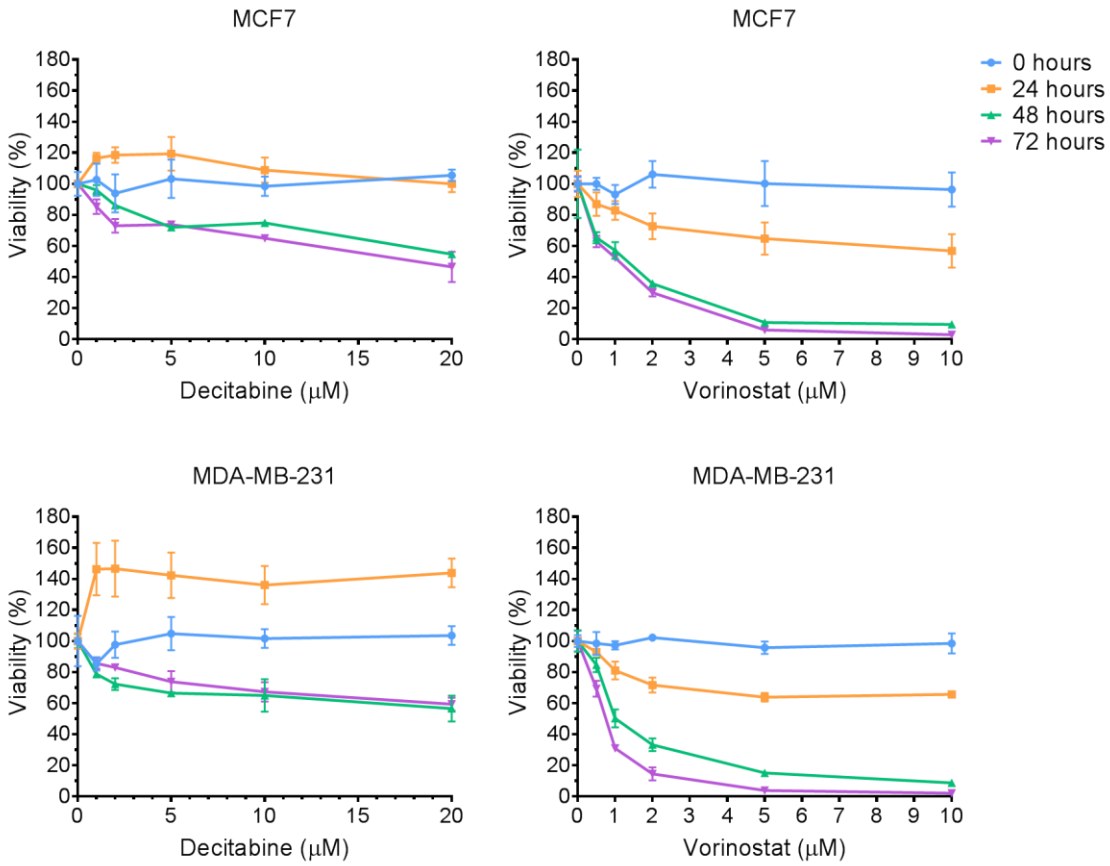

Figure 4.2 MCF7 and MDA-MB-231 viability after decitabine and vorinostat treatment. MCF7 cells (top) and MDA-MB-231 (bottom) were treated for 0 hours (blue), 24 hours (orange), 48 hours (green) or 72 hours (purple) with varied doses of decitabine (left) or vorinostat (right) and metabolic activity assessed using an MTS assay. The results were normalised to a DMSO control to determine the percentage of viable cells. Error bars indicate one standard deviation for three biological repeats.

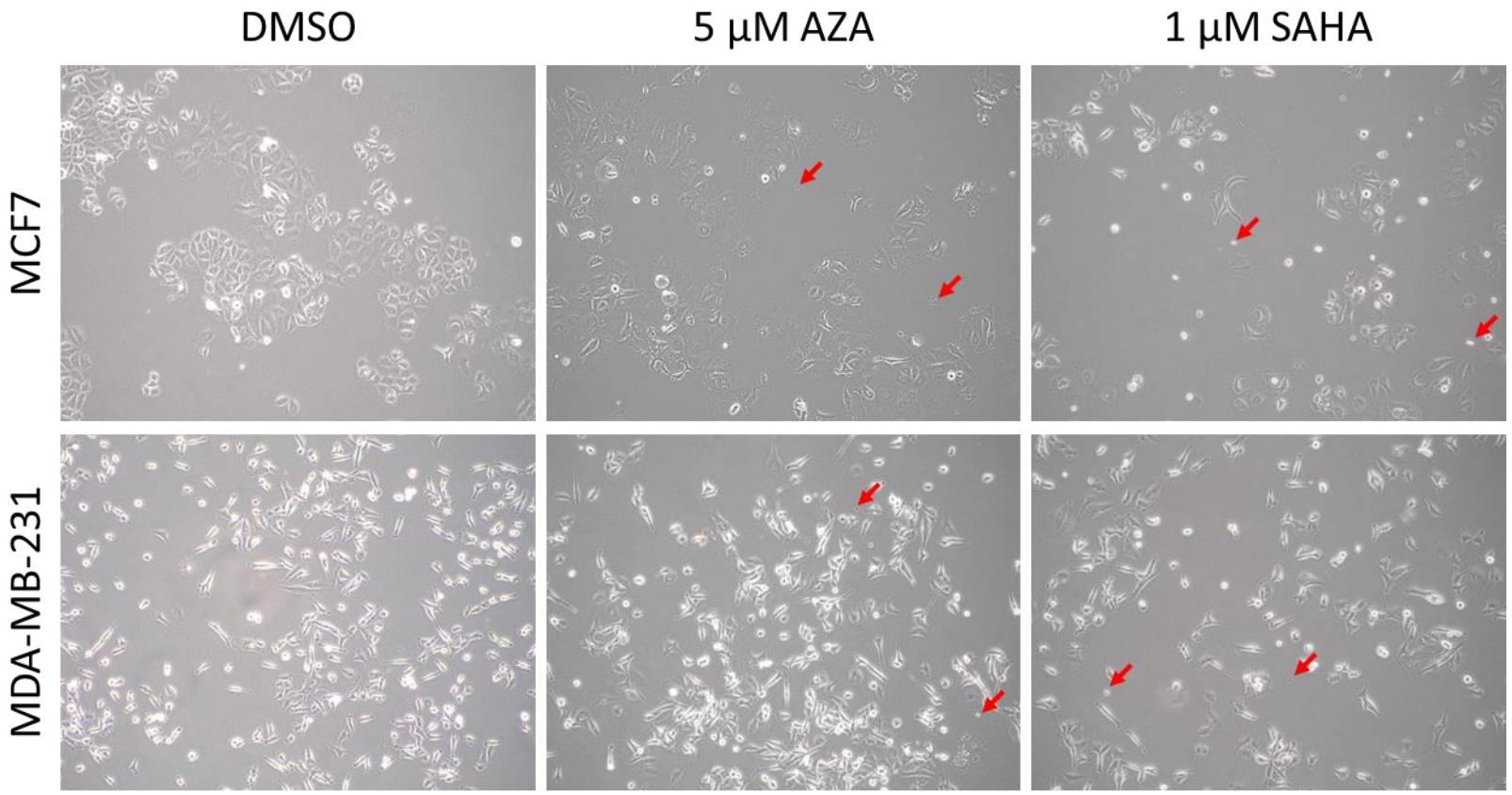

Figure 4.3 MCF7 and MDA-MB-231 cells after 72 hour epigenetic drug treatment. Images of MCF7 (top) and MDA-MB-231 (bottom) treated for 72 hours with DMSO control (left), 5 µM decitabine (centre) or 1 µM vorinostat (right). An increased number of floating cells and cell debris indicated by red arrows seen with decitabine and vorinostat treatment.

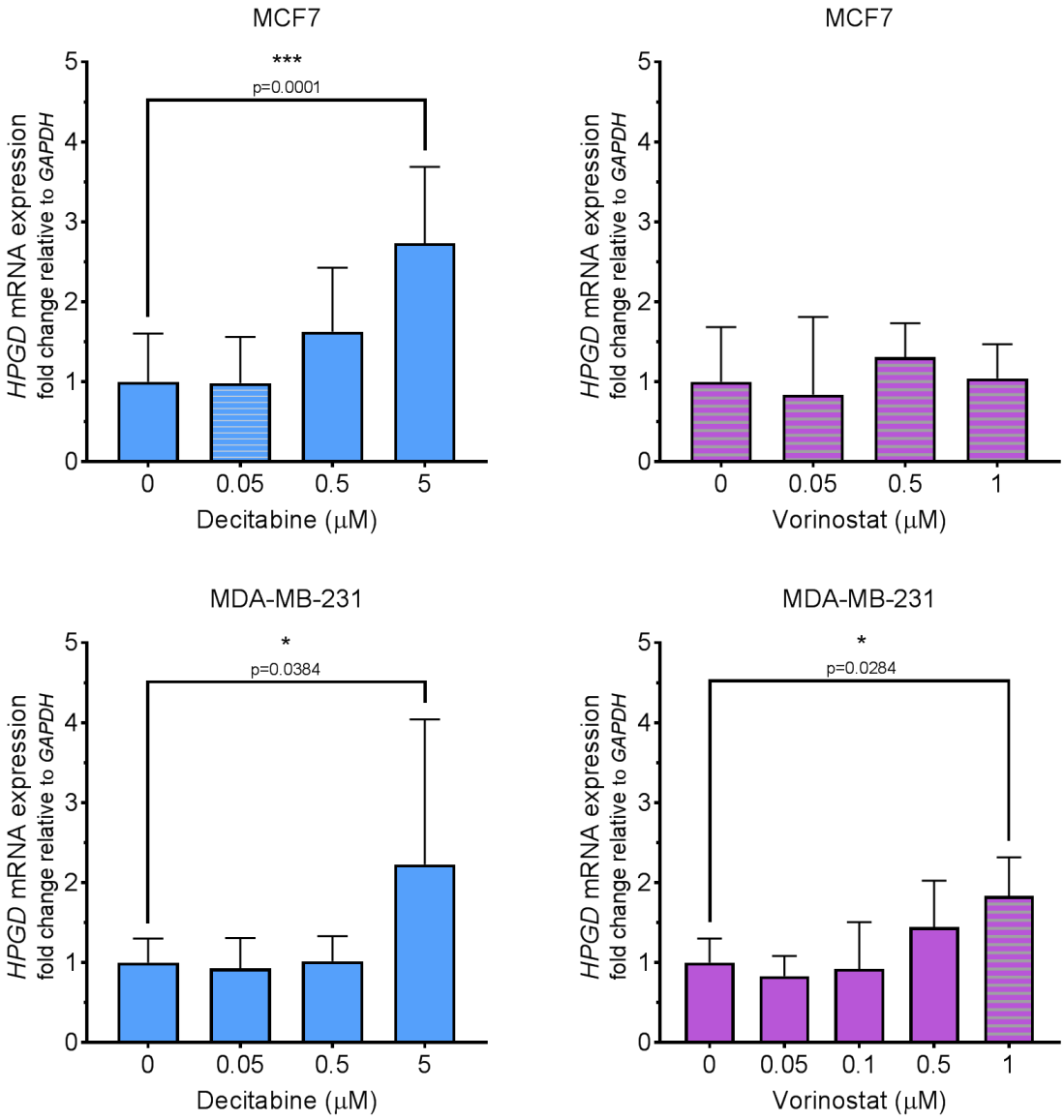

Figure 4.4 *HPGD* mRNA expression following epigenetic drug treatment. MCF7 and MDA-MB-231 cells were treated with a range of decitabine and vorinostat doses or a DMSO control, for 72 hours. RT-PCR was performed with both *HPGD* and *GAPDH* primers. The samples were quantified after gel electrophoresis using ImageLab software and *HPGD* expression normalised to the *GAPDH* loading control. Error bars indicate one standard deviation of one (striped colour bars) or two (solid colour bars) independent experiments. One-way ANOVA performed to determine statistical significance.

A significant 2.73-fold increase in *HPGD* mRNA was observed in MCF7 cells ($p = 0.0001$) after 5 µM decitabine treatment for 72 hours and 2.23-fold increase in MDA-MB-231 cells ($p = 0.0384$). Although these are significant, the variation between repeats resulted in the data having a large standard deviation. No significant difference was observed with vorinostat treatment after 72 hours in the MCF7 cell line, whereas a 1.83-fold increase was observed in the MDA-MB-231 cell line with 1 µM vorinostat ($p = 0.0284$).

The results indicate that 5 µM decitabine and 1 µM vorinostat have the largest effect on *HPGD* expression in MCF7 and MDA-MB-231 cell lines. Since both 5 µM decitabine and 1 µM vorinostat caused minimal cell death in both MCF7 and MDA-MB-231 cells (Figure 4.3 and Figure 4.4), these were the concentrations used for further work.

4.3.2 Increased *HPGD* mRNA in breast and colorectal cell lines following epigenetic drug treatment

HPGD mRNA expression was assessed after epigenetic drug treatment with demethylating agent decitabine and/or HDAC inhibitor vorinostat, using the more accurate method of qRT-PCR. As conventional RT-PCR is semi-quantitative, the reliability of the data is dependent upon the PCR and gel imaging not becoming saturated and reducing the linearity of the data. In comparison, qRT-PCR is a highly accurate and quantitative technique and as three independent experiments were performed, the qRT-PCR data represents a much more reliable dataset.

As the expression of 15-PGDH is low in breast cell lines, it was decided that performing the experiments with an intermediate or high 15-PGDH-expressing cell line would allow for clearer assessment of the results. The literature on the prostaglandin pathway and the role of 15-PGDH in breast cancer is very limited; in contrast, the role of 15-PGDH in colon cancer has been well established. As shown in Chapter 3, CaCo-2 and LoVo cell lines exhibit high and intermediate levels of *HPGD* expression, respectively. These two cell lines were therefore included in the qRT-PCR experiments for comparison.

HPGD mRNA expression was significantly increased by drug treatment in the MDA-MB-231 and LoVo cell lines. Despite an increase in average expression observed in MCF7 and CaCo-2 cells, these were not significant changes (Figure 4.5). A 5.17-fold increase in 15-PGDH expression was observed in MDA-MB-231 ($p < 0.0001$) and 7.72-fold in LoVo ($p < 0.0001$) with decitabine alone.

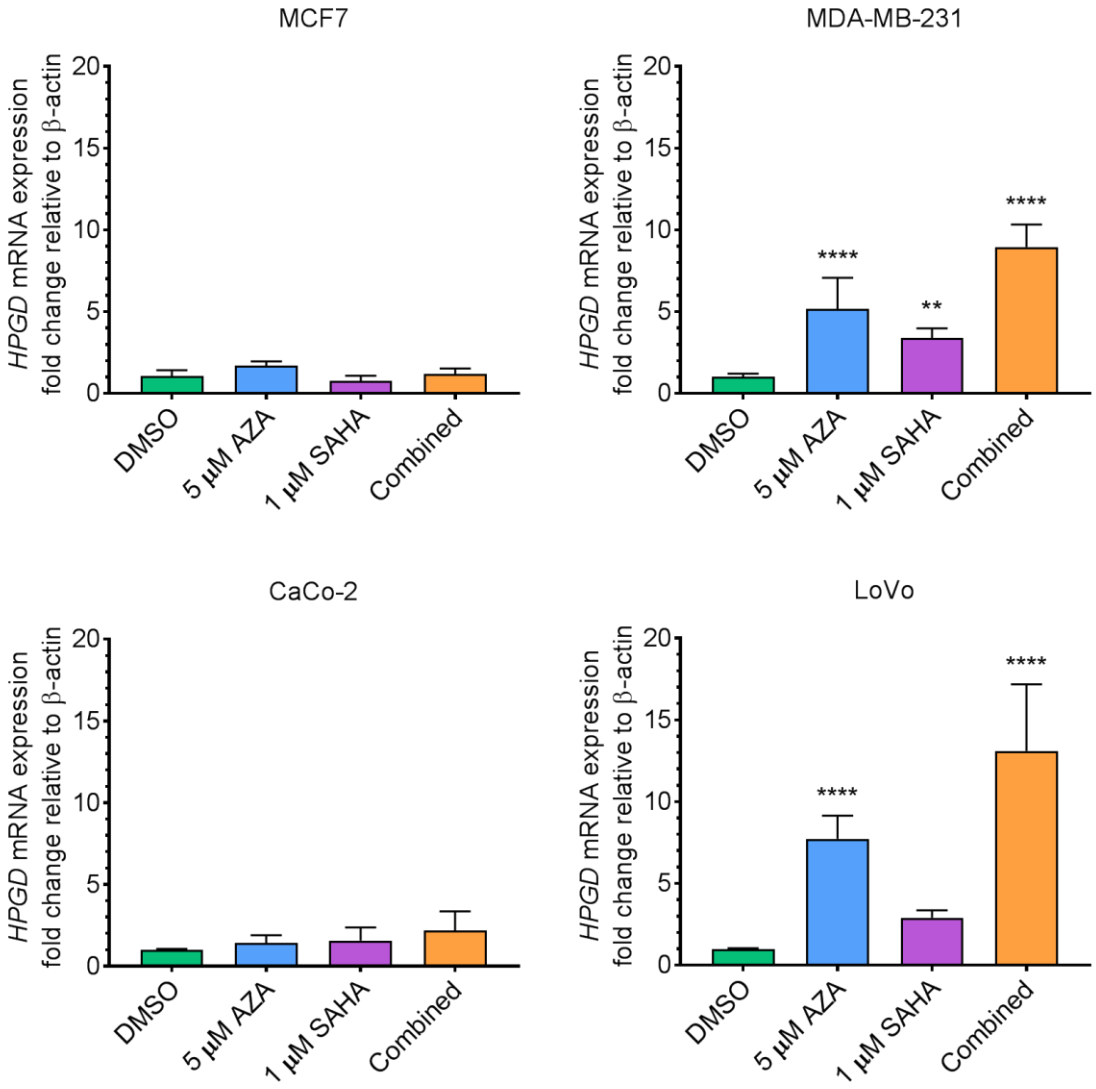

Figure 4.5 qRT-PCR with β-actin and *HPGD* primers in epigenetic drug-treated cell lines. qRT-PCR was performed on cells treated for 72 hours with 5 μM decitabine (AZA) and/or 1 μM vorinostat (SAHA) or DMSO control. 15-PGDH Ct values were normalised to their relative β-actin controls and the *HPGD* mRNA fold change calculated. Error bars show one standard deviation for two (MCF7 and MDA-MB-231) or three (CaCo-2 and LoVo) independent experiments. A significant increase in *HPGD* expression is observed where * $p < 0.01$, ** $p < 0.001$, *** $p < 0.0001$ and **** $p < 0.00001$ using a one-way ANOVA.

A significant 3.40-fold increase was seen in the vorinostat treatment alone with MDA-MB-231 ($p = 0.0072$); however, a 2.90-fold increase in the LoVo cell line was not significant ($p = 0.1723$). When the two epigenetic drugs were combined, an additive effect was observed, with an 8.96-fold increase ($p < 0.0001$) and 13.10-fold increase ($p < 0.0001$) in *HPGD* mRNA expression seen in MDA-MB-231 and LoVo cells, respectively.

4.3.3 Increased expression of 15-PGDH protein in cell lines following epigenetic drug treatment

Once an increase in *HPGD* transcript levels had been demonstrated, immunocytochemistry was performed to assess whether epigenetic drug treatment also increased 15-PGDH protein expression. 15-PGDH antibody optimisation for immunocytochemistry was performed on A549 and MCF7 cell lines (Section 3.3.2). A positive A549 lung control was included in the staining, with mainly cytoplasmic and some nuclear staining (results not shown). Labelling varied between cells within the sample.

15-PGDH protein (red label) was mainly localised to the cytoplasm in drug-treated MDA-MB-231 cells, with some variation in expression between cells (Figure 4.6). No change in 15-PGDH protein expression was observed in the MCF7 cell line. In contrast, in the MDA-MB-231 cell line an increase in 15-PGDH expression was observed with decitabine alone.

4.3.4 Epigenetic drug treatment has no significant effect on *HPGD* methylation

The *HPGD* gene contains three CpG islands (summarised in Table 4.1), meeting the criteria listed in Section 4.2.2. The CpG islands are relatively small, but have a GC content of at least 59.4% and an observed/expected CpG ratio of at least 0.85.

Pyrosequencing was performed to determine whether the *HPGD* gene was methylated and if epigenetic drug treatment was altering the methylation status of the gene to cause increased *HPGD* transcription. Several assays were designed to cover the three CpG islands located within the gene, as this is where the largest number of CpGs could be assessed.

The first CpG island, which is located over the ATG translation start site (Figure 4.1), was found to be essentially unmethylated (7.26% and 7.59%) in the untreated samples, in both MDA-MB-231 and LoVo cell lines (Figure 4.7) as well as MCF7 cells (Appendix 13).

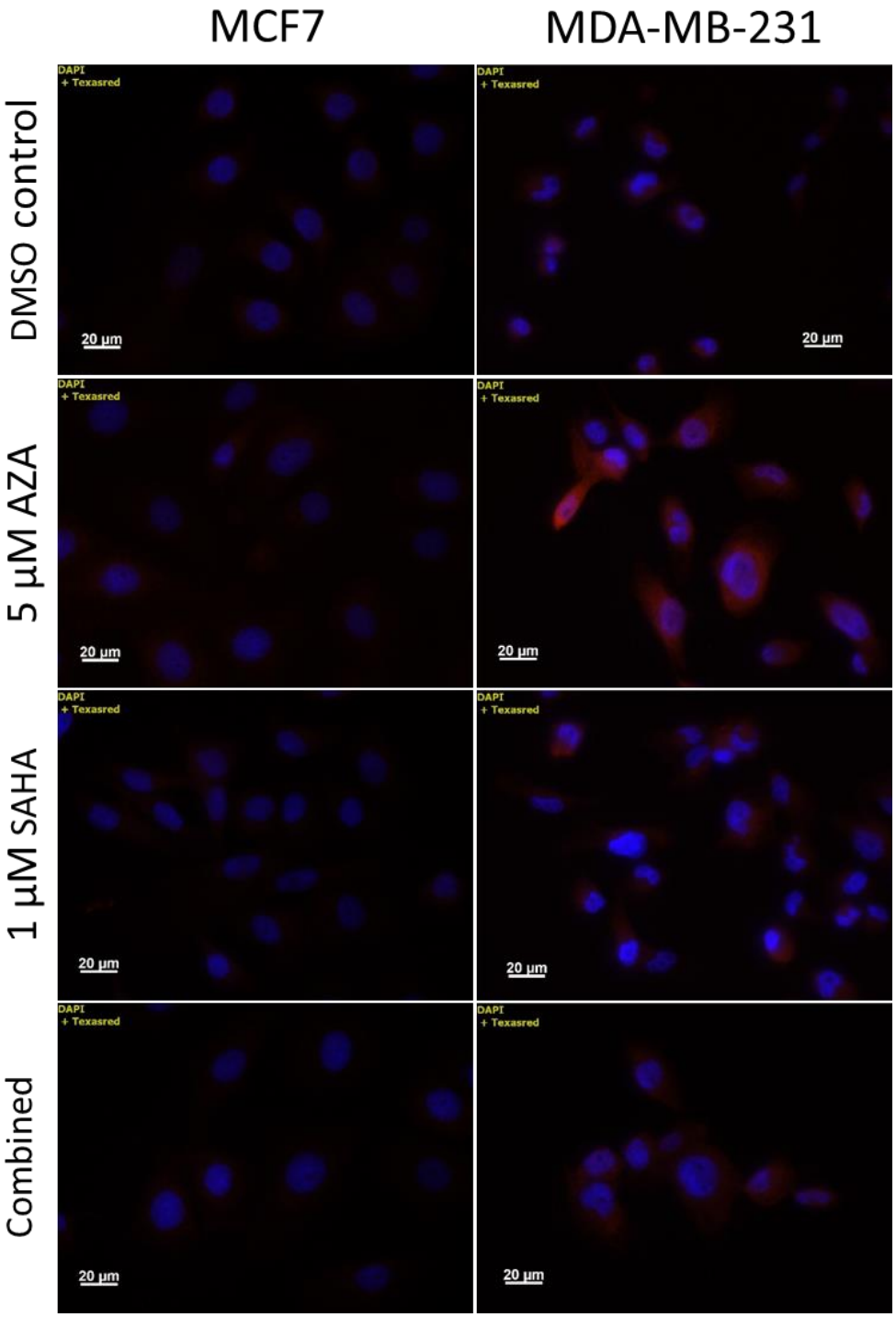

Figure 4.6 15-PGDH protein expression following epigenetic drug treatment. Immunocytochemistry using a fluorescent secondary antibody indicated the level of 15-PGDH protein expression in MCF7 and MDA-MB-231 cell lines following epigenetic drug treatment for 72 hours. AZA = decitabine, SAHA = vorinostat, combined = 5 µM decitabine and 1 µM vorinostat. Blue = DAPI nuclear staining, red = 15-PGDH cytoplasmic staining. Images were taken at x40 objective. The experiment was repeated twice. Scale bar = 20 µm.

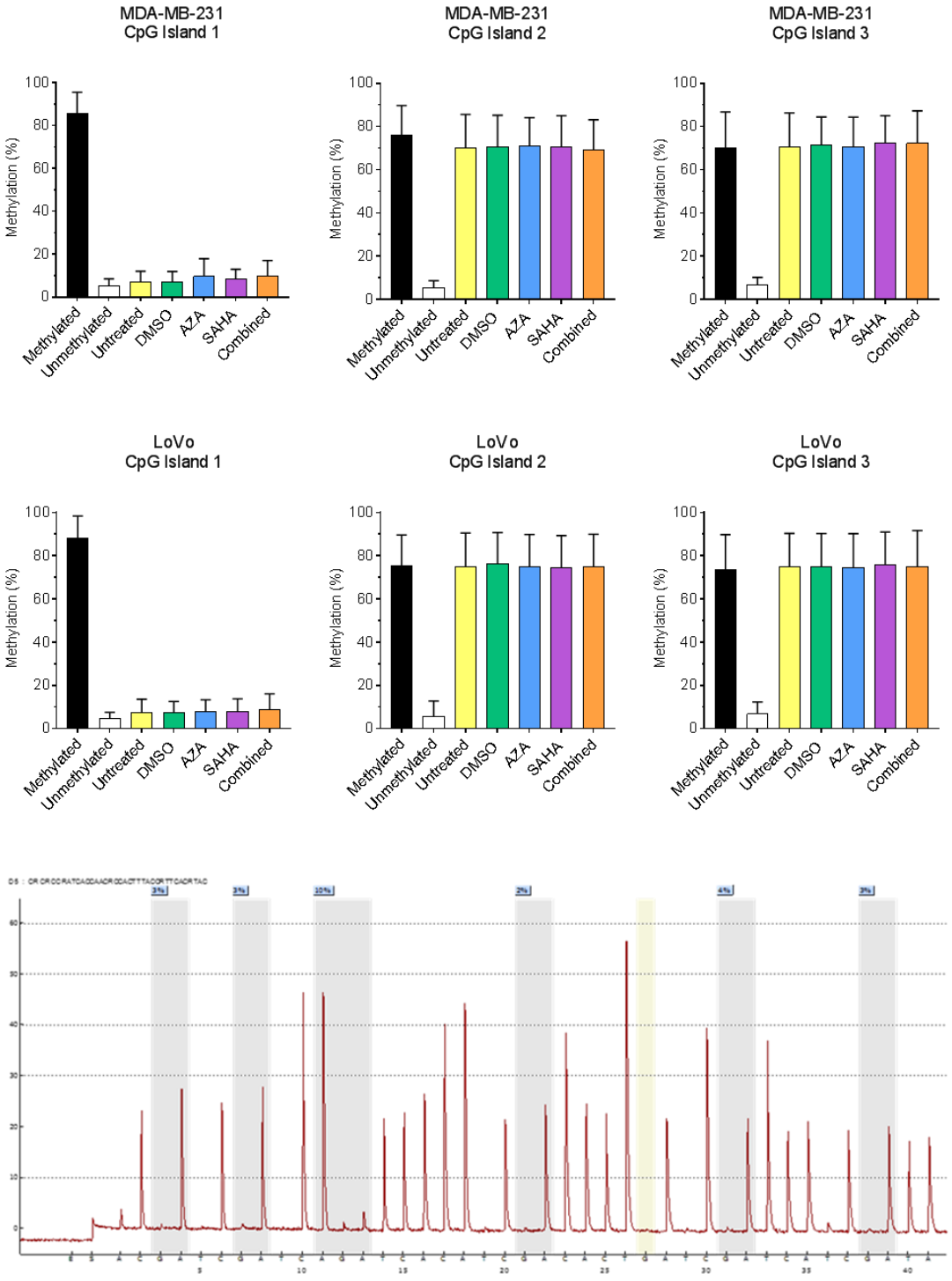

Figure 4.7 Methylation analysis of epigenetic drug-treated cell line samples at *HPGD* CpG islands. Black = methylated control DNA, white = unmethylated control DNA, yellow = untreated DNA, green = DMSO control DNA, blue = 5 µM decitabine-treated DNA, purple = 1 µM vorinostat-treated DNA, orange = combined decitabine and vorinostat treatment. Row 1 = MDA-MB-231 CpG Island 1, 2 and 3 respectively. Row 2 = LoVo CpG Island 1, 2 and 3 respectively. Row 3 = pyrogram for CpG island 1 PCR product 2, sequencing primer set 2, with untreated MDA-MB-231 DNA in the reverse complement orientation. Grey shading highlights the CpG locations, green indicates the bisulphite control. X-axis = nucleotide number, y-axis = arbitrary units (light).

In contrast, CpG islands 2 and 3, located in exons 3 and 4, were highly methylated (CpG island 2 = 70.21% and 71.97%, CpG island 3 = 70.71% and 74.96%) in both MDA-MB-231 and LoVo cell lines. No significant change was observed in methylation following epigenetic drug treatment in any of the cell lines assessed. There was some variation in the absolute level of methylation at individual CpG sites within the islands (Appendix 14), but there was no clear difference following drug treatment at the individual sites.

Pyrosequencing was selected as the primary method to assess methylation as the technique can simultaneously sequence a large set of samples and produces a quantitative output. The method cannot however be used to sequence long homopolymers, which result in high error rates (Siqueira et al., 2012). Bisulphite Sanger sequencing was performed with one of the PCR products to confirm the reliability of data.

Bisulphite Sanger sequencing was performed on a region including the 26 CpGs from CpG island 1, which covers the gene's ATG translation start site, on 10 clones of MDA-MB-231 untreated and decitabine-treated DNA (Figure 4.8). The results confirmed the pyrosequencing data, as only 3 out of 260 (1.15%) CpGs in the untreated control and 2 out of 260 (0.77%) decitabine-treated were methylated.

4.3.4.1 The *HPGD* promoter is largely unmethylated in breast tissue

To examine whether *HPGD* gene methylation status observed in the cell lines was representative of the *in vivo* situation, methylation of invasive breast carcinoma DNA samples was assessed using MEXPRESS. MEXPRESS uses data obtained for The Cancer Genome Atlas (TCGA) project to look at gene methylation in patients at specific probe locations. DNA methylation information was collected from samples using an Infinium HumanMethylation450 microarray and combined with RNA-seq-derived expression data alongside clinical data to generate the MEXPRESS platform (Koch et al., 2015).

The MEXPRESS results shown in Figure 4.9 and Appendix 15 are curated from 871 breast invasive carcinoma samples and some normal breast samples. There are 14 probes that have been assessed within the *HPGD* gene; the five highlighted in green in Table 4.2 have also been assessed by pyrosequencing. The *HPGD* gene promoter ± 1500 bp to the TSS is largely demethylated (probes 3-9) in most of the samples.

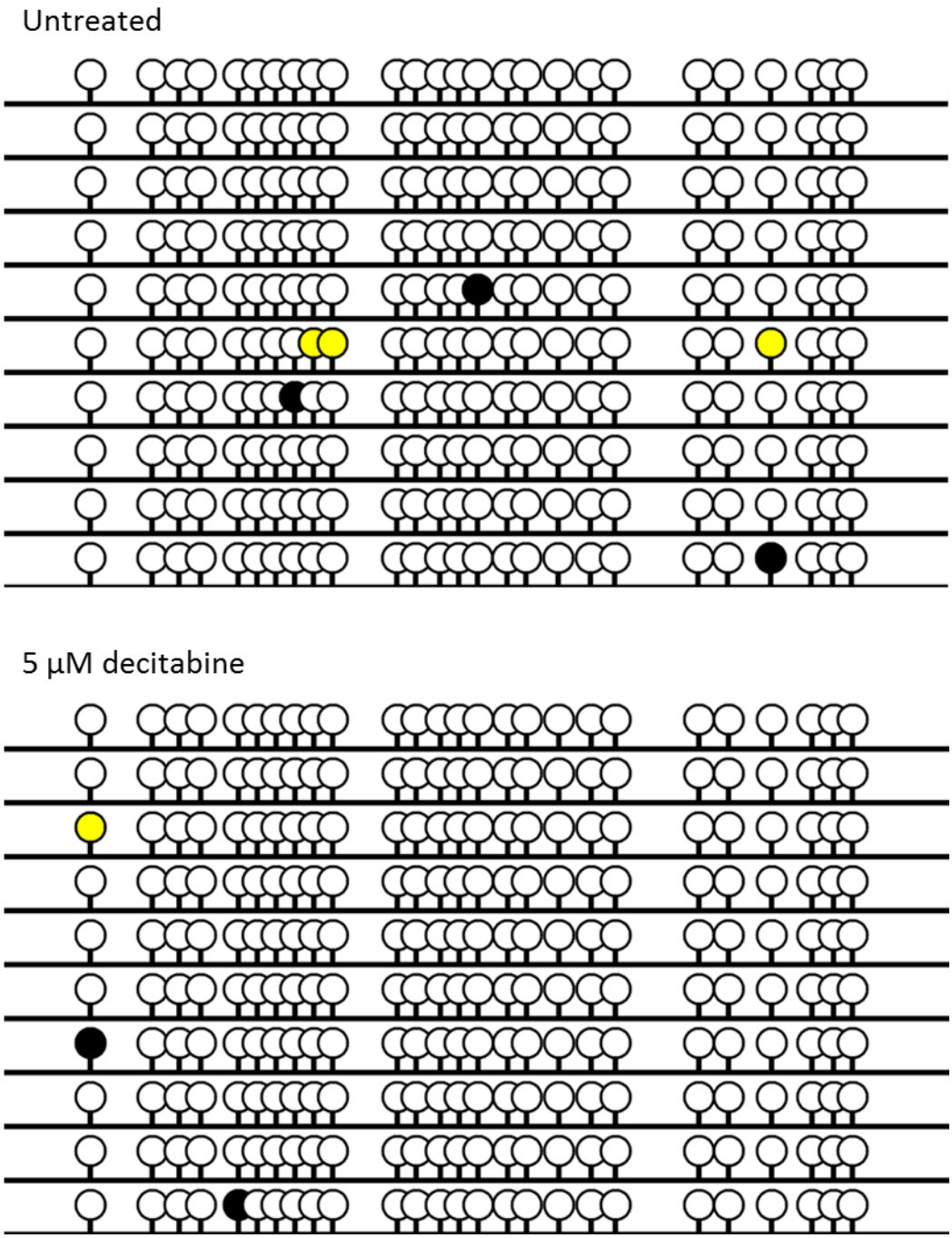

Figure 4.8 Bisulphite Sanger sequencing of LoVo DNA untreated or treated with decitabine. Bisulphite sequencing of LoVo DNA following 72 hours' incubation, either untreated or with 5 µM decitabine. White lollipop = unmethylated, black lollipop = methylated, yellow lollipop = undetermined. A total of 26 CpGs in the first *HPGD* CpG island were assessed in 10 clones in both the forward and reverse orientation. The figure shows the forward orientation only.

Figure 4.9 MEXPRESS data analysis for the *HPGD* gene and breast invasive carcinoma samples. Samples sorted by 15-PGDH expression, high to low shown in orange (left to right). The blue peaks show the level of methylation for each CpG site for the 871 individual patients. A significant increase in methylation is observed with decreased 15-PGDH expression at 13 of the 14 CpG probe sites.

Table 4.2 Summary of MEXPRESS data. Green indicates the CpG sites that were analysed by pyrosequencing. The Wilcoxon rank-sum test was performed to generate p values, $p < 0.05$ was classed as significant. Pearson correlation was calculated to generate the r values, positive value = positive correlation, negative value = negative correlation. * $r < 0.05$, ** $r < 0.01$, *** $r < 0.001$.

Probe		Chromosome 4 position (GRCh37/hg19)	Position		Statistical analysis based on:	
					Sample type	Expression
14	cg03772063	chr4:175440325	gene body	Intron 1	p < 2.2e-16	r = -0.000646
13	cg06366981	chr4:175443243	gene body	Intron 1	p = 2.24e-7	r = -0.0712 *
12	cg02822257	chr4:175443407	gene body	Intron 1 (CpG island 1)	p = 3.95e-4	r = -0.127 ***
11	cg11073923	chr4:175443752	1st exon, 5'UTR, gene body	Exon 1 (CpG island 1)	p = 6.23e-8	r = -0.127 ***
10	cg11073923	chr4:175443752	1st exon, 5'UTR, gene body	Exon 1 (CpG island 1)	p = 0.0168	r = -0.135 ***
9	cg00906130	chr4:175443797	TSS ± 200, gene body	Exon 1 (CpG island 1)	p = 3.96e-11	r = -0.133 ***
8	cg18164599	chr4:175443867	TSS ± 200, gene body	Exon 1 (Edge of CpG island 1)	p = 0.19	r = -0.0956 **
7	cg15474754	chr4:175444096	TSS ± 200, TSS ± 1500	Upstream of exon 1	p = 0.0205	r = -0.0751 *
6	cg13181537	chr4:175444120	TSS ± 200, TSS ± 1500	Upstream of exon 1	p = 0.819	r = -0.181 ***
5	cg05527430	chr4:175444181	TSS ± 200, TSS ± 1500	Upstream of exon 1	p = 0.00779	r = -0.222 ***
4	cg04555941	chr4:175444268	TSS ± 1500	Upstream of exon 1	p = 4.92e-5	r = -0.163 ***
3	cg01084566	chr4:175444482	TSS ± 1500	Upstream of exon 1	p = 1.09e-4	r = -0.0726 *
2	cg20455617	chr4:175444948	TSS ± 1500	Upstream of exon 1	p = 2.62e-10	r = -0.161 ***
1	cg06937164	chr4:175446087	Upstream of exon one	Upstream of exon 1	p = 6.21e-10	r = +0.314 ***

MEXPRESS data reveals a significant correlation between *HPGD* mRNA expression and methylation at probes 1-13 (Pearson correlation, $p < 0.05$). A very weak negative correlation ($r = -0.00$-0.19) was observed with probes 2-13, with the exception of probe 5 which showed weak negative correlation ($r = -0.20$-0.39). This demonstrates that increased methylation is associated with decreased *HPGD* mRNA expression, whereas a weak positive correlation was observed with probe 1 in the promoter region presenting increased methylation with increased *HPGD* mRNA expression.

When the samples were sorted by tissue origin (solid tissue normal, metastatic and primary solid tumour), a significant trend between methylation status and sample type was observed for 12 of the 14 probes (Wilcoxon rank-sum test, $p < 0.05$). This shows that a significant increase in methylation was observed in the cancer samples when compared to normal tissue at twelve CpG sites.

No statistical data was available when grouping the samples by PAM50 subtype (which divides the samples into normal, basal, HER2 positive, luminal A and luminal B subtypes) (data not shown). Visual inspection showed less methylation at probes 9 to 11 in normal and basal subtypes compared to the other subtypes.

When the samples were ordered by menopause status, no statistical significance was observed for 12 of the 14 CpG probe locations with r values of +0.101 and −0.09 for the two significant probes, indicating no strong trend. Similarly no statistical significance was observed when looking at the relationship between methylation and pathological stage or lymphocyte infiltration, except for a negative correlation with one CpG site for the lymphocyte infiltration.

A significant relationship between decreased methylation and positive ER and PR expression was observed for 8 and 6 probes, respectively, with most of the significant CpG sites in the upstream promoter region. Yet no statistical significance was observed between *HPGD* methylation and HER2 expression.

Interestingly, a significant positive link between *HPGD* methylation and age at diagnosis was observed for 6 of the CpG sites in the MEXPRESS data and a significant negative correlation at 3 CpG sites.

4.3.5 Transcription factor binding locations

As the methylation levels within the promoter region were inherently low and did not appear either to be strongly associated with transcript levels *in vivo*, or *in vitro*, an alternative approach

to understanding the mechanism of transcriptional regulation was pursued. To determine which transcription factors bind to the *HPGD* promoter and thus may alter *HPGD* expression, data obtained from the Cistrome online database was assessed.

Both high and low *HPGD* expressing cell lines were selected, as it was hypothesised that this might identify factors important for producing high *HPGD* transcriptional activity, and those that would repress or maintain basal gene activity, respectively. Transcription factors that were found to bind at the *HPGD* promoter region in the A549 and LoVo cell lines, which exhibit high to moderate endogenous 15-PGDH expression, are shown in Figure 4.10. Conversely, transcription factors shown to bind to the *HPGD* promoter region in cell lines with low endogenous 15-PGDH expression, including the breast MCF7 and MDA-MB-231 lines, are shown in Figure 4.11.

Fifteen transcription factors were found to bind in the A549 high expressing cell line and five in LoVo samples. Eleven transcription factors were shown to bind to the *HPGD* promoter region in the low expressing MCF7 cells, two in the MDA-MB-231 cell line and one in HT-29 cells. Twelve transcription factors were unique to the high expressing cell lines and eight to the low expressing cell lines. GATA3, POLR2A and SIN3A showed binding in both high and low expressing cell lines.

GATA3 showed a different binding pattern between the high and low expressing cells, binding within the CpG island in high expressing cell lines and further upstream in the low expressing cell lines. Overlap of the binding sites was seen with both SIN3A and POLR2A in the high and low expressing cell lines.

4.3.6 Transcription factor expression in cell lines

The expression levels of transcription factors that bind to the *HPGD* promoter region, according to the ChIP-Seq data from the Cistrome database (Figure 4.10 and Figure 4.11), were assessed in a range of cell lines to determine whether a trend was observable in high versus low 15-PGDH expressing cells (Figure **4.12**).

Thirteen transcription factors that bind to the *HPGD* promoter were identified for analysis (Table 4.3). They were selected if they bound to high *HPGD* expressing cells but not those with low expression, or *vice versa*, so as to identify potential 15-PGDH promoter activators and repressors.

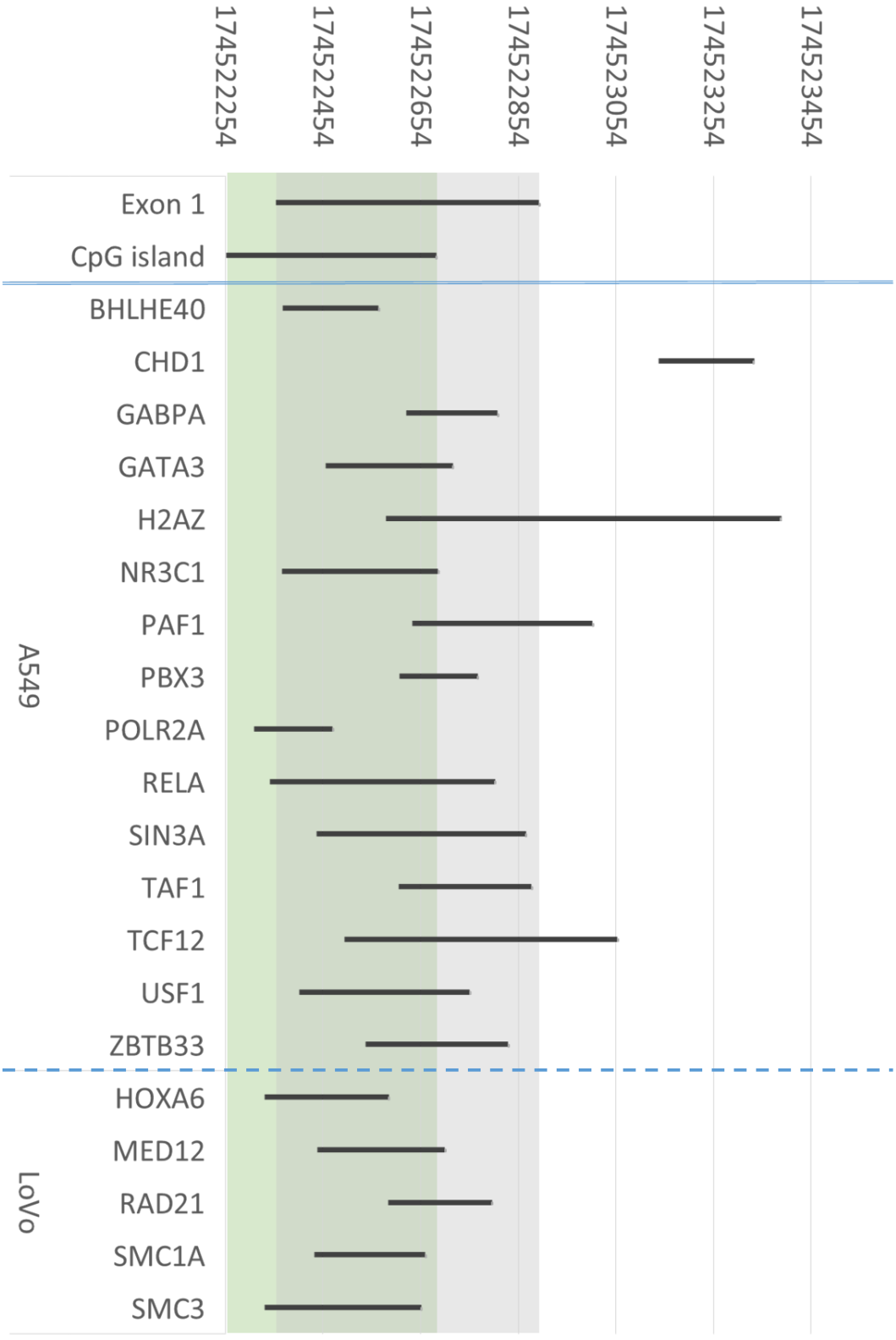

Figure 4.10 Transcription factor binding sites in high to moderate 15-PGDH expressing cell lines taken from the Cistrome database. Chromosome 4 position indicated at the top. Exon 1 = grey, CpG island 1 = green.

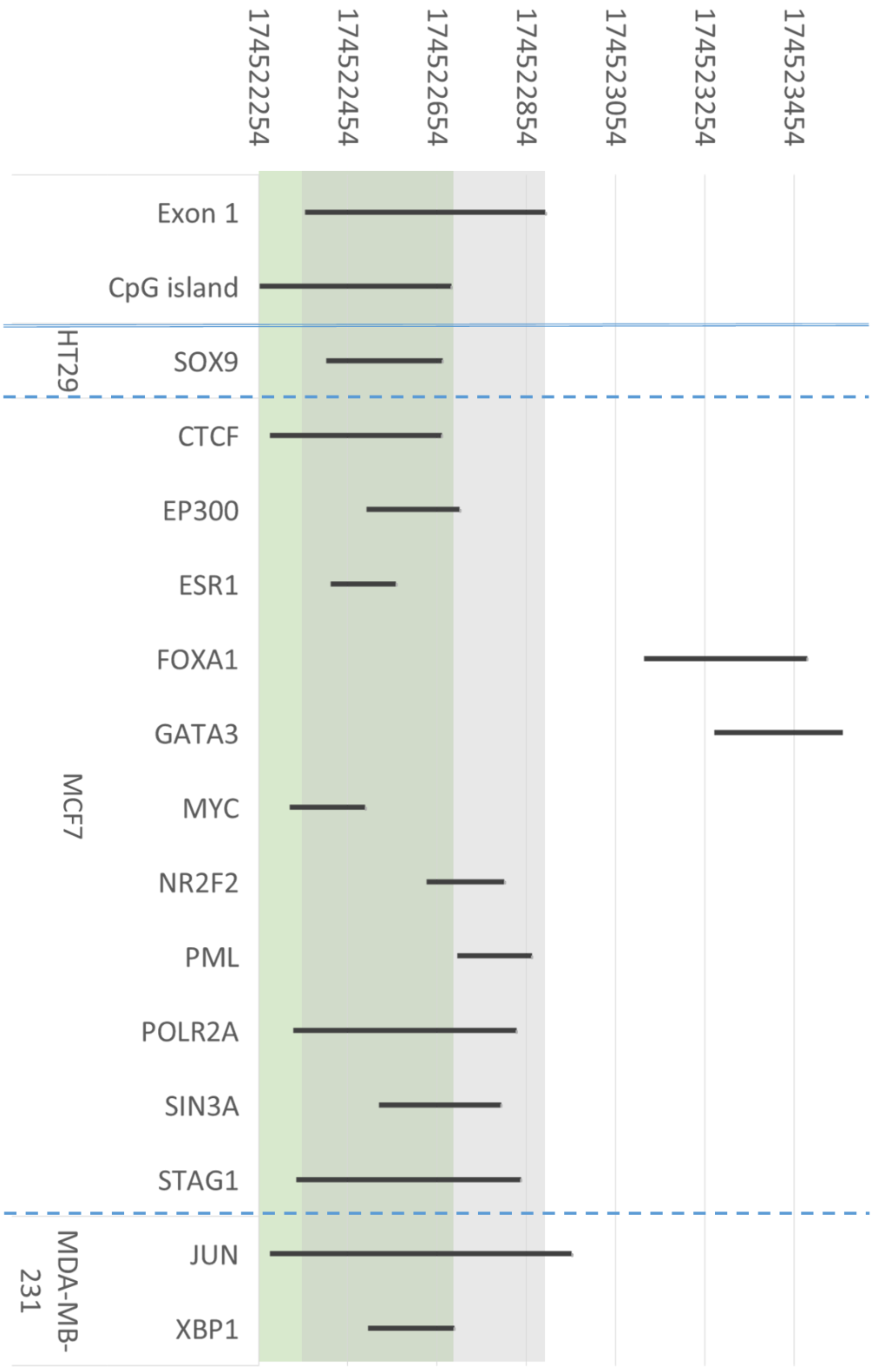

Figure 4.11 Transcription factor binding sites in low 15-PGDH expressing cell lines taken from the Cistrome database. Chromosome 4 position indicated at the top. Exon 1 = grey, CpG island 1 = green.

Table 4.3 Transcription factor binding patterns. Cistrome database *HPGD* promoter transcription factor binding patterns in cell lines. N = no data in the data sets analysed. Number = total number of samples assessed, NT = cells cultured under normal cell culture conditions, T = cells treated or cultured in non-standard culture conditions (e.g. serum starved). Red = No binding detected in *HPGD* promoter region, green = binding to *HPGD* promoter detected, orange = mixed binding observed, white = not assessed.

	High or intermediate *HPGD* expression			Low *HPGD* expression		
Transcription factor	A549	LoVo	CaCo-2	MCF7	MDA-MB-231	HT-29
CHD1	1T	N	N	N	N	N
CTCF	8NT and T	4NT	2NT	20 mix	N	N
ESR1	N	1NT	N	151 mix	N	N
GABPA	1T	N	N	1NT	N	N
GATA3	1T	N	N	23 mix	N	N
HOXA6	N	1NT	N	N	N	N
MED12	N	1NT	N	1T	N	N
PML	N	N	N	1NT	N	N
SMC1A	N	1NT	N	N	N	N
SOX9	N	2NT	N	N	N	1NT
TAF1	1T	N	N	1NT	N	N
USF1	3T	N	N	N	N	N
XBP1	N	1NT	N	N	+1T - 1NT	N

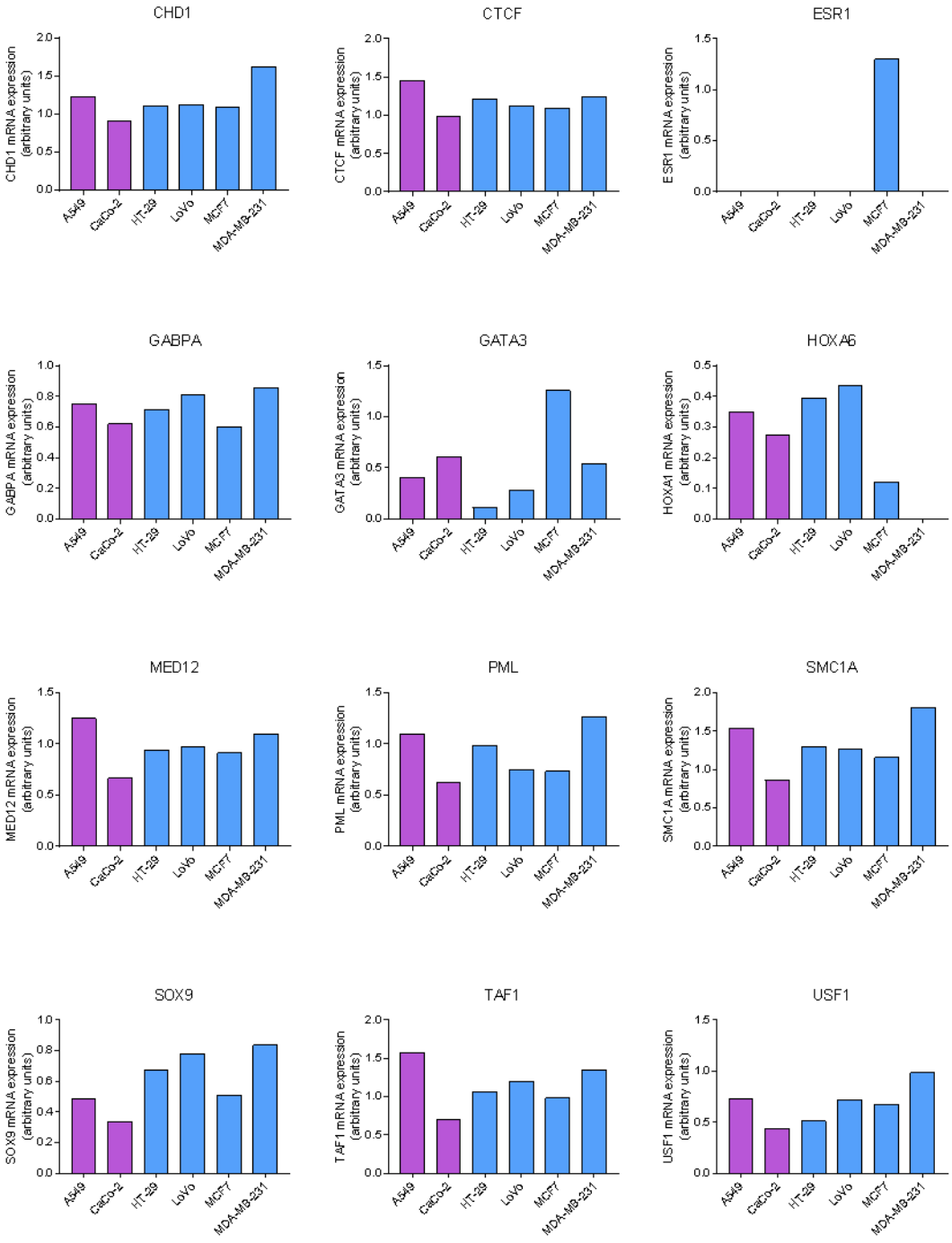

Figure 4.12 Transcription factor expression in cell lines. RT-PCR was performed on a range of cell line cDNA with transcription factor or *GAPDH* primers. The samples were quantified after gel electrophoresis using ImageLab software and transcription expression normalised to the *GAPDH* loading control. Purple = high 15-PGDH expression, blue = low or intermediate 15-PGDH expression.

Transcription factors were also chosen if the literature suggested that they might be of interest. For instance, *SOX9* has a CpG island that has been shown to be methylation-dependent in advanced melanoma (Cheng, P.F. et al., 2015), potentially therefore being relevant to the up-regulation of 15-PGDH on decitabine treatment. CHD1, HOXA6, PML, SMC1A and USF1 were randomly selected for the analysis, despite only having been assessed in one of the cell lines in the ChIP-Seq data. Literature suggests that the listed genes may be influenced by or influence methylation. For example, the USF and CTCF binding sites are methylation-sensitive (Huang, S. et al., 2007; Wolf et al., 2006; Qiao and May, 2011; Wang, H. et al., 2012) and PML has been implicated in regulation of DNA methylation through recruitment of ten-eleven translocation dioxygenase 2 (Song et al., 2018).

RT-PCR indicated that there were no consistent differences between the high and low 15-PGDH expressing cell lines for all of the transcription factors assessed (Figure **4.12**). A range of transcription factor expression levels were seen for eleven of the twelve transcription factors quantified, the exception being ESR1 (oestrogen receptor 1). ESR1 is expressed at a high level in the MCF7 cell line, known to be ER positive, and not expressed in any of the other cell lines assayed.

The effect of epigenetic drug treatment on the expression of SOX9, USF1 and XBP1 transcription factors was determined. This was to assess whether the up-regulation of 15-PGDH might be the indirect result of up-regulation of a transcription factor (Figure 4.13). As mentioned above, SOX9 and USF1 are known to show methylation-sensitive regulation (Cheng, P.F. et al., 2015; Qiao and May, 2011). No trend was observed between the cell lines with increased 15-PGDH expression following epigenetic drug treatment and those where there was no significant change.

4.3.7 *HPGD* mRNA expression is up-regulated in hypoxic conditions

The Cistrome data indicated that the transcription factor XBP1 binds to the *HPGD* promoter at a higher level in MDA-MB-231 cells exposed to hypoxic conditions (Table 4.3) (Chen, X. et al., 2014). The literature also suggested that 15-PGDH expression is induced under hypoxic conditions in colorectal cancer (Young et al., 2013). The effect of hypoxia was therefore investigated in the MCF7 breast cell line. MCF7 cells were starved of oxygen in a hypoxic incubator for 24, 48 and 72 hours before RNA was collected and RT-PCR performed with *HPGD* primers.

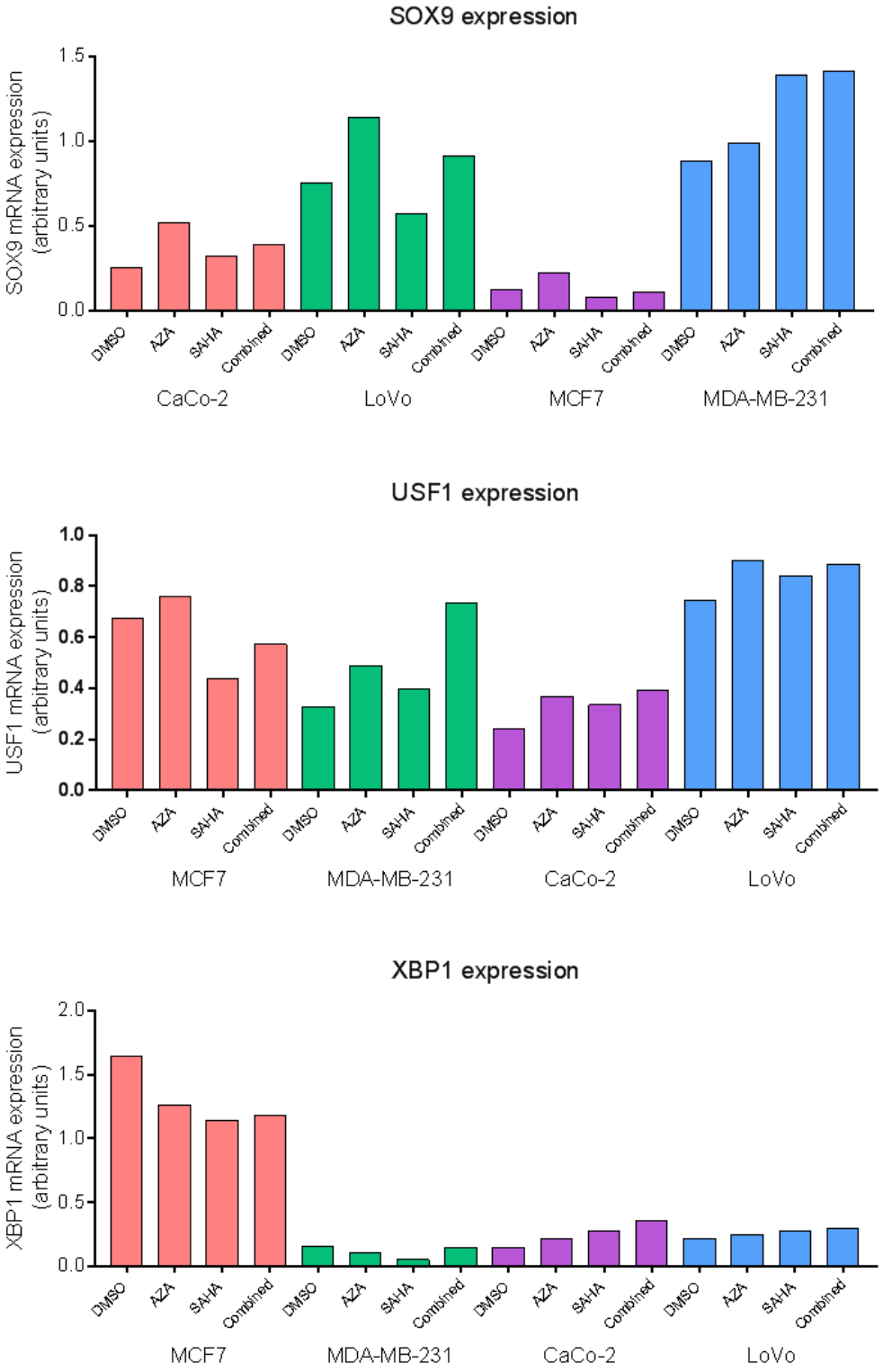

Figure 4.13 SOX9, USF1 and XBP1 expression in epigenetic drug-treated cell lines. RT-PCR was performed with epigenetic drug-treated cell line cDNA**.** The band was quantified from an agarose gel and normalised to a *GAPDH* control.

Little difference was observed in 15-PGDH mRNA expression after 24 or 48 hours, but a large decrease in 15-PGDH mRNA was observed following 72 hours' incubation in hypoxic conditions (Figure 4.14).

4.4 Discussion

Decitabine and vorinostat are well known epigenetic drugs, currently approved for the treatment of myelodysplastic syndromes and refractory cutaneous T-cell lymphoma (Ramalingam et al., 2010; Mann, B.S. et al., 2007; Saba, 2007). Because epigenetic regulation of 15-PGDH has been implicated in breast cancer, the first aims of the work described in this chapter were to assess the roles of methylation and histone acetylation in transcriptional regulation of *HPGD* in this disease.

The epigenetic drug doses were selected to reduce cytotoxic or cytostatic effects and maximise 15-PGDH expression in the cell lines, and were similar to those used previously. IC_{50} values for decitabine of 0.006 µM and 0.013 µM with MDA-MB-231 cells and 0.472 µM and 0.13 µM with MCF7 cells have been recorded after 72 and 48 hours' exposure respectively (Uhr et al., 2015; Karahoca and Momparler, 2013). These values are much lower than those calculated from Figure 4.2, in which an IC_{50} of ~18 µM was observed for the MCF7 cell line. No IC_{50} could be calculated using the range of decitabine concentrations tested for MDA-MB-231 cells, so these decitabine-resistant cells would require testing at a higher concentration range. Similar observations were reported by others using the same dose range (Cooper et al., 2012). Regardless of this, the data confirms that the 5 µM concentration taken forward for the expression experiments reduces proliferation rate to ~70% of the DMSO control. Previous studies assessing gene expression in the MCF7 and MDA-MB-231 cell lines have tended to use 5-12 µM decitabine over 72 and 96 hours (Mirza et al., 2013; Grandin et al., 2016; Phan et al., 2016; Wolf et al., 2006). Several studies have used similar decitabine doses (2.5-10 µM) for 72 hours, but with no data presented on the cytotoxicity of the drug, focusing instead on changes in gene expression for selection of the optimal drug concentration (Hesson et al., 2013; Lim et al., 2012). This may explain the wide range of drug doses that have been used in the literature.

One reason for the discrepancies in IC_{50} values for decitabine may involve the MTS assay. This assesses mitochondrial activity, which is associated with viability, but a limitation of it is that cells may become quiescent and thus exhibit reduced metabolic activity, giving a false negative

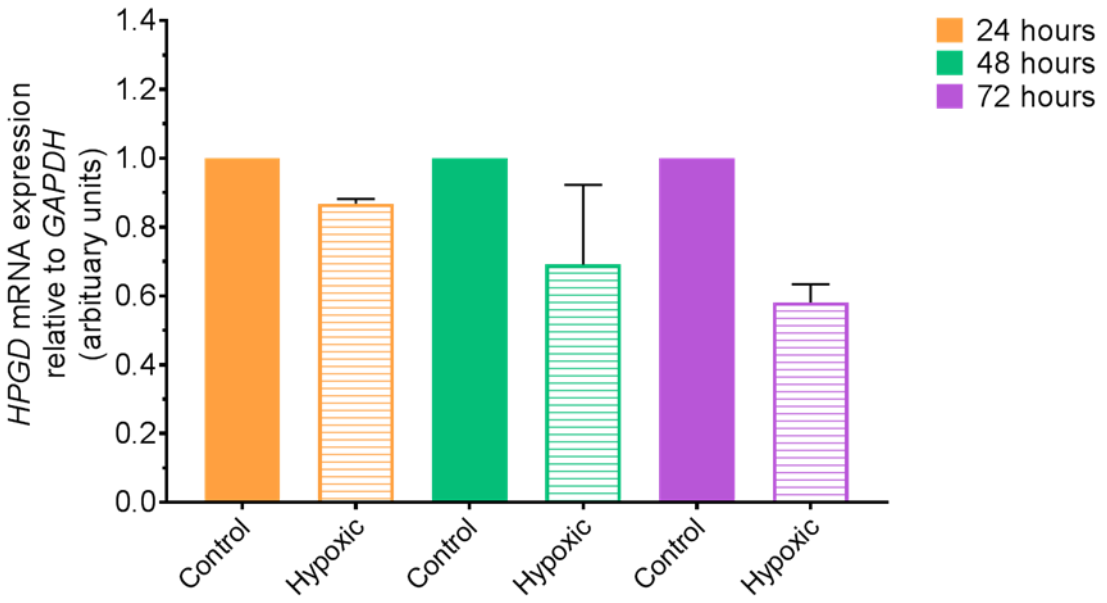

Figure 4.14 *HPGD* mRNA expression after exposure to hypoxic conditions. RT-PCR data to show *HPGD* mRNA expression after 24, 48 and 72 hours of culture in hypoxic conditions. Data normalised to the normoxic control. Error bars represent standard deviation from two independent experiments. One-way ANOVA performed for statistical analysis.

result. To overcome this, an assay based on apoptosis or on cell counting could be performed alongside the MTS assay, to determine the number of quiescent and viable cells.

Increased viability was observed with decitabine treatment after 24 hours' exposure, which has also been reported in the MDA-MB-231 cell line (Kastl et al., 2010). Decitabine requires metabolism and incorporation into the DNA to promote demethylation (Stresemann and Lyko, 2008), therefore the presence of decitabine may result in a surge in cellular metabolism as a result of its' incorporation into the DNA.

Vorinostat was more cytotoxic than decitabine, with IC_{50} values of ~1.1 µM for MCF7 and ~0.8 µM for MDA-MB-231 cells. These values are comparable to those reported in the literature of 0.783 µM and 1.32 µM for MCF7 and MDA-MB-231 respectively (Uhr et al., 2015). Higher IC_{50} values of 5.76 and 5.9 µM were reported for MCF7 and MDA-MB-231 cells respectively in the 'Genomics of Drug Sensitivity in Cancer' database after 72 hours' exposure; however, it is not reported whether the drug was replaced daily, which may explain the decreased sensitivity (Yang, W. et al., 2013). As with decitabine, studies assessing the optimal vorinostat dose have not always taken into account the toxicity of the drug. For instance, Dolskiy et al. assessed 0.25-5 µM vorinostat treatment over 1-96 hours and despite observing high toxicity, selected 5 µM for 72 hours for further experiments, because of the optimally increased gene expression (Dolskiy et al., 2017). Therefore, the 1 µM dose over 72 hours is within the range obtained from the literature.

Decitabine treatment resulted in increased *HPGD* mRNA expression in the MDA-MB-231 and LoVo cell lines (low and intermediate 15-PGDH expression respectively), but no significant change was observed in MCF7 and CaCo-2 cells (low and high 15-PGDH expression respectively). This data suggests that methylation can alter the expression of *HPGD* in some cell lines, MDA-MB-231 and LoVo; however, the up-regulation of 15-PGDH is not dependent upon the initial 15-PGDH expression level. Similar observations have been made in colorectal and gastric cancer cell lines (Thiel et al., 2009; Piepoli et al., 2009).

An increase in *HPGD* mRNA expression was also observed in MDA-MB-231 and LoVo cells with vorinostat treatment, but this was only significant in the breast cell line. HDAC inhibitors have been shown to increase 15-PGDH expression in colorectal and lung cancer cell lines (Tong et al., 2006a; Backlund et al., 2008; Wang, X. et al., 2013). These findings are therefore consistent with the literature and imply that histone deacetylation can reduce 15-PGDH expression, but not in all cell lines.

When the decitabine and vorinostat treatments were combined, a synergistic effect on *HPGD* mRNA expression was observed in MDA-MB-231 and LoVo cell lines, confirming that *HPGD* can be regulated by a combination of both methylation and histone acetylation. Others have reported similar results with the MDA-MB-231 cell line (Wolf et al., 2006). These authors reported a comparable trend with decitabine and vorinostat single and combination treatment, but their vorinostat treatment was for 24 rather than 72 hours. Up-regulation of *HPGD* expression has also been reported in various cancers including colorectal and prostate cell lines following epigenetic drug treatment (Piepoli et al., 2009; Lodygin et al., 2005).

Increased expression of the 15-PGDH protein, mainly localised in the cytosol, was observed in the MDA-MB-231 cell line upon decitabine treatment, which confirms the qRT-PCR data. This increase was not as pronounced in the combination treatment. Interestingly, the localisation of 15-PGDH differed between normal and hypoxic conditions in pulmonary artery endothelial cells, being both cytosolic and nuclear under normal conditions, but only nuclear in hypoxia (Ma, C. et al., 2014). Thus, the observed localisation of 15-PGDH was as expected under the normal conditions used. 15-PGDH has a short half-life of 47 minutes (Xun et al., 1991), which may account for the lower protein expression than expected overall. Moreover, the lower 15-PGDH expression in the combined drug treatment may be due to downstream effects of the vorinostat on other genes. For instance, vorinostat treatment resulted in induction of 1014 and 164 genes and decreased expression of 760 and 191 in the AGS and KATO-III gastric cell lines respectively (Claerhout et al., 2011). The expression of 15-PGDH may therefore change secondary to altered expression of other genes within the cell. Furthermore, increased mRNA expression does not always result in increased translation. Despite all this, the data shows that decitabine treatment directly increases 15-PGDH protein expression *in vitro*, confirming that it is of therapeutic interest.

Decitabine is a global demethylating agent, and so may be expected to alter the expression of many genes. Similarly, vorinostat inhibits histone deacetylation non-specifically, so altering expression of numerous genes. Because of these widespread effects, epigenetic treatment of different cell lines does not always result in the same changes in gene expression. This is likely to reflect variation in the epigenetic landscape within each cell type. For instance, variation in DNA methylation was observed among different cancer types, including colon, breast, lung, thyroid and Wilms' tumour (Hansen et al., 2011). Furthermore, methylation profiling of breast cell lines highlighted that the cell lines show differential susceptibility to *de novo* methylation, with the Hs578T breast cell line showing a lack of ability to methylate the HBC CpG island, unlike

MCF7 cells (Huang, T.H. et al., 1999). Although the specificity of vorinostat was not assessed, it is important to mention that HDAC inhibitors also show non-specific activity. They have been shown to interact with non-histone proteins and alter cell growth leading to gene expression changes (Marks and Dokmanovic, 2005).

Even though several studies have demonstrated increased *HPGD* mRNA expression following epigenetic drug treatment, none of them have confirmed that this is the direct result of demethylation of the gene. Given that no significant change in *HPGD* methylation was observed here following epigenetic drug treatment, either in the MDA-MB-231 breast or the LoVo colorectal cell line, the drugs are probably altering 15-PGDH expression through an indirect mechanism.

Previous studies have reported the *HPGD* promoter to be extensively methylated in prostate and bladder cancer cell lines, as well as 73% of primary prostate cancer tissue samples (Lodygin et al., 2005). Yet promoter methylation was not linked to decreased gene expression in prostate cancer (Lodygin et al., 2005) and *HPGD* promoter hypermethylation was not detected in gastric carcinomas with limited protein expression (Jang et al., 2008). *HPGD* promoter methylation was identified in 9/18 intestinal type gastric cancer specimens and 1/3 non-neoplastic samples, but despite this no significant association was observed between methylation and 15-PGDH expression (Thiel et al., 2009). Furthermore, no methylation was observed in five out of six breast cancer cell lines assessed (including MDA-MB-231 cells), with methylation observed only in the MDA-MB-436 cell line in the regions sequenced (Wolf et al., 2006). This corresponds with the pyrosequencing data obtained here for the first CpG island.

In contrast, methylation was detected in 3/10 primary breast cancers in the 13 CpG sites assessed (Wolf et al., 2006) and gastric carcinomas with >4% *HPGD* promoter methylation showed significantly less 15-PGDH mRNA expression (Ryu et al., 2013). MEXPRESS data also shows a significant trend between methylation of *HPGD* and gene expression in breast carcinoma samples. The data suggests overall that methylation of *HPGD* may be more prevalent *in vivo* than in *in vitro* cell line models. No significant effect on *HPGD* mRNA expression was observed on drug treatment of the MCF7 cell line, unlike MDA-MB-231. Similar methylation of the *HPGD* promoter in CpG island 1 was observed for both MCF7 and MDA-MB-231 cells, so the methylation status of the cell lines did not appear to determine *HPGD* expression changes after epigenetic drug treatment. The MCF7 cell line is ER positive, whereas the MDA-MB-231 cell line is a triple-negative cell line and has a highly invasive phenotype, both of which may alter the response to the epigenetic drugs.

Untreated MCF7 cells express higher levels of DNA methyltransferases DNMT1, DMNT3A and DNMT3B than MDA-MB-231 cells and upon treatment with decitabine and trichostatin A (TSA), expression was slightly increased (Kar et al., 2014). This suggests that despite treatment of the cell lines with epigenetic drugs, the effect of the treatment may be partially counteracted by increased DNA methyltransferase activity. A higher level of methylation was also observed in MCF7 than MDA-MB-231 when assessing 30 CpG island loci in untreated cells (Huang, T.H. et al., 1999). Furthermore, when compared to non-tumourigenic MCF10A cells a significant loss of global methylation and more epigenetic changes, such as histone acetylation, were observed in the MDA-MB-231 cell line in comparison to MCF7 cells (Tryndyak et al., 2006).

Indirect effects of decitabine on gene expression have also been reported in the literature, for example increased COX2 expression with decitabine treatment, without change in methylation (Evans et al., 2016). This indirect mechanism was shown to involve demethylation of the transcription factor, thyroid cancer protein 1 (Evans et al., 2016).

Decitabine is predominantly known for its demethylating properties. More and more alternative mechanisms altering gene expression are being reported as a result of decitabine treatment. Altered gene expression profiles have been demonstrated as a result of histone modifications and DNA damage resulting from decitabine treatment (Seelan et al., 2018). Interestingly, of 81/22,000 genes induced by decitabine in the AML cell line OCI-AML2, 50% did not contain CpG islands in the promoter region (Schmelz et al., 2005). Moreover, only one of five up-regulated genes assessed showed demethylation following decitabine treatment (Schmelz et al., 2005). This suggests that the primary method of gene regulation by decitabine may not actually be through demethylation of the gene.

Taking all of the epigenetic data into consideration, both methylation and histone acetylation play a role in controlling *HPGD* gene expression. The data suggests that the *HPGD* promoter is likely to be open and accessible under standard conditions. The recruitment of specific transcription factor complexes (repressors and activators) may therefore be more important in controlling expression for this gene in breast cancer.

As decitabine appeared to be only indirectly altering 15-PGDH expression in the MDA-MB-231 and LoVo cell lines, the Cistrome database was used to identify transcription factors that bind directly to the *HPGD* promoter. No distinct trends were observed of transcription factor expression in a panel of high versus low expressing cell lines using RT-PCR. As mentioned previously, the accuracy of RT-PCR is limited and the actual mRNA level of a transcription factor

may not always reflect its protein level. Furthermore, the expression level of a transcription factor does not necessarily correlate with the amount of transcription factor protein recruited to the *HPGD* promoter. Therefore, it would be beneficial to assess the transcription factor protein expression and perform immunoprecipitation assays to determine transcription factor binding at the *HPGD* promoter.

Several limitations have been identified with the Cistrome database. Firstly, a limited number of breast cell lines were assessed, and secondly, the experimental design for the datasets was not ideal. For instance, various treated samples were included in the database without matched controls, which may favour false positive results. Ideally an alternative approach to generate a list of methylation-sensitive transcription factors responding to decitabine treatment would be completed. For instance performing an Illumina methylation array on DMSO- and decitabine-treated breast cancer cell lines would give a more rounded overview of all of modified genes relevant in breast cancer.

The transcription factor X box protein 1 (XBP1) is required for cell survival and tumour growth in hypoxic conditions (Romero-Ramirez et al., 2004). Binding of XBP1 to the *HPGD* promoter was observed in the MDA-MB-231 cell line under hypoxic conditions, and so it was predicted that hypoxia may alter 15-PGDH expression. Decreased *HPGD* mRNA expression was indeed observed in the MCF7 cell line after 72 hours' exposure to hypoxic conditions. In contrast though, Young et al. have shown that 15-PGDH protein levels can vary within a tumour, with higher levels in the centre of colorectal cancer liver metastases than the periphery (Young et al., 2013). They have also shown that this variation in expression may be due to hypoxia, and using the human colon adenocarcinoma cell line HCA-7, have demonstrated that hypoxia-induced 15-PGDH expression is reversible. Furthermore, increased 15-PGDH protein expression has also been observed in pulmonary vasculature *in vivo* (Ma, C. et al., 2014) and increased mRNA in an oesophageal cell line when exposed to hypoxic conditions (Lee, J.J. et al., 2010). These observations are at odds with the results seen with the MCF7 breast cell line, which may be due to the difference in cell types and origin.

Several transcription factors have been implicated in transcriptional repression of *HPGD* including Snail, early growth response factor-1 (Egr-1) and hepatocyte nuclear factor 3β (Mann, J.R. et al., 2006; Miyaki et al., 2009; Huang, G. et al., 2008; Backlund et al., 2008). Few of these have been studies performed in breast cancer. The identification of potential transcription factors that act to activate and repress *HPGD* expression in this context is therefore of interest, as they are potential means of modulating *HPGD* levels in cancer.

Snail and Slug are regulated through DNA methylation during the EMT/mesenchymal-epithelial transition process (Chen, Y. et al., 2013). HDAC activity is also required for Snail repression of E-cadherin (Peinado et al., 2004); both methylation and histone acetylation therefore alter Snail activity. This suggests that Snail might be a component of the indirect mechanism involved in 15-PGDH expression, particularly in MDA-MB-231 cells.

In summary, 15-PGDH expression was increased by treatment with decitabine (DNMT1 inhibitor) and vorinostat (HDAC inhibitor) in specific cell lines. As no change in methylation status of the *HPGD* gene was observed following decitabine treatment, it is predicted that decitabine alters 15-PGDH expression through an indirect mechanism. Further research is required to reveal the components of this indirect mechanism of 15-PGDH regulation, which could be through altered expression of transcription factors or histone modifications.

Chapter 5 The role of 15-PGDH in breast cancer

5.1 Introduction

Up-regulation of COX2 has been observed in many cancers and has been implicated in cancer, including breast cancer (Kim, H.S. et al., 2012; Ghosh et al., 2010; Hashemi Goradel et al., 2018). Extensive research has been completed into COX inhibitors, yet limitations of COX inhibition due to toxicity and a lack of patient response has led to alternative approaches to counteract COX2 downstream signalling (Whitlock et al., 2015; Sostres et al., 2010; Hippisley-Cox and Coupland, 2005).

As COX2 is a key enzyme involved in prostaglandin production, recent research has focused on the prostaglandin metabolising enzyme, 15-PGDH. The majority of this research has been undertaken in colorectal and lung cancer with little emphasis on the role of 15-PGDH in breast cancer.

5.2 Aims

This chapter aims to assess the role of 15-PGDH in breast cancer. In order to do this the following was completed:

1. Generation of MCF7 cell line clones stably over-expressing 15-PGDH with varying levels of 15-PGDH expression, and control clones.
2. Validation of the MCF7 clones stably over-expressing 15-PGDH
    a. Protein expression
    b. mRNA expression
    c. Protein activity
3. Assessment of 15-PGDH over-expression effect on aspects of cell behaviour, and the additional effect of exogenous PGE_2 for:
    a. Proliferation
    b. Migration
    c. Invasion
    d. Clonogenicity

4. Complete RNA sequencing to evaluate downstream transcriptional effects of 15-PGDH up-regulation, and additional effects of exogenous PGE_2.

5.3 Methods

5.3.1 Generation of 15-PGDH stable over-expressing clones

The process involved in generating the 15-PGDH over-expressing clones is described below. MCF7 cells were selected as the parent cell line as it is a well-established and well-characterised breast cell line. The MCF7 cells were transfected using Gateway cloning vectors containing the 15-PGDH gene (*HPGD*) or an empty control vector. Twenty 15-PGDH control clones with the truncated vector and fourteen 15-PGDH over-expressing clones were generated.

5.3.1.1 pDEST510 HPGD vector preparation

5.3.1.1.1 *HPGD* open reading frame amplification from A549 cell line

The A549 cell line has high endogenous *HPGD* expression; therefore the cell line was chosen to amplify *HPGD's* coding sequence from its cDNA in order to generate the *HPGD* over-expression vector. The ORF was amplified with gateway primers designed according to the gateway cloning protocol using the mix and nested-PCR settings in Table 5.1 and Table 5.2.

Table 5.1 Reaction mixture for *HPGD* amplification for Gateway cloning.

Reagent	Volume (µl)
10 x Pfx amplification buffer	5
10 µM F/R gateway *HPGD* PCR primers	1.5
Platinum Pfx DNA polymerase (2.5 U/µl)	0.4
10 mM dNTP mix	1.5
50 mM $MgSO_4$	1
Nuclease free water	39.6
Template cDNA (~32 ng)	1
Total	**50**

Table 5.2 *HPGD* nested amplification for Gateway cloning

Step	Temperature	Time	Cycles
Initial denaturation	94°C	5 minutes	x1
Denaturation	94°C	15 seconds	x4
Annealing	54°C	30 seconds	
Extension	68°C	1 minute	
Denaturation	94°C	15 seconds	x31
Extension	68°C	1 minute	
Refrigeration	4°C	Forever	x1

7 µl of the PCR product was checked on a 1% (w/v) agarose gel. Two bands were seen which were identified as originating from two alternatively splices transcripts of *HPGD*. Variant 1 = 862 bp and *HPGD* variant 2 = 698 bp. The *HPGD* variant 1 (NM_000860) product was selected to take forward.

To isolate the *HPGD* variant one ORF sequence, gel electrophoresis was performed with the remaining 43 µl of PCR product diluted in 10 x Orange G loading dye (100 mg Orange G (Sigma-Aldrich), 15 ml glycerol, 35 ml dH_2O) and visualised using crystal violet (Section 2.3.5). The larger variant 1 band was excised and purified (Section 2.3.1).

5.3.1.1.2 BP reaction and transformation

A BP reaction facilitates recombination between an *att*B substrate (a sequence flanked by *att*B sequences) and an *att*P substrate (donor vector containing two attP sites) to create a vector containing the insert flanked by *att*L sequences. This reaction was performed to insert the *HPGD* ORF product into a pDONR201 vector (Invitrogen) (Appendix 10) as follows: 150 ng gateway *HPGD* product, 140 ng pDONR201 vector, 2 µl BP clonase II (Invitrogen 11789020) and made up to 8 µl with TE buffer was added to 1.5 ml microcentrifuge tube. The mixture was briefly vortexed twice for 2 seconds and incubated at room temperature for one hour. The reaction was terminated by adding 1 µl proteinase K and incubating for 10 minutes at 37°C.

1 µl of the BP reaction was added to 50 µl DH5a library efficiency cells (Invitrogen 18263-012) mixed by flicking and incubated on ice for 30 minutes followed by heat shocking the cells at 42°C for 45 seconds to transform the cells. The cells were immediately placed on ice for 5 minutes before 250 µl of SOC media was added and incubated at 37°C for 1 hour in a shaking incubator at 200 rpm. 50 µl of the cell suspension was plated onto a kanamycin LB agar plate (50 µg/ml) (prepared as described in Section 2.4.3). The plate was incubated at 37°C overnight and five single colonies selected to take forward. The colonies were grown overnight at 37°C in

5 ml of LB broth with 50 µg/ml of kanamycin. Glycerol stocks of each clone were prepared by mixing 200 µl autoclaved glycerol with 200 µl of the overnight *E.coli* culture and were stored at −80°C.

5.3.1.1.3 Mini-prep extraction and purification of pDONR201 HPGD plasmid

pDONR201 HPGD plasmid DNA was purified using the Mini-prep protocol as described in Section 2.4.1. The product was quantified using the Nanodrop (Section 2.3.2) before Sanger sequencing was then performed using the pDONR201 vector primers (Appendix 3) and the settings were as described for RT-PCR using mini-prep product diluted 1 in 10 in water for 35 cycles (see Section 2.3.7). This confirmed that the BP reaction was successful and that the *HPGD* sequence had been inserted into the pDONR201 vector in the correct orientation.

5.3.1.1.4 LR reaction (clone1) with pDEST510 and pDONR201 HPGD

A LR reaction was performed with *HPGD* pDONR201 clone 1 vector to transfect the *HPGD* ORF insert into the pDEST510 destination vector (Section 5.3.1.1.2). The pDEST510 vector has been adapted in-house from the pDEST47 vector (Appendix 11) by replacing the GFP tag with a smaller FLAG-tag, which is more hydrophilic and therefore less likely to denature or inactivate the protein generated. 150 ng *HPGD* pDONR201 clone 1 and 150 ng pDEST510 was made up to 8 µl in TE buffer. The LR clonase enzyme was thawed for 2 minutes and vortexed for 2 seconds before 2 µl was added into the LR reaction. The mix was incubated for 1 hour at room temperature and 1 µl proteinase K was added. The solution was mixed by vortexing briefly, and incubated at 37°C for 10 minutes.

5.3.1.1.5 Amplification, extraction and purification of pDEST510 HPGD plasmid

Transformation of DH5α cells was completed as described in Section 5.3.1.1.2 with pDEST510 HPGD vector and plated on an ampicillin plate (100 µg/ml). Five colonies on the ampicillin plate were grown overnight in 5 ml LB broth with ampicillin and glycerol stocks were prepared (as mentioned in Section 5.3.1.1.2). Mini-prep was performed with the five separate cultures to isolate the pDEST510 HPGD vector (Section 2.4.1).

5.3.1.1.6 Sanger sequencing to confirm correct insert and orientation

Colony PCR amplification (Section 2.3.7) of the *HPGD* ORF from the pDEST510 HPGD vectors using the T7 forward and *HPGD* reverse primers was performed with an annealing temperature of 60°C to confirm the correct orientation of the *HPGD* insert. Inserts in the correct orientation produced a 481 bp band on a 1% (w/v) agarose gel (Section 2.3.4). Sanger sequencing was

completed on each of the five successful colonies using the T7 forward and *HPGD* reverse primers to check the sequence of the insert (Section 2.3.8).

5.3.1.1.7 Maxi-prep extraction and purification of pDEST510 HPGD plasmid

Once the plasmid had been fully assessed a larger quantity of clone 1 was prepared using a maxi-prep (Section 2.4.2).

5.3.1.2 Preparation of pDEST510 X vector

5.3.1.2.1 Double digest

A control vector was prepared by completing a double digest of the pDEST510 HPGD vector using EcoR1-HF (New England Biolabs) and AflII (New England Biolabs). 5 µg pDEST510 HPGD DNA was added to a 50 µl ligation reaction (1 µl each enzyme, 5 µl 10 x cut smart buffer, 5 µg vector DNA in nuclease-free water) incubated at 37°C for 1 hour. This removed the majority of the *HPGD* gene and the FLAG-tag leaving the rest of the vector intact. The digest was confirmed on a 0.8% (w/v) agarose gel using ethidium bromide with digested products of 797 bp and ~5500 bp in size or un-digested vector of ~6200 bp.

5.3.1.2.2 Blunt ending of restriction digest

To blunt end the ligated vector and enable successful ligation a 70 µl reaction was prepared with the following reagents: 33 µM dNTPs, 1 x NEB cut smart buffer (New England Biolabs), 47 µl pDEST510 HPGD digest and 5 U Klenow (New England Biolabs). The reaction was incubated to 25°C for 30 minutes and the product checked on 0.8% (w/v) agarose gel with an expected band size of ~5500 bp. The product was then run on a 0.8% crystal violet gel and purified as described above.

5.3.1.2.3 Vector ligation and transformation

A ligation reaction was performed by mixing 5 µl T4 ligase buffer, 4 µl blunt ended digested pDEST510 HPGD sample and 1 µl T4 ligase and incubating at 16°C overnight along with a no ligase control. DH5α cells were transformed as previously described with the pDEST510 HPGD vector. Sixteen colonies from both reactions with and without the ligase enzyme were gently removed on a sterile scraper and transferred into 50 µl water. The samples were heated to 100°C for 10 minutes to kill the *E.coli* and colony PCR performed with pDEST510 HPGD forward and reverse primers using the PCR method as described in Section 2.2.9 for 35 cycles at 60°C annealing temperature. The samples were run on a 1% (w/v) agarose gel to test whether insert

was successful. The expected product sizes were 578 bp with the double digest product and 1365 bp with the undigested product.

The successful products were Sanger sequenced as described above to confirm successful insertion. Once confirmed a maxi-prep was performed to generate a stock of pDEST510 HPGD vector as in Section 5.3.1.1.7. The vector was then ready for transfection into mammalian cell lines.

5.3.2 Proliferation

5.3.2.1 Clone proliferation assays

MCF7 pDEST510 HPGD or X stable transfected clones were seeded at $1.5x10^3$ cells per 96 well in 100 µl media with 800 µg/ml G418 in triplicate for 72 hour assays and $4x10^3$ cells per well for 24 hour treatments. The cells were incubated at 37°C in 5% CO_2 (v/v) in air and the MTS assay performed as described in Section 2.1.6 to determine the rate of proliferation under standard culture conditions.

5.3.2.2 Proliferation with PGE_2 treatment

To assess whether the presence of exogenous PGE_2, a 15-PGDH substrate, affects the rate of proliferation, MCF7 clones were treated with a range of exogenous PGE_2 concentrations (0-10 µM). As the composition of FCS can vary between batches and contains compounds that affect proliferation, it was decided that performing the assay with reduced serum may increase the effect observed with PGE_2 addition. The MCF7 over-expressing clones and their matched controls were seeded as described above (Section 5.3.2.1) and incubated for 24 or 72 hours with 1% or 10% FCS media containing PGE_2.

5.3.3 Migration

Scratch wound assays were performed to measure spontaneous migration using the MCF7 clones stably over-expressing 15-PGDH as described in Section 2.1.7 in the presence of G418 (400 µg/ml). The assay was optimised with a range of PGE_2 concentrations in both 1% and 10% FCS with 1% FCS and 1 µM PGE_2 used in subsequent experiments.

The rate of MCF7 clone migration in response to a chemoattractant was also assessed using a transwell inserts as described in Section 2.1.9. Marked chemotaxis has been reported in the MDA-MB-231 and MCF7 breast cell lines with 50 ng/ml EGF as a chemoattractant (Wang, S.J. et al., 2004; Truong et al., 2016). Cells were therefore seeded in 1% FCS and media supplemented with 10% FCS or 10% FCS with added 50 ng/ml EGF.

5.3.4 Invasion

The capacity of MCF7 clones stably over-expressing 15-PGDH to invade a Matrigel layer was measured using transwell inserts as described in Section 2.1.8. As with the transwell migration assays, clones were seeded in 1% FCS and 10% FCS or 10% FCS with 50 ng/ml EGF used as a chemoattractant. Cell invasion was determined by normalising the results with reference to the control well lacking Matrigel.

5.3.5 Colony formation

MCF7 clones stably over-expressing 15-PGDH were assayed to determine the effect of 15-PGDH expression on colony formation as described in Section 2.1.10. Cells were cultured in either with media with 10% FCS (untreated) or 10% FCS media containing 1 µM PGE_2 (treated). The number of colonies were counted and the colony forming efficiency determined by calculating the percentage of cells seeded that successfully generated colonies.

5.3.6 RNA sequencing

RNA sequencing was performed on the highest 15-PGDH expressing MCF7 clone, H14, and its matched control clone, X17 as well as the original MCF7 cell line. The experiment was performed in triplicate with RNA from DMSO- or 1 µM PGE_2-treated cells in the presence of a maintenance dose of G418 (400 µg/ml) as described in Section 2.2.11. The aim of the experiment was to determine the downstream transcriptional effects of 15-PGDH expression.

Pair-wise comparisons were performed between each of the cell lines or clones and the treatments to identify the transcripts with the largest, statically significant, up- and down-regulated changes in expression. KEGG pathway analysis and gene ontology phrase enrichment was also preformed to gain greater insights in to the global effects of 15-PGDH expression in the presence of PGE_2. Validation of the RNA-Seq data was completed using RT-PCR and Western blotting for protocadherin-7 (PCDH7) as described in Sections 2.5.32.2.9.

5.4 Results

5.4.1 Generation of 15-PGDH stably over-expressing MCF7 clones

5.4.1.1 Preparation of gateway vector

Gateway cloning is a recombination cloning technology by Invitrogen that enables fast and accurate cloning as described in Section 2.4.5. The ORF in the *HPGD* variant 1 transcript

(NM_000860.5) was amplified by RT-PCR from RNA extracted from A549 cells and inserted in to the pDEST510 vector (based on pDEST47 with FLAG-tag instead of GFP) and sequenced by Sanger sequencing to confirm the integrity of the ORF and its orientation. The ORF was found to differ from the reference sequence at one position, equivalent to common single nucleotide polymorphism (SNP) rs1050145. This SNP consists of an A to G substitution with allele frequencies of: A = 0.38 and G = 0.61% allele frequency in dbSNP136. As both variants result in the same amino acid (glutamine) its presence does not alter the protein produced. A schematic of the final vectors used to generate the clones can be seen in Figure 5.1.

5.4.1.2 Transient transfection with pDEST510 HPGD and control vectors

Transient transfection of the MCF7 cell line by each vector preparation was performed and the presence of 15-PGDH and the FLAG-tag protein demonstrated using immunocytochemistry (Figure 5.2). Strong expression of 15-PGDH was seen throughout the MCF7 cells transfected with the pDEST510 HPGD vector, whereas no 15-PGDH expression was detected in the parent MCF7 cell line or cells transfected with the control vector. Similarly, strong FLAG-tag staining was observed in the 15-PGDH positive transfection and not in the controls. Co-localisation of the 15-PGDH and FLAG-tag staining was observed in the MCF7 cells transfected with the pDEST510 HPGD vector.

5.4.1.3 MCF7 geneticin kill curve

The pDEST510 vector also contains a neomycin resistance gene cassette, which confers geneticin (G418) resistance to transfected cells. To select for cells that had successfully incorporated the vector into the host genome, transfected cells were exposed to G418 for 14 days, causing cells not stably transfected to undergo G418 induced apoptosis.

The optimal concentration of G418 kills most of the cells after exposure for one week, however this concentration is cell line dependent, with the majority of mammalian cells requiring under 1 mg/ml to induce cell death (Amirkia and Qiubao, 2012). Consequently, a kill curve was generated for the MCF7 cells grown in the presence of 0-1000 µg/ml of G418 (Figure 5.3).

No considerable change in cell confluency was observed in the first 48 hours with G418 treatment. A decrease in confluency was seen after 72 hours with the highest doses of G418 (1000 µg/ml) and after 7 days an 80% decrease in confluency was observed with 500-1000 µg/ml doses. No change in confluency was observed with the lower doses of G418 over the duration of the experiment.

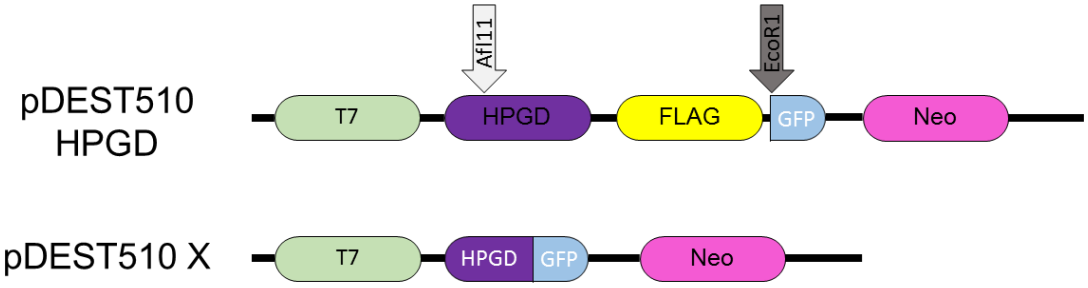

Figure 5.1 Destination vector diagrams. Following preparation of the pDEST510 HPGD vector (based on the pDEST47 vector with the GFP sequence truncated and FLAG-tag inserted) the pDEST510 X vector was generated using an AflII and EcoR1 restriction digest. White text indicates an inactive gene, while black indicates an active gene. T7 = T7 promoter, HPGD = *HPGD* gene, FLAG = FLAG-tag, GFP = green fluorescent protein (inactive), Neo = neomycin resistance gene (also encodes G418 resistance).

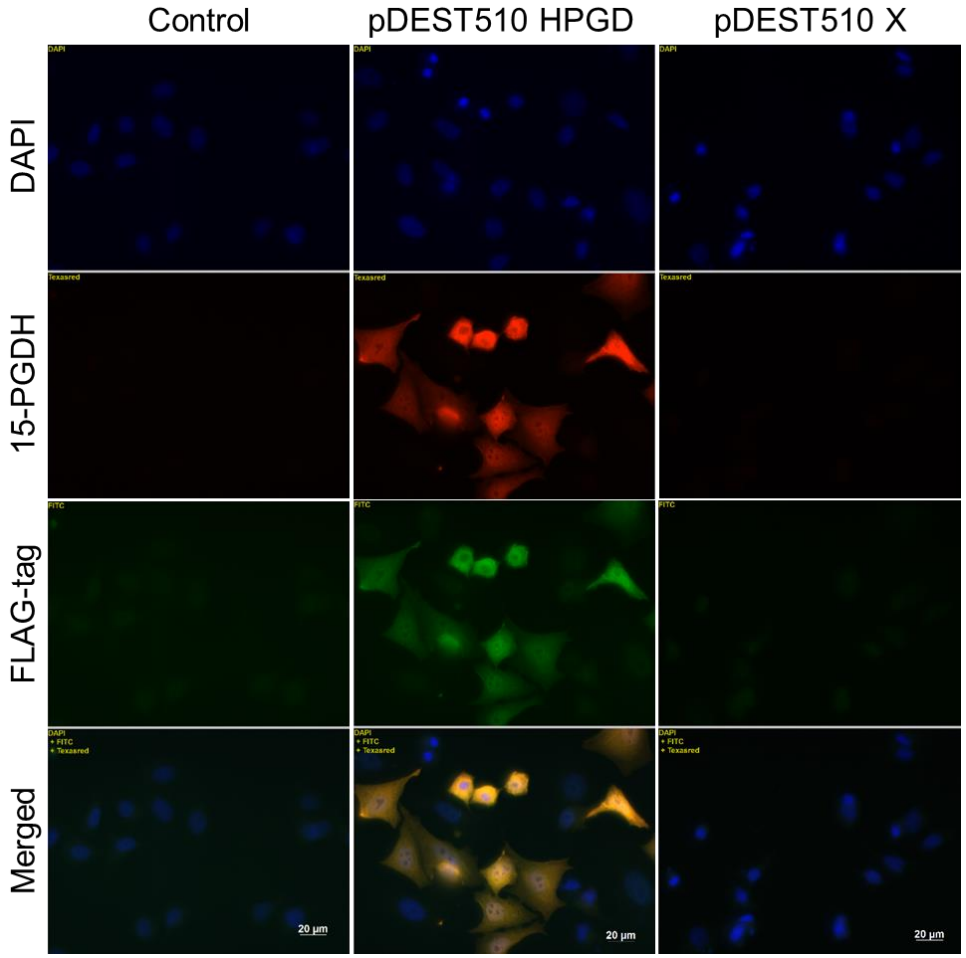

Figure 5.2 MCF7 transient transfection with 15-PGDH Gateway vectors. Immunocytochemistry was performed with untreated MCF7 cells (left), MCF7 cells transfected with the pDEST510 HPGD (centre) or pDEST510 X vector (right) and fixed after 24 hours (x40 objective). Blue = DAPI nuclear stain, red = 15-PGDH, green = FLAG-tag, yellow = co-localisation of 15-PGDH and FLAG-tag.

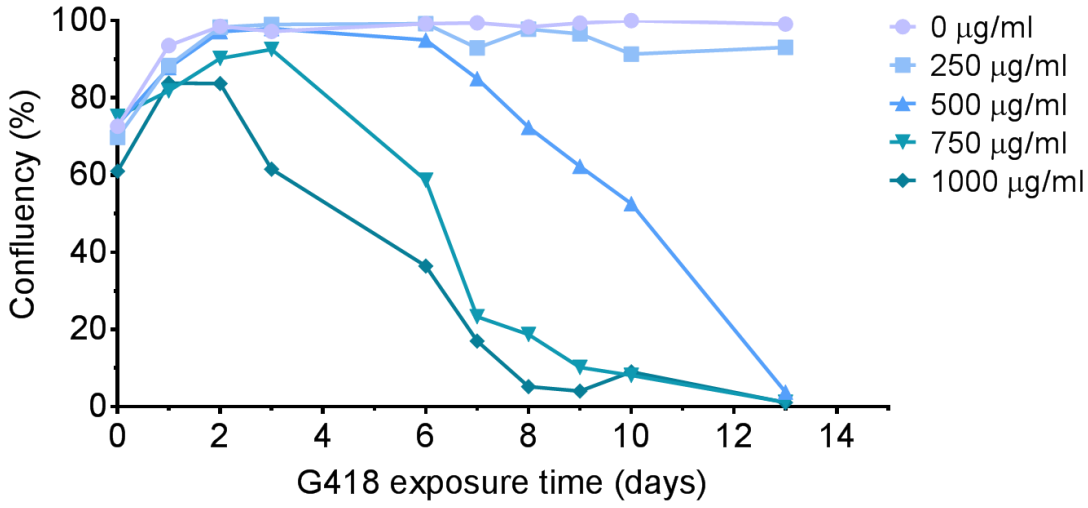

Figure 5.3 MCF7 geneticin (G418) kill curve. MCF7 cells were treated with a range of G418 concentrations and the confluency measured using ImageJ each day to determine the optimal dose of G418 for clone selection.

As the confluency was assessed rather than the metabolic activity it was believed that the cells that remained after 7 days of treatment in the higher doses were quiescent, therefore the cells were trypsinised and re-plated on day 10. As the cells did not re-adhere it was decided that the higher G418 concentration had killed the cells.

In line with the literature it was found that 800 µg/ml was the lowest concentration that killed the majority of the MCF7 cells after one week and so this concentration was used for the selection of stably transfected cells. The concentration was then reduced to 400 µg/ml to maintain the selection pressure.

5.4.2 Characterisation of MCF7 clones stably over-expressing 15-PGDH

5.4.2.1 15-PGDH protein expression in MCF7 clones

Cells were transfected with the pDEST510 vector that was either empty or contained the *HPGD* ORF and grown for two weeks in media supplemented with 800 µg/ml G418 (Section 2.1.11). Twenty control clones and fourteen 15-PGDH stable over-expressing clones were isolated and grown for use in further studies. Immunocytochemistry was performed with a 15-PGDH antibody to confirm protein expression in MCF7 stably transfected clones (Figure 5.4 and Figure 5.5). No data was obtained for X15 or X20 as the clones failed to grow sufficiently.

The control clones showed little to no 15-PGDH protein production, with a faint red glow seen in some of the clones. 15-PGDH protein was only found by immunocytochemistry in five of the fourteen over-expressing clones, localised predominantly in the cytoplasm with some nuclear staining as expected.

Cell morphology was similar between all of the clones. A range of 15-PGDH expression was observed in the 15-PGDH over-expressing clones, with the highest and lowest levels in clones H14 and H11 respectively. Clones H1, H3 and H4 exhibited intermediate levels of 15-PGDH expression. Interestingly, some of the clones, such as H1, displayed heterogeneous expression of 15-PGDH between cells in the same culture.

5.4.2.1 *HPGD* mRNA expression in MCF7 clones

Initially, conventional RT-PCR was performed to determine *HPGD* mRNA levels in the stably transfected MCF7 clones that demonstrated elevated 15-PGDH protein levels, alongside the control clones and parental MCF7 cell line. The data was normalised to the MCF7 parent cell line.

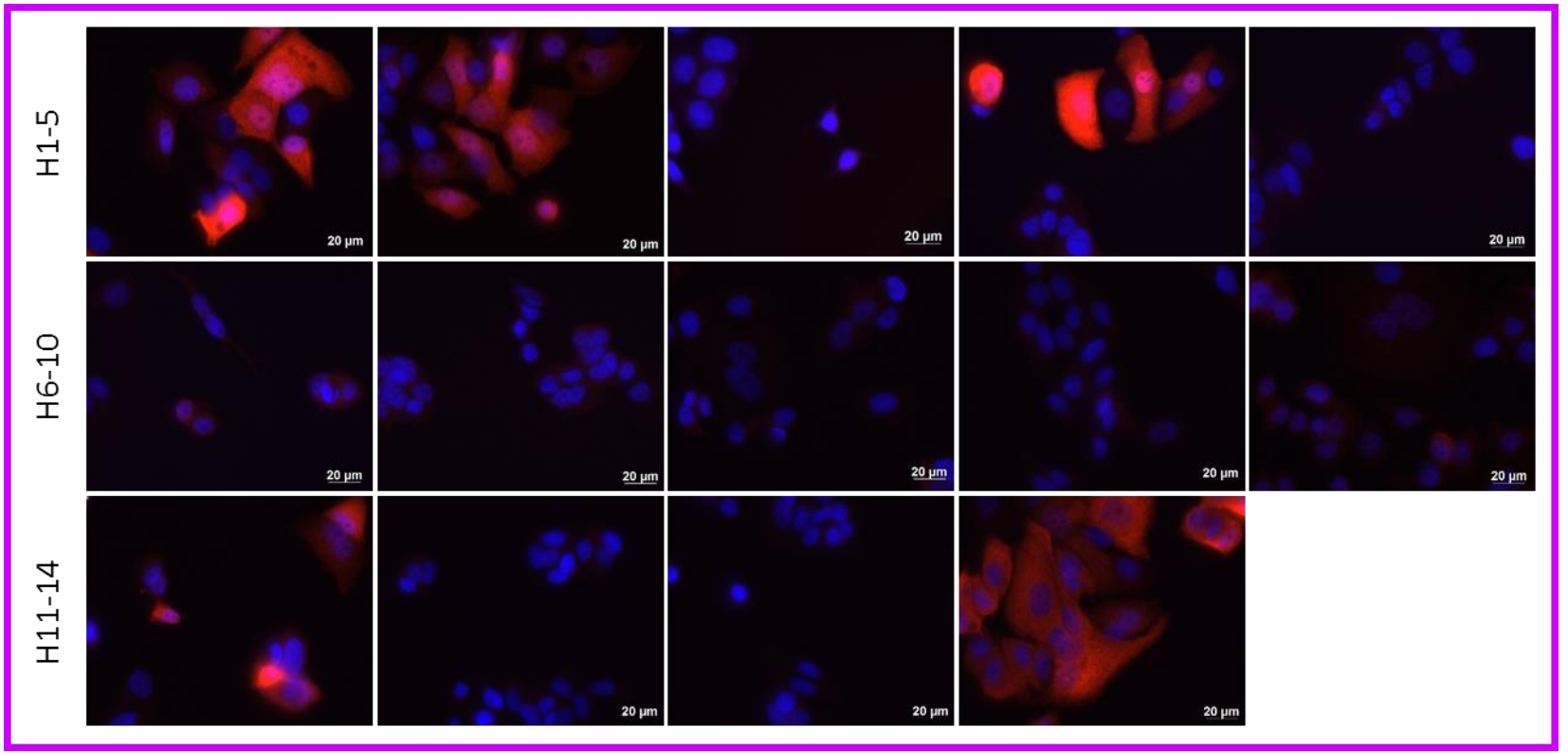

Figure 5.4 15-PGDH protein expression in MCF7 cells stably transfected with pDEST50 HPGD Immunocytochemistry with MCF7 pDEST510 HPGD clones using 15-PGDH antibody (x40 objective). Red = 15-PGDH stain, blue = nuclear staining DAPI. Clones displayed in numerical order left to right. Intensity set on H1 clone for each run of samples.

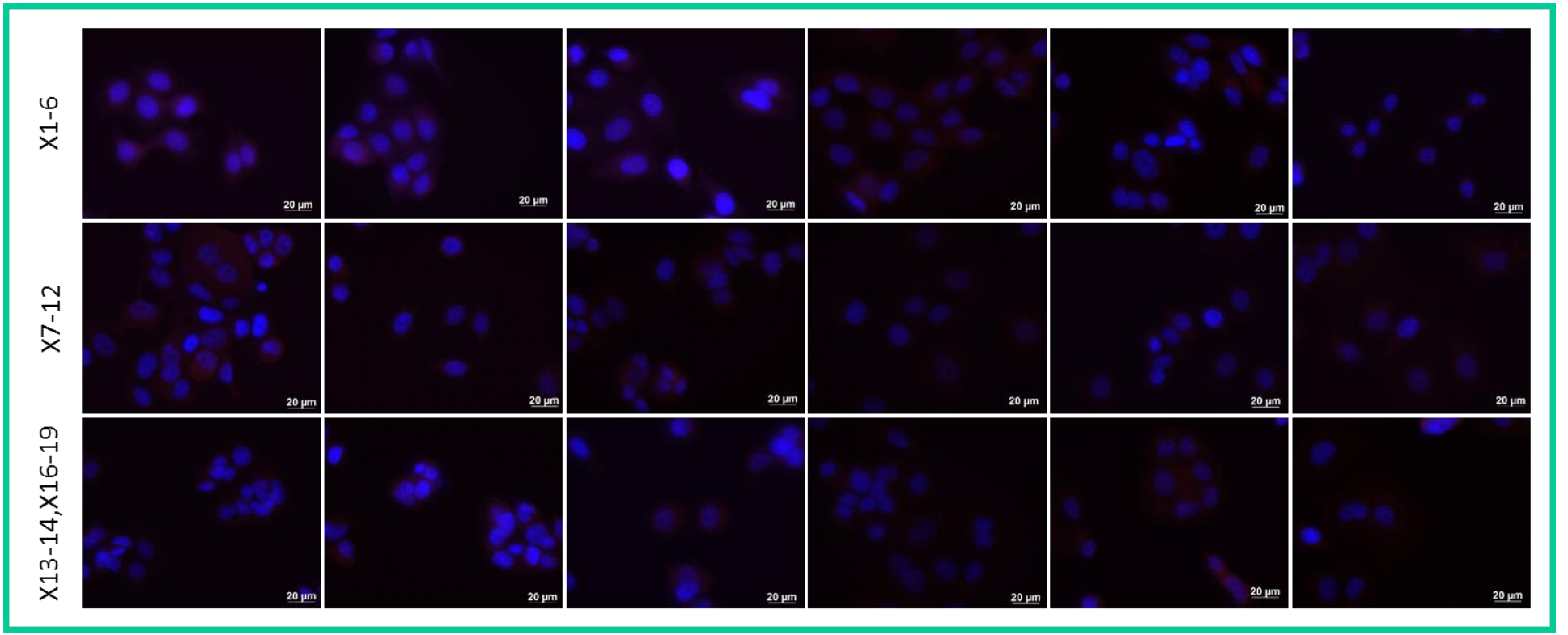

Figure 5.5 15-PGDH protein expression in MCF7 cells stably transfected with pDEST50 X. Immunocytochemistry with MCF7 pDEST510 X control clones using 15-PGDH antibody (x40 objective). Red = 15-PGDH stain, blue = nuclear staining DAPI. Clones displayed in numerical order left to right. Intensity set on H1 clone for each run of samples.

The 15-PGDH over-expressing clones (H1, H4, H2, H11 and H14) also showed increased *HPGD* mRNA levels (Figure 5.6), ranging from a 2.3-3.6-fold increase over the parental MCF7 cells. Variation in *HPGD mRNA* expression was observed between the control clones in comparison to the parent MCF7 cell line, but the levels did not appear to be unduly high when compared to the over-expressing clones. No data was collected for the X15 clone as the cells failed to grow sufficiently.

5.4.2.2 Stable clone proliferation

The metabolic activity, a measure of proliferation rate, of each MCF7 stably transfected clone was assessed using the MTS assay. The aim was to match each 15-PGDH over-expressing clone to a control clone with a similar rate of proliferation for further functional assays. This was to ensure that the intrinsic proliferation rate of the clones was not a confounding factor in the subsequent analysis.

A 4-fold difference in proliferation rates was found between the highest and lowest proliferation rates, with no apparent association between those over-expressing 15-PGDH and proliferation rate (Figure 5.7A). The clones were ordered by their rate of proliferation (Figure 5.7B) and the over-expressing clones matched to a control clone with the closest mean proliferation rate and smallest standard deviation. The MCF7 stable transfected clones were matched as follows:

- H1 and X6
- H2 and X1
- H4 and X3
- H11 and X2
- H14 and X17

H1 and H2 had very similar proliferation rates and each could be paired with X6 or X1, but it was decided to pair H1 with X6 and H2 with X1 as X6 was closer to H1 than to X1.

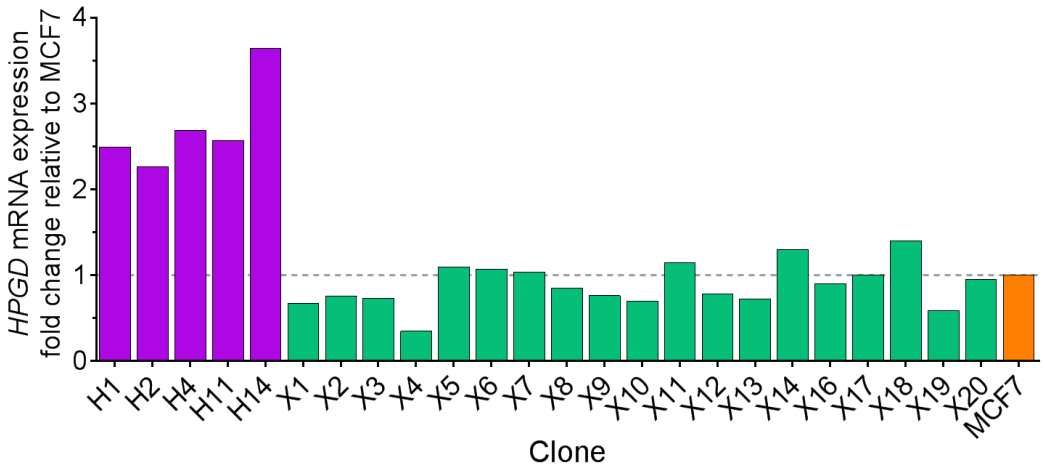

Figure 5.6 *HPGD* mRNA expression. Conventional RT-PCR was performed with *HPGD* and *GAPDH* primers. The mRNA expression as normalised to the matched exogenous *GAPDH* control expression and the fold change determined in relation to the MCF7 parent cell line. 15-PGDH over-expressing clones (purple), control vector clones (green) and the non-transfected parent MCF7 cell line (orange).

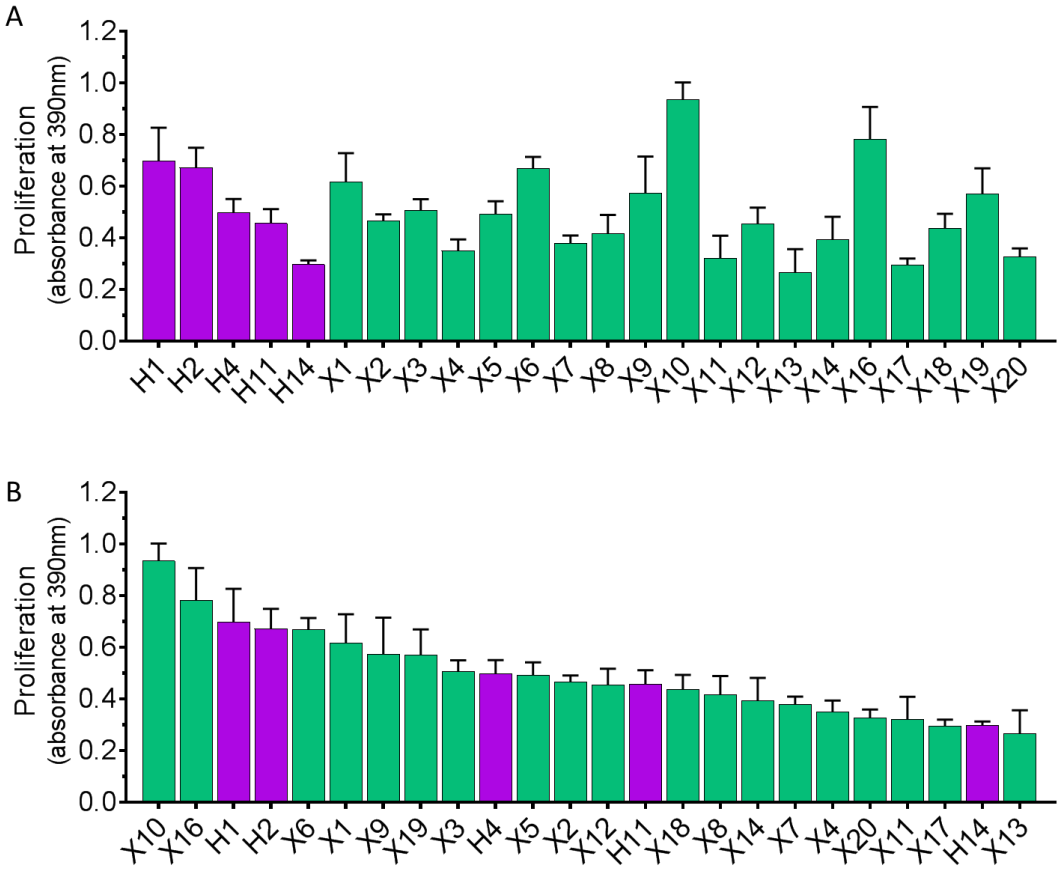

Figure 5.7 MCF7 stable transfected clone proliferation. Over-expressing clones (purple), and control clones (green) were grown for 72 hours before performing an MTS assay. Error bars represent one standard deviation from two experiments with three repeats per experiment. (A) Clones ordered by clone ID. (B) Ordered by proliferation.

5.4.2.3 *HPGD mRNA* expression in selected MCF7 clones

HPGD mRNA expression was confirmed in the selected clones listed above using the more accurate, quantitative RT-PCR (Figure 5.8).

No significant difference in *HPGD mRNA* expression was observed between the control clones and the MCF7 parent cell line. Whereas, a significant increase in *HPGD mRNA* expression was observed in the over expressing clones, with the fold change ranging from 52-fold increase ($p = 0.0013$) in the H11 clone to 1439-fold in H14 ($p < 0.0001$).

5.4.2.4 15-PGDH protein activity in selected MCF7 clones

The 15-PGDH protein activity was measured to confirm both the protein produced by the MCF7 15-PGDH stably over-expressing clones was functional and the clones had a detectable increase in enzyme activity. The assay was based on the principle that 15-PGDH breaks down prostaglandin PGE_2 into its 15-keto metabolite with the linked production of NADH, whose levels can be determined by increased absorbance at 340 nm. The assay was based on the method used by Uppal et al. (Uppal et al., 2008) and was confirmed using an *E.coli* induced 15-PGDH over-expressing construct model system (Figure 5.9).

The protocol was adapted to assay total protein lysate from mammalian cells, which produce noticeably less 15-PGDH protein than the *E.coli* based system. The assay was performed on the matched pairs of MCF7 stably transfected clones, using the A549 lung cell line as a positive control (Figure 5.10) with enzyme activity assessed following the addition of either DMSO (control) or PGE_2 in DMSO.

No change in NADH production was observed with DMSO treatment for all of the clones assessed. Furthermore, no change was observed following the addition of PGE_2 to the control clones (green). An increase in absorbance was however observed with the all the 15-PGDH expressing clones except clone H11. Clone H14 showed the largest increase in NADH production, followed by H2, H1 and H4, while H11 showed little change in NADH production after 20 minutes.

Together the RNA and protein analysis confirmed that the five over-expressing clones were suitable for downstream functional studies alongside their matched controls, and between them they displayed approximately a 10-fold difference of in 15-PGDH activity.

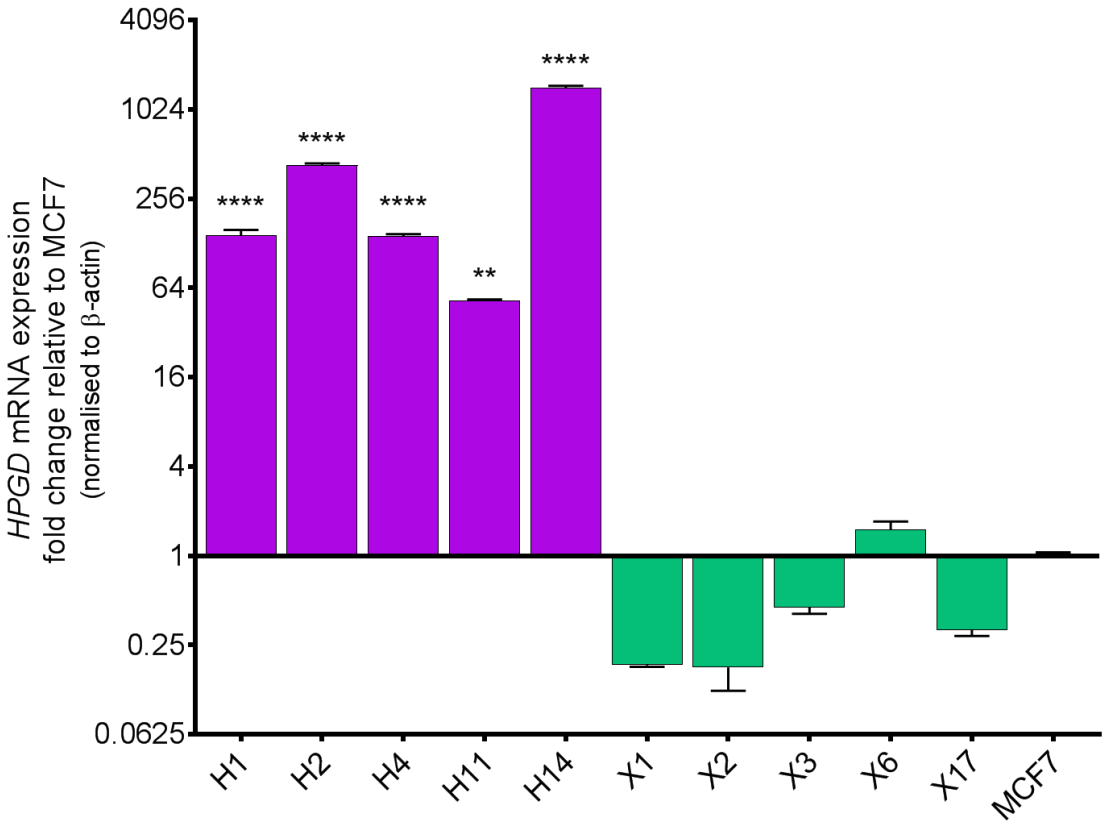

Figure 5.8 *HPGD* mRNA expression in MCF7 stably transfected clones. *HPGD* mRNA expression was assessed in the selected 15-PGDH over-expressing clones (purple), control clones (green) and parent MCF7 cell line (orange) by qRT-PCR. The graph shows log2 fold change mRNA expression and error bars indicate one standard deviation for each clone performed in triplicates. One-way ANOVA statistical analysis was performed, ** = $p < 0.005$, **** = $p < 0.0005$.

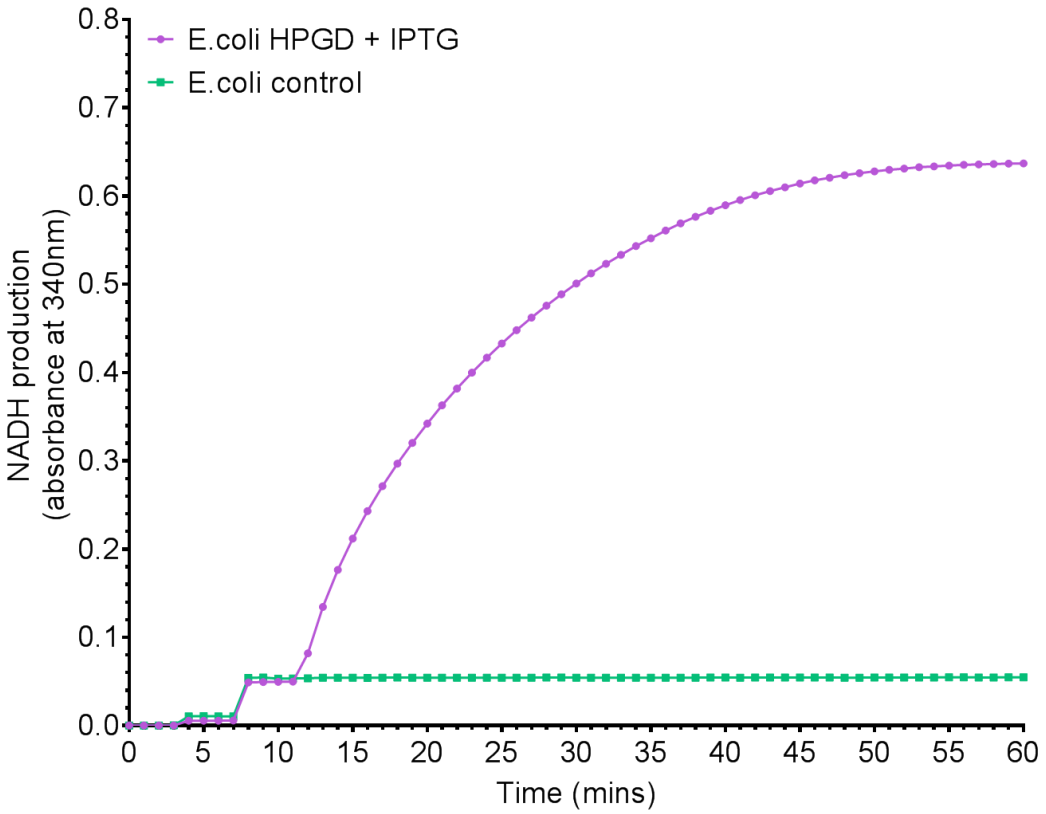

Figure 5.9 15-PGDH protein activity assay with *E.coli* positive control. Metabolism of PGE_2 by 15-PGDH produces NADH as a by-product. The NADH production was measured by an increase in absorbance at 340nm. 0 mins = buffer only, 3 mins = protein added, 8 mins = NAD+ added, 12 mins = PGE_2 substrate added. *E.coli* 15-PGDH positive control (purple), *E.coli* control (green).

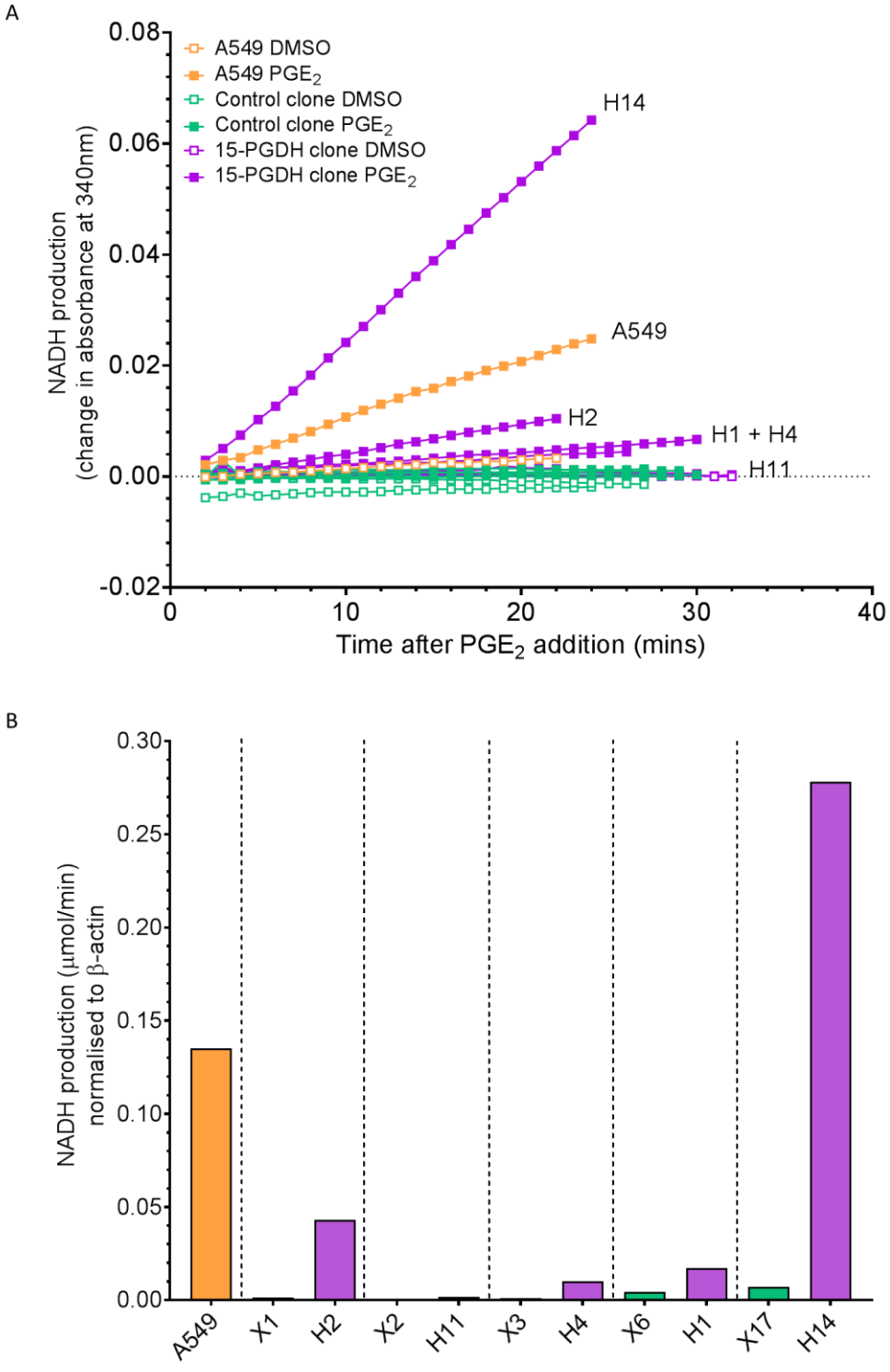

Figure 5.10 15-PGDH protein activity assay. Metabolism of PGE_2 by 15-PGDH produces NADH as a by-product. The NADH production was measured by an increase in absorbance at 340nm. Over-expressing 15-PGDH clones (purple), control clones (green), A549 control (orange). (A) Change in absorbance after PGE_2 or DMSO addition for MCF7 15-PGDH over-expressing clones. (B) Change in absorbance after 20 minutes of PGE_2 addition for each of the clones.

5.4.3 Functional effects of 15-PGDH expression on MCF7 cell line

5.4.3.1 15-PGDH and proliferation with PGE_2 substrate

As previously described, no trend in baseline proliferation was observed between MCF7 clones with low 15-PGDH expression compared to the over expressing clones (Figure 5.7). Therefore, to determine whether the effect of 15-PGDH expression on proliferation was dependent upon the presence of 15-PGDH substrates, MCF7 clones were treated with exogenous PGE_2. The cells were treated with 0-10 µM PGE_2 for 24 or 72 hours in standard culture media (10% FCS) and a reduced serum culture media (1% FCS) to determine the effect of exposure time and FCS on proliferation. The ability of the cells to survive and grow following each treatment was determined using the MTS assay to measure the cells metabolic activity.

A decrease in proliferation was observed in H4 and H11 over-expressing clones compared to their matched control clones when cultured with media containing 10% FCS and 10 µM PGE_2 after 24 hours (Figure 5.11). Furthermore, a decrease in proliferation in the over-expressing clone compared to the control clone was observed in one clone with 1 µM PGE_2 after 72 hours and reduced proliferation in the control clone compared to the over-expressing clone in one clone at 0.1 µM PGE_2 and 1 µM PGE_2. Similar observations were seen with clones grown in media with reduced serum (1% FCS) (Figure 5.12).

No significant difference between the control clones and over-expressing clones was seen at the PGE_2 concentrations and exposure times tested. Furthermore, the clone showing reduced proliferation with PGE_2 treatment switched between the controls and over-expressing clones.

A decrease in individual clone viability was observed after 10 µM PGE_2 treatment at 24 hours, which was amplified after 72 hours exposure in media supplemented with 1% FCS compared to 10% FCS. Equally, a decrease in viability was also observed in the 1 µM PGE_2 treatment after 72 hours, which was not present after 24 hours. This was confirmed through visual inspection of the plates, where floating cell debris was observed after treatment.

A comparable trend was seen between all of the matched MCF7 clone pairs, which was also observed when all of the data sets were combined (Figure 5.13). A significant reduction in viability was observed with higher doses of PGE_2 in both the control and 15-PGDH over-expressing clones.

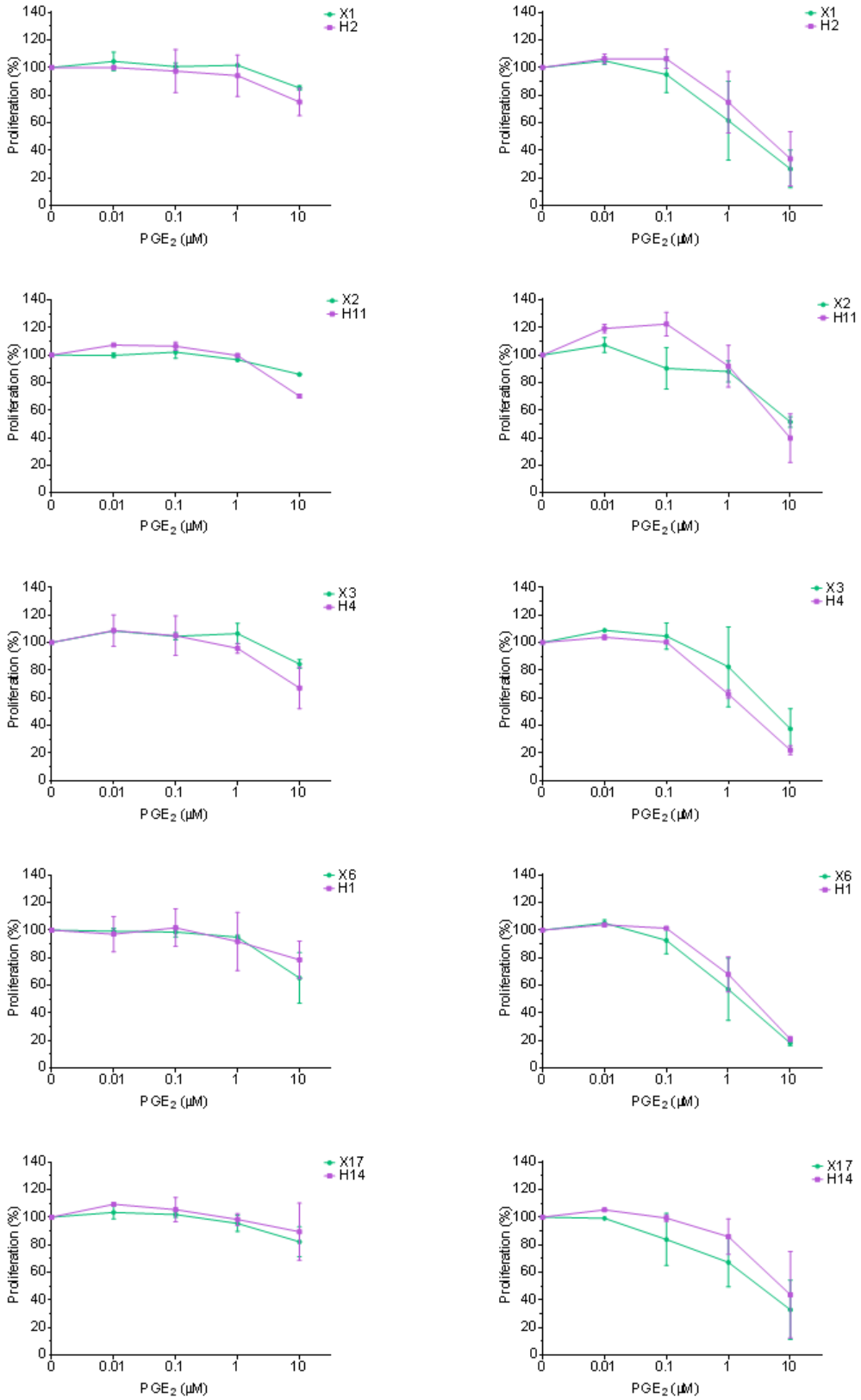

Figure 5.11 Proliferation of MCF7 clones stably over-expressing 15-PGDH. Cells grown in media containing 10% FCS. Left = 24 hours, right = 72 hours. Error bars = one standard deviation for two biological repeats.

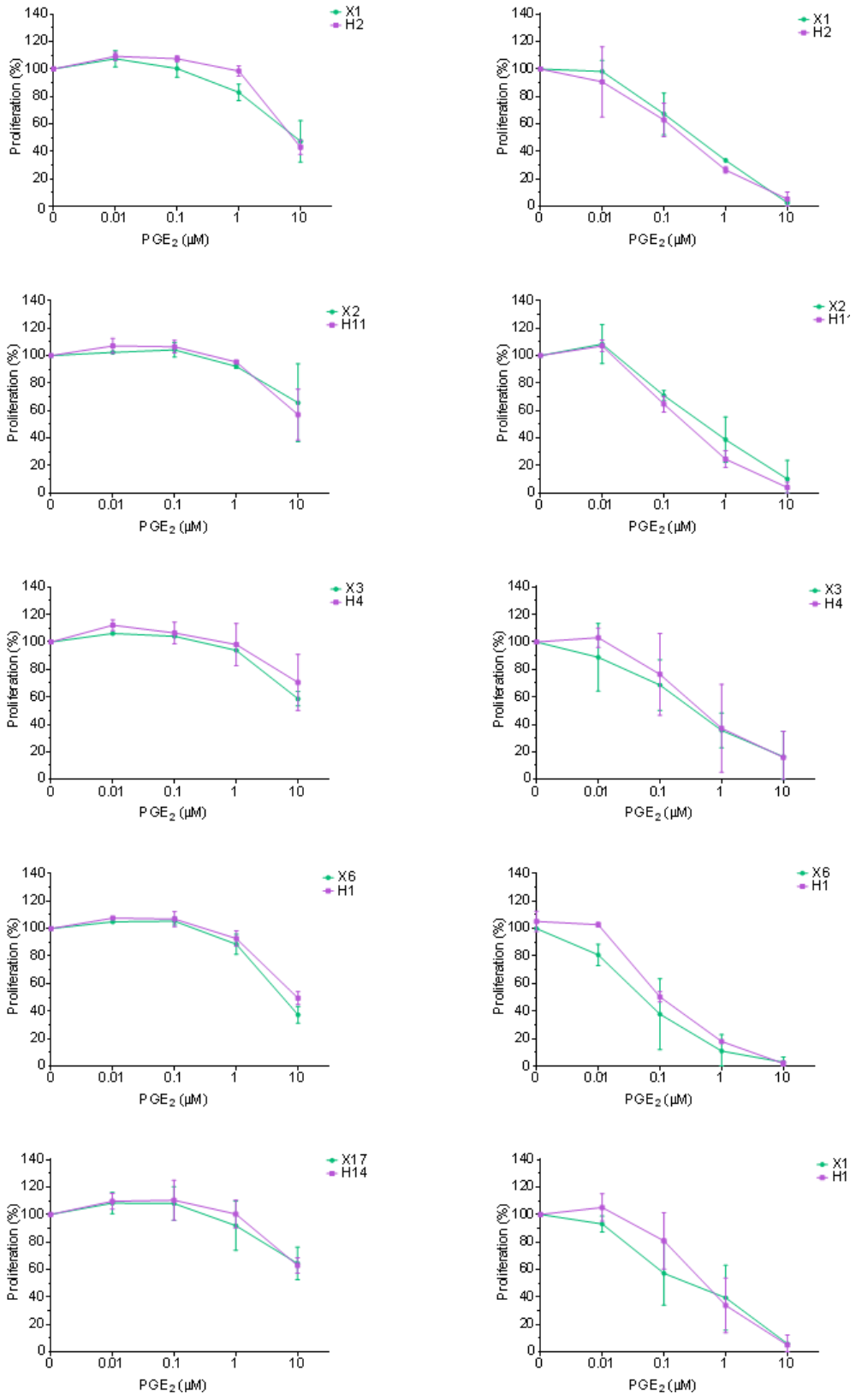

Figure 5.12 Proliferation of MCF7 clones stably over-expressing 15-PGDH in media with reduced serum. Cells grown in media containing reduced FCS (1%) for 24 hours prior to the addition PGE_2 in 1% FCS media. Left = 24 hours, right = 72 hours. Error bars = one standard deviation for two biological repeats.

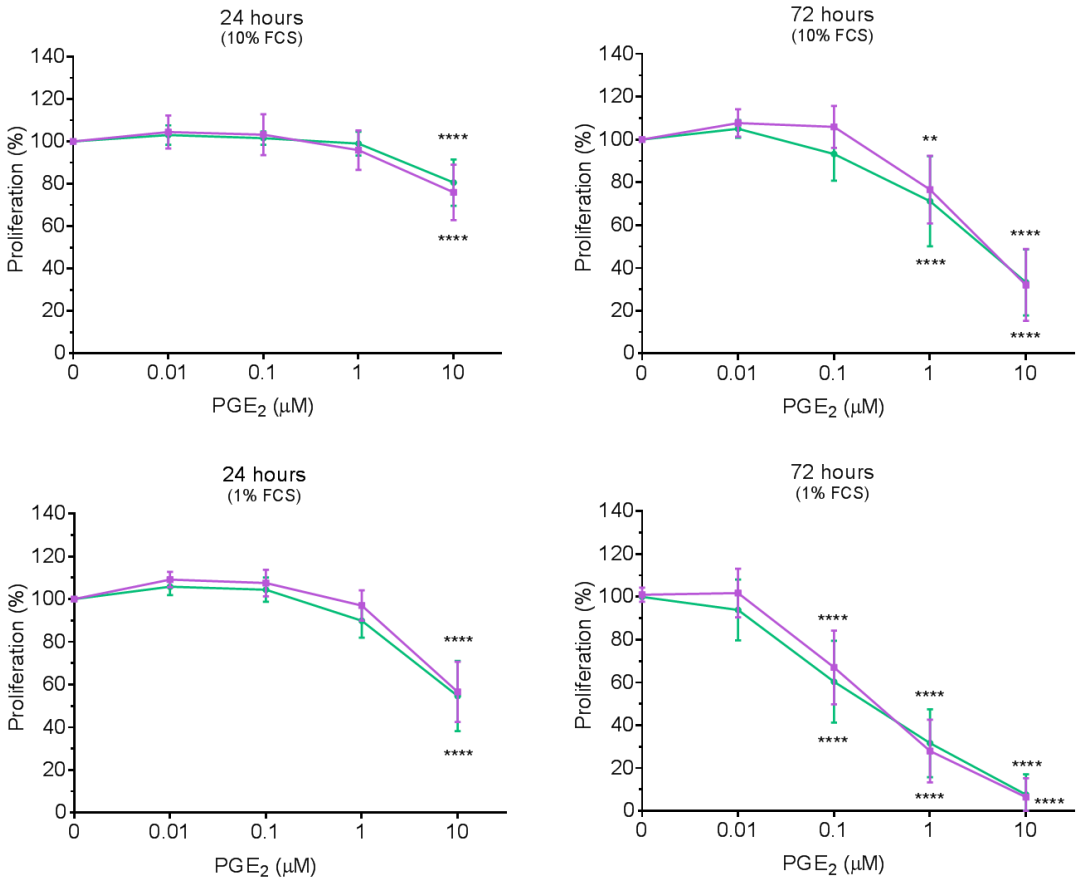

Figure 5.13 Summary of MCF7 clones stably over-expressing 15-PGDH proliferation with PGE_2 treatment. Cells were grown in media containing 10% FCS (top) or 1% FCS (bottom) for 24 hours (left), or 72 hours (right) with PGE_2. Error bars = one standard deviation for two biological repeats for the five clones combined. Green = control clones, purple = matched 15-PGDH over-expressing clones. Two-way ANOVA statistical analysis * $p < 0.05$, ** $p < 0.005$, *** $p < 0.0005$, **** $p < 0.0001$. Comparison between PGE_2 treatment within a clone above or below data point.

5.4.3.2 15-PGDH and migration

The effect of 15-PGDH expression on cell migration was examined in MCF7 clones stably over-expressing 15-PGDH compared to control clones matched for proliferation rate. To do this scratch wound and transwell assays were performed as described in Sections 2.1.7 and 2.1.9.

Optimisation of the scratch wound assay using a single matched clone pair indicated that growing the cells in media containing reduced serum (1% FCS) gave the largest difference between PGE_2 treatment and DMSO-treated samples compared to normal serum levels (10% FCS) (Figure 5.14). Treatment was then performed with 1 µM, 5 µM and 10 µM PGE_2 to determine the concentration that showed the largest change in cell migration (Figure 5.15).

A large difference was observed in the over-expressing clone with 1 µM and 5 µM PGE_2 treatment after 48 and 72 hours. A slight decrease in wound confluency was also observed with 10 µM PGE_2 compared to the lower concentrations. For this reason and given that PGE_2 binds EP receptors at a K_d value (binding affinity) of 1-40 nM (Sugimoto and Narumiya, 2007), the lowest concentration of 1 µM was taken forward to ensure optimal effect was observed with minimal toxicity. The optimisation experiments also indicated that the over-expressing clone tended to have a reduced migration rate compare to the matched control, and this was seen with and without addition of PGE_2.

Subsequent experiments performed with all five matched clone pairs showed that the rate of migration was reduced in DMSO-treated 15-PGDH over-expressing clones in comparison to their matched control clones in the scratch wound assay (Figure 5.16 and Figure 5.17), with the exception of X1 and H2 clones, which showed a similar wound confluency. This was observed across the independent experimental repeats, with a small standard deviation observed for all of the clones except X17. Compared to all of the other clones that reached 80-90% wound confluency after 72 hours, the rate of migration was slower in the X17, H14 and H4 clones, as the cells only reached an average of 60% confluency after 72 hours with DMSO treatment for the X17 clone, 40% for the H14 clone and 60% for the H4 clone.

The addition of PGE_2 did not significantly alter the rate of migration in the MCF7 control clones with the exception of the H4 clone after 72 hours. There was however a general increase in migration with PGE_2, and the effect of PGE_2 on wound confluency was more pronounced in the 15-PGDH over-expressing clones compared to their controls.

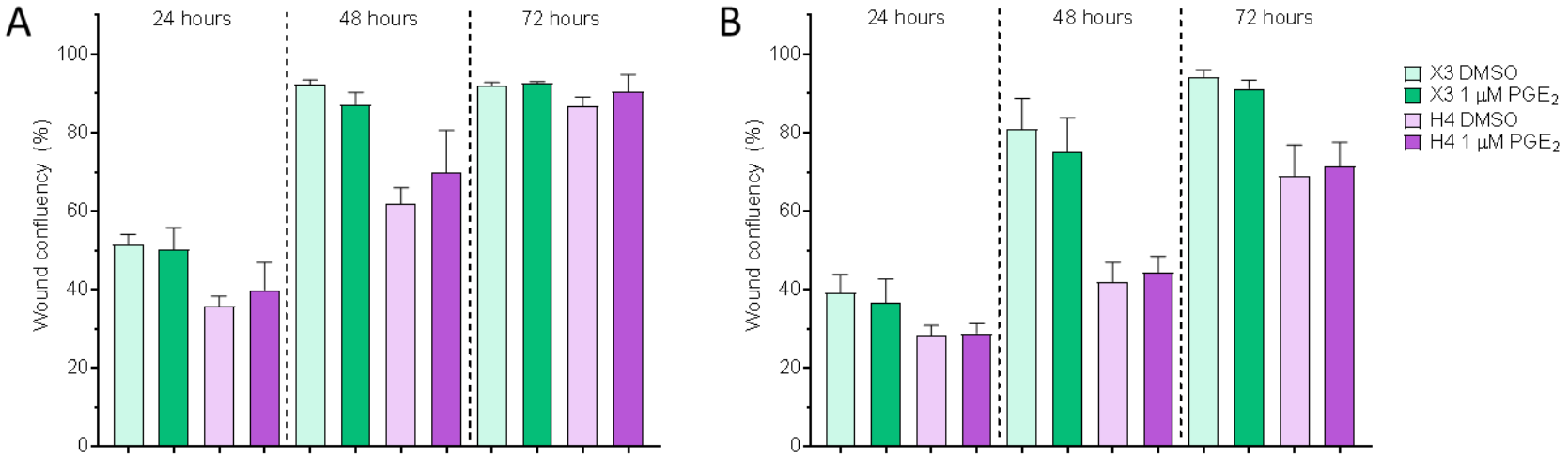

Figure 5.14 Optimisation of scratch wound migration assay FCS culture conditions. Performed with X3 (green) and H4 (purple) clones. (A) Cells cultured in media with reduced serum (1% FCS) treated with DMSO or 1 µM PGE_2 (B) Cells cultured in media with standard serum levels (10% FCS) treated with DMSO or 1 µM PGE_2. Error bars indicate one standard deviation for three repeats in a single experiment.

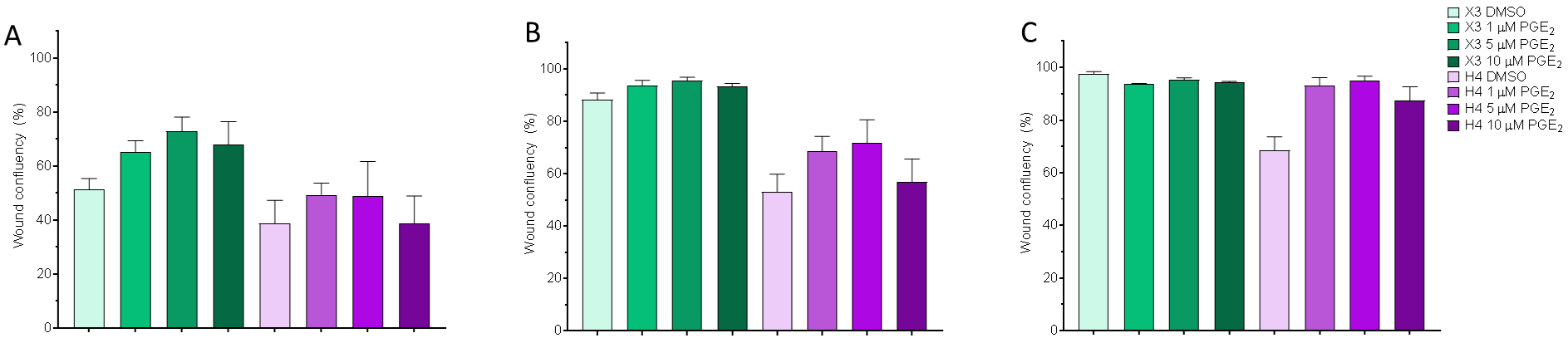

Figure 5.15 Optimisation of scratch wound migration assay PGE_2 concentration. Performed with X3 (green) and H4 (purple) clones. Cells cultured in media with reduced serum (1% FCS) treated with DMSO, 1 µM PGE_2, 5 µM PGE_2 or 10 µM PGE_2 for (A) 24 hours, (B) 48 hours or (C) 72 hours. Error bars indicate one standard deviation for three repeats in a single experiment.

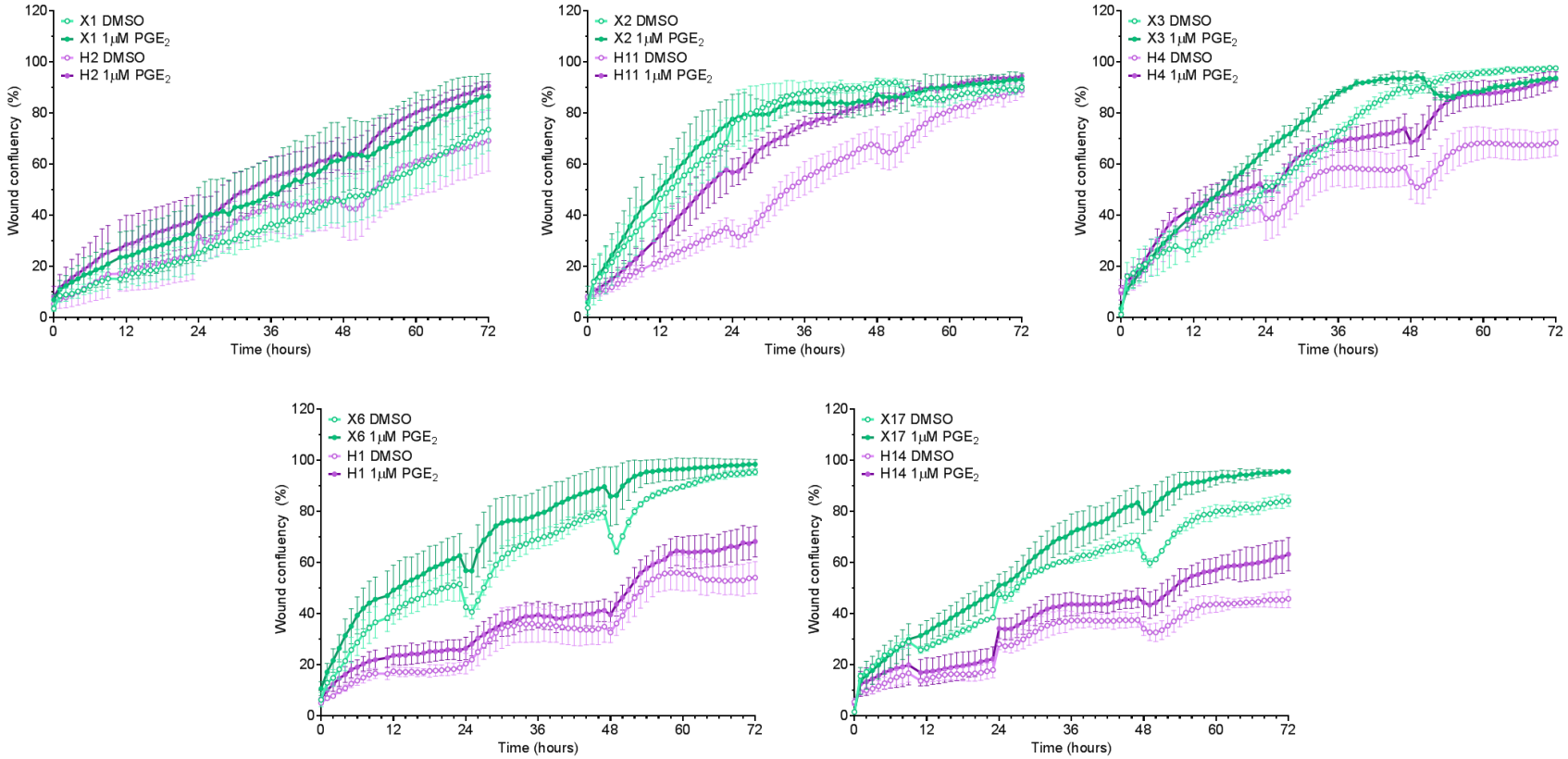

Figure 5.16 Scratch wound migration assays with MCF7 15-PGDH stably transfected clones. Migration data for one experiment containing two to four biological repeats per sample. Data is representative of the results seen in three independent experiments. Error bars indicate one standard deviation. Pale purple = 15-PGDH over-expressing clone DMSO control, dark purple = 15-PGDH over-expressing clone treated with PGE_2, pale green = control clone DMSO control, dark green = control clone treated with PGE_2. Troughs seen at 24 and 48 hours due addition of PGE_2 and plate repositioning.

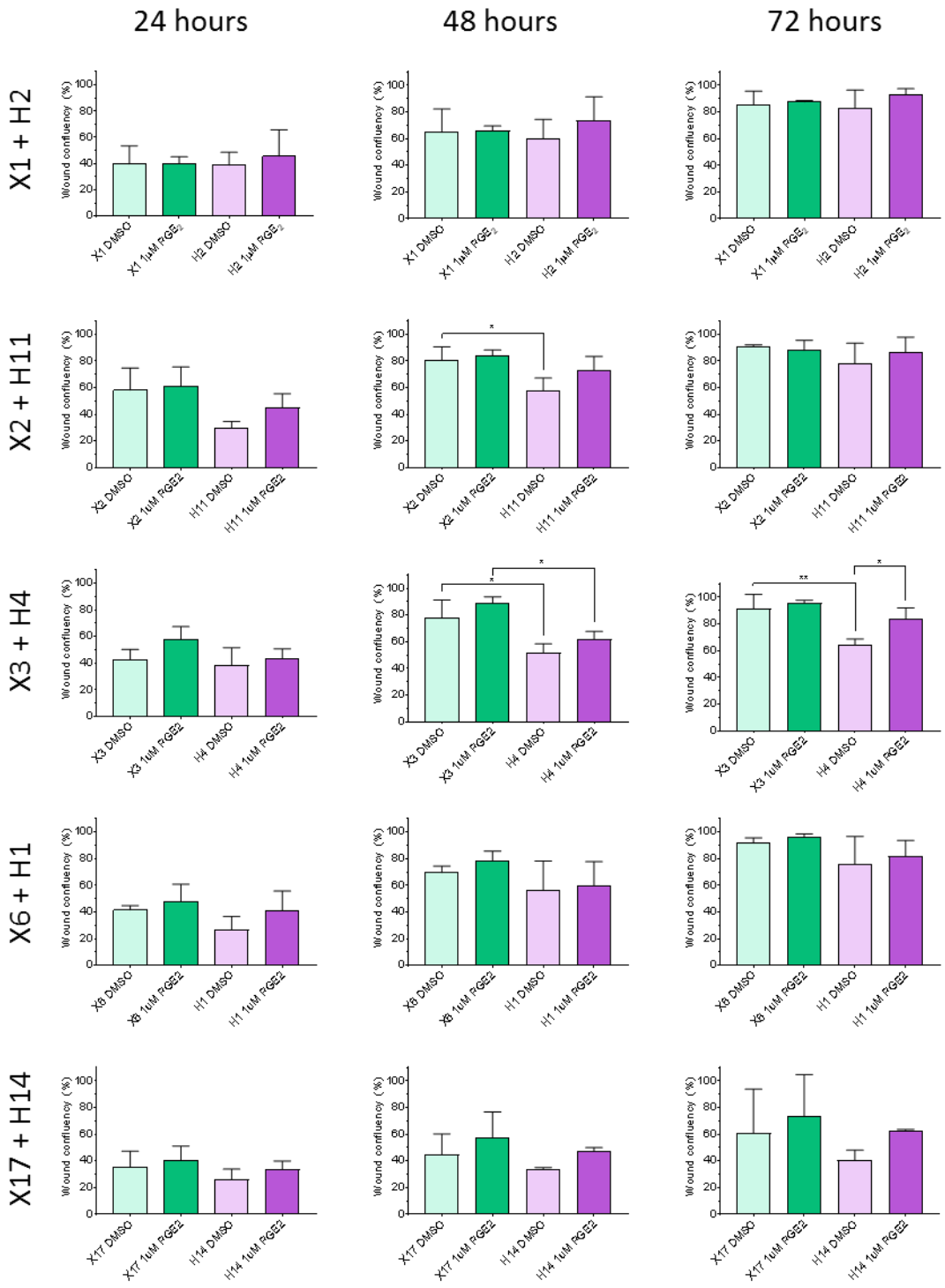

Figure 5.17 Scratch wound migration assay wound confluency bar graphs. Control clone = green, 15-PGDH over-expressing clones = purple. Left to right column shows 24, 48 and 72 hour data respectively. Each row represents the indicated clone pairs. Error bars show one standard deviation for three independent experiments (two for X2 and H11 and X17 and H14 72 hours).

The largest increase in migration following PGE_2 addition was observed in the H4 and H14 clones after 72 hours. The effect of exposure to PGE_2 was overall consistent between each of the 24, 48 and 72 hour time points.

Combining the data from all control clones and all 15-PGDH clones showed that the over-expressing clones had a lower migration rate than the controls on average at all time points (Figure **5.18**). This reached statistical significance at 48 hours ($p < 0.05$). More variability was observed overall with the combined data, due to differences in proliferation rates.

Transwell migration assays were also performed, where cells were seeded into transwell inserts with 8 µm pores for 48 hours. The number of cells able to migrate through the pores onto the underside of the insert was counted. 10% FCS with or without EGF was used as a chemoattractant. Two matched clone sets were assessed, clones X6 and H1 as well as X17 and H14. X17 and H14 were selected as they had the largest difference as judged by the scratch wound migration assay.

The transwell assay was optimised by comparing cells cultured in reduced serum for 24 hours prior to the experiment in comparison to normal culture conditions (Figure 5.19). Increased cell migration was observed with cells cultured under normal culture conditions rather than serum starved, therefore the cells were not serum starved prior to the experiment.

Migration was increased in the presence of 10% FCS as a chemoattractant compared to 1% FCS, and even more so with the addition of EGF in all of the clones assessed (Figure 5.20). Although reduced migration was observed in the H14 clone compared to the X17 control clone under all conditions, increased migration was seen with the H1 clone with chemoattractant compared to its matched control (X6). As the data was not consistent and none of the differences between the control and over-expressing clones were sufficient to reach statistical significance, it indicated that 15-PGDH levels did not influence migration when assessed by this assay.

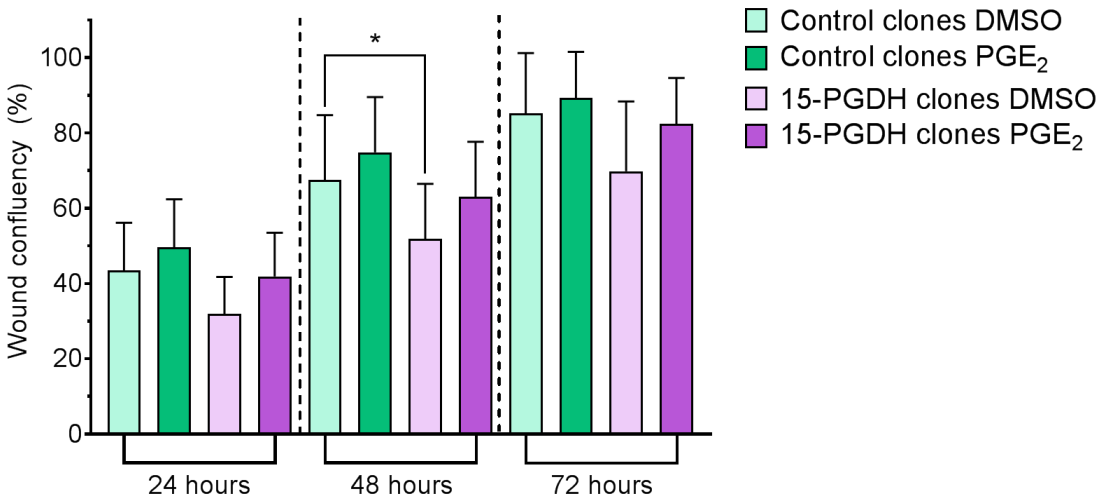

Figure 5.18 Scratch wound migration data for MCF7 15-PGDH stably transfected clones. Combined wound confluency scratch wound data for the MCF7 clones at 24, 48 and 72 hours. Cells were treated with DMSO (control) or 1 µM PGE_2. Error bars indicate one standard deviation for the three independent experiments. A one-way ANVOA statistical test was performed, * $p < 0.05$.

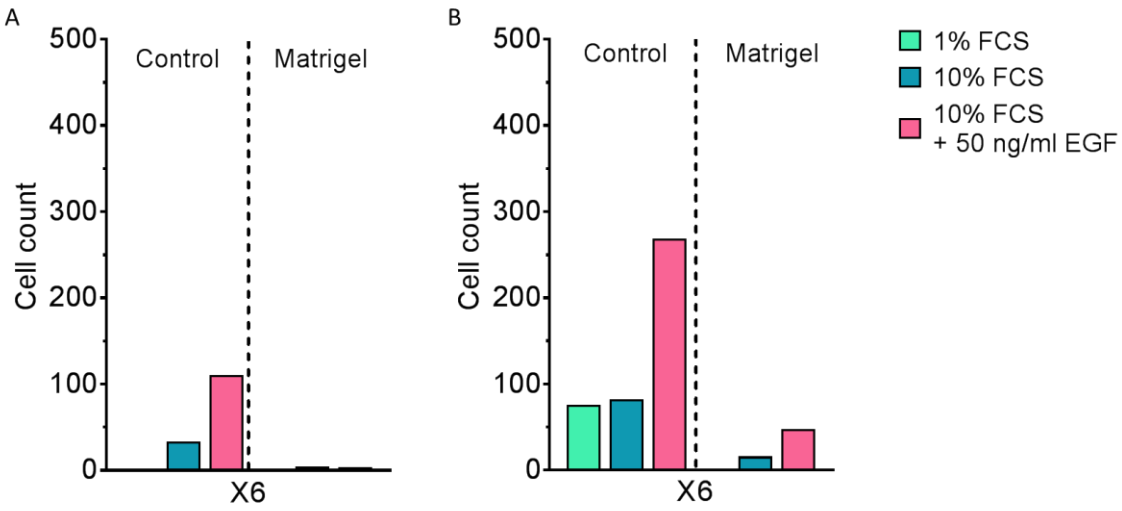

Figure 5.19 Transwell migration and invasion assay optimisation. X6 migration and invasion assay cell count. (A) Reduced serum (1%) for 24 hours prior to assay. (B) Normal serum (10%) conditions prior to assay.

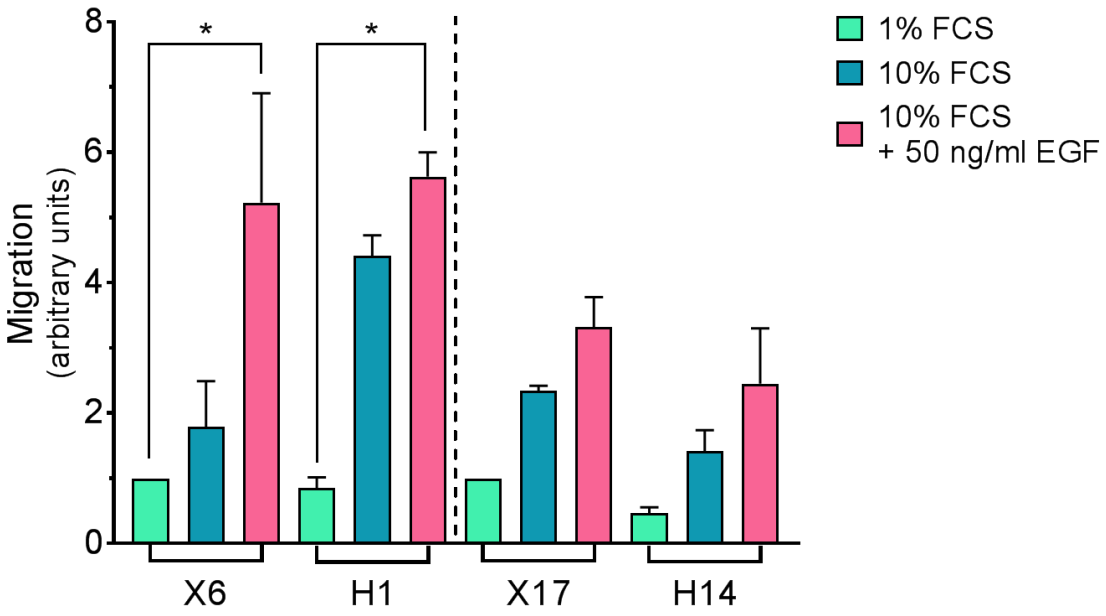

Figure 5.20 Transwell migration data for MCF7 15-PGDH stably transfected clones. Transwell migration data for X6, H1, X17 and H14 clones. Average of two independent experiments. Error bars indicate one standard deviation. Data normalised to relative control clone 1% FCS. One-way ANOVA statistical test performed. * $p < 0.05$.

5.4.3.3 15-PGDH and invasion

MCF7 clones with and without stable over-expression of 15-PGDH were next assessed for their ability to invade using a transwell Matrigel invasion assay. Matrigel contains a number of components of the extracellular matrix, including laminin, collagen and heparin sulphate, and models the basement membrane through which epithelial cells must cross in order to invade during cancer progression.

Optimisation of the invasion assay was required as the parent MCF7 cell line is regarded as relatively non-invasive. Additional chemoattractants were tested to see whether a potential decrease in invasion may be recorded. A standard chemoattractant for transwell assays is FCS, which the cells require to grow. EGF was also selected as an addition chemoattractant due to its ability to induced speed motility and directionality of both MCF7 and MDA-MB-231 breast cells (Wang, S.J. et al., 2004; Truong et al., 2016). Increased invasion was observed with cells grown in normal culture conditions prior to the experiment in comparison to reduced serum, which increased further with the additional chemoattractants (10% FCS and EGF) (Figure 5.19).

The percentage of invading cells increased when 10% FCS was used as the chemoattractant in comparison to the 1% FCS control for three of the clones assessed, but this was not statistically significant due to large variation between repeats (Figure 5.21A). The effect of additional EGF in 10% serum showed no clear trend for both the control and 15-PGDH over-expressing clones when compared to the 1% basal serum control.

When compared to the number of invading cells with no chemoattractant, the invasive index for the both X6 and H1 were higher than the X17 and H14 clones (Figure 5.21B). A higher invasive index was determined for the clones with 10% FCS as a chemoattractant in comparison to the 10% FCS and EGF in both clone sets. The invasive index was slightly lower for the over-expressing clones in comparison to their matched control clones, though no statistical difference was observed.

5.4.3.4 15-PGDH and clonogenicity

Colony forming assays were performed with the MCF7 clones to determine the ability of a single cell to recolonise (Figure 5.22). The process mimics the formation of a metastases from a single cell that has become detached from the primary tumour, invaded healthy tissue and proliferated to form a secondary tumour.

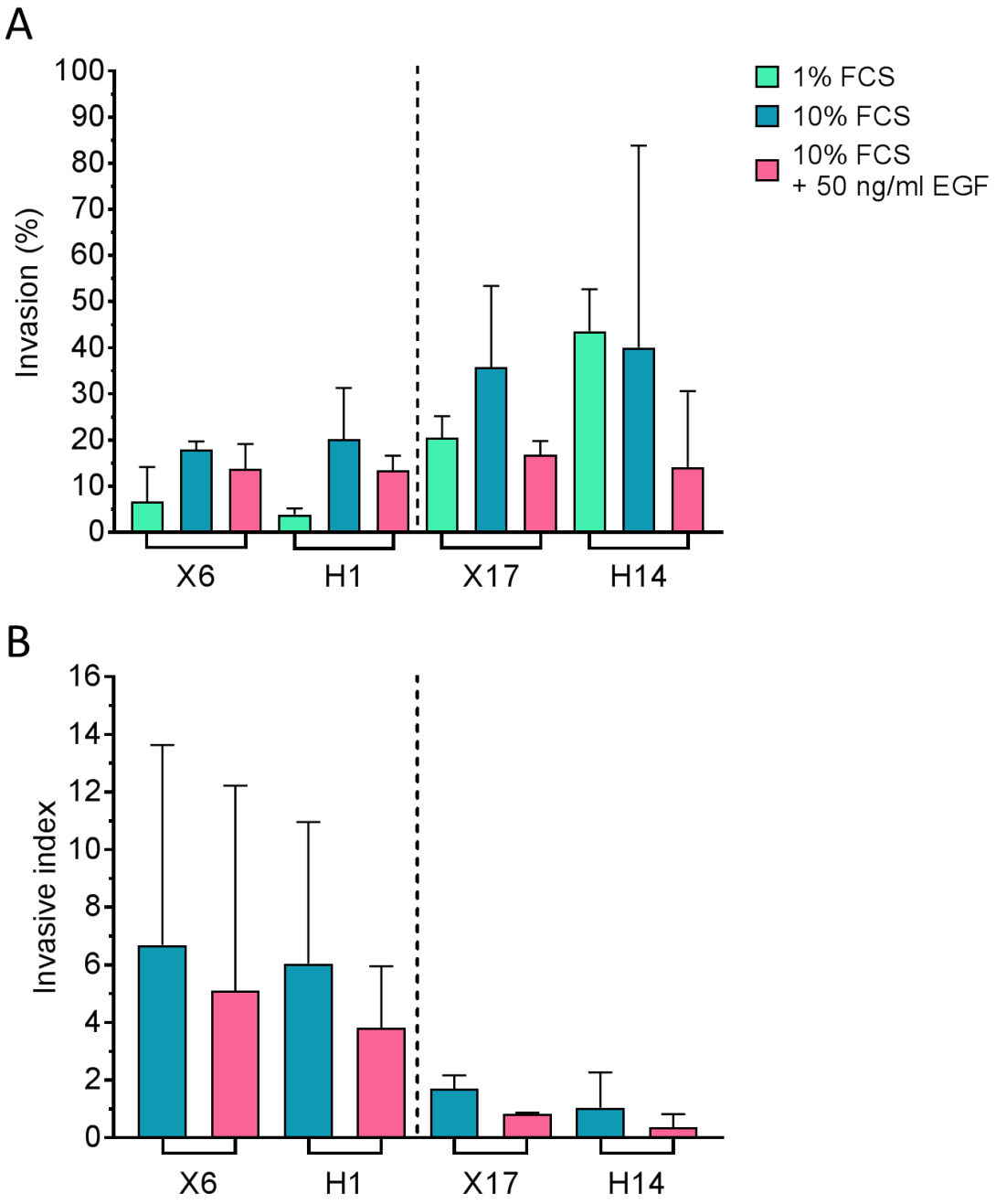

Figure 5.21 The effect of 15-PGDH expression on MCF7 invasion. Transwell invasion assay with MCF7 cells stably over-expressing 15-PGDH and their matched control clones. Error bars indicate one standard deviation. (A) Percent of cells invading the Matrigel layer normalised to the number of migrating cells. (B) Invasive index of clones when normalising to the 1% FCS control. No significant results were identified using a one-way ANOVA analysis.

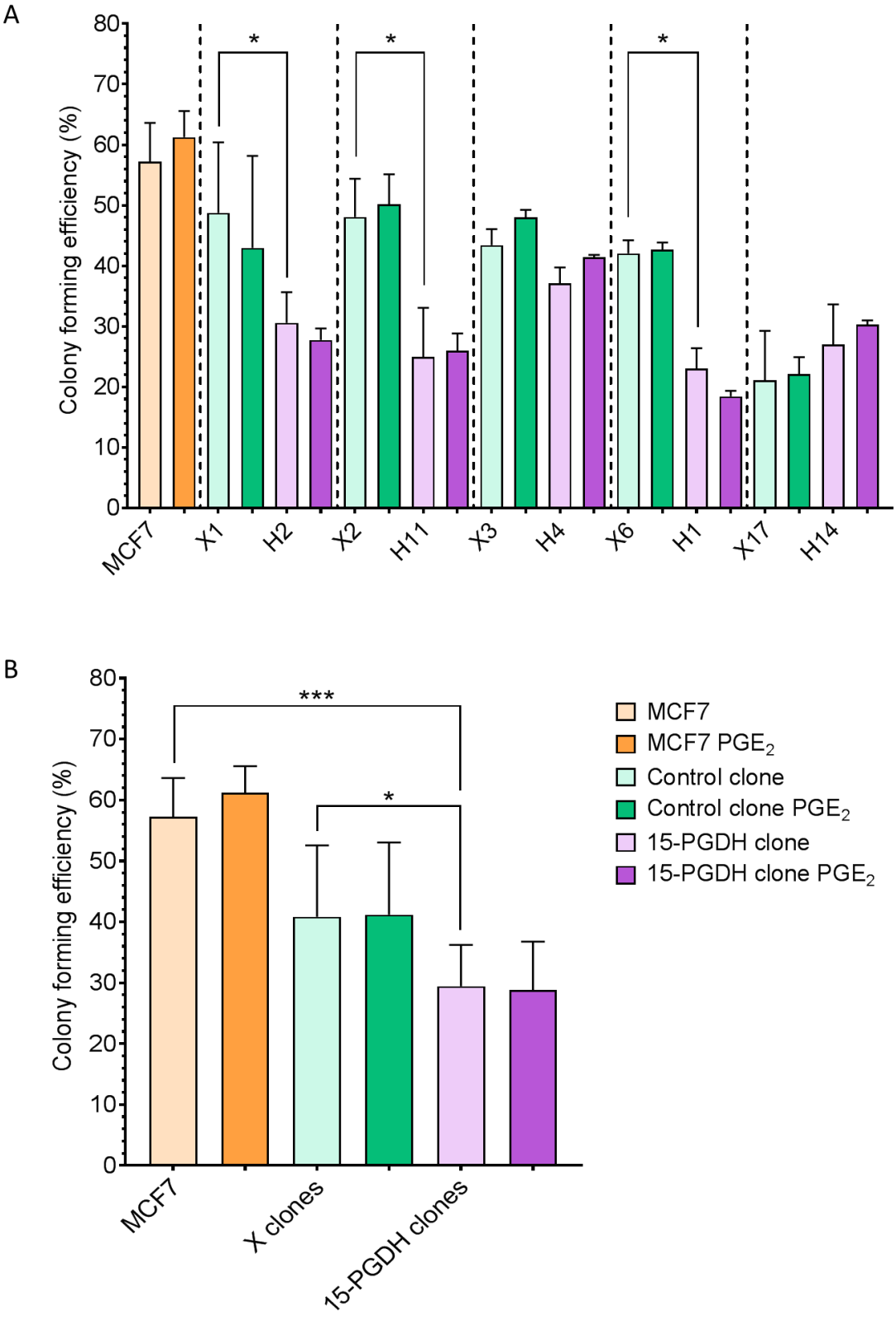

Figure 5.22 Clonogenicity of MCF7 15-PGDH stably transfected clones. The capacity of untreated MCF7 15-PGDH stably transfected clones and 1 µM PGE_2-treated clones to form colonies. Error bars indicate one standard deviation. One-way ANOVA performed, * $p < 0.05$, *** $p < 0.0005$. (A) Individual clones (B) Combines control and over-expressing clone data.

A significant decrease in colony forming efficiency was observed between three out of the five MCF7 15-PGDH over-expressing clones and their matched control clones. No significant difference was observed in the highest 15-PGDH expressing clone (H14) and its matched control, where H14 showed a slight increase in colony count.

To determine whether exposure to 15-PGDH substrate, PGE_2, increased clonogenicity of the MCF7 clones, the colony forming assay was performed in the presence of 1 µM PGE_2. No significant trend was observed in the ability of the clones to form colonies from a single cell with PGE_2 treatment with any of the clones assessed.

Larger colonies were observed in the control clones compared to their matched over-expressing clones, with the exception of H14 and X17. Additionally, the colony size for these clones was generally much smaller than the other clones assessed (Figure 5.23). No substantial difference in colony size was observed with any of the clones when comparing treatment with or without PGE_2.

A summary of the functional effect of 15-PGDH over-expression is shown in Table 5.3. No significant difference was observed for proliferation with any of the clone sets. A decrease in migration was observed in four of the clone sets, two of which were significant. Conflicting results were observed for invasion with the two clone sets assessed, however there was no significant difference. Finally, four of the five clone sets showed reduced clonogenicity, three of which were statistically significant.

5.4.4 Downstream transcriptional effects of 15-PGDH over-expression

RNA-Seq was performed with the highest 15-PGDH over-expressing MCF7 clone (H14) and it's matched control clone (X17), to assess the downstream transcriptional effects of 15-PGDH over-expression, and identify gene expression changes that may have functional significance. The samples were treated with DMSO (control) or PGE_2 to determine the effect of the presence of 15-PGDH substrate on the transcriptome.

Analysis was performed to assess the quality of the RNA-Seq data obtained throughout the library preparation and in the analysis. RNA in-put into the mRNA library preparation were of a high quality with a RIN number of at least 9.5.

Heatmaps were generated to show clustering of differentially expressed genes between the samples and their repeats (Figure 5.24). PCA plots were prepared to show grouping of the repeats depending on variation between the samples (Figure 5.25).

Table 5.3 A summary of the functional assay experiments with each clone set.

The table shows the effect of 15-PGDH over-expression on proliferation, migration, invasion and clonogenicity in each clone compared to its matched control clone. / = no change, ↓ = decrease, ↑ = increase, ns = non-significant change, * = significant change ($p < 0.05$).

Clone set	Proliferation	Migration (scratch wound)	Migration (transwell)	Invasion	Clonogenicity
X1 and H2	/ (ns)	/ (ns)			↓ (*)
X2 and H11	/ (ns)	↓ (*)			↓ (*)
X3 and H4	/ (ns)	↓ (*)			↓ (ns)
X6 and H1	/ (ns)	↓ (ns)	/ (ns)	↓ (ns)	↓ (*)
X17 and H14	/ (ns)	↓ (ns)	↓ (ns)	↑ (ns)	↑ (ns)

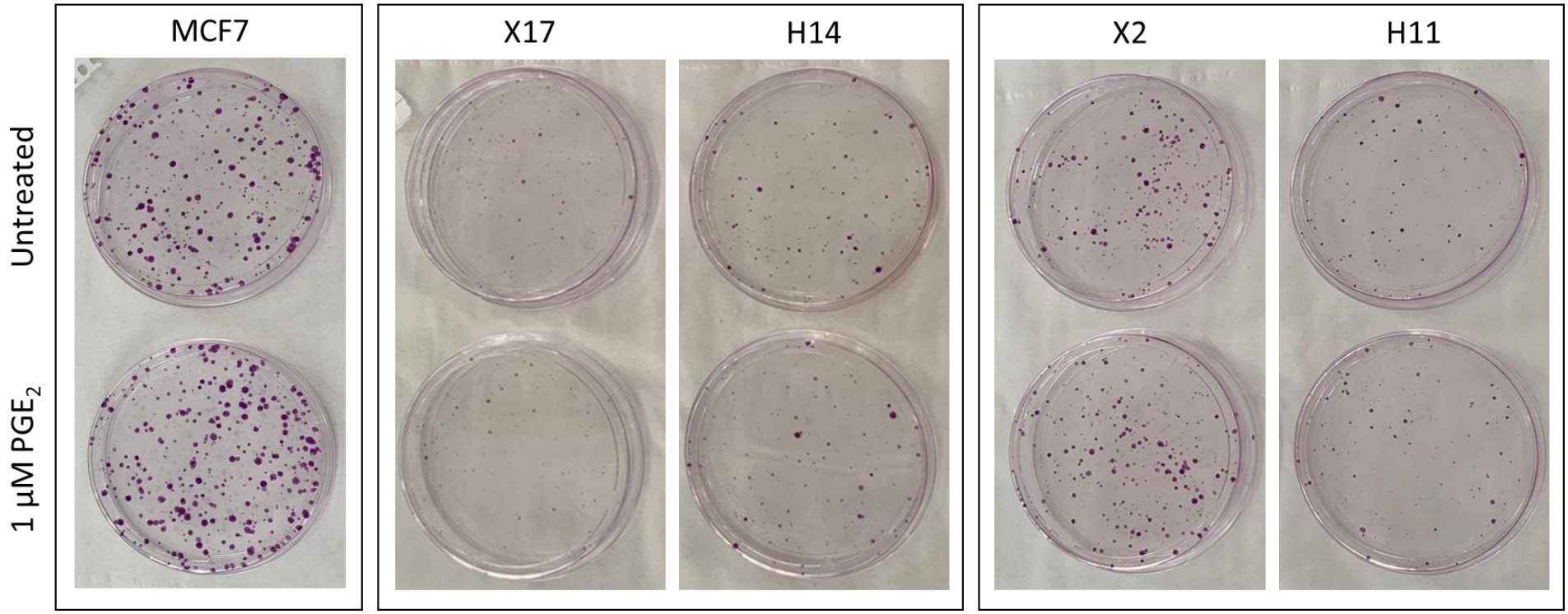

Figure 5.23 MCF7 15-PGDH stably transfected clones colony forming assay images. MCF7 clones stably over-expressing 15-PGDH were grown with or without 1 µm PGE_2 for two weeks before counting the number of colonies. MCF7 parent cell line, X17 and H14 clone set and X2 and H11 clone set s hown above.

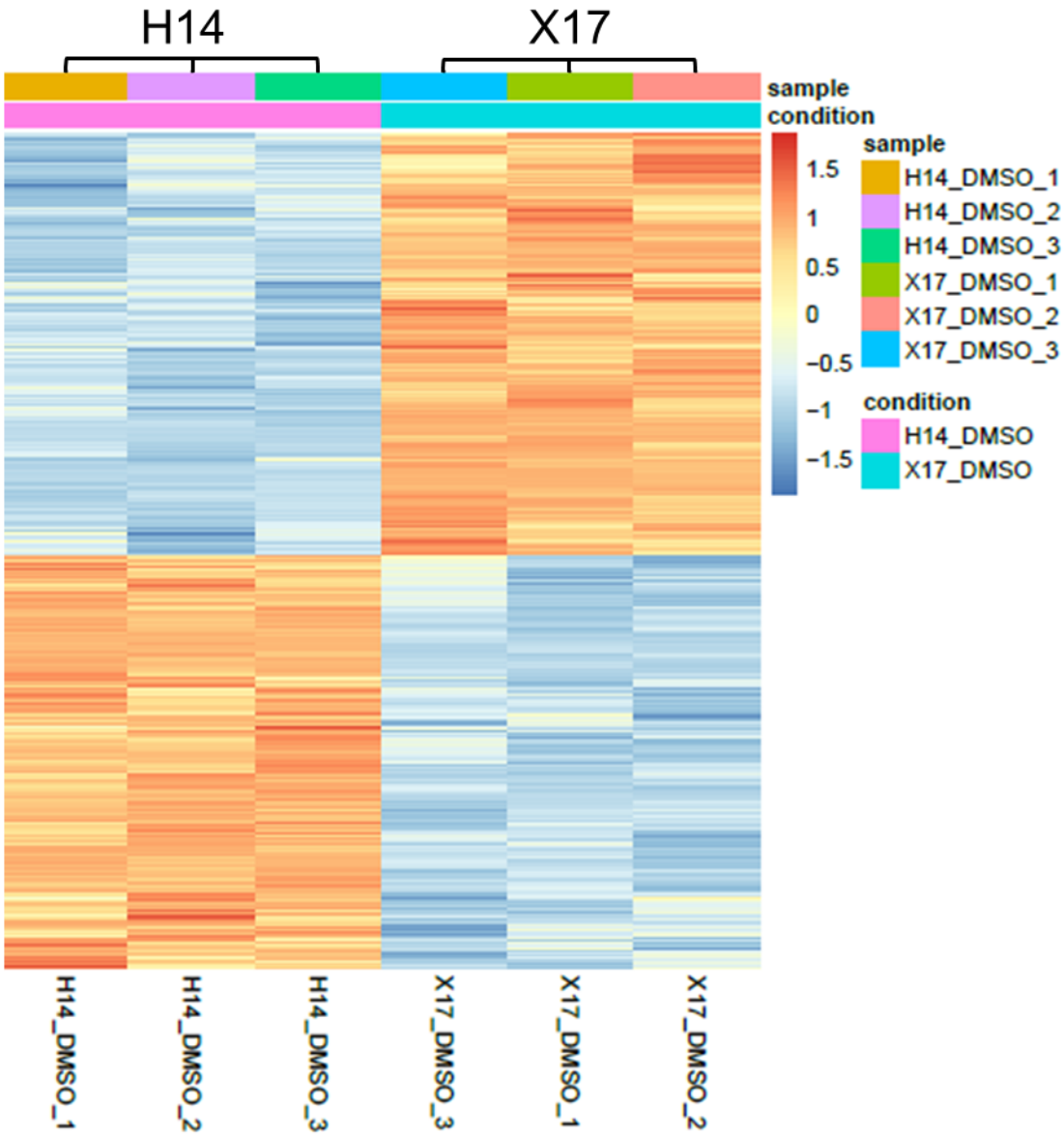

Figure 5.24 RNA-Seq quality assessment. Heat map with X17 and H14 clones, showing differentially expressed genes.

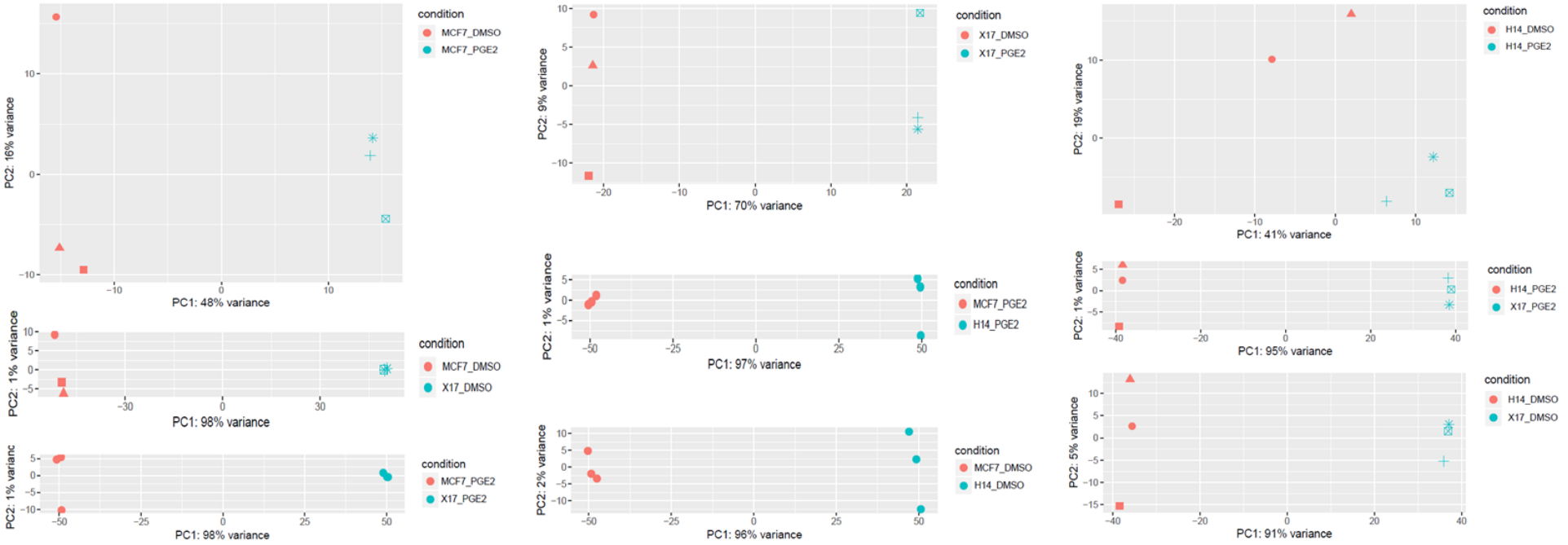

Figure 5.25 RNA sequencing PCA plots for pair-wise comparison data. Principle component analysis (PCA) plots for pair-wise comparisons between RNA sequencing samples.

MA plots, M being log ratio and A being mean average, were also generated to show the significantly differentially expressed genes between two sets of sample (Figure **5.26**). The X17 and H14 clones show a significant level of variation between the groups while demonstrating minimal variation between replicates. Similar data was observed for each of the other samples, with the H14 DMSO versus PGE2 showing a smaller degree of variation between the groups. This is possibly due to the exact same cell lines being used and a limited effect of the PGE2 treatment.

Gene ontology analysis was completed for each pairwise analysis (Figure 5.27), which highlighted cell adhesion molecule binding and cadherin binding as two of the most up-regulated cellular functions when comparing H14 to X17. Other cellular activities found to be differential modulated include DNA, RNA binding and NADH dehydrogenase activity. Many GO terms associated with 'binding' were also identified when comparing H14 to MCF7 cells (Appendix 16), yet cell adhesion was not in the top 40 GO terms.

The top 40 significant KEGG pathways when comparing the X17 and H14 clone included apoptosis, DNA repair and cell cycle check points (Figure 5.28). Both apoptosis and cell cycle pathways also contain a large number of transcript's whose expression was significantly different in the MCF7 versus H14 comparison (Appendix 17).

KEGG pathway analysis was performed to determine the genes expression changes in a number of pathways. The majority of the genes in the arachidonic acid metabolism pathway (hsa00590) are up-regulated (green) in H14 compared to X17, with the exception of EC 5.3.99.3 and EC 3.3.2.6 (Figure 5.29). Those up-regulated enzymes include epoxide hydrolase (EC 3.3.2.10), monooxygenases (EC 1.14.14.1), glutathione peroxidase (EC 1.11.1.9) and phospholipase A2 (EC 3.1.1.4). On the other hand, EC 5.3.99.3, which is down-regulated, denotes prostaglandin E synthase. Furthermore, leukotriene A4 hydrolase (EC 3.3.2.6) is also down-regulated. These patterns were consistent in the MCF7 and H14 comparison for prostaglandin E synthase, leukotriene A4 hydrolase, phospholipase A2, glutathione peroxidase and epoxide hydrolase (Appendix 18).

The KEGG cell cycle pathway (hsa04110) for the X17 and H14 DMSO samples can be seen in Figure 5.30. The majority of the genes in the cell cycle pathway are down-regulated (red) in the H14 15-PGDH over-expressing clone compared to the X17 control, but this is not consistent when comparing the H14 clone to the parent MCF7 cell line (Appendix 19), which shows a more even number of up- and down-regulated genes.

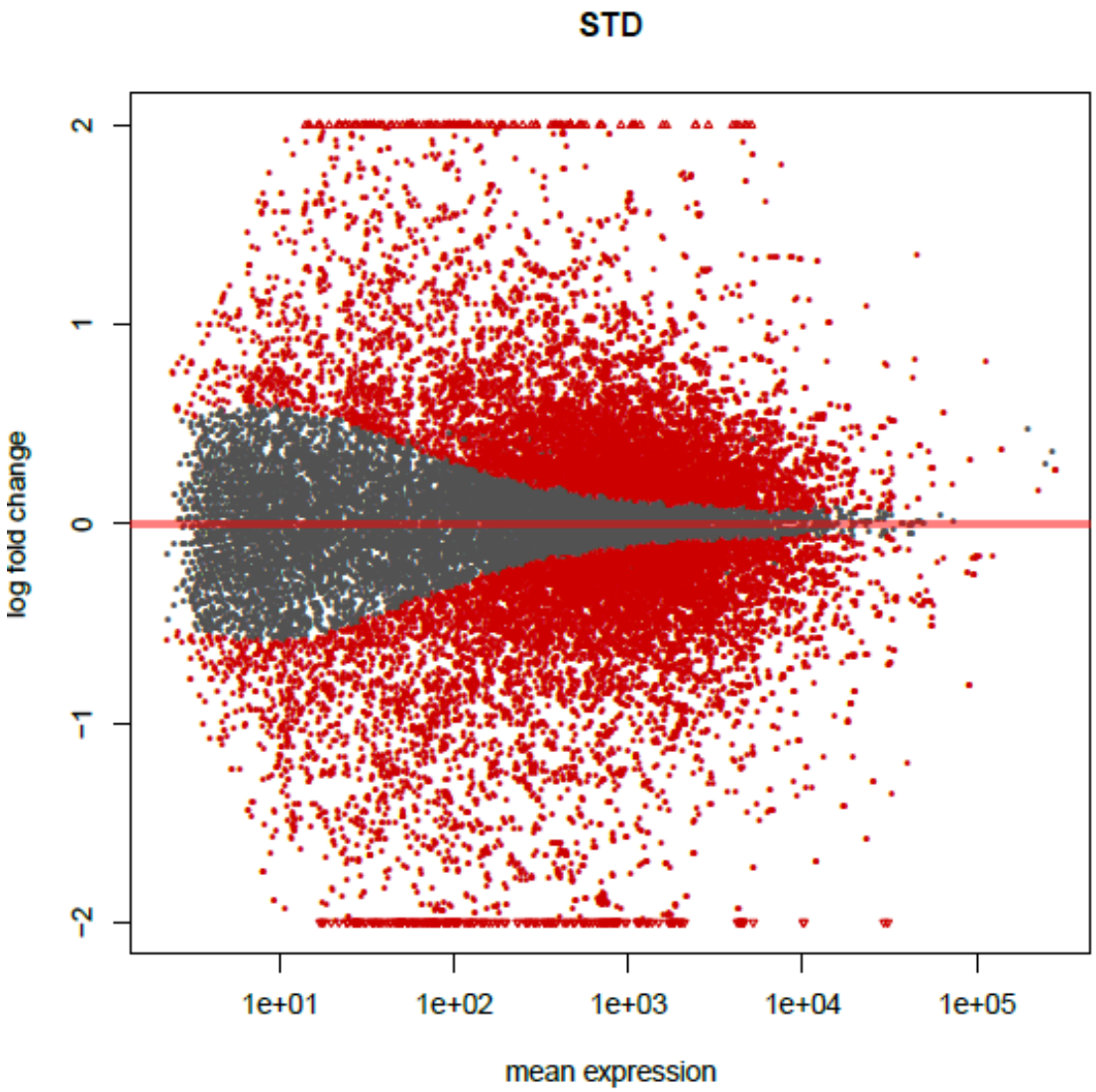

Figure 5.26 MA plot for X17 versus H14 DMSO. Grey represents genes with non-significant differential expression, red represents genes with significant differential expression using the adjusted P-values.

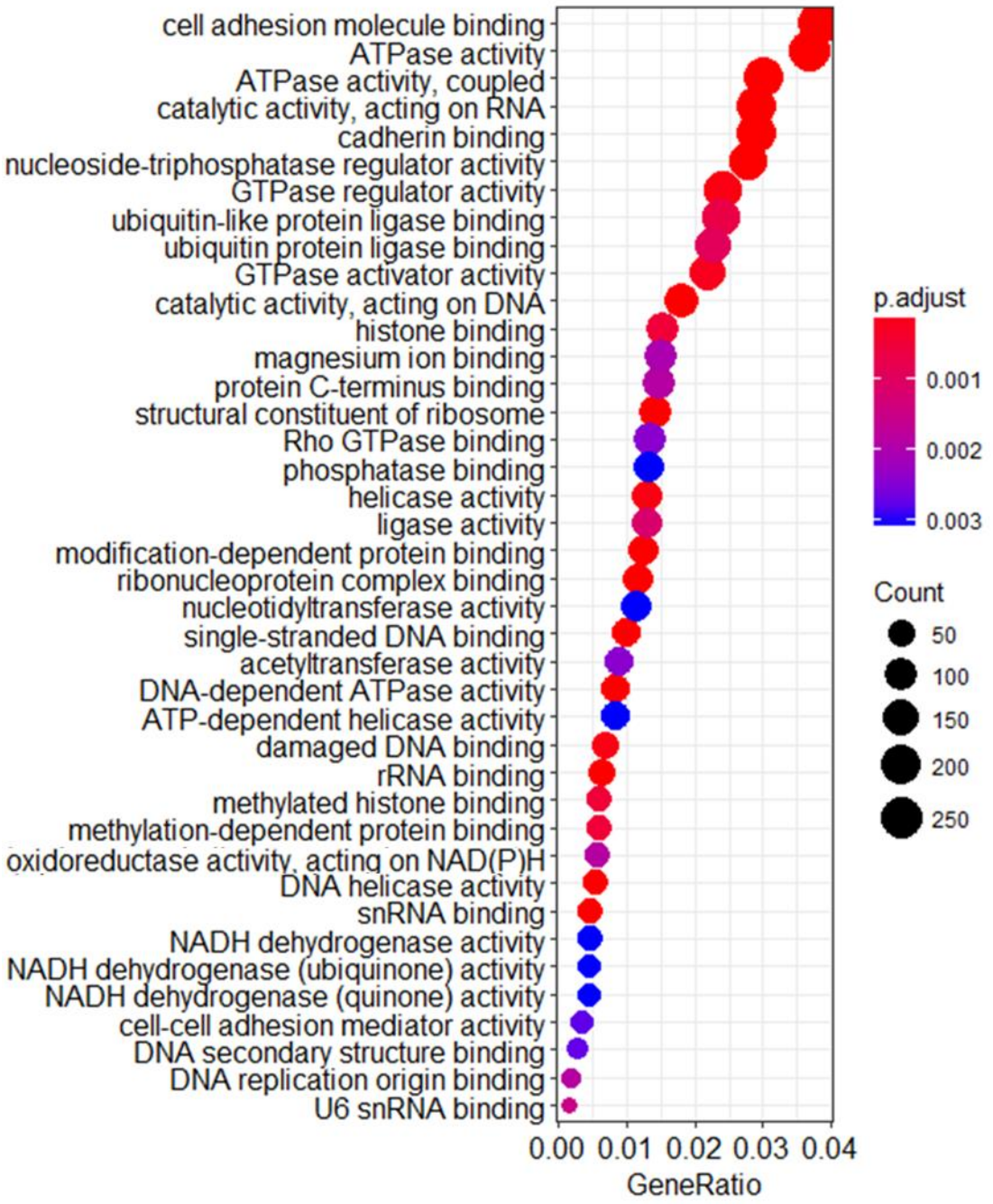

Figure 5.27 Top 40 up-regulated gene ontology enrichment in H14 clone compared to X17 with DMSO treatment. GeneRatio = ratio between the number of differentially expressed genes in the pathway and the number of differentially expressed genes. Count = the number of genes in the pathway. Gradient red to blue shows adjusted p value with decreasing significance.

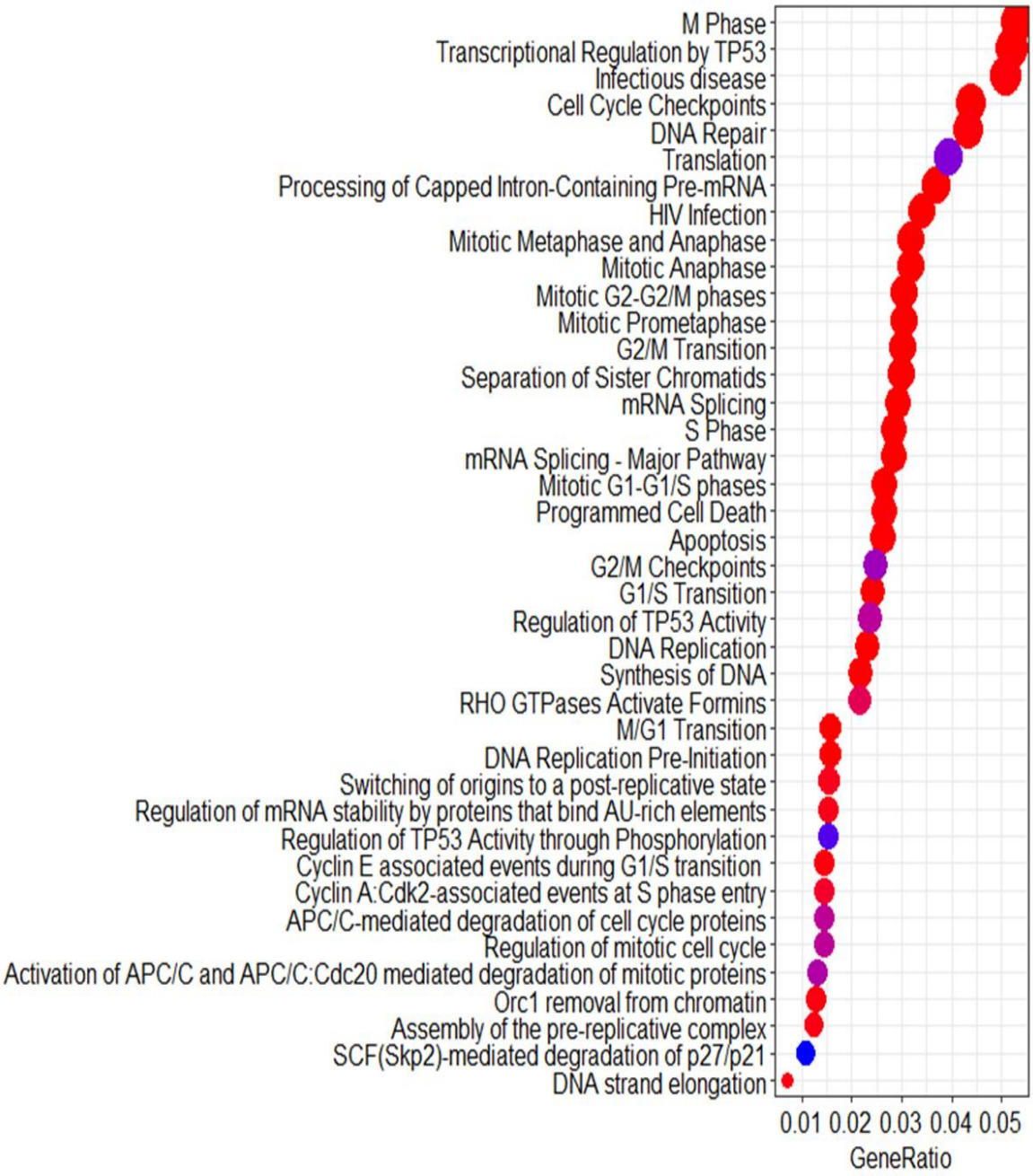

Figure 5.28 Top 40 up-regulated KEGG pathway enrichment in H14 clone compared to X17 with DMSO treatment. GeneRatio = ratio between the number of differentially expressed genes in the pathway and the number of differentially expressed genes. Count = the number of genes in the pathway. Gradient red to blue shows adjusted p value with decreasing significance.

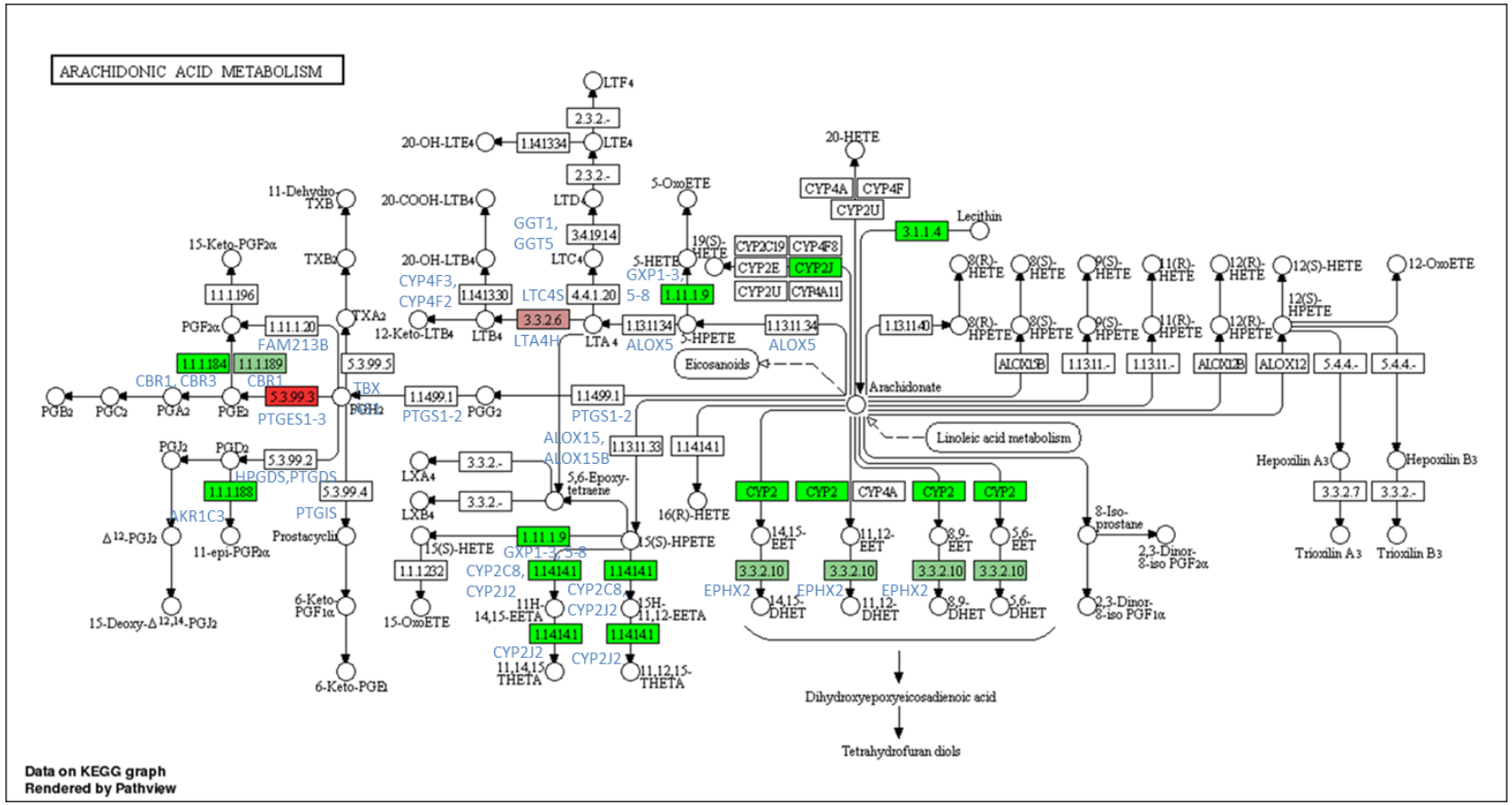

Figure 5.29 KEGG arachidonic acid metabolism pathway analysis comparing differentially expressed genes in DMSO-treated clones X17 and H14. Green = up-regulated, red = down-regulated in H14 compared to X17. Names based on enzyme number. Genes associated with the EC numbers are annotated in blue below or to the left.

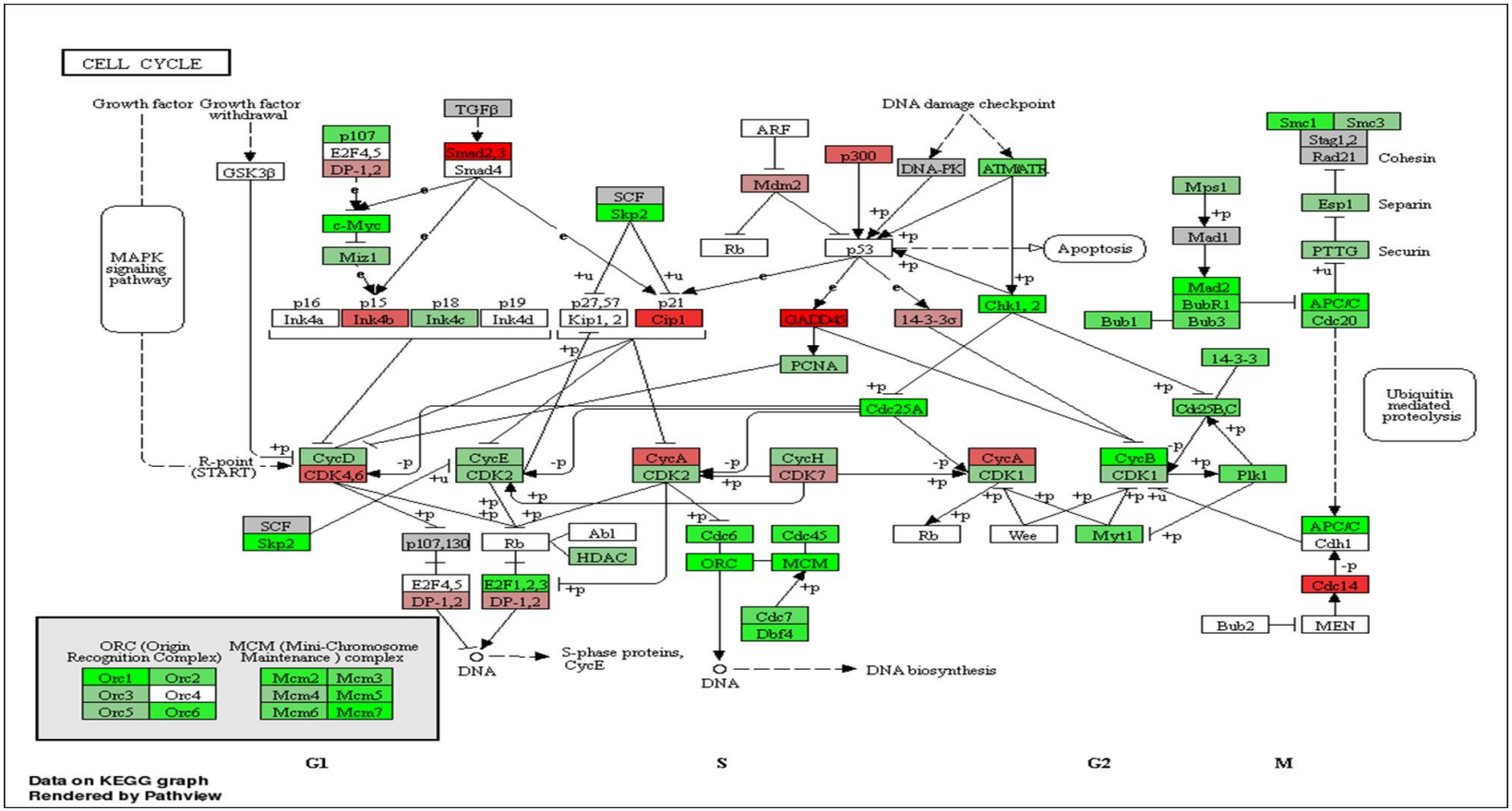

Figure 5.30 KEGG cell cycle pathway analysis comparing differentially expressed genes in DMSO-treated clones X17 and H14. Green = up-regulated, red = down-regulated in H14 compared to X17.

The main genes in the breast cancer pathway (hsa05224) are down-regulated when comparing the X17 and H14 clone, but this is not consistent in the MCF7 and H14 comparison (Figure 5.31 and Appendix 20).

PGE_2 treatment resulted in differential expression of many genes in the KEGG pathways of cancer (hsa05200) gene set when comparing in the X17 clone (Figure 5.32). Whereas the H14 clone showed limited change in gene expression (Figure 5.33).

Changes in the expression of prostaglandin pathway components between the clones and DMSO (control) and PGE_2 exposure was assessed (Table 5.4). Cut offs of 1.5-fold increase and 0.8-fold decrease were selected. *HPGD* was up-regulated 14-fold in the X17 clone and 835-fold in H14, compared to the MCF7 parent cell line. These were increased to 14.3-fold and 1253-fold in the presence of PGE_2 in the X17 and H14 clone respectively.

Significant down-regulation of prostaglandin receptors EP2 and EP3 (*PTGER2*, *PTGER3*), were observed in the H14 clone compared to the MCF7 parent cell line. Although this result was not significant between the X17 and H14 clone. Furthermore, significant down-regulation of EP4 (*PTGER4*) was observed in the H14 clone compared to the X17 clone, yet no significant change was observed between the MCF7 and H14 samples. PGE_2 exposure had little effect on prostaglandin receptor expression when comparing the H14 clone to the MCF7 and X17 samples.

Significant down-regulation of microsomal prostaglandin E synthase (*PTGES*) was observed in the H14 clone compared to both X17 and MCF7 samples, also seen in Figure 5.29 (EC 5.3.99.3). A similar fold change was observed between the DMSO- and PGE_2-treated samples in the H14 clone. The fold change observed for the cytosolic prostaglandin E synthases (*PTGES2* and *PTGES3*) were small (below 1.5-fold cut off) when comparing the X17 and H14 clones, but m-PGES3 was up-regulated in the H14 clone and with PGE_2 treatment surpassed the 1.5-fold cut off.

No significant fold change (>1.5 fold change) in COX1 or COX2 transcripts were detected in any of the pair-wise comparisons. Additionally, the MRP4 transporter was significantly down-regulated in the H14 clone compared to the MCF7 cells with DMSO treatment and compared to X17 clone with PGE_2 treatment, yet this observation as not consistent between treatments.

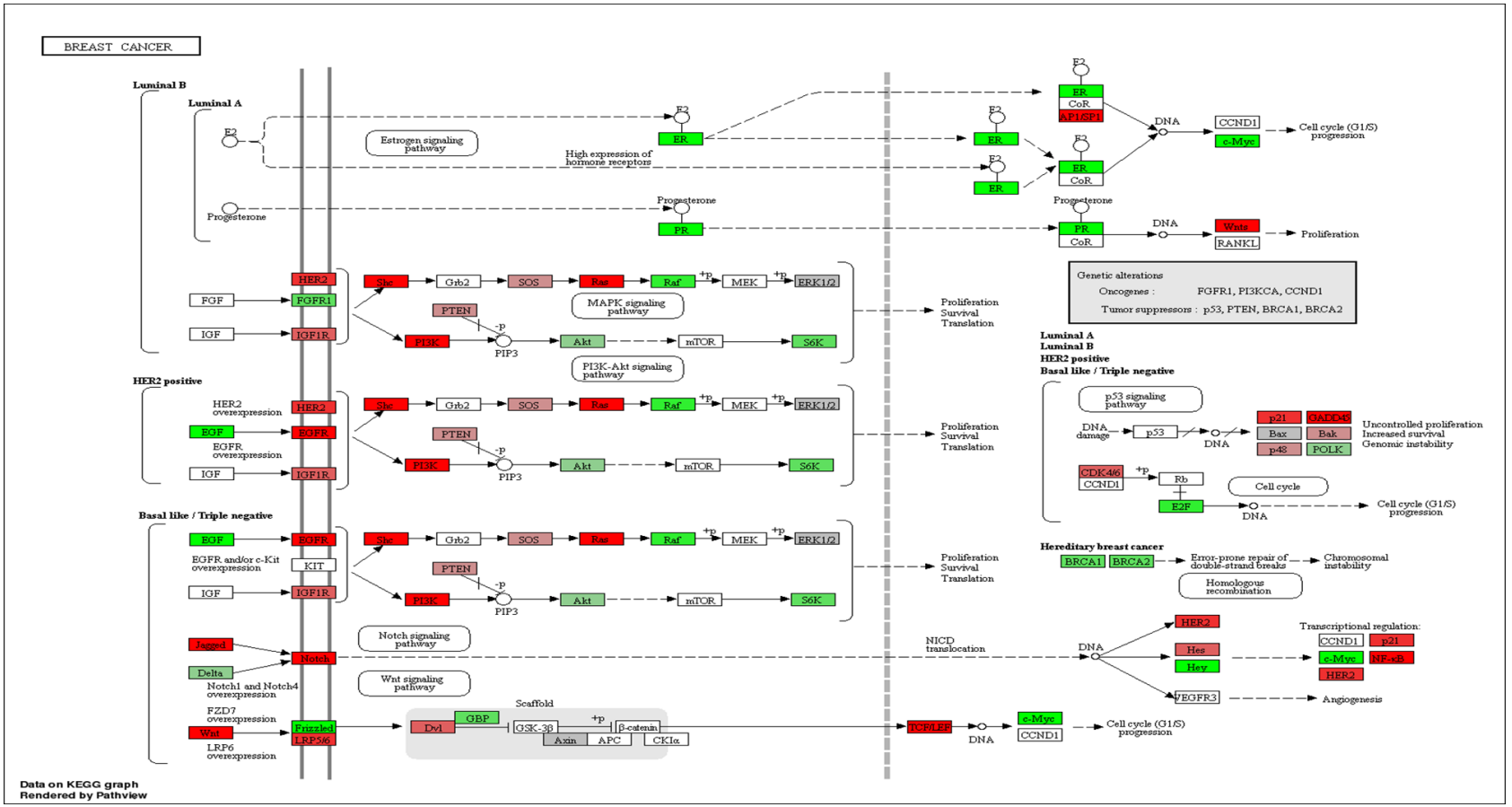

Figure 5.31 KEGG breast cancer pathway analysis comparing differentially expressed genes in DMSO-treated clones X17 and H14. Green = up-regulated, red = down-regulated in H14 compared to X17.

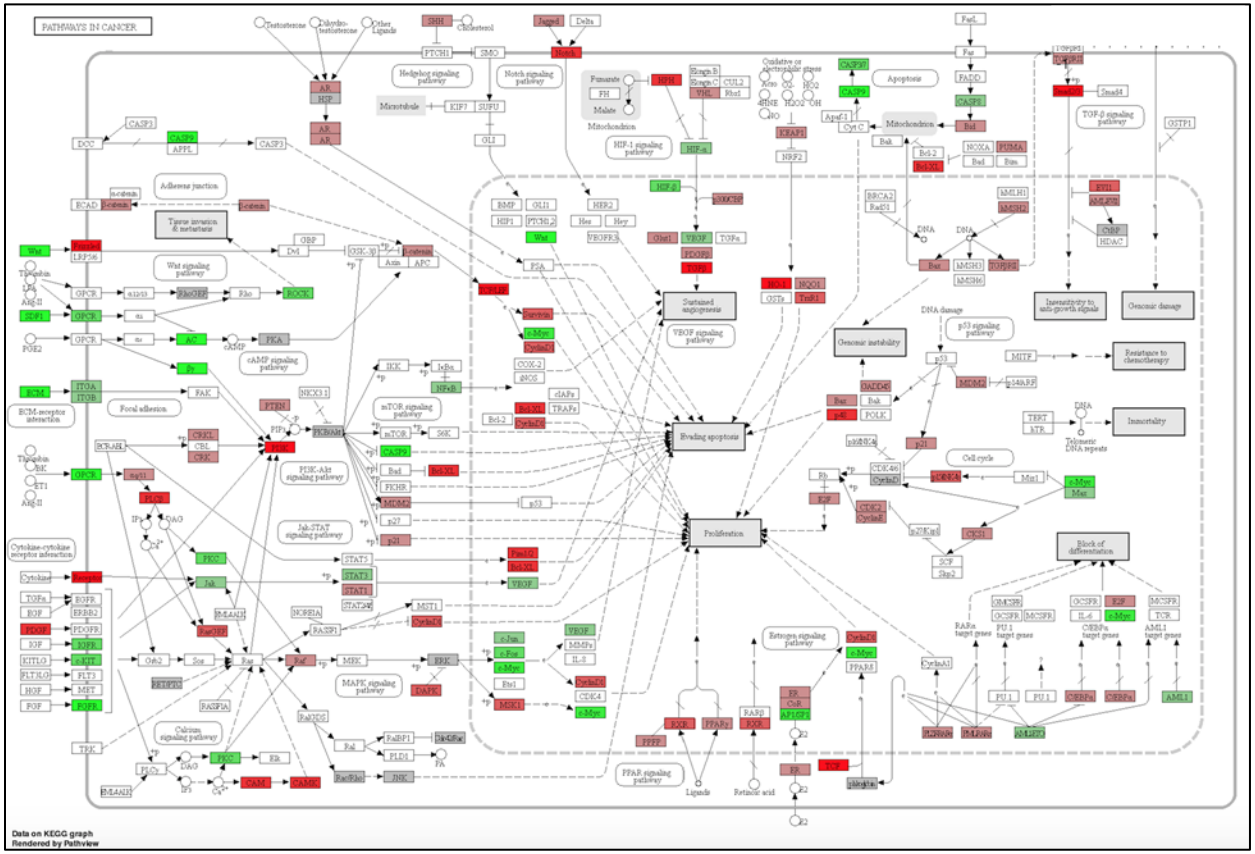

Figure 5.32 KEGG pathways in cancer analysis comparing differentially expressed genes in clone X17 with DMSO and PGE_2 treatment. Green = up-regulated, red = down-regulated in clone X17 with PGE_2 treatment compared to the DMSO control.

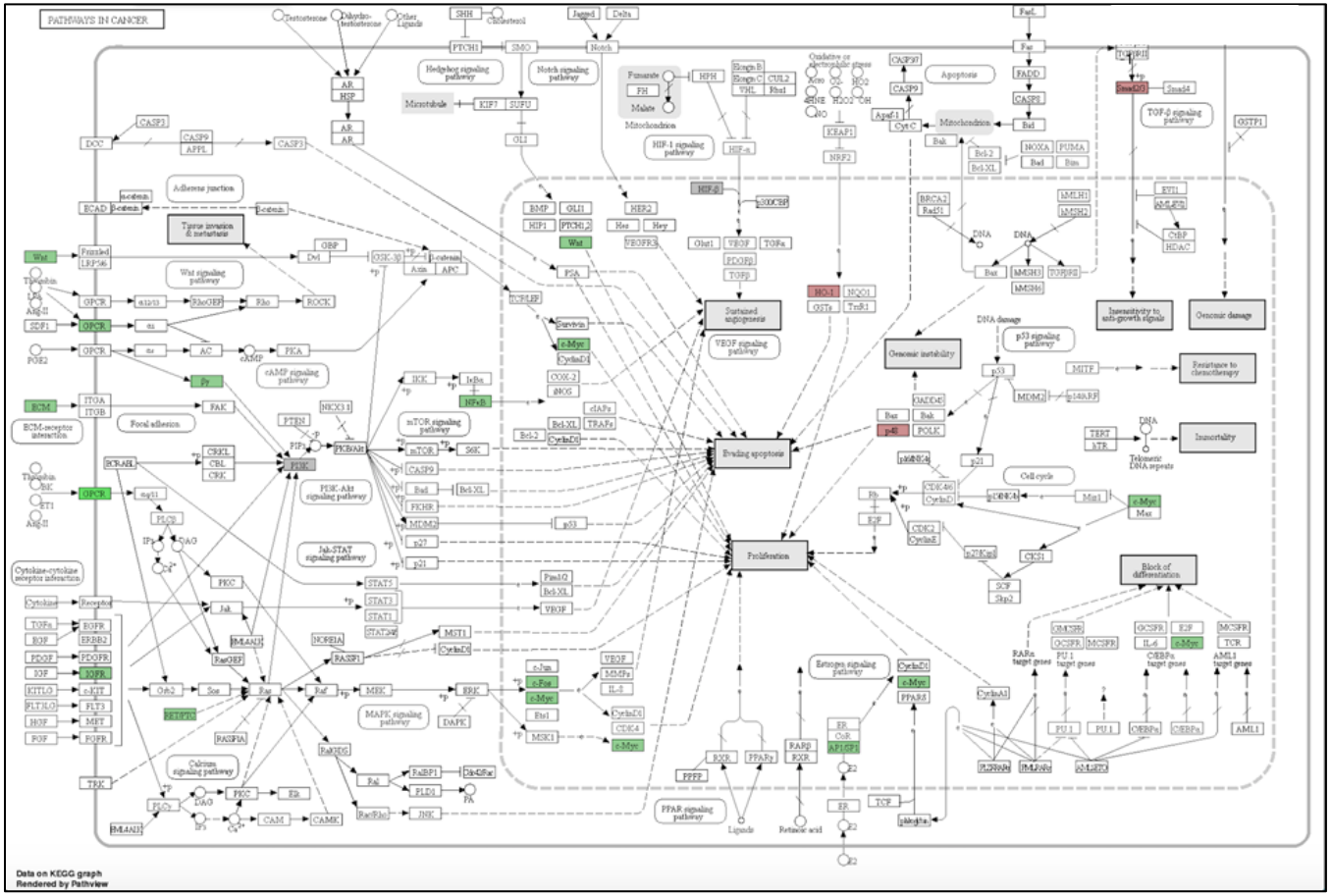

Figure 5.33 KEGG pathways in cancer analysis comparing differentially expressed genes in clone H14 with DMSO and PGE_2 treatment. Green = Up-regulated, red = down-regulated in clone H14 with PGE_2 treatment.

Table 5.4 RNA sequencing fold change in prostaglandin pathway components.

Green = significant > 1.5 fold increased expression. Red = significant < 0.8 fold decreased expression. Blue = not significant but in cut off. Yellow = significant but not in cut off. N/A indicates transcripts not detected in the samples or no significant differential expression.

ABCC4 = multidrug resistance binding protein 4 (MRP4), *HPGD* = 15-PGDH, *PTGER1-4* = prostaglandin E2 receptor 1-4 (EP1-4), *PTGES* = prostaglandin E synthase, *PTGES2* = prostaglandin E synthase 2, *PTGES3* = prostaglandin E synthase 3, *PTGS* = cyclo-oxygenase 1 (COX1), *PTGS2* = cyclo-oxygenase 2 (COX2), *SLCO2A1* = prostaglandin transporter.

	Fold change								
Baseline	MCF7 DMSO	X17 DMSO	H14 DMSO	MCF7 DMSO	MCF7 PGE_2	MCF7 DMSO	MCF7 PGE_2	X17 DMSO	X17 PGE_2
Comparison	MCF7 PGE_2	X17 PGE_2	H14 PGE_2	X17 DMSO	X17 PGE_2	H14 DMSO	H14 PGE_2	H14 DMSO	H14 PGE_2
ABCC4	1.153	1.569	1.131	0.800	1.131	0.780	0.819	1.100	0.757
HPGD	0.995	1.079	1.399	14.006	14.285	835.164	1253.00	668.671	923.612
PTGER1	N/A	1.020	N/A	2.258	N/A	N/A	N/A	0.690	0.674
PTGER2	0.974	0.890	0.945	0.754	0.945	0.594	0.468	0.787	0.696
PTGER3	1.004	0.880	0.984	0.725	0.984	0.542	0.498	0.715	0.793
PTGER4	0.944	0.995	1.081	2.250	1.081	0.957	1.201	0.425	0.498
PTGES	1.287	0.912	1.070	1.325	1.071	0.496	0.420	0.375	0.482
PTGES2	0.991	1.100	1.054	0.691	1.046	0.790	0.838	1.132	1.100
PTGES3	0.962	0.960	0.989	0.731	0.989	1.089	1.117	1.464	1.511
PTGS1	0.987	1.172	1.009	0.849	1.009	0.965	1.442	N/A	0.808
PTGS2	N/A	N/A	N/A	N/A	N/A	N/A	N/A	N/A	N/A
SLCO2A1	0.954	0.801	0.990	1.014	0.990	0.433	0.455	0.456	0.557

On the other hand, the PGT (*SLCO2A1*) transcriptional expression was significantly down-regulated in the H14 clone compared to the MCF7 and X17 samples. PGE_2 addition did not alter the fold change overall.

Transcript expression of epithelial and mesenchymal markers was assessed in the MCF7, X17 and H14 RNA sequencing data (Table 5.5). A significant decrease in vimentin expression, a mesenchymal marker, was observed in the H14 clone compared to both MCF7 and X17 samples with DMSO and PGE_2 treatment. Additionally, down-regulation of mesenchymal marker fibronectin was observed in the H14 clone compared to the X17 clone. Conversely, up-regulation of fibronectin was observed in the H14 clone compared to the MCF7 parent cell line.

Slight up-regulation of E-cadherin was observed in the DMSO treatment of the H14 clone compared to both MCF7 and X17 cells, but this was not the case in the presence of PGE_2. Furthermore, no large change in epithelial marker, E-cadherin, was observed in any of the samples. *SOX9* which inhibits EMT in thyroid cancer cells (Huang, J. and Guo, 2017) was up-regulated in the X17 up to 5-fold and up to 12-fold in the H14 clone compared to the MCF7 parent cell line. *SNAI2* encoding Snail-2 induces EMT (Mathsyaraja and Ostrowski, 2012) and is significantly reduced in the H14 clone compared to both the X17 clone and MCF7 parent cell line. *XNF503* conversely promotes invasion and metastasis (Shahi et al., 2015) and was up-regulated in the H14 clone.

5.4.4.1 RNA sequencing validation

RT-PCR was performed to validate the RNA sequencing data analysis in the X17 and H14 clones. Five genes were selected from the significantly differential expressed genes that were up-regulated in the H14 clone compared to the MCF7 and X17 samples with DMSO treatment (Table 5.6). *PCDH7,* which encodes protocadherin-7, is downregulated in the X17 control compared to the MCF7 parent cell line, and was found to be up-regulated by 25-fold in the clone H14 compared to X17. Protocadherin-7 is part of the cadherin superfamily associated with cell-cell adhesion. *FMOD* encodes fibromodulin, which is associated with collagen fibre assembly.

Glutathione S-transferase A1 (*GSTA1*) mentioned earlier is linked to detoxification, and *SERPINA4* encodes the kallistatin protein. All of which were up-regulated 4-fold in the H14 clone compared to the X17 and MCF7 samples. RT-PCR showed that *PCDH7* was up-regulated in the 15-PGDH over-expressing clone in four out of the five sets of clones including clone H14 (Figure 5.34).

Table 5.5 RNA sequencing fold change in epithelial and mesenchymal markers.

Green = significant > 1.5 fold increased expression. Red = significant < 0.8 fold decreased expression. Blue = not significant but in cut off. Yellow = significant but not in cut off. *VIM* = vimentin, *FN1* = fibronectin, *CHD2* = N-cadherin, *CDH1* = E-cadherin. E-cadherin is an epithelial marker. Vimentin, fibronectin and N-cadherin are mesenchymal markers. The remaining genes are transcription factors associated with EMT (Lamouille et al., 2014).

	Fold change								
Baseline	MCF7 DMSO	X17 DMSO	H14 DMSO	MCF7 DMSO	MCF7 PGE_2	MCF7 DMSO	MCF7 PGE_2	X17 DMSO	X17 PGE_2
Comparison	MCF7 PGE_2	X17 PGE_2	H14 PGE_2	X17 DMSO	X17 PGE_2	H14 DMSO	H14 PGE_2	H14 DMSO	H14 PGE_2
VIM	1.066	0.874	1.003	1.144	1.003	0.391	0.351	0.350	0.413
FN1	1.576	1.624	1.234	1.739	1.234	1.599	1.259	0.908	0.709
CDH2	1.009	1.036	0.988	0.876	0.987	1.264	1.039	1.344	1.111
CDH1	1.057	0.974	1.007	1.131	1.007	1.152	1.095	1.008	1.048
SNAI1	1.007	1.322	0.983	1.471	0.983	1.535	1.411	1.039	0.708
SNAI2	0.955	1.159	1.035	0.681	1.035	0.359	0.531	0.549	0.575
ZEB1	1.041	1.234	1.022	1.297	1.022	1.510	1.434	1.166	0.941
FOXD3	1.008	N/A	N/A	0.985	N/A	0.496	0.593	0.594	0.713
FOXF1	1.004	0.946	1.014	0.747	1.014	0.506	0.689	0.726	1.066
FOXQ1	N/A	N/A	N/A	N/A	N/A	N/A	N/A	0.722	0.539
FOXO3	0.914	0.963	0.959	1.730	0.958	1.543	1.614	0.883	0.878
FOXA1	1.109	1.239	1.012	1.453	1.012	1.443	1.312	0.982	0.806
GATA4	1.007	N/A	1.014	N/A	1.014	N/A	1.081	N/A	N/A
GATA6	0.943	0.822	0.966	2.591	0.966	0.903	0.918	0.348	0.404
SOX9	0.967	1.341	1.031	5.489	1.031	10.542	12.233	1.919	1.476
KLF8	0.903	0.744	0.983	2.202	0.991	2.177	2.648	0.999	1.357
ZNF703	0.913	0.857	1.017	1.054	1.017	1.642	1.838	1.538	1.844

Table 5.6 Genes selected for RNA sequencing validation

The fold change with a dark grey background shows those not significant. N/A indicates no data was found due to no transcripts in one of the data sets.

	Fold change		
Baseline	MCF7 DMSO	MCF7 DMSO	X17 DMSO
Comparison	X17 DMSO	H14 DMSO	H14 DMSO
FMOD	NA	5.924	6.419
GSTA1	0.917	4.858	4.206
KLHL4	NA	3.233	3.792
PCDH7	0.191	4.787	25.607
SERPINA4	NA	4.251	3.034

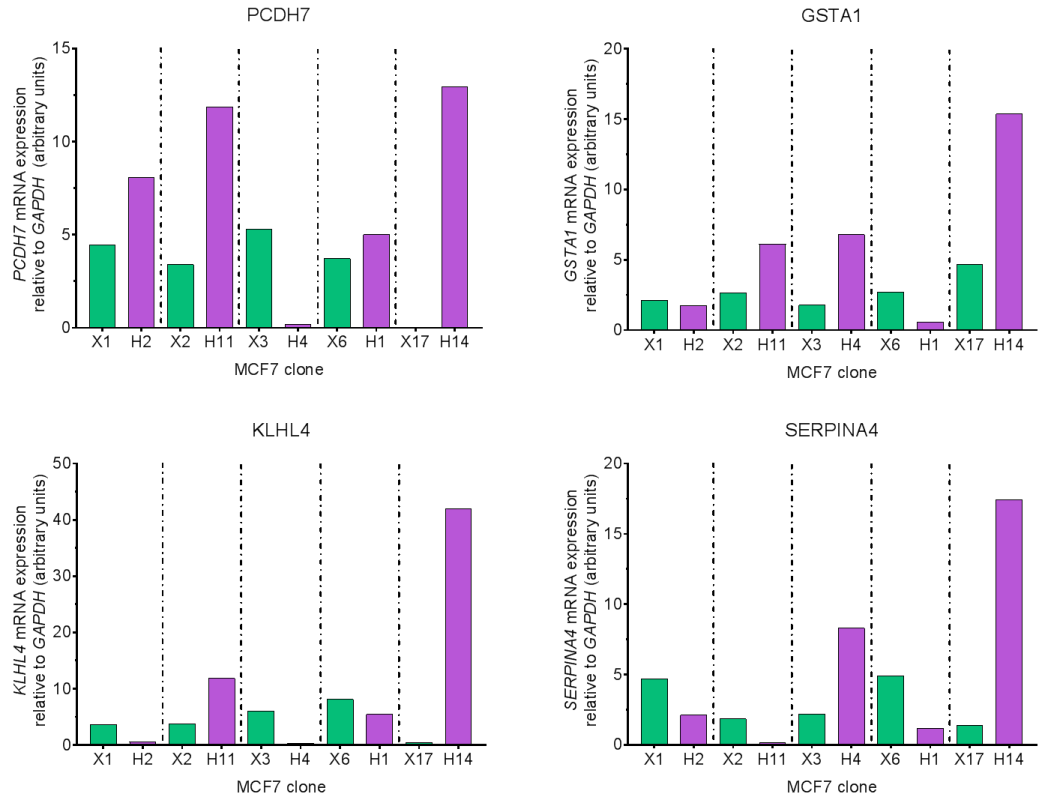

Figure 5.34 RT-PCR validation of RNA sequencing data. Conventional RT-PCR with genes over-expressed in the H14 clone compared to the MCF7 parent cell line and X17 clone. Samples normalised to *GAPDH* control. Green = control clone, purple = 15-PGDH over-expressing clone.

No bands were seen with the *FMOD* primers in the MCF7 clones (data not shown), despite up-regulation of the transcript in clone H14. Up-regulation of *GSTA1* and was observed in three clones sets and *SERPINA4* and KLHL were up-regulated in two of the clone sets.

As up-regulation of protocadherin-7 was most consistent at the transcriptional level in the 15-PGDH over-expressing clones, protein expression was assessed in the clones by Western blot. Optimisation of the antibody was completed with two different antibody concentrations (Figure 5.35).

Four isoforms of PCDH7 have been reported in the literature (Zhou, X. et al., 2017), which may account for some of the additional bands. The remaining bands may be PCDH7 degradation products or non-specific protein binding. PCDH7 is predicted to be between 116 kDa and 135 kDa. A faint band just under 150 kDa was observed for the MCF7 parent cell line, whereas two strong bands were observed in the H14 15-PGDH over-expressing clone for both antibody dilutions which are believed to be PCDH7. As 1:2000 gave cleaner bands for PCHD7 it was the dilution taken forward.

A Western blot was performed with all of the MCF7 clones stably over-expressing 15-PGDH and the matched control clones (Figure 5.35 and Figure 5.36). The two bands generated from alternative splicing for PCDH7 were quantified using ImageLab software. PCDH7 bands 1 and 2 were both up-regulated in the H14 clone compared to the X17 control clone, further validating the RNA-Seq data. Furthermore, band 1 was up-regulated in three out of the five clone sets in the 15-PGDH over-expressing clones compared to the matched control. Three out of the five sets were up-regulated when quantifying band 2 and X3 and H4 showed similar levels of expression.

5.5 Discussion

Five over-expressing clones were generated and matched with control clones with similar proliferation rates. The panel of over-expression clones were generated to ensure that the observations in the clones were not due to the position of the inserted genetic information but a direct result of 15-PGDH expression. Furthermore, assessing a panel of 15-PGDH over-expressing clones enabled assessment of the consistency of the data.

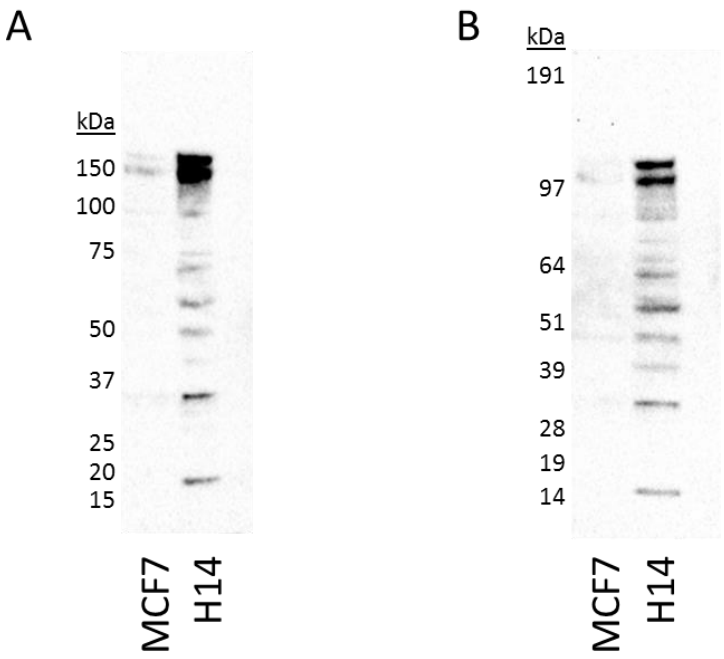

Figure 5.35 Western blot optimisation with PCDH7 antibody. Optimisation of the PCDH7 antibody dilution. PCDH7 = ~116 kDa to 135 kDa. (A) 1:1000 antibody dilution (B) 1:2000 antibody dilution. Exposure time = 5 seconds.

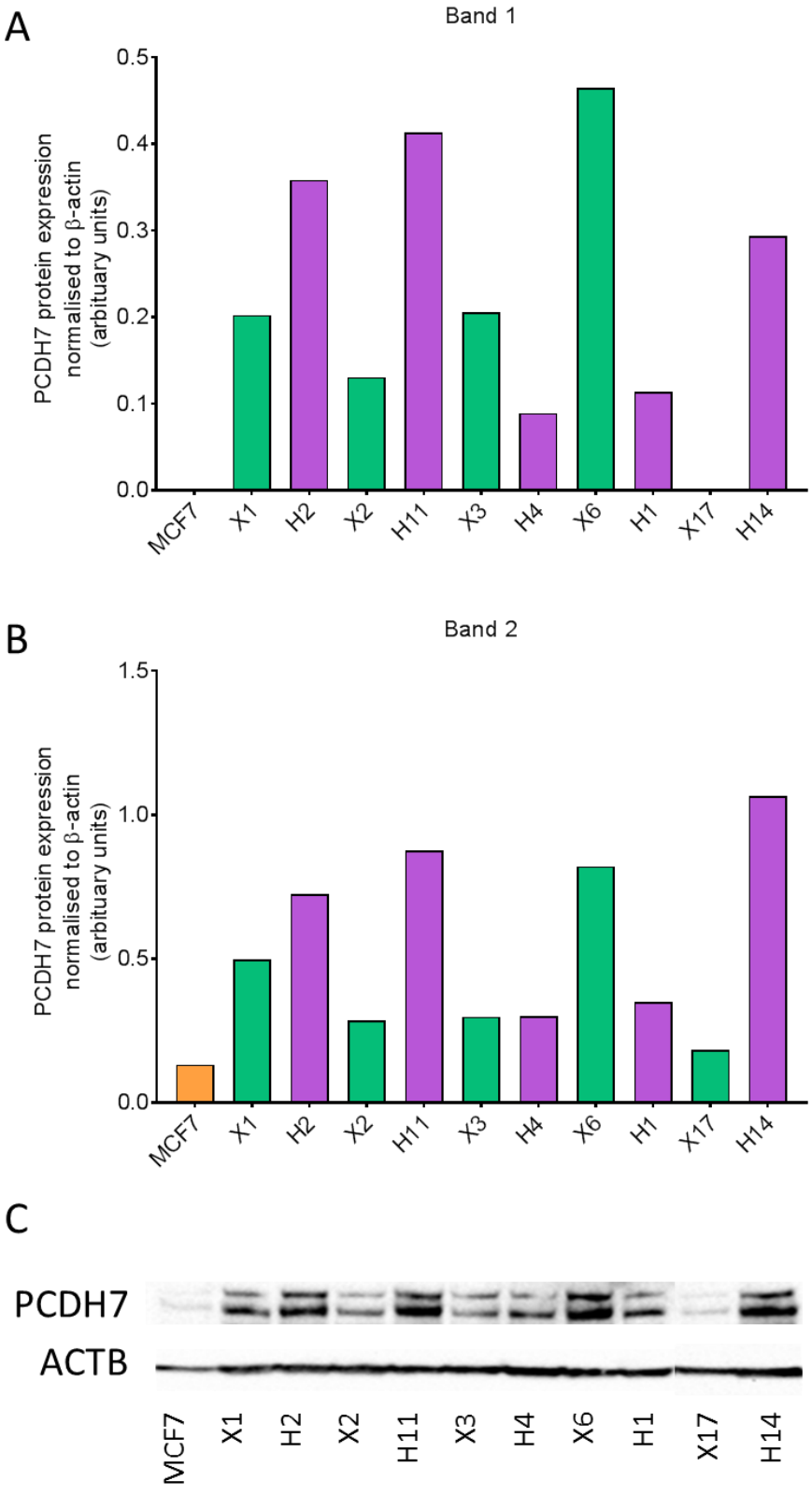

Figure 5.36 Western blot quantification with PCDH7 antibody for MCF7 clones. Green = Control clone, purple = 15-PGDH over-expressing clone, orange = MCF7 parent cells. (A) PCDH7 band 1 quantification (B) PCDH7 band 2 quantification. (C) Western blot PCDH7 and β-actin expression in MCF7 clones. PCDH7 ~132.5 kDa and β-actin ~42 kDa.

Stably transfected clones allowed the study of long term over-expression of 15-PGDH rather than its transient up-regulation. Despite several papers studying over-expression of 15-PGDH, through both transient and stable transfection, only one other known paper using the A549 cell line has looked at a range of clones with varied level of expression (Ding et al., 2005). As 15-PGDH is generally expressed at a low level in breast tissue and even lower in breast cancers and breast cancer derived cell lines derived (Backlund et al., 2005), its over-expression was required to assess its role in breast cancer. The generation of stably transfected clones does however have its limitations.

The presence of geneticin to select for cells in which the trans-genes are inserted in the host genome puts the cells under intense selective pressure. Consequently, an advantage is given to those cells that can grow rapidly in tissue culture at low seeding concentrations. This may generate cell lines significantly different from the parental cell line with a very different biological profile. In addition, the expansion of a single colony to generate sufficient cells to perform functional assays may also influence cell behaviour. The number of cell doublings will be substantially higher than used in normal cell culture work allowing the accumulation of additional genetic alterations, especially when using tumour derived cell lines that can have compromised DNA repair mechanisms. The insertion of the plasmid in to the host genome may also have important consequences through the disruption of gene function and regulation around the site(s) of integration.

HPGD mRNA and 15-PGDH protein expression in the over-expressing clones varied significantly. Clone H14 showed the largest increase in *HPGD* mRNA with a 1439-fold increase compared to the MCF7 parental cell line. In comparison, the H11 clone showed a 52-fold increase. This wide range of expression suggests that the vector may have inserted into the host genome multiple times at one or more loci in clone H14. Despite the large variation in expression, the expression level of *HPGD* mRNA was still less than β-actin, as determined by RNA-Seq. Although the clones had different *HPGD* mRNA levels, across the clones the level of mRNA did correlate with protein levels, indicating that altering the level of gene transcription would be reflected in the production of functional protein.

The effect of PGE_2, a 15-PGDH substrate, on the MCF7 stably over expressing clones was assessed to determine whether the functional effects of 15-PGDH expression were increased in response to increased substrate. The suggested normal range of PGE_2 in human serum is 18–200 pg/ml (Busch et al., 2012; Sasaki, T. et al., 2012; Malachi et al., 1981), which equates to 0.05-0.57 nM PGE_2. Average plasma levels in control patients, and patients with benign or

malignant breast tumours were 34.4 pg/ml, 59.9 pg/ml and 62.3 pg/ml respectively (Malachi et al., 1981). Nevertheless, higher plasma levels have been reported in colon cancer at 1000 pg/ml (Narisawa et al., 1990). Furthermore, the K_d of PGE_2 for the receptor is 1-40 nM (Sugimoto and Narumiya, 2007). For experimental purposes 1 μM (3.52 $x10^5$ pg/ml) was selected for most experiments to ensure maximum effect and saturation of the receptors, whist showing minimal toxicity.

The oncogenic effects of PGE_2 are the result of downstream signalling in response to binding to the EP receptors. Expression of the EP receptors was not accessed by RT-PCR in this study, yet the RNA-Seq data shows that mRNA transcripts for EP2, EP3 and EP4 are present in the MCF7 cell line. mRNA expression of all four EP receptors have also been demonstrated in the literature (Timoshenko et al., 2003). The Protein Atlas suggests that there is little to no mRNA expression of the EP receptors in the MCF7 cell line, as well as SKBR3 and A549 cells, compared to other cell lines (Uhlen et al., 2017). As the MCF7 cell line has no COX2 expression and produces very little PGE_2 itself (Kochel et al., 2017) there may be no need for EP receptor expression and thus limited effect of PGE_2 treatment. The A549 lung cell line does however produce PGE_2 regardless of the low EP receptor mRNA expression (Takai et al., 2013). As PGE_2 can act in an autocrine and paracrine manner, PGE_2 produced in the tumours microenvironment may influence cancer cell behaviour, therefore the effect of exogenous PGE_2 on the MCF7 cell line is still of concern. Interestingly, protein expression of EP4 has been demonstrated in the MCF7 cell line despite the low levels of the mRNA transcript suggested in the Protein Atlas (Kochel et al., 2017). This may be the result of a much shorter half-life for the mRNA transcript in comparison to the protein and may also be the case for the other EP receptors. Future work assessing the protein expression of the prostaglandin pathway components in the MCF7 cell line would therefore be important to help determine if PGE_2 is binding to EP receptors and thus altering cellular signalling. This would facilitate understanding the MCF7 cell lines response to exogenous PGE_2 treatment.

The rate of proliferation of the ten selected stable clones did not correlate with 15-PGDH expression. A significant decrease in proliferation was observed at several PGE_2 concentrations in both the control and 15-PGDH over-expressing clones compared to the untreated samples. Despite this, there was no significant difference in proliferation between the 15-PGDH over-expressing and control clones. This suggests that 15-PGDH does not alter the rate of proliferation in the MCF7 cell line. While PGE_2 is often described as enhancing cellular proliferation (Nakanishi, M. and Rosenberg, 2013) this was not demonstrated here, suggesting

the effect may be cell line specific. Similar observations to this study have been reported with MCF7 cells after 24 and 48 hours' incubation with 10 µM PGE_2 using the MTT assay (Bronger et al., 2012). No change in proliferation was also reported in gastrointestinal cells over-expressing 15-PGDH after 9 days of culture, yet a significant decrease in tumour formation was seen when the cells were injected into athymic mice (Yan et al., 2004). This observation was attributed to the fact that the tumour promoting effect of increased prostaglandin synthesis is primarily the result of increased tumour angiogenesis (Yan et al., 2004). Decreased proliferation was only observed after 4 days of culture in 15-PGDH over-expressing murine forestomach carcinoma (MFC) cancer cells and 7 days with a gastric cell line (Li, L. et al., 2014; Liu, Z. et al., 2010), therefore performing the assay over a longer time course may result in a decreased rate of proliferation *in vitro*. Decreased tumour size and formation with 15-PGDH over-expression *in vivo* has been observed in carcinoma, gastric, breast and colorectal cell xenographs (Kaliberova et al., 2009; Castro-Sanchez et al., 2013; Liu, Z. et al., 2010; Yan et al., 2004). It would therefore be interesting to see whether increasing the time course *in vitro* and assessing the MCF7 clones stably over-expressing 15-PGDH *in vivo* would result in decreased proliferation and tumour formation.

Cytotoxicity with higher doses of PGE_2 (5-10 µM) has also been reported in microglial cells after 24 hours (He, G.L. et al., 2016). Increased toxicity with PGE_2 treatment was observed in the cells treated with media containing 1% FCS compared to 10% FCS. Although many studies serum starve cells in order to synchronise the cell cycle, research suggests that serum starvation also causes environmental stress and induces apoptosis (Pirkmajer and Chibalin, 2011). The cells treated with 1% FCS may therefore be under additional stress resulting in increased toxic effect of PGE_2.

Adenoviral mediated 15-PGDH expression decreased migration of breast and colorectal cancer established cell lines and human umbilical vein endothelial cells (HUVEC) using a transwell assay (Kaliberova et al., 2009). The assay was performed over five days, therefore proliferation may have been an influencing factor in the results. No difference was observed between the two 15-PGDH over-expressing MCF7 clones and their matched control clones after 48 hours with the 3D transwell migration assay in this project. When combining all of the five sets of clones the results were statistically significant in the 2D wound healing assay after 48 hours. Increased migration was observed in the MCF7 cell line following 15-PGDH silencing (Wu, R. et al., 2017), which confirms the wound healing data. In addition, there was a non-statistically significant

trend that exogenous PGE_2 further increased migration in the wound healing assay, for control clones and possibly to a higher degree in the over-expressing clones.

The transwell migration assay requires chemotaxis, which involves a range of complex processes including cell motility, polarity and directional sensing (Decaestecker et al., 2007). Furthermore the cells also have to pass through a physical barrier, therefore mimicking the effects of migration in response to the cellular environment. In contrast, the wound healing assay requires the cells to repopulate the wound area taking into account migration and proliferation. Although the two assays assess the ability of the clones to migrate, the migration is in response to different stimuli and involves different mechanisms explaining the difference in results of each assay.

15-PGDH expression decreased invasion in the H1 clone compared to the matched control clone (X6), yet this was not statistically significant due to the large standard deviation between repeats. This is most likely due to the low number of cells invading through the Matrigel layer, creating noisy data and displaying a large standard deviation that masked any underlying trend, if present. Furthermore, the same trend was not observed in the H14 over-expressing clone compared to its control. It would be interesting to repeat this with the other clones to see whether the H14 clone is the only clone not following this trend, as observed with the colony forming assay. To overcome the low number of invading cells in the control, it would be valuable to repeat the experiment with a more invasive breast cell line, such as MDA-MB-231 cells. Silencing of 15-PGDH expression also promoted EMT with over-expression decreasing invasion in the A549 lung cell line (Wang, W. et al., 2018). Additionally, It has been reported that EGF decreases 15-PGDH enzymatic activity and expression (Backlund et al., 2005), therefore the clone migration and invasion data in this study may be influenced by the change in 15-PGDH expression.

Increased N-cadherin and fibronectin, together with decreased E-cadherin and β-catenin were reported in an A549 15-PGDH over-expressing cell line, together with a more mesenchymal morphology (Tai et al., 2007). This suggests that 15-PGDH expression in the lung cell line leads to EMT. The data supporting this was not shown however and the group had also reported 15-PGDH has a tumour suppressor role in lung cancer (Ding et al., 2005). The MCF7 breast cell line on the other hand, showed decreased vimentin, a mesenchymal marker, and no large change in E-cadherin expression in the 15-PGDH over-expressing cells. This was further verified by a decrease in *SNAI2* (EMT inducer) and increase in *SOX9* (EMT inhibitor) transcripts. Together this

data suggests that in these cells 15-PGDH could contribute to generate a more epithelial profile that is important in reducing the potential for migration and invasion.

15-PGDH over-expression significantly decreased the ability of MCF7 cells to form colonies in three out of the five clone pairs. One pair do not reach statistical significance and the highest 15-PGDH expressing clone and its matched control (H14 and X17) did not follow the same trend. This may be due to the X17 clone showing a reduced rate of proliferation compared to the H14 clone. Overall there is a significant decreased in colony formation in the 15-PGDH over-expressing clones compared to both the MCF7 parent cell line and control vector clones. Similar observations have been reported in the literature following 15-PGDH silencing in MCF7 cells resulting in increased colony formation (Wu, R. et al., 2017). Up-regulation of 15-PGDH also showed decreased colony formation in gastric carcinoma and murine MFC cells (Li, L. et al., 2014; Liu, Z. et al., 2010). The increase in colony size with PGE_2 treatment has also been observed in colorectal cells at 1 µM and 10 µM concentrations (Young et al., 2013).

RNA sequencing data highlighted that elevated 15-PGDH expression leads to increased expression of genes involved in cell adhesion and cadherin binding. Coincided repression of 15-PGDH and E-cadherin expression was reported in a colorectal cell line with EGF treatment (Mann, J.R. et al., 2006) which supports this observation. Furthermore, genes involved in apoptosis were up-regulated in the 15-PGDH over-expressing clones with increased apoptosis seen in A549 over-expressing cells (Ding et al., 2005). A number of significantly differentially expressed genes identified following the addition of PGE_2 to the X17 clone were not seen following addition of PGE_2 treatment of the H14 clone, suggesting that 15-PGDH is metabolising PGE_2 and therefore inhibiting downstream signaling.

A 25-fold increase in PCDH7 was observed in the H14 clone compared to its matched control clone (X17). Validation of the RNA-Seq data with RT-PCR confirmed that PCDH7 mRNA was up-regulated in four out of the five 15-PGDH over-expressing clone sets including the H14 clone. Western blotting confirmed that only three of the four showed increased PCDH7 at the protein level. Low expression of PCDH7 has been reported in gastric and colorectal carcinoma, moreover down-regulation of PCDH7 in gastric cell lines lead to increased migration and invasion (Chen, H.F. et al., 2017; Bujko et al., 2015). Despite this, an alternative phenomenon has been reported in breast cancer. Knock-down of PCDH7 in the MDA-MB-231 breast cell line increased migration and invasion *in vitro* and *in vivo* (Li, A.M. et al., 2013). Consequently, it would be interesting to see what the effect of PCDH7 up-regulation alone has in the breast MCF7 cell line.

The MCF7 cell line has relatively low PGT expression at a transcriptional level (refer to Chapter 3), therefore PGE_2 is not likely to be actively reabsorbed by the cell where it could be metabolised by 15-PGDH. As a result the major route for absorption of PGE_2 by the cell may be via relatively slow passive diffusion and thus limiting the effect of 15-PGDH over-expression. To counteract this it would be interesting to transfect the cells with the PGT and assess whether 15-PGDH over-expression has a more pronounced functional effect.

In conclusion, 15-PGDH over-expression does not have a significant effect on MCF7 clones proliferation, but does decrease the rate of migration and colony formation. Furthermore, increased cell adhesion and cadherin binding resulting from 15-PGDH downstream signalling may be advantageous in preventing cancer cell migration. This data suggests that 15-PGDH over-expression may be beneficial as a breast cancer treatment. Further research to assess the functional effects of 15-PGDH expression on cancer metastasis formation in *in vivo* models may give rise to important insights into its role in breast cancer progression.

Chapter 6 Discussion

6.1 Introduction

Extensive research has assessed the effect of COX2 expression and PGE_2 production in cancer progression. There is a strong link between induced expression of COX2 and increased proliferation, migration, invasion and angiogenesis in cancer (Lee, E.J. et al., 2007; Tomozawa et al., 2000; Hashemi Goradel et al., 2018; Sobolewski et al., 2010). Development of COX2 inhibitors has shown promising results in cancer treatment, including breast cancer (Regulski et al., 2016; Giercksky, 2001). Due to adverse side effects resulting from COX2 inhibition, recent focus has shifted to the role of PGE_2 metabolising enzyme, 15-PGDH, in cancer progression.

This study aimed to assess the expression of 15-PGDH in breast cancer, determine mechanisms behind the regulation of its expression and the effect of 15-PGDH over-expression in the MCF7 breast cell line.

6.2 Expression of 15-PGDH in breast cancer

The first aim of the project was to determine the expression of 15-PGDH in primary breast cancer. Immunohistochemistry revealed only 3% of primary breast cancer samples exhibited strong expression and 1% intermediate 15-PGDH expression out of 253 samples. As 15-PGDH expression was rare in this cohort of primary breast cancers, 15-PGDH gene expression therapy may be a therapeutic option. No trend was observed between 15-PGDH expression and sample staging, with high expressing samples in all three breast cancer grades. This was also the case at the mRNA level in the TCGA dataset, yet *HPGD* expression was linked to subtype, with high expression in normal breast tissue, intermediate in luminal A and B subtypes and low in basal and HER2 positive samples (Kochel et al., 2016). Due to limited clinical data associated with the TMA samples a link between high 15-PGDH expression and subtype could not be assessed in this dataset.

Published data suggests 15-PGDH is down-regulated in breast cancer compared to normal breast tissue (Backlund et al., 2005; Thill et al., 2010a; Kochel et al., 2016). Conversely, one study suggests it may be up-regulated (Thill et al., 2010b), but this result may be due to their cohort containing an excess of apocrine cancers which are thought to highly express 15-PGDH (Celis et al., 2008), and so creating an erroneous result. In addition to this, the study used the

HPGD2 antibody for IHC, which was found to demonstrate a high level of non-specific staining in this thesis. No 15-PGDH staining was observed in the small number of normal breast tissue samples assayed in this thesis, but assessment in a larger cohort is required to make an accurate conclusion.

Loss of 15-PGDH expression is seen in early colorectal and gastric cancer, but is yet to be reported in breast cancer (Myung et al., 2006; Park et al., 2018; Tseng-Rogenski et al., 2010). This early loss of 15-PGDH may contribute to a poor prognosis, therefore assessing whether this is the case in breast cancer would help determine patient prognosis and influence treatment selection. Future work assessing 15-PGDH expression in a large cohort of early stage breast carcinoma and matched adjacent tissue samples would enable a comprehensive assessment of whether 15-PGDH expression is lost during carcinogenesis. Regardless of whether 15-PGDH expression is lost in breast cancer or 15-PGDH expression is low in the breast in general, induction of 15-PGDH may still be advantageous in reducing migration and invasion of the cancer cells and improving patient prognosis.

15-PGDH is a biomarker of apocrine breast cancer (Celis et al., 2008). In this thesis, two apocrine samples were identified in the six high 15-PGDH expressing patient samples and a further two exhibited apocrine features, which suggests there may be a link between 15-PGDH and apocrine breast cancer. In the Farmer breast data set only one out of six apocrine samples showed high *HPGD* mRNA expression (Kochel et al., 2016). As the Farmer breast data set was based on mRNA data and not protein expression this does not necessarily correspond to protein expression and activity levels. Together with the findings in this thesis, where not all of the samples highly expressing 15-PGDH were apocrine breast cancer, the data suggests that 15-PGDH expression alone may not facilitate accurate identification of apocrine breast carcinoma. Interestingly, other components of the prostaglandin and lipoxygenase pathways have also been identified as apocrine biomarkers. High COX2 and 15-LOX-2 expression have also been described as indicators of apocrine carcinoma (Celis et al., 2006; Celis et al., 2008). Intermediate COX2 expression was observed with the two apocrine samples in this study, agreeing with this observation, but 15-LOX-2 expression was not assessed in this study. This data indicates that the prostaglandin pathway and arachidonic metabolism may have a key role in apocrine breast cancer, but the importance of this role is yet to be determined.

Patients with invasive apocrine breast carcinoma have a significantly lower frequency of lymphatic invasion and axillary node metastasis than those with invasive ductal carcinoma (Tanaka et al., 2008), which is consistent with the *in vitro* metastasis and invasion data with 15-

PGDH over-expression in this thesis. Still, no difference in survival rates was observed between invasive apocrine breast cancer and other invasive ductal carcinomas (Tanaka et al., 2008). Consequently, the anti-carcinogenic effects associated with 15-PGDH expression has no effect on overall survival in this patient group, which may be due to COX2 expression, which is also up-regulated in apocrine carcinoma (Celis et al., 2006). The advantage, if there is one, of high 15-PGDH expression in apocrine breast cancer compared to other breast cancer subgroups is currently unknown. One hypothesis is that 15-PGDH expression is increased in response to COX2 expression to counteract excess prostaglandin production. Hence 15-PGDH expression may be a consequence of COX2 expression in apocrine breast carcinoma, rather than driving apocrine tumour development.

There is no standard treatment for apocrine carcinoma. As the apocrine molecular profile is ER-/PgR-/AR+ with varied HER2 expression, treatment is either consistent with that of TNBC or utilises HER2 targeted therapy. A more targeted therapy for this subgroup is therefore required to improve patient outcome. 15-PGDH expression would not be a suitable target in these patients and its down-regulation would potentially lead to a worse prognosis via increased PGE_2 signalling. Nevertheless, understanding the cause and role of 15-PGDH expression in apocrine carcinoma would help to identify other potential therapeutic targets in these patients.

Studies suggest that 15-PGDH and COX2 are reciprocally regulated in gastric and lung cancer (Tong et al., 2006b; Liu, Z. et al., 2008) although this does not appear to be the case in breast cancer. Intermediate COX2 expression was seen in half of the high 15-PGDH expressing samples and very weak COX2 expression was observed in samples with no epithelial 15-PGDH expression. As COX2 expression was not assessed in any samples negative for epithelial or leukocyte 15-PGDH expression, no comparison can be made. It is possible that 15-PGDH is up-regulated in response to COX2 expression in some cases and could be confirmed by assessing the effect of COX2 up-regulation on 15-PGDH expression in breast cancer both *in vitro* and *in vivo*. Furthermore, assessing a larger patient tumour cohort for COX2 and 15-PGDH expression would improve the statistical power of any correlation identified between their expression.

The identity of isolated cells in tumour samples that expressed high levels of 15-PGDH was not confirmed, but are most likely leukocytes consisting of macrophages, B cells and T cells. While they have been reported once before in the literature in the context of abdominal aortic aneurysm (Sola-Villa et al., 2015), they have yet to be reported in cancer. The interaction of various cell types found in breast tumours, such as fibroblasts, macrophages, epithelial cells, T and B cells, may all play a role in the tumours prostaglandin microenvironment. The tumours

progression may be the result of a poorly understood, complex interaction of different cell types producing, degrading and responding to various prostaglandins. Tumour associated macrophages are known to drive breast cancer development (Mahmoud et al., 2012), therefore future work should determine whether this is the case with the over-expressing 15-PGDH isolated cells, or whether they have a protective phenotype as suggested by the *in vitro* experiments. This raises the possibility that treatment may be directed at modulating 15-PGDH activity in normal cells associated with a tumour rather than the cancerous cells themselves.

A study has shown that co-culture of several breast cancer cell lines, including the MCF7 and MDA-MB-231 cell lines, with polarised THP-1 monocytes (M1 and M2 macrophages) increased migration in ER positive cell lines and mammosphere formation (Ward et al., 2015). In this thesis RT-PCR with polarised THP-1 cells did not show 15-PGDH expression, therefore an alternative model would be required to assess whether leukocytes expressing 15-PGDH have a protective effect *in vitro*. Alternatively, if increased 15-PGDH expression is a response to the tumour microenvironment, assessing 15-PGDH expression in macrophages co-cultured with PGE_2 producing cells may help to elucidate this interaction. Furthermore, comparing macrophage co-culture data with a normal breast cell line expressing all the components of the prostaglandin pathway and those exhibiting genetic defects in parts of the pathway would allow an enhanced assessment of 15-PGDH expression in macrophages infiltrating a tumour.

The presence of 15-PGDH expressing isolated cells had no significant effect on metastasis or cancer related death in patients present in the small cohort assessed in this thesis. Interestingly, when mice with targeted 15-PGDH expression in the liver were treated with LPS, a reduced number of infiltrating macrophages were observed compared to the control (Yao et al., 2017). It would therefore be interesting to assess the number of macrophages in all of the samples and determine whether those with isolated cell 15-PGDH expression contain as many infiltrating macrophages as those that do not expression 15-PGDH.

In summary, 15-PGDH expression is often low in both normal and cancerous breast tissue, with the exception of the apocrine subgroup. Consequently, up-regulation of 15-PGDH or exogenous 15-PGDH is a possible approach to treating most types of breast cancer. Furthermore, the novel observation of 15-PGDH expression in isolated cells in breast cancer may suggest that not all tumour associated macrophages are associated with poor prognosis and warrants further investigation.

6.3 Regulation of 15-PGDH in breast cancer

In order to exploit the low levels of 15-PGDH expression in breast cancer as a potential therapy, it would be valuable to understand the factors regulating 15-PGDH in breast cancer. The second purpose of this thesis was therefore to elucidate the mechanisms involved in 15-PGDH regulation in breast cancer, with focus on epigenetic and transcriptional regulation.

Treatment of breast cell lines with demethylating agent, decitabine, increased 15-PGDH mRNA and protein expression up to 5-fold in MDA-MB-231 cells *in vitro*. Given that 15-PGDH expression is low in breast cancer, a 5-fold up-regulation would still result in a lower level of expression compared to the lung positive control, therefore the physiological effect of this up-regulation is unclear. Measuring PGE_2 levels in decitabine-treated cells or quantifying the production of its metabolite (PGE-M) from exogenous PGE_2 would enable further assessment. Low endogenous PGE_2 production has been reported in both MCF7 and MDA-MB-231 cells compared to MDA-MB-436 and BT549 breast cells under standard culture conditions (Kochel et al., 2017). The addition of exogenous PGE_2 may therefore enable a more accurate assessment of decitabine induced 15-PGDH expression on prostaglandin metabolism.

Pyrosequencing and bisulphite sequencing showed no change in methylation status at the *HPGD* gene locus with decitabine, which has also been reported previously (Lodygin et al., 2005; Thiel et al., 2009; Wolf et al., 2006). This thesis looked at 97 CpG sites covering three CpG islands located over the promoter - exon/intron 1 boundary and within introns 3 and 4 and thus assessed a much larger proportion of the gene locus than previous studies. Both Thie l et al. and Lodygin et al. assessed methylation by methylation-specific PCR, which solely targets CpG sites within the primer binding region. Lodygin et al. covered 4 CpG sites in the promoter region and 7 CpG sites within the first intron. Wolf et al. on the other, hand used bisulphite sequencing and assessed 13 CpG sites between −122 bp to +39 bp of the transcription start site covering a small region of the promoter. It has been shown that methylation as far as 42.5 Kb upstream and 74.5 Kb downstream of the COX2 genes transcription start site can influence gene expression though altering CCCTC-binding factor/cohesion-mediated chromatin looping and as a consequence enrichment of transcriptional components (Kang et al., 2015). Consequently, studying such a small section of the promoter may not allow complete assessment of the true effect of methylation on 15-PGDH expression. Even though there was no change in methylation observed at the loci studied in this thesis, 15-PGDH expression was up-regulated at both the mRNA and protein level following decitabine treatment. This data suggests that 15-PGDH

expression is indeed influenced by epigenetic mechanisms, but the effect is most likely the indirect result of demethylation, possibly on genes that bind *HPGD*'s promoter.

Treatment of breast cell lines with the HDAC inhibitor, vorinostat, increased 15-PGDH expression at the transcript level but not at the protein level. Combination treatment with decitabine also resulted in a synergistic effect on gene transcription. While histone acetylation was not assessed in this study, it would be interesting to determine how vorinostat influences 15-PGDH expression via histone acetylation in the future. Analysis of MDA-MB-231 cells treated with 10 µM vorinostat for 24 or 48 hours identified lysine acetylation of 61 proteins including non-histone proteins such as transcription factors and cell structure proteins (Zhou, Q. et al., 2010). Although 15-PGDH was not one of these proteins, seven transcription factors were acetylated. This indicates that vorinostat may also act indirectly on 15-PGDH expression through altering transcription factor activity. It would therefore be interesting to assess the effect of 1 µM vorinostat over 72 hours on acetylation in the four cell lines used in this study.

Vorinostat and decitabine have been approved for the treatment of haematological malignancies (Ramalingam et al., 2010; Mann, B.S. et al., 2007; Saba, 2007), but their use has yet to be approved in solid tumours such as breast cancer. Current literature suggests epigenetic mechanisms play a strong role in breast cancer development and the methylation status of tumour suppressor genes including *DKK3*, *ITIH5*, *DOK7*, *HYAL2* and *RASSF1A* which are biomarkers of breast cancer (Yang, R. et al., 2015; Kloten et al., 2013; Heyn et al., 2013). As 15-PGDH is up-regulated in breast cancer cell lines by vorinostat and decitabine treatment *in vitro*, this may also translate in the clinic, increasing 15-PGDH expression in patients.

Decitabine induced demethylation requires cells to undergo proliferation for its incorporation into the genome (Derissen et al., 2013), consequently the efficacy of the drug relies on the cells' proliferation rate. As the number of proliferating cells is much lower in solid tumours compared to haematological malignancies, decitabine efficacy is better in haematological malignancies than solid tumours. Other factors influencing the efficacy of decitabine on solid tumours are: ease of drug penetration, blood supply to the tumour, activation of the prodrug and the effect of methylation changes on carcinogenesis (Issa and Kantarjian, 2009). These factors need to be considered if epigenetic drug treatment is to be used in breast cancer patients. A phase I clinical trial assessing the efficacy of decitabine in combination with the cytotoxic agent, carboplatin, in patients with a range of solid tumours (including breast cancer) has confirmed an optimal regime with minimal toxicity and detectable demethylation (Appleton et al., 2007). Combination therapies with chemotherapy drugs and HDAC inhibitors such as olaparib

(poly(ADP-ribose) polymerase inhibitor) and vorinostat have also shown promising results in TNBC cells both *in vitro* and *in vivo* (Min et al., 2015). Further research is required to determine the efficacy and long term effects of epigenetic treatment in breast cancer.

Decitabine's reduced efficacy on solid tumours may mean it is either ineffective or requires a higher dose, which often results in unacceptable levels off-target adverse effects. Targeting decitabine directly to the site of the breast carcinoma using novel delivery systems such as microbubbles, may reduce these adverse effects. A microbubble consists of small micro-vesides made of polymers, lipopolymers, lipids, proteins and surfactants, which can be loaded with drugs such as decitabine (Ambika Rajendran, 2018). The microbubbles are introduced into the circulation and can be burst at the site of the tumour using ultrasound targeting the cancer cells. Similarly, the microbubbles can incorporate antibodies that bind to antigens presented only on the membrane of cancerous cells, improving the targeted effect. The use of microbubbles loaded with doxorubicin has shown positive results with breast cancer cell lines *in vitro*, with increased up-take of the drug and cell death (Lentacker et al., 2010). This targeted therapy could offer a potential approach to increasing 15-PGDH expression in patients, overcoming the toxicities observed with decitabine and reducing off-target demethylation.

15-PGDH showed limited methylation *in vitro*, but correlation between 15-PGDH expression and methylation was seen in MEXPRESS patient data, whereas COX2 has a similar methylation trend both *in vitro* and *in vivo*. Methylation of the COX2 promoter has been reported in the murine mammary cell line 410 and treatment with decitabine increased COX2 protein expression and PGE_2 synthesis (Ma, X. et al., 2004). Furthermore, 18.2% of primary breast cancers exhibited methylation at the 5' region of COX2, associated with decreased tumour size, metastasis and overall improved prognosis (Chow et al., 2005). Regardless of this, decitabine treatment increased apoptosis and suppressed cell growth with increased COX2 expression and PGE_2 production in pulmonary fibrosis and hepatocellular carcinoma (Murata et al., 2004; Evans et al., 2016). This suggests other genes altered by decitabine treatment counteract reactivation of COX2 expression *in vitro*. When taken together with the epigenetic regulation of 15-PGDH, it appears that breast cancer patients with high COX2 expression may be a suitable target group for epigenetic treatment. As 15-PGDH and COX2 are part of the prostaglandin pathway consisting of many genes, altering their expression can impact on other bioactive lipids levels e.g. lipoxygenase products. It is probable that these compounds would need to be monitored to prevent excessive side effects. Further work would need to be completed to identify specific markers and gene expression profiles of patients likely to benefit from this type of treatment.

COX2 expression was observed in 36% of primary breast cancer patients (Denkert et al., 2003). Increased COX2 expression was associated with postmenopausal, and larger, node positive tumours (Jana et al., 2014; Denkert et al., 2003). Additionally, high COX2 expression correlated with TNBC, an aggressive cancer with poor overall survival rates (Tian et al., 2017). As the aggressive phenotype of COX2 expressing TNBC is linked to PGE_2 signalling, 15-PGDH expression may counteract the oncogenic effects of COX2 by degrading the PGE_2 synthesised via COX2 over-expression. Consequently, TNBC patients may be another target group for 15-PGDH therapy, possibly in combination with COX2 inhibitors.

Research in this thesis indicates that up-regulation of 15-PGDH by decitabine treatment is through indirect demethylation, therefore the role of transcription factors in regulation of 15-PGDH was investigated. Examples of targeting a transcription factor to reduce the repression of oncogenic genes are the drugs including tamoxifen and raloxifene. These compete with oestrogen to bind to the ER, blocking the proliferative effects of oestrogen (Fiorito et al., 2013; Williams and Lin, 2013). Research implicates the role of Slug, Snail, EGF and HNF3β in regulation of 15-PGDH expression in colorectal, NSCLC, and lung cancer (Backlund et al., 2008; Yang, L. et al., 2007; Huang, G. et al., 2008; Mann, J.R. et al., 2006), but little research has focused on transcription factor regulation of 15-PGDH in breast cancer.

Initial screening of transcription factors binding at the *HPGD* locus was performed using the Cistrome database. As this study is focused on breast cancer, the panel of cell lines assessed would ideally consist of breast derived cell lines with varied levels of 15-PGDH expression. This would enable the correlation of 15-PGDH and transcription factor expression in breast cell lines to be assessed, giving more specific breast cancer data and improved interpretation. A significant constraint of the Cistrome data analysis was a lack of a high 15-PGDH expressing breast cell line as a reference point. To overcome this a panel of six cell lines including breast, colon and lung carcinoma cell lines were used for the study. Analysis of the data identified twelve and eight unique transcription factors binding to high and low 15-PGDH expressing cell lines, respectively. RT-PCR amplification of these transcription factor's mRNA sequences however did not reveal any distinct trends between high and low 15-PGDH expressing cell lines. Furthermore, limitations associated with Cistrome database data, such as a lack of relevant untreated controls, as well as the small panel of cell lines assessed, reduced the reliability of the observations. Consequently, further research is required to identify the transcription factors associated with 15-PGDH expression in breast cancer.

Interestingly, the Cistrome data highlighted the binding of XBP1 in hypoxic MDA-MB-231 cells. 15-PGDH expression is influenced by hypoxic culture conditions, yet there are conflicting results between the literature and this study. The literature suggests 15-PGDH expression is increased in hypoxic tissue in colorectal and pulmonary artery epithelial cells (Young et al., 2013; Ma, C. et al., 2014), whereas a decrease in *HPGD* mRNA expression was observed in hypoxia-treated MCF7 breast cells. Furthermore, no link between expression of the hypoxia marker, HIF-1α, and 15-PGDH epithelial expression was seen in the primary breast tissue samples. This may be due to the sample selection bias towards samples with high or intermediate 15-PGDH expression, whether in epithelial or isolated cells. As hypoxia is linked to cancer progression, metastasis and angiogenesis (Liu, Z.J. et al., 2015; Maxwell et al., 1997), decreased 15-PGDH expression may in part play a role in this in the context of breast cancer. Due to conflicting data with the literature describing other types of cancer, it would be interesting to repeat the experiment with a wider range of breast cell lines with differing molecular profiles and to assess both the protein and mRNA levels of 15-PGDH.

High 15-PGDH expression in apocrine breast carcinoma makes this subgroup an ideal model to help improve our understanding of 15-PGDH regulation in breast cancer. Establishing how 15-PGDH expression is regulated in apocrine breast cancer would offer an insight in to how to increase 15-PGDH expression in other cancer types, aiding the development of a novel cancer treatment. As apocrine cancers are relatively rare they are poorly understood and it would be interesting to determine whether 15-PGDH expression occurs in early apocrine breast carcinoma or increases as the disease progresses. Future work should assess the apocrine lipid profile, to determine whether there are increased prostaglandin levels in the microenvironment and how 15-PGDH may influence them and ultimately cancer progression.

In summary, the data confirms that regulation of 15-PGDH is highly complex and involves interplay between epigenetics, transcription factor expression and environmental factors. Further investigation to understand this regulatory network could be valuable in helping to develop a potential treatment in breast cancer.

6.4 Functional effects of 15-PGDH over-expression in MCF7 cells

To assess the functional effect of 15-PGDH in breast cancer five MCF7 clones stably over-expressing 15-PGDH to different degrees and five control clones were generated. This enabled a more comprehensive assessment of the functional effects of 15-PGDH in breast cancer than

that described in the literature which utilised either transiently expressed 15-PGDH or a single stably transfected clone.

15-PGDH over-expression had no effect on proliferation in the MCF7 cell line, although there was a significant decrease in colony forming efficiency. Furthermore, significantly decreased migration was observed in the 15-PGDH over-expressing clones, compared to the matched controls after 48 hours. This suggests that although 15-PGDH does not alter the rate of proliferation of breast cancer cells it reduces the cells ability to migrate and successfully populate at a secondary site. Downstream transcriptional effects of 15-PGDH over-expression lead to increased expression of genes associated with cell adhesion and cadherin binding. Protocadherin-7 (*PCDH7*) was one of the genes highly expressed in the H14 clone compared to the control clone and is known for its role in adhesion. Lower expression of *PCDH7* has been reported in colorectal and gastric cancer with increased expression found to inhibit cell migration and invasion via E-cadherin (Chen, H.F. et al., 2017; Bujko et al., 2015), a marker for differentiation and invasiveness (Otto et al., 1993). Taken together this data indicates that 15-PGDH up-regulation may be more beneficial in cancers with an aggressive phenotype, by increasing cell adhesion and reducing the occurrence of metastasis. Further *in vitro* work to assess expression of genes associated with adhesion in different breast cell lines would confirm whether this is the case in other breast cancer subtypes as well as the luminal A MCF7 cell line. Moreover, assessing the effect of 15-PGDH expression on metastasis in breast cancer *in vivo* would provide vital information to determine how 15-PGDH up-regulation could modulate cancer progression.

It has been reported that 15-PGDH inhibits tumour growth through lowering PGE_2 levels and thus inhibiting angiogenesis in lung cancer (Huang, G. et al., 2008). For this reason it would be interesting to assess whether varied levels of 15-PGDH expression alters the angiogenic properties of breast cell line xenographs or *in vitro* co-culture of breast epithelial cells and endothelial cells such as the HUVEC cell line. Co-culture of epithelial lung adenocarcinoma cell line CL1-5 with HUVEC cells increased tube formation *in vitro*, which was reduced with COX2 inhibitor celecoxib (Cheng, H.W. et al., 2017). As COX2 expression is linked to angiogenesis it would be interesting to see whether 15-PGDH attenuates tube formation in a co-culture system with HUVEC and breast epithelial cells that express COX2 or following addition of PGE_2.

All of this data indicates that 15-PGDH may be more important in cell survival and metastasis than in proliferation alone and therefore assessing the effects of 15-PGDH expression *in vivo* would be the next logical step. Viral transfection in BALB/c mice, using an oncolytic herpes

simplex virus containing a 15-PGDH expression cassette, significantly reduced tumour growth and inhibited pulmonary metastases compared to the PBS control (Walker et al., 2011). No statistical significance was observed between the control and 15-PGDH virus, despite a slight improved response with 15-PGDH. Consequently, it would be interesting to see whether 15-PGDH over-expressing breast cell line xenographs gave a similar result.

6.5 General discussion

Tumour suppressor genes inhibit cell proliferation and tumour development and are often lost or inactivated in cancer. For instance disruption of the tumour suppressor gene BRCA1 is associated with inherited breast cancer (Miki et al., 1994). 15-PGDH has been described as a tumour suppressor in several cancers (Backlund et al., 2005; Ding et al., 2005; Liu, Z. et al., 2010). Increased risk of colon cancer is associated with the SNP rs2555639, which caused decreased expression of 15-PGDH (Thompson et al., 2013). Despite this, 15-PGDH does not meet the traditional criteria of a tumour suppressor, as patients with non-functional 15-PGDH did not exhibit increased occurrence of breast cancer (Uppal et al., 2008). Additionally, over-expression of 15-PGDH in the apocrine subgroup, suggests that 15-PGDH alone does not suppress cancer. As 15-PGDH over-expression in MCF7 resulted in a decreased rate of migration and colony formation, 15-PGDH may have an important role in tumour progression, but a lack of 15-PGDH activity itself does not drive cancer.

The half-life of prostaglandins ranges between seconds to minutes (Wymann and Schneiter, 2008), therefore the effect of 15-PGDH may be limited by the rate of cellular absorption of PGE_2 by its transporters such as PGT. Increasing the rate of uptake of PGE_2 back into the cell for degradation may decrease PGE_2 signalling. Consequently, altering the expression of the PGT may amplify the effect of increased 15-PGDH expression in cancer treatment. As evidence suggests that PGE_2 is the main prostaglandin involved in breast cancer development, inhibition of PGE_2 production may be an even more specific target than non-specific prostaglandin degradation.

Development of mPGES-1 inhibitors has been an on-going endeavour leading to a clinical trial comparing the effect of the mPGES-1 inhibitor LY3023703 to the anti-inflammatory COX2 inhibitor celecoxib. The results showed that inhibiting PGE_2 production with LY3023703 resulted in increased prostacyclin production by 115% in comparison to a 44% decrease with celecoxib (Jin et al., 2016). This increase in prostacyclin production reduces the side effects associated

with celecoxib, which is advantageous to its use as an anti-inflammatory. Inhibition of mPGES-1 redirects the PGH_2 intermediate, producing more of the other prostaglandins as well as prostacyclin. As summarised in Table 1.3, $PGF_{2\alpha}$, PGD_2 and TXA_2 have also been implicated in cancer, therefore increased production and thus signalling of these molecules may be detrimental. Consequently, targeting 15-PGDH expression circumvents altering the prostaglandin profile by metabolising the final prostaglandin products and possibly making it a more suitable target.

TNBCs are associated with a more aggressive phenotype than other cancers and is more likely to metastasise leading to shorter overall survival (Kim, J.E. et al., 2012). High mRNA expression of *HPGD* in TNBC patients correlated with higher overall survival and higher probability of recurrence-free survival (Kochel et al., 2016). Due to a lack of ER, PR and HER2 expression, TNBCs do not benefit from endocrine or molecular targeted treatment. Current treatment relies on a comparatively ineffective combination of chemotherapy, radiotherapy and non-HER2 targeted therapy, meaning there is a demand for more targeted treatments of TNBC patients to improve their outcome. This study observed low expression of 15-PGDH in the TNBC cell line MDA-MB-231 and its up-regulation following epigenetic drug treatment. Furthermore, since the 5 year recurrence-free survival rate was 85% and 70% in those with high versus low 15-PGDH expression and overall survival was 92.6% and 81.4%, respectively (Wu, R. et al., 2017), possibly making TNBC patients ideal candidates for 15-PGDH therapy or epigenetic drug treatment.

Vascular endothelial growth factor (VEGF) is well known for its role in angiogenesis, and research has shown that PGE_2 stimulates VEGF production (Tamura et al., 2006). Combination treatment of adenoviral mediated 15-PGDH expression and anti-VEGF antibody (bevacizumab) reduced tumour growth in colorectal cell line LS174T xenographs (Kaliberova et al., 2009). It would therefore be interesting to see whether 15-PGDH expression combined with current breast cancer therapies decreased tumour growth and metastasis. Combination treatment with COX2 inhibitors and aromatase inhibitors had a similar response rate to frontline treatment, with some patients showing a complete clinical response (Chow et al., 2008). Therefore it would be interesting to assess whether 15-PGDH up-regulation in combination with exemestane improves patient outcome, particularly in those patients with metastatic disease. Furthermore, although the MCF7 cell line has low COX2 mRNA expression, 15-PGDH over-expression still resulted in a less aggressive phenotype as measured by colony formation and cell migration. This suggests that even if COX2 expression is not increased in the cancerous cells, 15-PGDH

expression may still reduce tumour progression and metastasis in breast cancer by degrading PGE_2 produced by non-cancerous cells. Combining current endocrine therapies with 15-PGDH therapy may therefore improve patient outcome in most breast cancer subtypes, with the exception of apocrine carcinoma.

15-PGDH gene therapy in murine breast cancer using a liposome-encapsulated 15-PGDH plasmid in combination with celecoxib significantly reduced tumour growth and lung metastases (Zhang, B. et al., 2013). This not only highlights the benefit of combining COX2 inhibition and 15-PGDH expression in breast cancer, but also the potential of 15-PGDH gene therapy. As this study is one of very few 15-PGDH gene therapy studies further work on 15-PGDH gene therapy *in vivo* would be highly advantageous.

In conclusion, 15-PGDH activity slows down the hallmarks of breast cancer *in vitro* and therefore further investigation as to whether this is the case *in vivo* would be advantageous. As 15-PGDH activity is generally low in breast cancer, induction of 15-PGDH activity within the tumour environment may be effective in slowing down breast cancer development. While the majority of breast cancer patients may benefit from increased 15-PGDH activity, patients with high COX2 expression or TNBC may benefit the most.

6.6 Future work

Though this study has provided an important insight into the role of 15-PGDH in breast cancer with regards to its expression, regulation and functional effects *in vitro*, there is scope for more research to be conducted in this area. Future work investigating the role of 15-PGDH in breast cancer should aim to assess the effect of 15-PGDH expression on breast cancer development *in vivo* and elucidate the mechanisms regulating 15-PGDH expression in order to develop a treatment that will increase 15-PGDH expression. Alternatively, further work on 15-PGDH gene therapy may be advantageous.

Only a small number of normal breast tissue samples were available for this project, therefore it was not possible to accurately determine the level of 15-PGDH in normal breast tissue. Furthermore, limited clinical data was associated with the primary breast cancer TMAs used in this study. It would therefore be highly advantageous to assess 15-PGDH expression in matched normal adjacent and primary breast cancer tissue with clinical data. This would enable the difference in 15-PGDH expression between cancer subtypes, receptor status and other clinical

features to be determined and help decide which patients would benefit the most from 15-PGDH based therapy.

An interesting observation discovered while assessing 15-PGDH expression in breast cancer was 15-PGDH labelling in isolated cells. Pathological assessment indicated the cells were macrophage or mast cells, but no co-localisation of 15-PGDH and pan macrophage marker CD68 was seen. A literature search suggests that the cells labelling with 15-PGDH may be a selection of different leukocytes. To determine the identity of the isolated cells future work should include flow cytometry to assess expression of known leukocyte markers in the 15-PGDH positive cell population. For example CD45, CD68, CD20 and CD3, which are pan-leukocyte, pan macrophage, B-cell and T-cell markers could be used. Alternatively immunohistochemistry with two fluorescently labelled antibodies could be used on tissue, but using an alternative fixation method to paraffin/formalin to reduce the tissue auto-fluorescence.

The presence of 15-PGDH labelling in immune cells highlights the significance of 15-PGDH expression and the tumour microenvironment in breast cancer. This is an area that has yet to be investigated, therefore future work should aim to determine the significance of 15-PGDH immune cell labelling. As 15-PGDH expression in isolated cells was observed in 41% of primary breast cancers, it would be interesting to see whether this is more common in a particular subset of breast cancers and whether it has any implications in overall patient survival.

Further studies should assess the effect of the microenvironment on 15-PGDH epithelial expression *in vitro*. This could be achieved by assessing the hallmarks of breast cancer in co-culture experiments. One example of this is to assess the ability of breast cancer cells to proliferate in the presence of a macrophage cell line such as THP-1 monocytes. This could be further developed by looking at the effect of epithelial co-culture with other immune cells or fibroblasts.

This study has shown that 15-PGDH expression is in theory indirectly regulated through methylation. Further work should aim to confirm this observation by determining the mechanism responsible for 15-PGDH up-regulation with decitabine treatment. A first step would be to perform RNA-Seq with MCF7 and MDA-MB-231 cells, both untreated and decitabine-treated. This would allow the differentially expressed genes between the treatments to be verified. The list of candidate genes could also be further narrowed by comparing the MDA-MB-231 and MCF7 cell lines, which showed a different change in 15-PGDH expression in response to decitabine treatment. Those genes showing up- or down-regulation

following decitabine treatment may be a key player in the regulation of 15-PGDH expression. Immunoprecipitation assays targeting the candidate protein would enable identification of transcription factors or proteins directly binding to the *HPGD* locus. Furthermore, functional studies would confirm the significance of these proteins in relation to the regulation of 15-PGDH expression.

As 15-PGDH was down-regulated in the MCF7 cell line in response to hypoxic conditions in this study, it would be useful to assess this in a larger panel of breast cell lines as well as breast cancer tissue. If 15-PGDH is down-regulated in hypoxic tissue leading to an increase in PGE_2 signalling, up-regulation of 15-PGDH may be advantageous in breast cancer with areas of hypoxia, such as large solid breast tumours.

An alternative way to identify a method of 15-PGDH up-regulation is by completing a drug screen using a luciferase reporter assay. Using a vector containing *HPGD* and the luciferase reporter gene enables easy quantification of *HPGD* transcription. This system would allow the effect of an array of commercially or otherwise available drugs on *HPGD* transcription to be quantified. Identification of a drug that increases the expression of 15-PGDH could potentially be beneficial in breast cancer treatment.

This study assessed the effect of 15-PGDH over-expression in the MCF7 breast cancer cell line on proliferation, migration, invasion and clonogenicity. Future work could also assess its role in apoptosis and angiogenesis. Additionally, the effect of 15-PGDH over-expression on the hallmarks of cancer should be assessed in a panel of breast cancer cell lines, including the T47D cell line, which expresses all the components of the prostaglandin pathway.

A key focus of this study was to assess the functional effect of 15-PGDH over-expression *in vitro*. If 15-PGDH over-expression, albeit by gene therapy or via drug treatment, was to be used in clinic a significant amount of research would need to prove the efficacy of 15-PGDH over-expression *in vivo*. Although some studies have shown positive results with 15-PGDH over-expression, further work to validate this would be highly beneficial.

6.7 Considerations for the interpretation of the results

The level of expression of 15-PGDH in primary breast cancer was determined using the primary breast cancer TMA samples obtained from the Leeds Breast Tissue Bank. These samples were a representative selection of cancers, with individual slides containing tumours grouped by

staging. While this minimised bias for tumour type and treatment, as the samples came from a specific geographic region they may be skewed for factors such as diet and lifestyle. The TMA used to optimise the 15-PGDH antibodies was created for the AZURE clinical trial, therefore the patients had either stage II or III cancer and all patients had undergone selection for the suitability for inclusion in the clinical trial. Both of the TMAs consisted of a limited number of samples which constrained the availability of rarer tumour types such as apocrine tumours or tumours with a range of 15-PGDH activity. This in turn limited the statistical power of any test, while meaning some comparisons could not be performed. For instance, it was only possible to obtain tissue blocks for thirteen 15-PGDH positive samples, limiting the ability to identify samples with a range of 15-PGDH, COX2 and HIF-1α expression which were required to determine the interplay of their expression on disease progression.

The clinical data linked to the TMA samples was limited as the samples were collected over 20 years ago. Consequently, the data available to this study was incomplete and restricted by the diagnostic tests available 20 years ago, for instance the receptor status was not always available. Most of the samples were ER positive, which is to be expected, but ER expression (as well as other receptors) for several samples were unknown. This may be because the receptor status was not assessed or recorded in the patients' notes, or because the results were negative and therefore not noted. As a result the clinical analysis of this dataset was restricted and what could be done is probably unreliable. Consequently, this work would have benefited from the availability of cohort linked to high quality clinical data.

The MCF7 cell line was selected for the 15-PGDH over-expression experiments as it is well characterised and commonly used in breast cancer research. The MCF7 cell line also has a luminal A molecular profile, which is the most common breast cancer subtype, accounting for 50-60% of all breast cancers (Yersal and Barutca, 2014). As such it expresses the oestrogen and progesterone receptor but not HER2 protein. Subsequent investigation into the expression of the prostaglandin pathway components in breast cell lines revealed that no PGT (*SLCO2A1*) was detected in the MCF7 cell line as determined by RT-PCR, although *SLCO2A1* transcripts were detected by RNA-Seq. The lack of *SLCO2A1* expression would limit the up-take of both exogenous and endogenous PGE_2 into the cell, reducing its metabolism by 15-PGDH. Despite this, PGE_2 would be able to diffuse through the cell membrane, although at a slower rate. Ideally the experiments would be repeated with other breast cancer cell lines that expressed *SLCO2A1,* such as MDA-MB-453. Further to this the MCF7 cell line does not express COX2 and therefore does not produce PGE_2 (Kochel et al., 2017). This suggests that PGE_2 may not play a large role

in the MCF7 cell line, but as PGE_2 can act in both an autocrine and paracrine manner, PGE_2 produced by cells in the tumours microenvironment may influence the cells behaviour. Additionally, the MCF7 cell line is known for its non-metastatic properties, therefore repeating this work on a more metastatic cell line such as the MDA-MB-231 cell line may yield a more pronounced effect than seen with MCF7 cells. Repeating this work in a cell line that expresses all of the components of the prostaglandin pathway such as the T47D cell line would also be advantageous. This ties in to the current goal of personalised medicine in which treatment is directed by the expression and mutation profile of each tumour rather than its histological subtype.

One of the constraints of the project was assessing the indirect mechanisms involved in methylation regulation of 15-PGDH. Establishing which transcription factors or other genes that are demethylated by decitabine and target 15-PGDH expression was difficult given time and monetary constraints. Using the Cistrome database to identify transcription factors binding within the *HPGD* promotor region was a useful starting point. The database contained limited data on transcription factor expression and binding in breast cancer cell lines, and what was available was designed for other purposes and so subject to the treatments and tissue culture conditions that were not ideal for the analysis required for this thesis. Consequently, colorectal and lung cell lines with known 15-PGDH expression were also included in the screen for transcription factors linked to 15-PGDH expression. A drawback of this approach is that the transcription factors influencing one cell or cancer type may not directly translate to breast cancer cells.

An alternative approach to determine transcription factors influencing 15-PGDH expression would be to assess genome-wide methylation analysis on a panel of epigenetic drug- and control-treated breast cell lines. The data could then be used to identify transcription factors demethylated in drug-treated cells, but not control cells, in cell lines whose 15-PGDH expression increased after treatment. These transcription factors could then be assessed for binding to the *HPGD* gene's promoter. Once a small subset of transcription factors was identified chromatin immunoprecipitation could be performed to detect their binding to *HPGD* in treated and untreated cells.

This study has focused on the anti-carcinogenic effects of 15-PGDH metabolism of PGE_2, but the endogenous levels of PGE_2 or its metabolite were not measured. The literature suggests that very little endogenous PGE_2 is produced by the MCF7 and MDA-MB-231 cells compared to MDA-MB-436 cells (Kochel et al., 2017), yet decreased colony formation was observed in the

untreated MCF7 clones over-expressing 15-PGDH. This data suggests that PGE_2 might not be the sole target of 15-PGDH. It would therefore be interesting to determine how other substrates respond to 15-PGDH overexpression and what their function is.

In vitro models of breast cancer are a useful tool in research, particularly when looking at a molecular level, but there are significant limitations of *in vitro* work due to the culture microenvironment. The assays used in this study have enabled the effect of 15-PGDH expression on the hallmarks of breast cancer to be investigated *in vitro*. A logical progression to this work would be to assess whether the observed effects are also found in *in vivo* experiments. Research indicates that over-expression of 15-PGDH in breast xenographs slowed tumour growth in colorectal, lung and cancer (Yan et al., 2004; Ding et al., 2005; Kaliberova et al., 2009). A 15-PGDH knock-out model also resulted in increased colorectal tumour growth (Myung et al., 2006). Stable siRNA down-regulation of 15-PGDH increased tumour growth in MCF7 xenographs and stable over-expression in the MDA-MB-231 cell line decreased tumour growth (Wolf et al., 2006). These studies focus on tumour growth and not metastasis, therefore it would be interesting to see whether increased 15-PGDH expression reduces the metastatic capacity of breast xenographs *in vivo*.

The RNA sequencing data was used to identify genes up- or down-regulated in the over-expressing clone versus the matched control clone. The expression of these genes were then assessed in the panel of MCF7 over-expressing and control clones to determine whether this expression change was consistent. Since, RNA sequencing was only performed on one set of clones, identifying genes that was consistently up- or down-regulated across the panel of over-expressing clones compared to their matched controls proved challenging. Many factors alter a gene's transcription, such as cell cycle and environmental factors, meaning that many false positive results are detected in RNA-Seq experiments with limited numbers of samples. This may be confounded in this experiment due to each clone having different integration sites for the expression cassette which may affect the expression of flanking genes and any gene expression network linked to these genes. Repeating the RNA sequencing with more of the clones would make it easier to determine the genes whose expression is linked to 15-PGDH activity and PGE_2 levels.

6.8 Final conclusion

The aim of this study was to investigate the effect of 15-PGDH expression on hallmarks of breast cancer *in vitro*. Research indicates that 15-PGDH expression is low in breast cancer and regulation of its expression is highly complex and requires further investigation. Regardless of this, 15-PGDH over-expression decreased migration and colony formation *in vitro* and increased expression of cell adhesion proteins. Together this data indicates 15-PGDH has anti-metastatic properties and has the potential to be highly beneficial in breast cancer treatment, particularly those with an aggressive phenotype and high COX2 expression.

Appendix

Appendix 1 Gene expression primers (1)

Gene	Primer sequence		Product size (bp)	Annealing temp. (°C)
ABCC4 (MRP4)	F	ctgccagaagaccgctcac	307	61 hot start
	R	tagccaaaatgagcgtgcaaa		
ACSM1 (ACSM1)	F	gctgccggtctttatcaga	356	56
	R	cttcaacaggatggtcgcag		
BCL2 (Bcl-2)	F	ggtggtggaggagctcttc	303	57
	R	cccagggtgatgcaagct		
CD24 (CD24)	F	gagagataaccctgcccgag	369	56 two bands
	R	gacgtttcttggcctgagtc		
CHD1 (CDH1)	F	agttctggaagcagtagtgatg	301	60 hot start
	R	agtcatcggaatcttcactgc		
CTCF (CTCF)	F	tgtccacggcgttcaaattt	359	60 hot start
	R	agcttgtatgtgtccctgct		
ERBB2 (HER2)	F	atagggttaagggaaggcgg	305	57
	R	tgtgactctttgctcaggga		
ESR1 (ER)	F	gccctactacctggagaacg	307	59
	R	atcaatggtgcactggttgg		
FMOD (FMOD)	F	attaggaatttggggcggga	321	60 hot start
	R	gggtaaggctcgtaggtctc		
GABPA (GABPA)	F	tgctagaaccaagactacagtgt	302	60 hot start
	R	ggttgtgatgtgttttgtgcc		
GAPDH (GAPDH)	F	acaacagcctcaagatcatcag	312	60
	R	ggtccaccactgacacgttg		
GATA3 (GATA3)	F	agtacagctccggactcttc	319	57
	R	ccattggcattcctcctcca		
GSTA1 (GSTA1)	F	attcagttgtcgagccagga	268	60 hot start
	R	caccagcttcatcccatcaa		
HOXA6 (HOXA6)	F	ttttctcccgagcagcagta	351	60 hot start
	R	ctgcgtggaattgatgagct		
HPGD (15-PGDH)	F	tagcgctggtggattggaat	306	57
	R	taatgatgccgccttcacct		
HPGD nested PCR	F	cctggatgagcagtttgaacc	247	57 hot start
	R	gccttcacctccattttgct		
KLHL4 (KLHL4)	F	agaagcttgtgagaaacgcg	333	60 hot start
	R	actccttccatcctgacctc		

Appendix 2 Gene expression PCR primers (2)

Gene	Primer sequence		Product size (bp)	Annealing temp. (°C)
MED12 (MED12)	F	cccttgccccatgatgtaga	379	60 hot start
	R	taaagggagtcgagggtgtg		
NR3C3 (PR)	F	tggtgtttggtctaggatgga	301	56
	R	cactcagtgcccgggact		
NR3C4 (AR)	F	gacctgcctgatctgtggag	306	57
	R	agcttctgggttgtctcctc		
PCDH7 (PCHD7)	F	tctaccaccagccaacacat	356	62 hot start
	R	cagtcagggctacatctgga		
PML (PML)	F	tgtaccggcagattgtggat	337	60 hot start
	R	ctgatgtcgcacttgagctc		
PTGES (mPGES-1)	F	tggtcatcaagatgtacgtggt	323	54
	R	gtaggtcacggagcggatgg		
PTGES2 (mPGES-2)	F	ccatgaaggctgtgaacgag	369	54
	R	acttgtcagcagcctcataga		
PTGES3 (cPGES)	F	agtggtacgatcgaagggac	237	57 hot start
	R	atgactggccagattctcct		
PTGS2 (COX2)	F	atctacggtttgctgtgggg	493	57
	R	ttctgtactgcgggtggaac		
SERPINA4 (SERPINA4)	F	agtgagctcaagaaggacgt	381	60 hot start
	R	gccagaaatggagaacttggg		
SLCO2A1 (PGT)	F	gctttgggctctccagttct	377	57
	R	aataggcactgtcccgatgc		
SMC1A (SMC1A)	F	gacctgatccatggagctcc	306	60 hot start
	R	cagctccccagaacgactaa		
SOX9 (SOX9)	F	ctccagcaagaacaagccg	448	60 hot start
	R	ctgcacgtcggttttggg		
TAF1 (TAF1)	F	tgaggaagatgctgggagtg	439	60 hot start
	R	agagtccaagtcactgtccc		
USF1 (USF1)	F	gatggccaaactgagggaac	309	60 hot start
	R	gcttcctccctgcagtactt		
XBP1 (XBP1)	F	gggacccctaaagttctgct	376	60 hot start
	R	ccaagcgctgtcttaactcc		

Appendix 3 Gateway cloning and sequencing primers

Gene	Primer sequence		Product size (bp)	Annealing temp. (°C)
HPGD gateway	F	GGGGACAAGTTTGTACAAAAAAGCAGGCTTCACCATGCACGTGAACGGC	862	54 Pfx
	R	GGGGACCACTTTGTACAAGAAAGCTGGGTCTTGGGTTTTTGCTTGAAATGGAGTTG	(*HPGD* variant 1)	
M13	F (-20)	GTAAAACGACGGCCAG	Variable	55
	R	CAGGAAACAGCTATGAC		
pDEST510 vector	F	GTGGGAGGTCTATATAAGCAGAG	Variable	60
	R	GCAACTAGAAGGCACAGTCG		
pDONR201 vector	F	TCGCGTTAACGCTAGCATGGATCTC	1082	60
	R	GTAACATCAGAGATTTTGAGACAC		
T7	F	TAATACGACTCACTATAGGG	Variable	60

Appendix 4 Pyrosequencing PCR primers

Primer set ID	Primer sequence		CpGs in product	Product size (bp)	Annealing temp. (°C)
CpG1 (1)	F	[Btn]GGTTTTTAGGGTATTGAAGGAAATT	12	221	52
	R	AAAAAAAACTATCAAACCAAC			
CpG1 (2)	F	[Btn]GTTGGTTTGATAGTTTTTTTT	26	206	57
	R	AAAAACTCTACCTATACCCTAAACC			
CpG1 (3)	F	[Btn]GGGTATAGGTAGAGTTTTTGTAGAGG	16	241	60
	R	AACAATTAAATTTAAATTCCCTCCC			
CpG2 (1)	F	[Btn]TTGTTTAGAATATAGAAGAAATGTTTA	12	210	52
	R	CCTCCTAAATAACTAAAACTACAAAC			
CpG2 (2)	F	[Btn]TAGTTATTTAGGAGGTTGAGGTAGG	8	183	52
	R	TATTAATAATTTTACAAAAACTCATTCTTT			
CpG3 (1)	F	[Btn]TTGAGTTATTAGAAATTGTTATTAAATATA	9	216	52
	R	CAAAAAACTAAAACAAAAAAATAAC			
CpG3 (2)	F	[Btn]TTTTTTGAGTAGTTGAGATTATAGG	14	247	52
	R	CTCATTCTTATAAATACCATTAAATTATAC			
MGMT	F	GTTTAGGATATGTTGGGATAGT	12	103	52
	R	[Btn]CCCAAACACTCACCAAAT			

Appendix 5 Pyrosequencing sequencing primers.

Primer name	Seq size (bp)	Primer sequence		CpGs in product
CpG1 (1) S1	127	R	AAAAAACTATCAAACCAA	12
CpG1 (2) S1	109	R	TACATAATACAACCACTACT	20
CpG1 (2) S2	50	R	CTCTACCTATACCCTAAAC	6
CpG1 (3) S1	48	R	ATATATAAACAAAAAAATTTC	6
CpG1 (3) S2	83	R	CAACCTCAACTTCAACAAAT	10
CpG2 (1) S1	66	R	TAATCTCAATCTCCTAACC	6
CpG2 (1) S2	64	R	CTCCTAAATAACTAAAACTAC	6
CpG2 (2) S1	123	R	TTACAAAAACTCATTCTTTCCTAAACA	8
CpG3 (1) S1	89	R	CAAAAAACTAAAACAAAA	9
CpG3 (2) S1	70	R	TCAAAAAATAATAACCATCC	5
CpG3 (2) S2	116	R	CTCATTCTTATAAATACCA	9
MGMT S1	81	F	GGATATGTTGGGATAGTT	12

Appendix 6 *HPGD* CpG island 1 pyrosequencing sequences and dispensation order

Light blue = CpG site, grey = CpG region, green = bisulphite conversion control, red = SNP location, dark blue = heterozygous SNP location. R denotes the cytosine location in a CpG site when sequencing in the reverse orientation and Y in the forward orientation.

Assay	Cell line	Sequence to analyse	Dispensation order
CpG1 P1 S1	CaCo-2 LoVo MCF7 231	CRCCCRCCRAAAAACCCACRACTAT ATCACCTACCCCCTAAACRTTCTAA AACRCCAAACTTCRCRATCTTTACC TTCCRAACTCRCAAACCRACTCAAA ACCTCCCCTCAACCTCTAACTCCRT AA	ACGATCGATCAAGAACATCAGACTG ATATCACTACCTATCGATCTAATCGA CACTACGATCAGATCTACTACAGACT ACGACATCAGACTCAACTCCTCACTC TACTACGAT
CpG1 P2 S1	CaCo-2 LoVo MCF7 231	AAAACRAACRATAAACRAACTCCRC RTCTCCRCRCRACCRCRACTTTTATA CCCCCCTACRCRCRCRCRCRTACAA CCCRACRAAACRCTCCCCTACCAAT AAACRAAAAAAAAAC	CGAATCAGATCAGATATCAGACTAC GATCGATCTACGATCGATCAGATCG ATCAGACTTATACCTATCGATCGATC GATCGATCGATCGATACATCAGATC AAGATCGACTCCTACATATCAAGAA
CpG1 P2 S2	CaCo-2 LoVo MCF7 231	CRCRCCRATCACCAACRCCACTTTA CCRTTCACRTAC	ACGATCGATCAGATCACATCGACACT GATCGATCATCGATA
CpG1 P3 S1	CaCo-2 LoVo MCF7 231	CRCRACTAAACRCCRAACTTACCTT AACRCCCTTAAACAACAACRCCT	ACGATCAGACTGATCGATCAGACTA CTATCGACTACACATCGAC
CpG1 P3 S2	CaCo-2 LoVo MCF7 231	TTTAAAAATAACAAAATAAACACRC CRAACRCRACCTCCCTATCTCCRCC AATACACCTCRAACRACRAAACRAA TCTCRAAAT	CTGAATACAATACATCGATCAGATCG ATCAGACTCTATCTACGACATACACT ACAGATCAGATCAAGATCAGATCTA CAAGA

Appendix 7 *HPGD* CpG island 2 pyrosequencing sequences and dispensation order

Light blue = CpG site, grey = CpG region, green = bisulphite conversion control, red = SNP location, dark blue = heterozygous SNP location. R denotes the cytosine location in a CpG site when sequencing in the reverse orientation and Y in the forward orientation.

Assay	Cell line	Sequence to analyse	Dispensation order
CpG2 P1 S1	CaCo-2	TTATAATCCRCCCRCCTCRATCTCCC AAAATACTAAAATTACAAACRTAA ATCACCRCTCCCRACC	CTGATATACGATCGACTACAGATCTC AATACTAATACATCGATATCATCGAC TACAGA
	LoVo		
	MCF7		
	231		
CpG2 P1 S2	CaCo-2	AAACRTCCRCCACCACRCCCRACTA AATTTTTATATTTTTAATAAAAACR AAATTTCACCRTAT	CGATCGATACGACACATCGATCAGA CTATTATATTATAATCAAGATCATCG ATA
	LoVo	AAACRTCCRCCACCACRCCCRACTA AATTTTTATATTTTTAATAAAAACR AAATTTCATCRTAT	CGATCGATACGACACATCGATCAGA CTATTATATTATAATCAAGATCATAC GATA
	MCF7		
	231	AAACRTCCRCCACCACTCCCRACTA AATTTTTATATTTTTAATAAAAACTA AATTTCATCRTAT	CGATCGATACGACACACTACAGACT ATTATATTATAACTATCATACGATA
CpG2 P2 S1	CaCo-2	TTTCTTTTTTTTAATTTTATTTTATTT TTAAAACAAAATCTCRCTCTATCRC CCAAACTAAAATACAATAACRCAAT CTCRACTCACTACAAACTCCRCCTC CCRAATTCACRCCATTCRCCT	CTCTTGATTATTATTAACAATCTACG ACTCTATACGACACTAATACATATCG ACATCTACAGACTCACTACACTACGA CTACAGATCATCGACATACGAC
	LoVo		
	MCF7		
	231		

Appendix 8 *HPGD* CpG island 3 and *MGMT* pyrosequencing sequences and dispensation order

Light blue = CpG site, grey = CpG region, green = bisulphite conversion control, red = SNP location, dark blue = heterozygous SNP location. R denotes the cytosine location in a CpG site when sequencing in the reverse orientation and Y in the forward orientation.

Assay	Cell line	Sequence to analyse	Dispensation order
CpG3 P1 S1	CaCo-2	AAATAACRTAAACCCRTAAAACRA AACTTACAATAAACCRAAATTACRC CACCACACTCCAACCTAAACRACAA AACRAAACTCCRTCT	CGATATCGATATCGATAATCAAGACT ACATATCAAGATATCGACACACACTC ACTATCAGACAATCAAGACTACGATC
	LoVo	AAATAACRTAAACCCRAAAAACRA AACTTACAATAAACCRAAATTACRC CACCRCACTCCAACCTAAACRACAA AACRAAACTCCRTCT	CGATATCGATATCAAGAATCAAGACT ACATATCAAGATATCGACATCGACAC TCACTATCAGACAATCAAGACTACGA TC
	MCF7	AAATAACRTAAACCCRAAAAACRA AACTTACAATAAACCRAAATTACRC CACCRCACTCCAACCTAAACRACAA AACRAAACTCCRTCT	
	231	AAATAACRTAAACCCRAAAAACRA AACTTACAATAAACCRAAATTACRC CAC/ACRCACTCCAACCTAAACRAC AAAACRAAACTCCRTCT	CGATATCGATATCAAGAATCAAGACT ACATATCAAGATATCGACACGACACT CACTATCAGACAATCAAGACTACGAT C
CpG3 P2 S1	CaCo-2	TAACTAACACRATAAAACCCCRTCT CTACTAAAAATACAAAAAATTAACC AAACRTAATAACRAACRCCT	ATGACTACATCAGATAACCGATCTCT ACTAATACAATACATCGATATATCAG ATCGAC
	LoVo		
	MCF7		
	231		
CpG3 P2 S2	CaCo-2	TTAAATTATACTTTAAAATATAACA CRACATTAAAAAATAACACATACRA CCRAACRCRATAACTAACRCCTATA ATCCCAACACTTTAAAAAACCRAAA TAAACRAATCACRAAAT	ATGATATACTAATATACATCAGACAT AATACACATATCAGATCAGATCGATC AGATACTATCGACTATATCACACTAA TCAAGATATCAGATCATCAAGA
	LoVo		
	MCF7		
	231		
MGMT S1	CaCo-2	YGYGTTTTTAGAAYGTTTTGYGTTTY GAYGTTYGTAGGTTTTYGYGGTGYG TATYGTTTGYGATTTGGTGAGTGTT TGGGT	GTCTGTCGCTTAGTATCGTTAGTCTG TTCGTATCAGTCGCTATGTTCAGTCG TAGTCGTGATCGTAGTCGAT
	LoVo		
	MCF7		
	231		

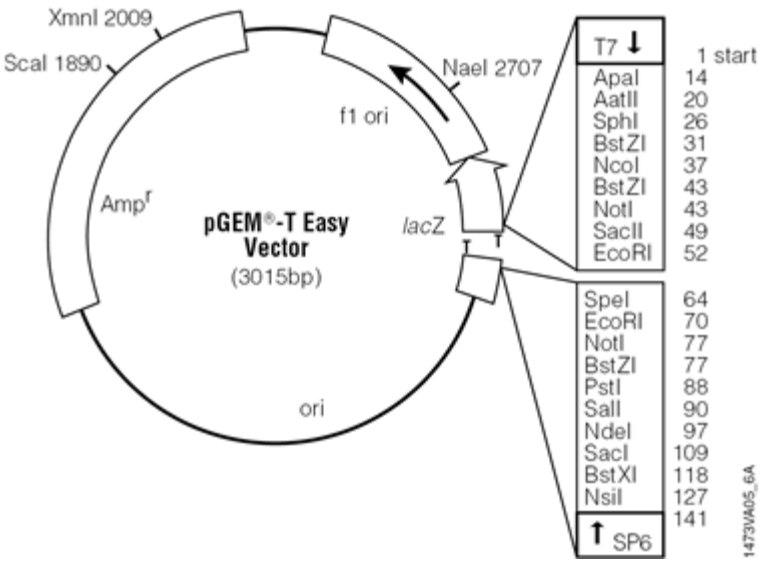

Appendix 9 Map of pGEM-T Easy Vector. Amp^r = ampicillin resistance, f1 ori = f1 origin, *lac*Z = encodes β-galactosidase.

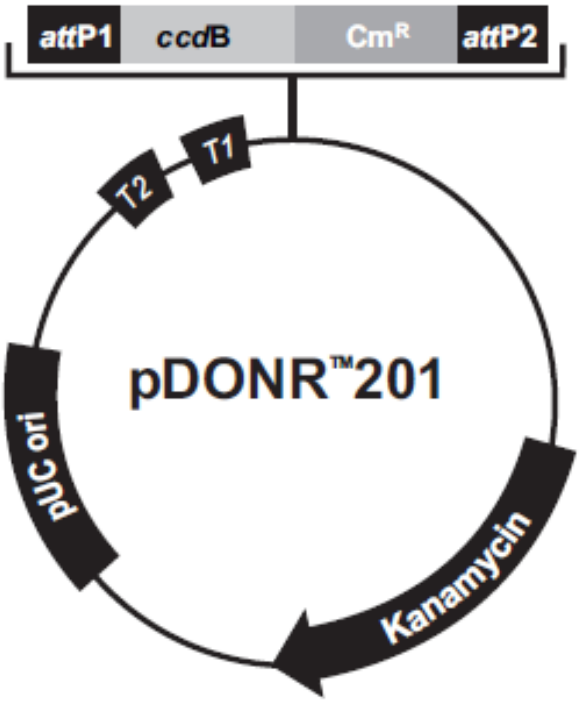

Appendix 10 Map of Gateway pDONR201 vector. Kanamycin = kanamycin resistance, pUC = pUC origin, T2 = *rrn*B T2 transcription termination sequence, T1 = rrnB T1 transcription termination sequence, *att*P1 = *att*P1 restriction site, *ccd*B = *ccd*B gene, Cm^R = chloramphenicol resistance, *att*P2 = *att*P2 restriction site.

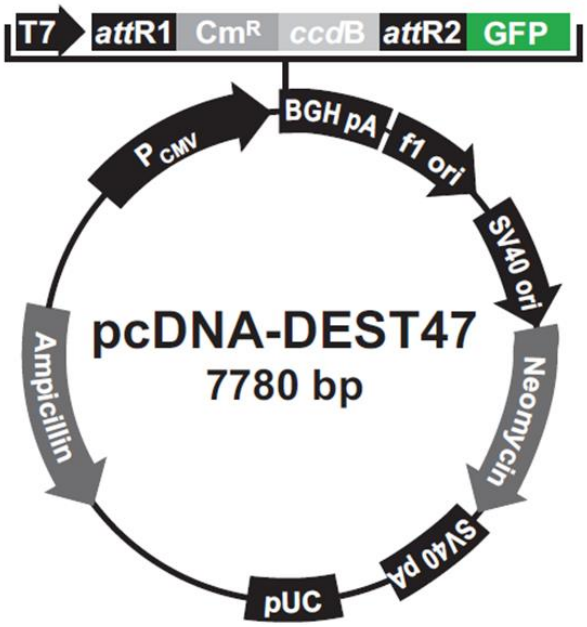

Appendix 11 Map of Gateway pcDNA-DEST47 vector. pDEST510 vector is based on the above vector, with the replacement of the GFP tag with a FLAG-tag. P_{CMV} = CMV promoter, BGH pA = BGH polyadenylation region, f1 ori = f1 origin, SV40 ori = SV40 early promoter and origin, Neomycin = neomycin resistance, SV40 pA = SV40 early polyadenylation region, pUC = pUC origin, Ampicillin = ampicillin resistance, T7 = T7 promoter, *att*R1 = attR1 recombination site, Cm^R = chloramphenicol resistance, *ccd*B = *ccd*B gene, *att*R2 = *att*R2recombination site, GFP = Cycle 3 green fluorescent protein (GFP) (C-terminal).

Marker	Apocrine (Celis et al. 2009)	Molecular apocrine (Vranic et al. 2011)
ACSM1	+	/
NR3C4	+	+
BCL2	-	/
CD24	+	/
ERBB2	/	+
ESR1	-	-
GATA3	-	/
HPGD	+	/
NR3C3	-	-
GAPDH	/	/

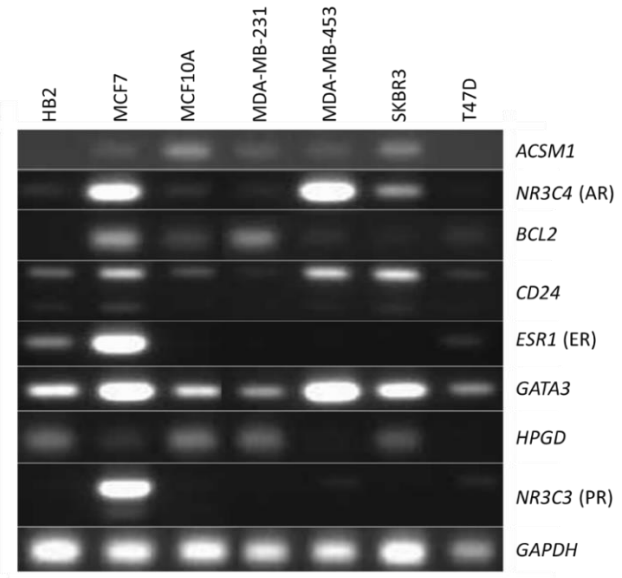

Appendix 12 Identification of an *in vitro* apocrine model. A list of biomarkers for apocrine breast cancer were taken from Celis 2009 (Celis et al., 2009) and Vranic 2011 (Vranic et al., 2011). Vranic et al. also looked at GCDFP-15, EGFR, KRAS, BRAF, p16INK4A. The profiles of the breast cell lines assessed were compared to the exprected apocrine profile. RT-PCR was performed with 35 cycles. * 40 cycles were performed for *ACSM1* as the expression was extremely low. The MDA-MB-453 cell lines has been described as apocrine in the literature.

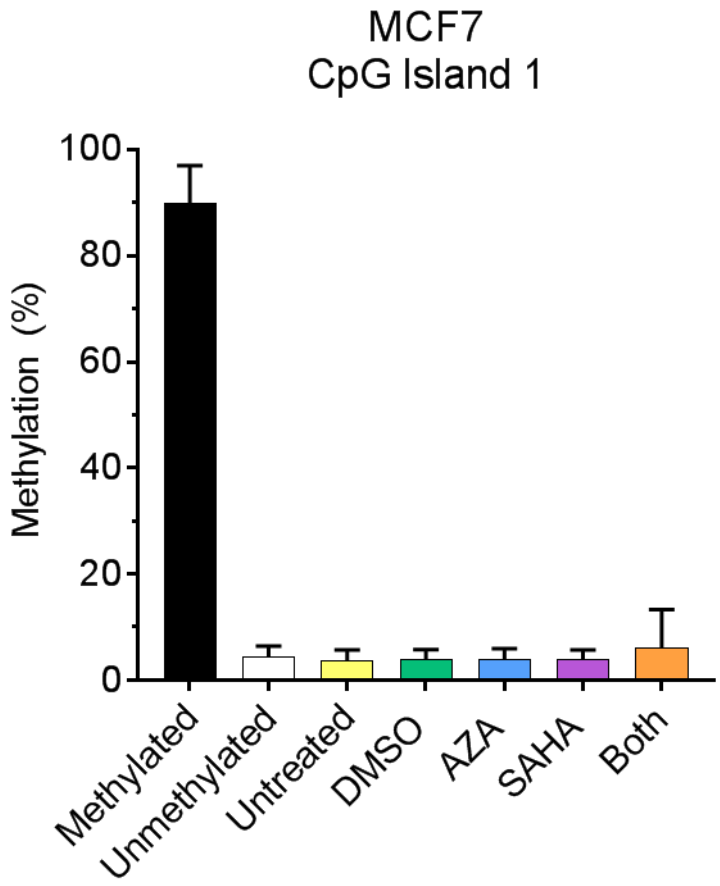

Appendix 13 Methylation analysis of epigenetic drug-treated MCF7 cells at *HPGD* CpG Island 1. Black **=** methylated control DNA, white = unmethylated control DNA, yellow = untreated DNA, green = DMSO control DNA, blue = 5 µM decitabine-treated DNA, purple = 1 µM vorinostat-treated DNA, orange = combined decitabine and vorinostat treatment.

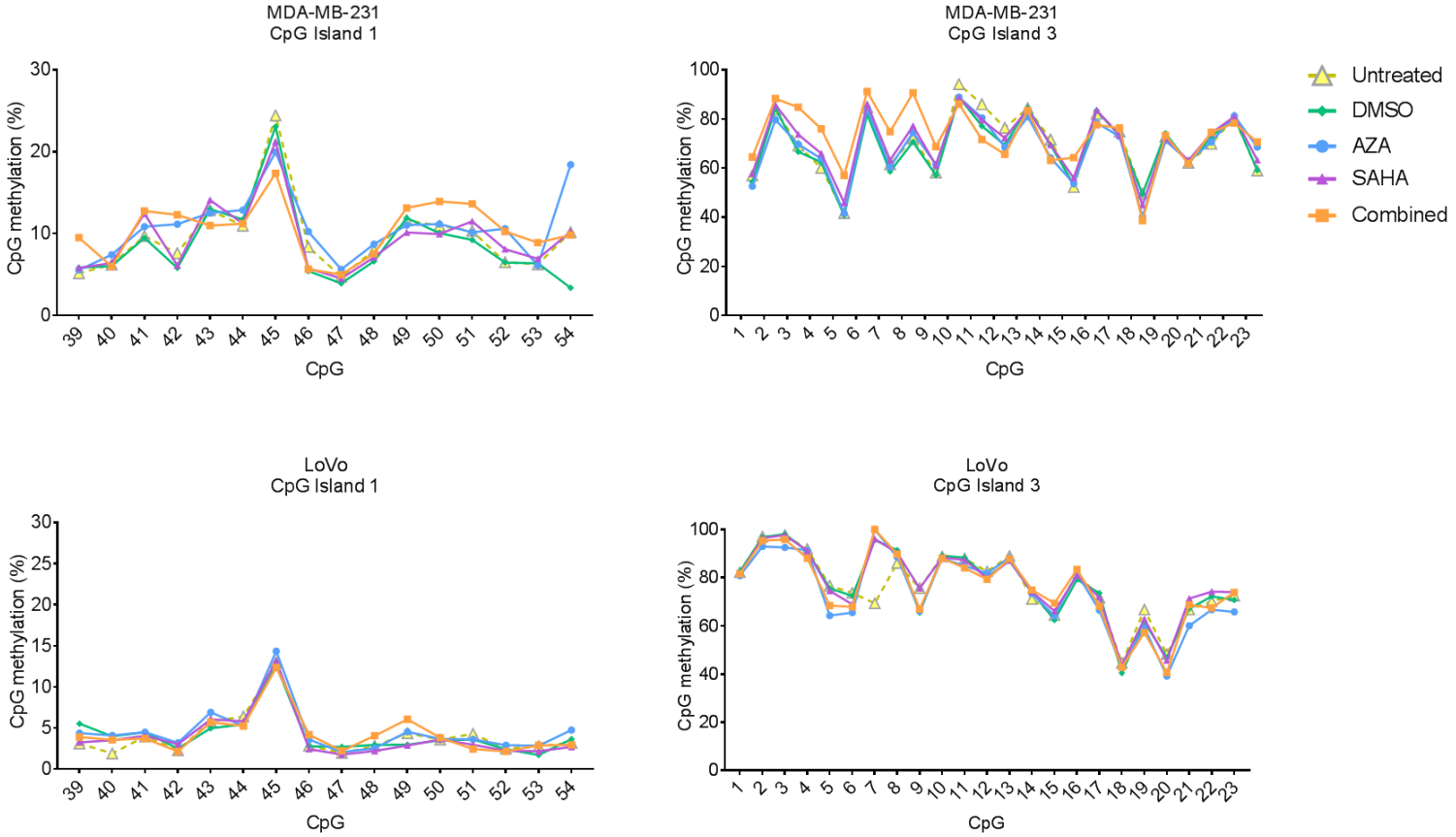

Appendix 14 Individual CpG methylation status after epigenetic drug treatment. Yellow = untreated DNA, green = DMSO control DNA, blue = 5 µM decitabine-treated DNA, purple = 1 µM vorinostat-treated DNA, orange = combined decitabine and vorinostat treatment. Top row = MDA-MB-231, bottom row = LoVo. CpG island 1 product 3 = CpG positions 39-54. CpG island 3 products 1 and 2 = CpG positions 1-23.

Appendix 15 MEXPRESS data analysis for the *HPGD* gene and breast invasive carcinoma samples. Samples sorted by sample type, dark blue=solid normal tissue (left), yellow = metastatic (middle), pale blue = primary solid tumour (right).). Significant p values = black, non-significant =grey. A significant increase in methylation was observed in the cancer samples when compared to normal tissue at twelve CpG sites.

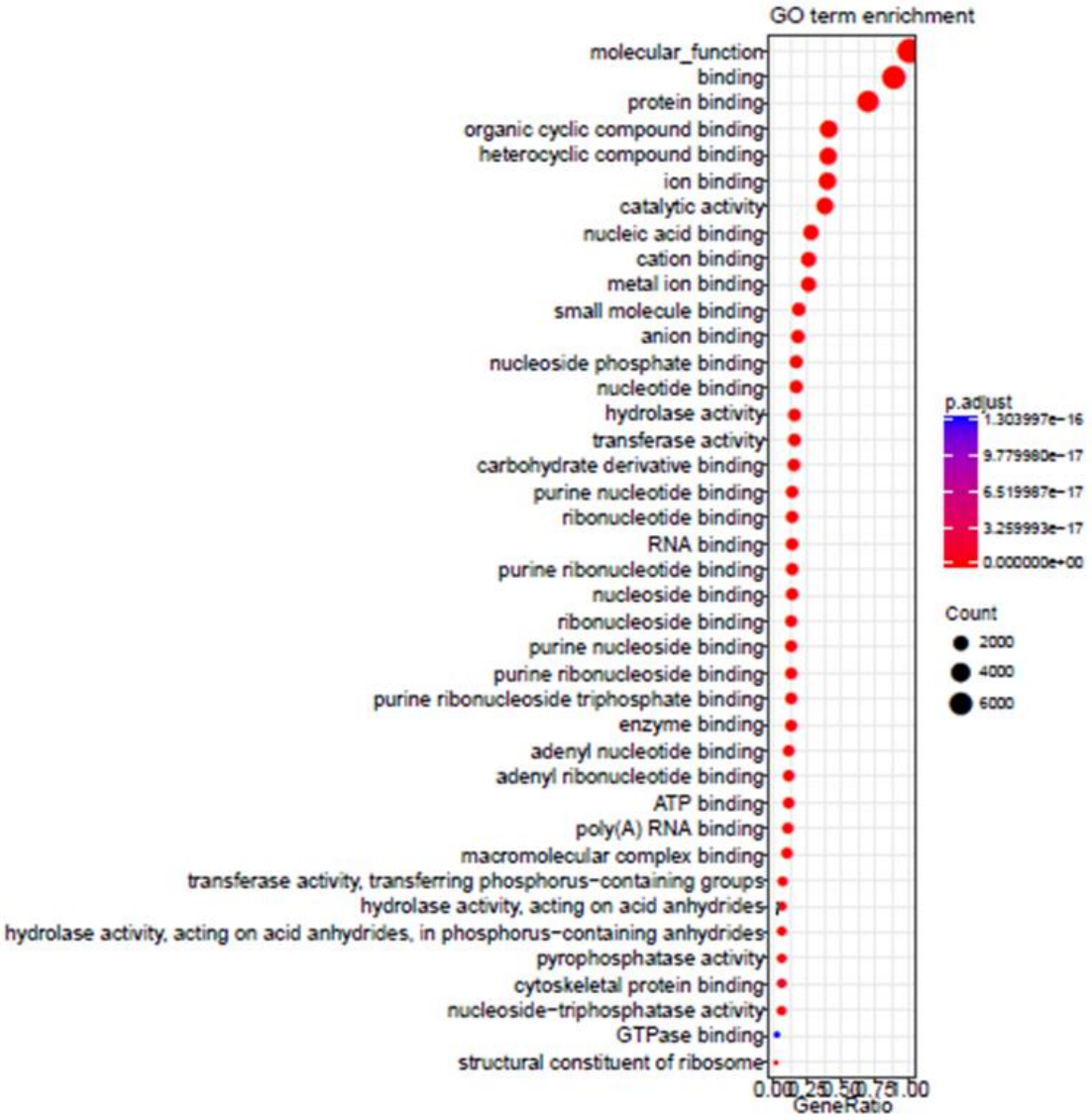

Appendix 16 Top 40 up-regulated GO term enrichment in H14 clone compared to parent MCF7 cell line. GeneRatio = ratio between the number of differentially expressed genes in the pathway and the number of differentially expressed genes. Count = the number of genes in the pathway. Gradient red to blue shows adjusted p value with decreasing significance.

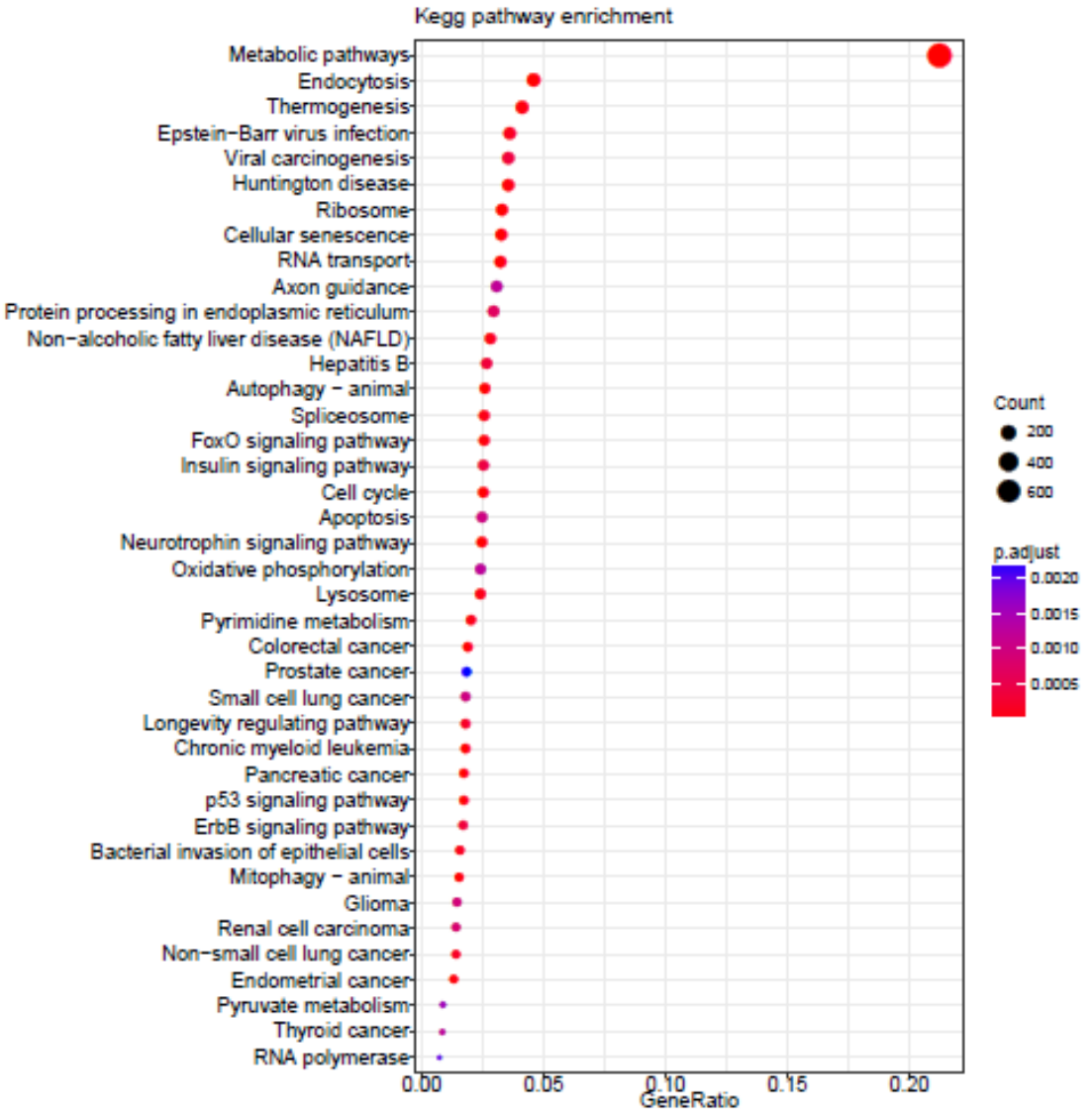

Appendix 17 Top 40 up-regulated KEGG pathway enrichment in H14 clone compared to MCF7 parent cell line. GeneRatio = ratio between the number of differentially expressed genes in the pathway and the number of differentially expressed genes. Count = the number of genes in the pathway. Gradient red to blue shows adjusted p value with decreasing significance.

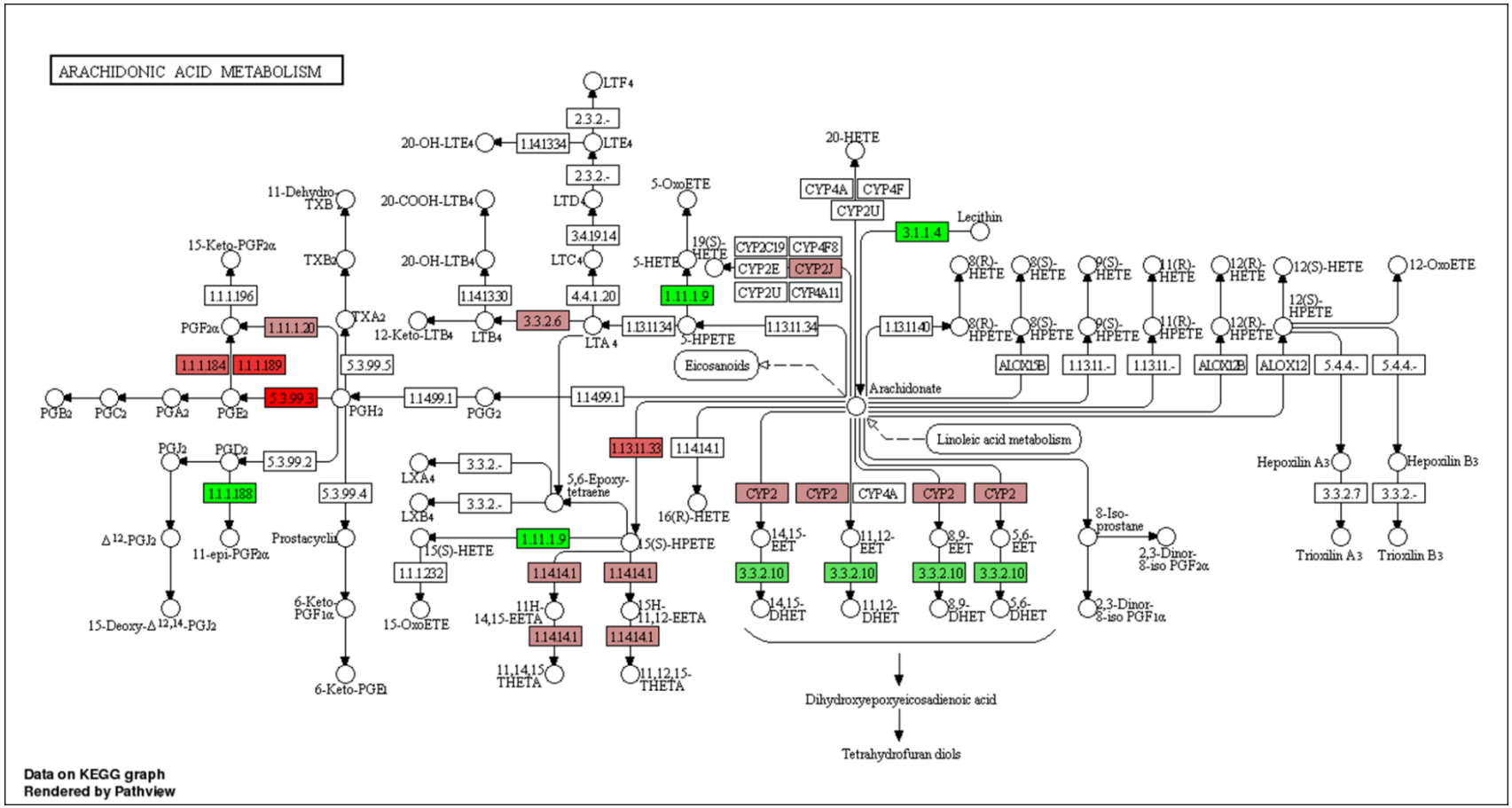

Appendix 18 KEGG arachidonic acid metabolism pathway analysis comparing differentially expressed genes in DMSO-treated parent MCF7 cells and clone H14.
Green = up-regulated, red = down-regulated in H14 compared to MCF7.

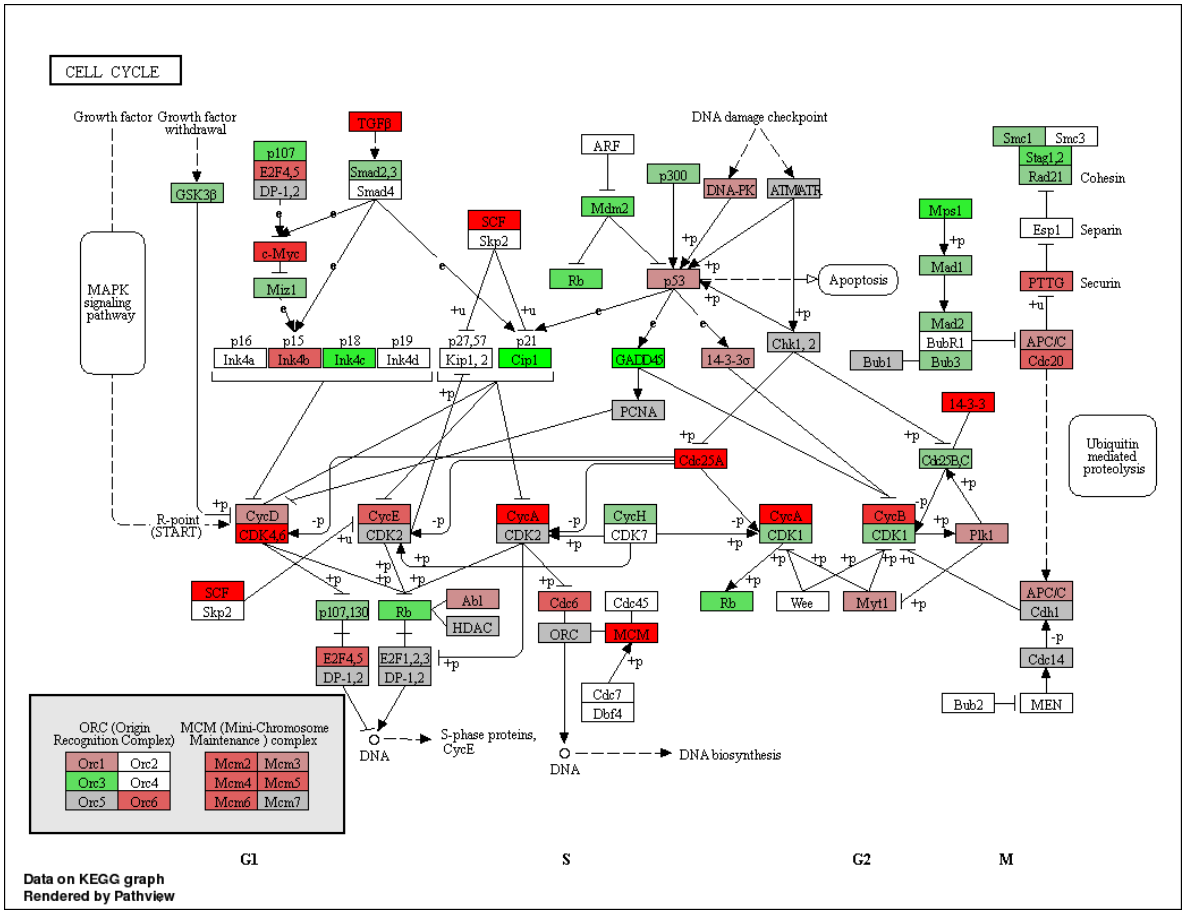

Appendix 19 KEGG cell cycle pathway analysis comparing differentially expressed genes in DMSO-treated parent MCF7 cells and clone H14. Green = up-regulated, red = down-regulated in H14 compared to MCF7 cells.

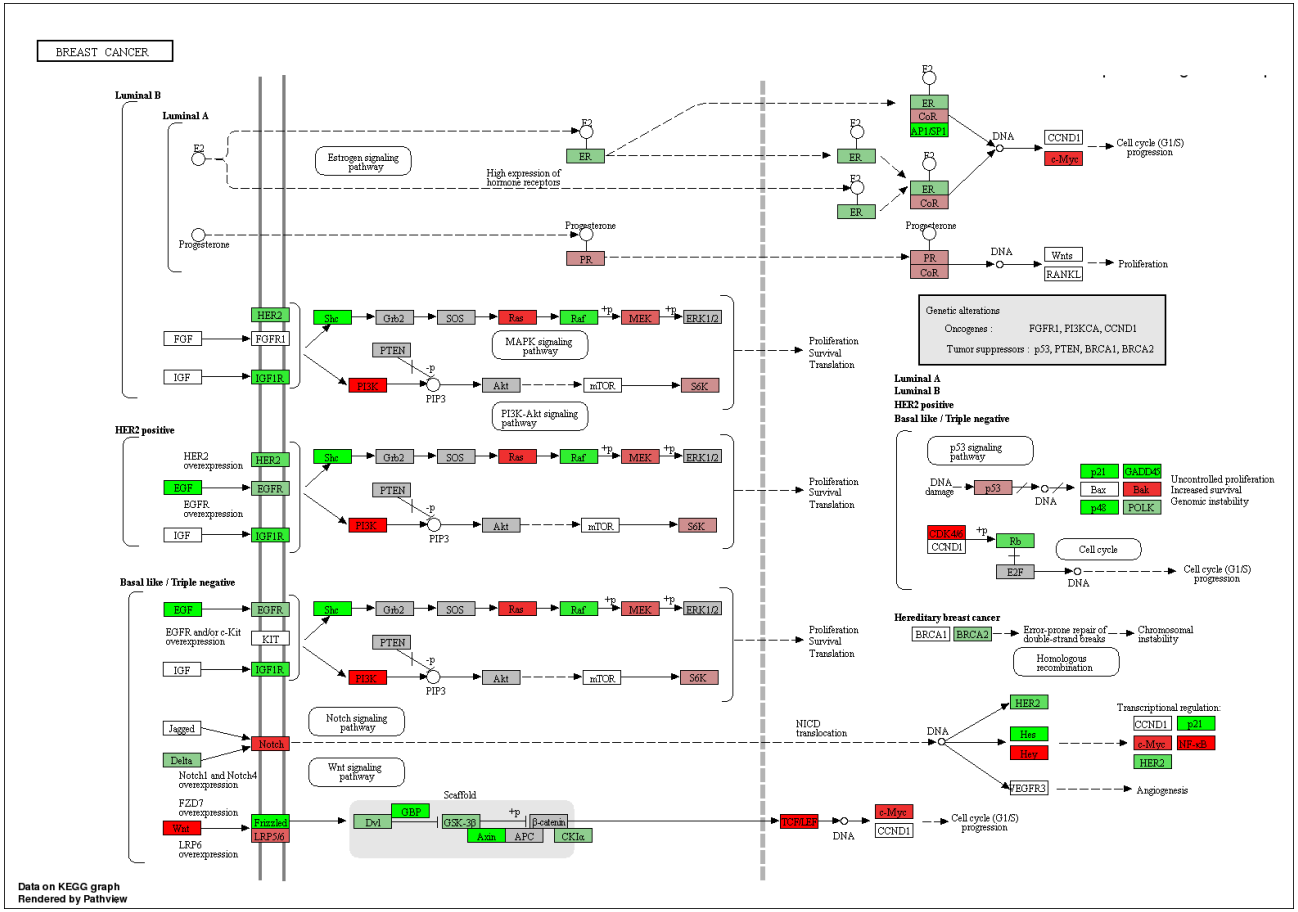

Appendix 20 KEGG breast cancer pathway analysis comparing differentially expressed genes in DMSO-treated MCF7 parent cells and clone H14. Green = up-regulated, red = down-regulated in H14 compared to MCF7 cells.

Bibliography

Abu-Jamous, B., Buffa, F.M., Harris, A.L. and Nandi, A.K. 2017. In vitro downregulated hypoxia transcriptome is associated with poor prognosis in breast cancer. *Mol Cancer.* **16**(1), p105.

Achiwa, H., Yatabe, Y., Hida, T., Kuroishi, T., Kozaki, K., Nakamura, S., Ogawa, M., Sugiura, T., Mitsudomi, T. and Takahashi, T. 1999. Prognostic significance of elevated cyclooxygenase 2 expression in primary, resected lung adenocarcinomas. *Clin Cancer Res.* **5**(5), pp.1001-1005.

Ali, S. and Coombes, R.C. 2000. Estrogen receptor alpha in human breast cancer: occurrence and significance. *J Mammary Gland Biol Neoplasia.* **5**(3), pp.271-281.

Ambika Rajendran, M. 2018. Ultrasound-guided Microbubble in the Treatment of Cancer: A Mini Narrative Review. *Cureus.* **10**(9), pe3256.

Amirkia, V. and Qiubao, P. 2012. Cell-culture Database: Literature-based reference tool for human and mammalian experimentallybased cell culture applications. *Bioinformation.* **8**(5), pp.237-238.

Anderson, B.J. 2008. Paracetamol (Acetaminophen): mechanisms of action. *Paediatr Anaesth.* **18**(10), pp.915-921.

Antoniou, A., Pharoah, P.D., Narod, S., Risch, H.A., Eyfjord, J.E., Hopper, J.L., Loman, N., Olsson, H., Johannsson, O., Borg, A., Pasini, B., Radice, P., Manoukian, S., Eccles, D.M., Tang, N., Olah, E., Anton-Culver, H., Warner, E., Lubinski, J., Gronwald, J., Gorski, B., Tulinius, H., Thorlacius, S., Eerola, H., Nevanlinna, H., Syrjakoski, K., Kallioniemi, O.P., Thompson, D., Evans, C., Peto, J., Lalloo, F., Evans, D.G. and Easton, D.F. 2003. Average risks of breast and ovarian cancer associated with BRCA1 or BRCA2 mutations detected in case Series unselected for family history: a combined analysis of 22 studies. *Am J Hum Genet.* **72**(5), pp.1117-1130.

Appleton, K., Mackay, H.J., Judson, I., Plumb, J.A., McCormick, C., Strathdee, G., Lee, C., Barrett, S., Reade, S., Jadayel, D., Tang, A., Bellenger, K., Mackay, L., Setanoians, A., Schatzlein, A., Twelves, C., Kaye, S.B. and Brown, R. 2007. Phase I and pharmacodynamic trial of the DNA

methyltransferase inhibitor decitabine and carboplatin in solid tumors. *J Clin Oncol.* **25**(29), pp.4603-4609.

Arps, D.P., Healy, P., Zhao, L., Kleer, C.G. and Pang, J.C. 2013. Invasive ductal carcinoma with lobular features: a comparison study to invasive ductal and invasive lobular carcinomas of the breast. *Breast Cancer Res Treat.* **138**(3), pp.719-726.

Auclair, G. and Weber, M. 2012. Mechanisms of DNA methylation and demethylation in mammals. *Biochimie.* **94**(11), pp.2202-2211.

Aysola, K., Desai, A., Welch, C., Xu, J., Qin, Y., Reddy, V., Matthews, R., Owens, C., Okoli, J., Beech, D.J., Piyathilake, C.J., Reddy, S.P. and Rao, V.N. 2013. Triple Negative Breast Cancer - An Overview. *Hereditary Genet.* **2013**(Suppl 2).

Backlund, M.G., Mann, J.R., Holla, V.R., Buchanan, F.G., Tai, H.H., Musiek, E.S., Milne, G.L., Katkuri, S. and DuBois, R.N. 2005. 15-Hydroxyprostaglandin dehydrogenase is down-regulated in colorectal cancer. *J Biol Chem.* **280**(5), pp.3217-3223.

Backlund, M.G., Mann, J.R., Holla, V.R., Shi, Q., Daikoku, T., Dey, S.K. and DuBois, R.N. 2008. Repression of 15-hydroxyprostaglandin dehydrogenase involves histone deacetylase 2 and snail in colorectal cancer. *Cancer Res.* **68**(22), pp.9331-9337.

Badowska-Kozakiewicz, A.M., Liszcz, A., Sobol, M. and Patera, J. 2017. Retrospective evaluation of histopathological examinations in invasive ductal breast cancer of no special type: an analysis of 691 patients. *Arch Med Sci.* **13**(6), pp.1408-1415.

Bae, S.Y., Choi, M.Y., Cho, D.H., Lee, J.E., Nam, S.J. and Yang, J.H. 2011. Mucinous carcinoma of the breast in comparison with invasive ductal carcinoma: clinicopathologic characteristics and prognosis. *J Breast Cancer.* **14**(4), pp.308-313.

Bignold, L.P. 2003. Pathogenetic mechanisms of nuclear pleomorphism of tumour cells based on the mutator phenotype theory of carcinogenesis. *Histol Histopathol.* **18**(2), pp.657-664.

Boocock, D.J., Brown, K., Gibbs, A.H., Sanchez, E., Turteltaub, K.W. and White, I.N. 2002. Identification of human CYP forms involved in the activation of tamoxifen and irreversible binding to DNA. *Carcinogenesis.* **23**(11), pp.1897-1901.

Bos, R., Zhong, H., Hanrahan, C.F., Mommers, E.C., Semenza, G.L., Pinedo, H.M., Abeloff, M.D., Simons, J.W., van Diest, P.J. and van der Wall, E. 2001. Levels of hypoxia-inducible factor-1 alpha during breast carcinogenesis. *J Natl Cancer Inst.* **93**(4), pp.309-314.

Bougnoux, P., Hajjaji, N., Ferrasson, M.N., Giraudeau, B., Couet, C. and Le Floch, O. 2009. Improving outcome of chemotherapy of metastatic breast cancer by docosahexaenoic acid: a phase II trial. *Br J Cancer.* **101**(12), pp.1978-1985.

Branca, G., Ieni, A., Barresi, V., Tuccari, G. and Caruso, R.A. 2017. An Updated Review of Cribriform Carcinomas with Emphasis on Histopathological Diagnosis and Prognostic Significance. *Oncol Rev.* **11**(1), p317.

Bronger, H., Kraeft, S., Schwarz-Boeger, U., Cerny, C., Stockel, A., Avril, S., Kiechle, M. and Schmitt, M. 2012. Modulation of CXCR3 ligand secretion by prostaglandin E2 and cyclooxygenase inhibitors in human breast cancer. *Breast Cancer Res.* **14**(1), pR30.

Buchanan, F.G., Gorden, D.L., Matta, P., Shi, Q., Matrisian, L.M. and DuBois, R.N. 2006. Role of beta-arrestin 1 in the metastatic progression of colorectal cancer. *Proc Natl Acad Sci U S A.* **103**(5), pp.1492-1497.

Buchanan, F.G., Wang, D., Bargiacchi, F. and DuBois, R.N. 2003. Prostaglandin E2 regulates cell migration via the intracellular activation of the epidermal growth factor receptor. *J Biol Chem.* **278**(37), pp.35451-35457.

Bujko, M., Kober, P., Mikula, M., Ligaj, M., Ostrowski, J. and Siedlecki, J.A. 2015. Expression changes of cell-cell adhesion-related genes in colorectal tumors. *Oncol Lett.* **9**(6), pp.2463-2470.

Busch, J., Frank, V., Bachmann, N., Otsuka, A., Oji, V., Metze, D., Shah, K., Danda, S., Watzer, B., Traupe, H., Bolz, H.J., Kabashima, K. and Bergmann, C. 2012. Mutations in the prostaglandin transporter SLCO2A1 cause primary hypertrophic osteoarthropathy with digital clubbing. *J Invest Dermatol.* **132**(10), pp.2473-2476.

Camargo Cde, Q., Mocellin, M.C., Pastore Silva Jde, A., Fabre, M.E., Nunes, E.A. and Trindade, E.B. 2016. Fish oil supplementation during chemotherapy increases posterior time to tumor progression in colorectal cancer. *Nutr Cancer.* **68**(1), pp.70-76.

Cancer Research UK. 2016. *Breast Cancer Statistics.* [Online]. [Accessed 25/03/2019]. Available from: https://www.cancerresearchuk.org/health-professional/cancer-statistics/statistics-by-cancer-type/breast-cancer

Carr, I.M., Camm, N., Taylor, G.R., Charlton, R., Ellard, S., Sheridan, E.G., Markham, A.F. and Bonthron, D.T. 2011. GeneScreen: a program for high-throughput mutation detection in DNA sequence electropherograms. *J Med Genet.* **48**(2), pp.123-130.

Carr, I.M., Valleley, E.M., Cordery, S.F., Markham, A.F. and Bonthron, D.T. 2007. Sequence analysis and editing for bisulphite genomic sequencing projects. *Nucleic Acids Res.* **35**(10), pe79.

Castellone, M.D., Teramoto, H., Williams, B.O., Druey, K.M. and Gutkind, J.S. 2005. Prostaglandin E2 promotes colon cancer cell growth through a Gs-axin-beta-catenin signaling axis. *Science.* **310**(5753), pp.1504-1510.

Castro-Sanchez, L., Agra, N., Llorente Izquierdo, C., Motino, O., Casado, M., Bosca, L. and Martin-Sanz, P. 2013. Regulation of 15-hydroxyprostaglandin dehydrogenase expression in hepatocellular carcinoma. *Int J Biochem Cell Biol.* **45**(11), pp.2501-2511.

Celis, J.E., Cabezon, T., Moreira, J.M., Gromov, P., Gromova, I., Timmermans-Wielenga, V., Iwase, T., Akiyama, F., Honma, N. and Rank, F. 2009. Molecular characterization of apocrine carcinoma of the breast: validation of an apocrine protein signature in a well-defined cohort. *Mol Oncol.* **3**(3), pp.220-237.

Celis, J.E., Gromov, P., Cabezon, T., Moreira, J.M., Friis, E., Jirstrom, K., Llombart-Bosch, A., Timmermans-Wielenga, V., Rank, F. and Gromova, I. 2008. 15-prostaglandin dehydrogenase expression alone or in combination with ACSM1 defines a subgroup of the apocrine molecular subtype of breast carcinoma. *Mol Cell Proteomics.* **7**(10), pp.1795-1809.

Celis, J.E., Gromova, I., Gromov, P., Moreira, J.M., Cabezon, T., Friis, E. and Rank, F. 2006. Molecular pathology of breast apocrine carcinomas: a protein expression signature specific for benign apocrine metaplasia. *FEBS Lett.* **580**(12), pp.2935-2944.

Chandrasekharan, N.V. and Simmons, D.L. 2004. The cyclooxygenases. *Genome Biol.* **5**(9), p241.

Chang, S.H., Liu, C.H., Conway, R., Han, D.K., Nithipatikom, K., Trifan, O.C., Lane, T.F. and Hla, T. 2004. Role of prostaglandin E2-dependent angiogenic switch in cyclooxygenase 2-induced breast cancer progression. *Proc Natl Acad Sci U S A.* **101**(2), pp.591-596.

Chen, H.F., Ma, R.R., He, J.Y., Zhang, H., Liu, X.L., Guo, X.Y. and Gao, P. 2017. Protocadherin 7 inhibits cell migration and invasion through E-cadherin in gastric cancer. *Tumour Biol.* **39**(4), p1010428317697551.

Chen, X., Iliopoulos, D., Zhang, Q., Tang, Q., Greenblatt, M.B., Hatziapostolou, M., Lim, E., Tam, W.L., Ni, M., Chen, Y., Mai, J., Shen, H., Hu, D.Z., Adoro, S., Hu, B., Song, M., Tan, C., Landis, M.D., Ferrari, M., Shin, S.J., Brown, M., Chang, J.C., Liu, X.S. and Glimcher, L.H. 2014. XBP1 promotes triple-negative breast cancer by controlling the HIF1alpha pathway. *Nature.* **508**(7494), pp.103-107.

Chen, Y., Wang, K., Qian, C.N. and Leach, R. 2013. DNA methylation is associated with transcription of Snail and Slug genes. *Biochem Biophys Res Commun.* **430**(3), pp.1083-1090.

Cheng, H.W., Chen, Y.F., Wong, J.M., Weng, C.W., Chen, H.Y., Yu, S.L., Chen, H.W., Yuan, A. and Chen, J.J. 2017. Cancer cells increase endothelial cell tube formation and survival by activating the PI3K/Akt signalling pathway. *J Exp Clin Cancer Res.* **36**(1), p27.

Cheng, P.F., Shakhova, O., Widmer, D.S., Eichhoff, O.M., Zingg, D., Frommel, S.C., Belloni, B., Raaijmakers, M.I., Goldinger, S.M., Santoro, R., Hemmi, S., Sommer, L., Dummer, R. and Levesque, M.P. 2015. Methylation-dependent SOX9 expression mediates invasion in human melanoma cells and is a negative prognostic factor in advanced melanoma. *Genome Biol.* **16**, p42.

Chow, L.W., Yip, A.Y., Loo, W.T., Lam, C.K. and Toi, M. 2008. Celecoxib anti-aromatase neoadjuvant (CAAN) trial for locally advanced breast cancer. *J Steroid Biochem Mol Biol.* **111**(1-2), pp.13-17.

Chow, L.W., Zhu, L., Loo, W.T. and Lui, E.L. 2005. Aberrant methylation of cyclooxygenase-2 in breast cancer patients. *Biomed Pharmacother.* **59 Suppl 2**, pp.S264-267.

Claerhout, S., Lim, J.Y., Choi, W., Park, Y.Y., Kim, K., Kim, S.B., Lee, J.S., Mills, G.B. and Cho, J.Y. 2011. Gene expression signature analysis identifies vorinostat as a candidate therapy for gastric cancer. *PLoS One.* **6**(9), pe24662.

Cockbain, A.J., Volpato, M., Race, A.D., Munarini, A., Fazio, C., Belluzzi, A., Loadman, P.M., Toogood, G.J. and Hull, M.A. 2014. Anticolorectal cancer activity of the omega-3 polyunsaturated fatty acid eicosapentaenoic acid. *Gut.* **63**(11), pp.1760-1768.

Coleman, R., Woodward, E., Brown, J., Cameron, D., Bell, R., Dodwell, D., Keane, M., Gil, M., Davies, C., Burkinshaw, R., Houston, S.J., Grieve, R.J., Barrett-Lee, P.J. and Thorpe, H. 2011. Safety of zoledronic acid and incidence of osteonecrosis of the jaw (ONJ) during adjuvant therapy in a randomised phase III trial (AZURE: BIG 01-04) for women with stage II/III breast cancer. *Breast Cancer Res Treat.* **127**(2), pp.429-438.

Coleman, R.E., Marshall, H., Cameron, D., Dodwell, D., Burkinshaw, R., Keane, M., Gil, M., Houston, S.J., Grieve, R.J., Barrett-Lee, P.J., Ritchie, D., Pugh, J., Gaunt, C., Rea, U., Peterson, J., Davies, C., Hiley, V., Gregory, W., Bell, R. and Investigators, A. 2011. Breast-cancer adjuvant therapy with zoledronic acid. *N Engl J Med.* **365**(15), pp.1396-1405.

Colotta, F., Allavena, P., Sica, A., Garlanda, C. and Mantovani, A. 2009. Cancer-related inflammation, the seventh hallmark of cancer: links to genetic instability. *Carcinogenesis.* **30**(7), pp.1073-1081.

Cong, Y., Qiao, G., Zou, H., Lin, J., Wang, X., Li, X., Li, Y. and Zhu, S. 2015. Invasive cribriform carcinoma of the breast: A report of nine cases and a review of the literature. *Oncol Lett.* **9**(4), pp.1753-1758.

Cooper, S.J., von Roemeling, C.A., Kang, K.H., Marlow, L.A., Grebe, S.K., Menefee, M.E., Tun, H.W., Colon-Otero, G., Perez, E.A. and Copland, J.A. 2012. Reexpression of tumor suppressor, sFRP1, leads to antitumor synergy of combined HDAC and methyltransferase inhibitors in chemoresistant cancers. *Mol Cancer Ther.* **11**(10), pp.2105-2115.

Cortes, J., Andre, F., Goncalves, A., Kummel, S., Martin, M., Schmid, P., Schuetz, F., Swain, S.M., Easton, V., Pollex, E., Deurloo, R. and Dent, R. 2019. IMpassion132 Phase III trial: atezolizumab and chemotherapy in early relapsing metastatic triple-negative breast cancer. *Future Oncol.* **15**(17), pp.1951-1961.

Coyle, C., Cafferty, F.H., Rowley, S., MacKenzie, M., Berkman, L., Gupta, S., Pramesh, C.S., Gilbert, D., Kynaston, H., Cameron, D., Wilson, R.H., Ring, A., Langley, R.E. and Add-Aspirin, i. 2016. ADD-ASPIRIN: A phase III, double-blind, placebo controlled, randomised trial assessing the effects of aspirin on disease recurrence and survival after primary therapy in common non-metastatic solid tumours. *Contemp Clin Trials.* **51**, pp.56-64.

Dawson, M.A. and Kouzarides, T. 2012. Cancer epigenetics: from mechanism to therapy. *Cell.* **150**(1), pp.12-27.

De Leeneer, K., Coene, I., Crombez, B., Simkens, J., Van den Broecke, R., Bols, A., Stragier, B., Vanhoutte, I., De Paepe, A., Poppe, B. and Claes, K. 2012. Prevalence of BRCA1/2 mutations in sporadic breast/ovarian cancer patients and identification of a novel de novo BRCA1 mutation in a patient diagnosed with late onset breast and ovarian cancer: implications for genetic testing. *Breast Cancer Res Treat.* **132**(1), pp.87-95.

Decaestecker, C., Debeir, O., Van Ham, P. and Kiss, R. 2007. Can anti-migratory drugs be screened in vitro? A review of 2D and 3D assays for the quantitative analysis of cell migration. *Med Res Rev.* **27**(2), pp.149-176.

Denkert, C., Winzer, K.J., Muller, B.M., Weichert, W., Pest, S., Kobel, M., Kristiansen, G., Reles, A., Siegert, A., Guski, H. and Hauptmann, S. 2003. Elevated expression of cyclooxygenase-2 is a negative prognostic factor for disease free survival and overall survival in patients with breast carcinoma. *Cancer.* **97**(12), pp.2978-2987.

Dent, R., Trudeau, M., Pritchard, K.I., Hanna, W.M., Kahn, H.K., Sawka, C.A., Lickley, L.A., Rawlinson, E., Sun, P. and Narod, S.A. 2007. Triple-negative breast cancer: clinical features and patterns of recurrence. *Clin Cancer Res.* **13**(15 Pt 1), pp.4429-4434.

Derissen, E.J., Beijnen, J.H. and Schellens, J.H. 2013. Concise drug review: azacitidine and decitabine. *Oncologist.* **18**(5), pp.619-624.

Deshpande, S.P., Mazzeffi, M.A., Strauss, E., Hollis, A. and Tanaka, K.A. 2018. Prostacyclins in Cardiac Surgery: Coming of Age. *Semin Cardiothorac Vasc Anesth.* **22**(3), pp.306-323.

Diesch, J., Zwick, A., Garz, A.K., Palau, A., Buschbeck, M. and Gotze, K.S. 2016. A clinical-molecular update on azanucleoside-based therapy for the treatment of hematologic cancers. *Clin Epigenetics.* **8**, p71.

Ding, Y., Tong, M., Liu, S., Moscow, J.A. and Tai, H.H. 2005. NAD+-linked 15-hydroxyprostaglandin dehydrogenase (15-PGDH) behaves as a tumor suppressor in lung cancer. *Carcinogenesis.* **26**(1), pp.65-72.

Dolskiy, A.A., Pustylnyak, V.O., Yarushkin, A.A., Lemskaya, N.A. and Yudkin, D.V. 2017. Inhibitors of Histone Deacetylases Are Weak Activators of the FMR1 Gene in Fragile X Syndrome Cell Lines. *Biomed Res Int.* **2017**, p3582601.

Dunne, B. and Going, J.J. 2001. Scoring nuclear pleomorphism in breast cancer. *Histopathology.* **39**(3), pp.259-265.

Durning, P., Schor, S.L. and Sellwood, R.A. 1984. Fibroblasts from patients with breast cancer show abnormal migratory behaviour in vitro. *Lancet.* **2**(8408), pp.890-892.

Early Breast Cancer Trialists' Collaborative, G. 2005. Effects of chemotherapy and hormonal therapy for early breast cancer on recurrence and 15-year survival: an overview of the randomised trials. *Lancet.* **365**(9472), pp.1687-1717.

Eberhart, C.E., Coffey, R.J., Radhika, A., Giardiello, F.M., Ferrenbach, S. and DuBois, R.N. 1994. Up-regulation of cyclooxygenase 2 gene expression in human colorectal adenomas and adenocarcinomas. *Gastroenterology.* **107**(4), pp.1183-1188.

Eliyatkin, N., Yalcin, E., Zengel, B., Aktas, S. and Vardar, E. 2015. Molecular Classification of Breast Carcinoma: From Traditional, Old-Fashioned Way to A New Age, and A New Way. *J Breast Health.* **11**(2), pp.59-66.

Ensor, C.M. and Tai, H.H. 1995. 15-Hydroxyprostaglandin dehydrogenase. *J Lipid Mediat Cell Signal.* **12**(2-3), pp.313-319.

Esbona, K., Inman, D., Saha, S., Jeffery, J., Schedin, P., Wilke, L. and Keely, P. 2016. COX-2 modulates mammary tumor progression in response to collagen density. *Breast Cancer Res.* **18**(1), p35.

Evans, I.C., Barnes, J.L., Garner, I.M., Pearce, D.R., Maher, T.M., Shiwen, X., Renzoni, E.A., Wells, A.U., Denton, C.P., Laurent, G.J., Abraham, D.J. and McAnulty, R.J. 2016. Epigenetic regulation of cyclooxygenase-2 by methylation of c8orf4 in pulmonary fibrosis. *Clin Sci (Lond).* **130**(8), pp.575-586.

Fabian, C.J., Kimler, B.F. and Hursting, S.D. 2015. Omega-3 fatty acids for breast cancer prevention and survivorship. *Breast Cancer Res.* **17**, p62.

Fazzari, M.J. and Greally, J.M. 2004. Epigenomics: beyond CpG islands. *Nat Rev Genet.* **5**(6), pp.446-455.

Finak, G., Bertos, N., Pepin, F., Sadekova, S., Souleimanova, M., Zhao, H., Chen, H., Omeroglu, G., Meterissian, S., Omeroglu, A., Hallett, M. and Park, M. 2008. Stromal gene expression predicts clinical outcome in breast cancer. *Nat Med.* **14**(5), pp.518-527.

Finnin, M.S., Donigian, J.R., Cohen, A., Richon, V.M., Rifkind, R.A., Marks, P.A., Breslow, R. and Pavletich, N.P. 1999. Structures of a histone deacetylase homologue bound to the TSA and SAHA inhibitors. *Nature.* **401**(6749), pp.188-193.

Fiorito, E., Katika, M.R. and Hurtado, A. 2013. Cooperating transcription factors mediate the function of estrogen receptor. *Chromosoma.* **122**(1-2), pp.1-12.

Funk, C.D. 2001. Prostaglandins and leukotrienes: advances in eicosanoid biology. *Science.* **294**(5548), pp.1871-1875.

Geninatti Crich, S., Cadenazzi, M., Lanzardo, S., Conti, L., Ruiu, R., Alberti, D., Cavallo, F., Cutrin, J.C. and Aime, S. 2015. Targeting ferritin receptors for the selective delivery of imaging and therapeutic agents to breast cancer cells. *Nanoscale.* **7**(15), pp.6527-6533.

Ghosh, N., Chaki, R., Mandal, V. and Mandal, S.C. 2010. COX-2 as a target for cancer chemotherapy. *Pharmacol Rep.* **62**(2), pp.233-244.

Giercksky, K.E. 2001. COX-2 inhibition and prevention of cancer. *Best Pract Res Clin Gastroenterol.* **15**(5), pp.821-833.

Godone, R.L.N., Leitao, G.M., Araujo, N.B., Castelletti, C.H.M., Lima-Filho, J.L. and Martins, D.B.G. 2018. Clinical and molecular aspects of breast cancer: Targets and therapies. *Biomed Pharmacother.* **106**, pp.14-34.

Gomes, R.N., Felipe da Costa, S. and Colquhoun, A. 2018. Eicosanoids and cancer. *Clinics (Sao Paulo).* **73**(suppl 1), pe530s.

Grandin, M., Mathot, P., Devailly, G., Bidet, Y., Ghantous, A., Favrot, C., Gibert, B., Gadot, N., Puisieux, I., Herceg, Z., Delcros, J.G., Bernet, A., Mehlen, P. and Dante, R. 2016. Inhibition of DNA methylation promotes breast tumor sensitivity to netrin-1 interference. *EMBO Mol Med.* **8**(8), pp.863-877.

Greenland, K.J., Jantke, I., Jenatschke, S., Bracken, K.E., Vinson, C. and Gellersen, B. 2000. The human NAD+-dependent 15-hydroxyprostaglandin dehydrogenase gene promoter is controlled by Ets and activating protein-1 transcription factors and progesterone. *Endocrinology.* **141**(2), pp.581-597.

Gruber, G., Greiner, R.H., Hlushchuk, R., Aebersold, D.M., Altermatt, H.J., Berclaz, G. and Djonov, V. 2004. Hypoxia-inducible factor 1 alpha in high-risk breast cancer: an independent prognostic parameter? *Breast Cancer Res.* **6**(3), pp.R191-198.

Gupta, R.A. and Dubois, R.N. 2001. Colorectal cancer prevention and treatment by inhibition of cyclooxygenase-2. *Nat Rev Cancer.* **1**(1), pp.11-21.

Gyorki, D.E. and Lindeman, G.J. 2008. Macrophages, more than just scavengers: their role in breast development and cancer. *ANZJ Surg.* **78**(6), pp.432-436.

Hahm, K.B., Lim, H.Y., Sohn, S., Kwon, H.J., Lee, K.M., Lee, J.S., Surh, Y.J., Kim, Y.B., Joo, H.J., Kim, W.S. and Cho, S.W. 2002. In vitro evidence of the role of COX-2 in attenuating gastric inflammation and promoting gastric carcinogenesis. *J Environ Pathol Toxicol Oncol.* **21**(2), pp.165-176.

Half, E., Tang, X.M., Gwyn, K., Sahin, A., Wathen, K. and Sinicrope, F.A. 2002. Cyclooxygenase-2 expression in human breast cancers and adjacent ductal carcinoma in situ. *Cancer Res.* **62**(6), pp.1676-1681.

Han, C., Michalopoulos, G.K. and Wu, T. 2006. Prostaglandin E2 receptor EP1 transactivates EGFR/MET receptor tyrosine kinases and enhances invasiveness in human hepatocellular carcinoma cells. *J Cell Physiol.* **207**(1), pp.261-270.

Hanahan, D. and Weinberg, R.A. 2011. Hallmarks of cancer: the next generation. *Cell.* **144**(5), pp.646-674.

Hansen, K.D., Timp, W., Bravo, H.C., Sabunciyan, S., Langmead, B., McDonald, O.G., Wen, B., Wu, H., Liu, Y., Diep, D., Briem, E., Zhang, K., Irizarry, R.A. and Feinberg, A.P. 2011. Increased methylation variation in epigenetic domains across cancer types. *Nat Genet.* **43**(8), pp.768-775.

Harris, R.E., Chlebowski, R.T., Jackson, R.D., Frid, D.J., Ascenseo, J.L., Anderson, G., Loar, A., Rodabough, R.J., White, E., McTiernan, A. and Women's Health, I. 2003. Breast cancer and nonsteroidal anti-inflammatory drugs: prospective results from the Women's Health Initiative. *Cancer Res.* **63**(18), pp.6096-6101.

Hashemi Goradel, N., Najafi, M., Salehi, E., Farhood, B. and Mortezaee, K. 2018. Cyclooxygenase-2 in cancer: A review. *J Cell Physiol.*

Hassiotou, F. and Geddes, D. 2013. Anatomy of the human mammary gland: Current status of knowledge. *Clin Anat.* **26**(1), pp.29-48.

He, G.L., Luo, Z., Yang, J., Shen, T.T., Chen, Y. and Yang, X.S. 2016. Curcumin Ameliorates the Reduction Effect of PGE2 on Fibrillar beta-Amyloid Peptide (1-42)-Induced Microglial Phagocytosis through the Inhibition of EP2-PKA Signaling in N9 Microglial Cells. *PLoS One.* **11**(1), pe0147721.

He, N., Zheng, H., Li, P., Zhao, Y., Zhang, W., Song, F. and Chen, K. 2014. miR-485-5p binding site SNP rs8752 in HPGD gene is associated with breast cancer risk. *PLoS One.* **9**(7), pe102093.

He, Z., Hu, B., Tang, L., Zheng, S., Sun, Y., Sheng, Z., Yao, Y. and Lin, F. 2015. The overexpression of MRP4 is related to multidrug resistance in osteosarcoma cells. *J Cancer Res Ther.* **11**(1), pp.18-23.

Hefti, M.M., Hu, R., Knoblauch, N.W., Collins, L.C., Haibe-Kains, B., Tamimi, R.M. and Beck, A.H. 2013. Estrogen receptor negative/progesterone receptor positive breast cancer is not a reproducible subtype. *Breast Cancer Res.* **15**(4), pR68.

Hesson, L.B., Patil, V., Sloane, M.A., Nunez, A.C., Liu, J., Pimanda, J.E. and Ward, R.L. 2013. Reassembly of nucleosomes at the MLH1 promoter initiates resilencing following decitabine exposure. *PLoS Genet.* **9**(7), pe1003636.

Heyn, H., Carmona, F.J., Gomez, A., Ferreira, H.J., Bell, J.T., Sayols, S., Ward, K., Stefansson, O.A., Moran, S., Sandoval, J., Eyfjord, J.E., Spector, T.D. and Esteller, M. 2013. DNA methylation profiling in breast cancer discordant identical twins identifies DOK7 as novel epigenetic biomarker. *Carcinogenesis.* **34**(1), pp.102-108.

Hippisley-Cox, J. and Coupland, C. 2005. Risk of myocardial infarction in patients taking cyclo-oxygenase-2 inhibitors or conventional non-steroidal anti-inflammatory drugs: population based nested case-control analysis. *BMJ.* **330**(7504), p1366.

Holla, V.R., Backlund, M.G., Yang, P., Newman, R.A. and DuBois, R.N. 2008. Regulation of prostaglandin transporters in colorectal neoplasia. *Cancer Prev Res (Phila).* **1**(2), pp.93-99.

Holmes, M.D., Chen, W.Y., Li, L., Hertzmark, E., Spiegelman, D. and Hankinson, S.E. 2010. Aspirin intake and survival after breast cancer. *J Clin Oncol.* **28**(9), pp.1467-1472.

Hossain, P., Kawar, B. and El Nahas, M. 2007. Obesity and diabetes in the developing world--a growing challenge. *N Engl J Med.* **356**(3), pp.213-215.

Howe, L.R., Subbaramaiah, K., Kent, C.V., Zhou, X.K., Chang, S.H., Hla, T., Jakobsson, P.J., Hudis, C.A. and Dannenberg, A.J. 2013. Genetic deletion of microsomal prostaglandin E synthase-1 suppresses mouse mammary tumor growth and angiogenesis. *Prostaglandins Other Lipid Mediat.* **106**, pp.99-105.

Howell, A., Anderson, A.S., Clarke, R.B., Duffy, S.W., Evans, D.G., Garcia-Closas, M., Gescher, A.J., Key, T.J., Saxton, J.M. and Harvie, M.N. 2014. Risk determination and prevention of breast cancer. *Breast Cancer Res.* **16**(5), p446.

Huang, G., Eisenberg, R., Yan, M., Monti, S., Lawrence, E., Fu, P., Walbroehl, J., Lowenberg, E., Golub, T., Merchan, J., Tenen, D.G., Markowitz, S.D. and Halmos, B. 2008. 15-Hydroxyprostaglandin dehydrogenase is a target of hepatocyte nuclear factor 3beta and a tumor suppressor in lung cancer. *Cancer Res.* **68**(13), pp.5040-5048.

Huang, J. and Guo, L. 2017. Knockdown of SOX9 Inhibits the Proliferation, Invasion, and EMT in Thyroid Cancer Cells. *Oncol Res.* **25**(2), pp.167-176.

Huang, S., Li, X., Yusufzai, T.M., Qiu, Y. and Felsenfeld, G. 2007. USF1 recruits histone modification complexes and is critical for maintenance of a chromatin barrier. *Mol Cell Biol.* **27**(22), pp.7991-8002.

Huang, T.H., Perry, M.R. and Laux, D.E. 1999. Methylation profiling of CpG islands in human breast cancer cells. *Hum Mol Genet.* **8**(3), pp.459-470.

Huang, X., Taeb, S., Jahangiri, S., Korpela, E., Cadonic, I., Yu, N., Krylov, S.N., Fokas, E., Boutros, P.C. and Liu, S.K. 2015. miR-620 promotes tumor radioresistance by targeting 15-hydroxyprostaglandin dehydrogenase (HPGD). *Oncotarget.* **6**(26), pp.22439-22451.

Isono, M., Suzuki, T., Hosono, K., Hayashi, I., Sakagami, H., Uematsu, S., Akira, S., DeClerck, Y.A., Okamoto, H. and Majima, M. 2011. Microsomal prostaglandin E synthase-1 enhances bone cancer growth and bone cancer-related pain behaviors in mice. *Life Sci.* **88**(15-16), pp.693-700.

Issa, J.P. and Kantarjian, H.M. 2009. Targeting DNA methylation. *Clin Cancer Res.* **15**(12), pp.3938-3946.

Ito, H., Duxbury, M., Benoit, E., Clancy, T.E., Zinner, M.J., Ashley, S.W. and Whang, E.E. 2004. Prostaglandin E2 enhances pancreatic cancer invasiveness through an Ets-1-dependent induction of matrix metalloproteinase-2. *Cancer Res.* **64**(20), pp.7439-7446.

Iyengar, N.M., Hudis, C.A. and Gucalp, A. 2013. Omega-3 fatty acids for the prevention of breast cancer: an update and state of the science. *Curr Breast Cancer Rep.* **5**(3), pp.247-254.

Jana, D., Sarkar, D.K., Ganguly, S., Saha, S., Sa, G., Manna, A.K., Banerjee, A. and Mandal, S. 2014. Role of Cyclooxygenase 2 (COX-2) in Prognosis of Breast Cancer. *Indian J Surg Oncol.* **5**(1), pp.59-65.

Jang, T.J., Ji, Y.S. and Jung, K.H. 2008. Decreased expression of 15-hydroxyprostaglandin dehydrogenase in gastric carcinomas. *Yonsei Med J.* **49**(6), pp.917-922.

Jania, L.A., Chandrasekharan, S., Backlund, M.G., Foley, N.A., Snouwaert, J., Wang, I.M., Clark, P., Audoly, L.P. and Koller, B.H. 2009. Microsomal prostaglandin E synthase-2 is not essential for in vivo prostaglandin E2 biosynthesis. *Prostaglandins Other Lipid Mediat.* **88**(3-4), pp.73-81.

Jin, Y., Smith, C.L., Hu, L., Campanale, K.M., Stoltz, R., Huffman, L.G., Jr., McNearney, T.A., Yang, X.Y., Ackermann, B.L., Dean, R., Regev, A. and Landschulz, W. 2016. Pharmacodynamic comparison of LY3023703, a novel microsomal prostaglandin e synthase 1 inhibitor, with celecoxib. *Clin Pharmacol Ther.* **99**(3), pp.274-284.

Jones, M.E., Schoemaker, M.J., Wright, L.B., Ashworth, A. and Swerdlow, A.J. 2017. Smoking and risk of breast cancer in the Generations Study cohort. *Breast Cancer Res.* **19**(1), p118.

Judson, B.L., Miyaki, A., Kekatpure, V.D., Du, B., Gilleaudeau, P., Sullivan-Whalen, M., Mohebati, A., Nair, S., Boyle, J.O., Granstein, R.D., Subbaramaiah, K., Krueger, J.G. and Dannenberg, A.J. 2010. UV radiation inhibits 15-hydroxyprostaglandin dehydrogenase levels in human skin: evidence of transcriptional suppression. *Cancer Prev Res (Phila).* **3**(9), pp.1104-1111.

Kaliberova, L.N., Kusmartsev, S.A., Krendelchtchikova, V., Stockard, C.R., Grizzle, W.E., Buchsbaum, D.J. and Kaliberov, S.A. 2009. Experimental cancer therapy using restoration of NAD+ -linked 15-hydroxyprostaglandin dehydrogenase expression. *Mol Cancer Ther.* **8**(11), pp.3130-3139.

Kalinski, P. 2012. Regulation of immune responses by prostaglandin E2. *J Immunol.* **188**(1), pp.21-28.

Kaminska, M., Ciszewski, T., Lopacka-Szatan, K., Miotla, P. and Staroslawska, E. 2015. Breast cancer risk factors. *Prz Menopauzalny.* **14**(3), pp.196-202.

Kaminskas, E., Farrell, A., Abraham, S., Baird, A., Hsieh, L.S., Lee, S.L., Leighton, J.K., Patel, H., Rahman, A., Sridhara, R., Wang, Y.C., Pazdur, R. and Fda. 2005. Approval summary: azacitidine for treatment of myelodysplastic syndrome subtypes. *Clin Cancer Res.* **11**(10), pp.3604-3608.

Kang, J.Y., Song, S.H., Yun, J., Jeon, M.S., Kim, H.P., Han, S.W. and Kim, T.Y. 2015. Disruption of CTCF/cohesin-mediated high-order chromatin structures by DNA methylation downregulates PTGS2 expression. *Oncogene.* **34**(45), pp.5677-5684.

Kar, S., Sengupta, D., Deb, M., Shilpi, A., Parbin, S., Rath, S.K., Pradhan, N., Rakshit, M. and Patra, S.K. 2014. Expression profiling of DNA methylation-mediated epigenetic gene-silencing factors in breast cancer. *Clin Epigenetics.* **6**(1), p20.

Karagiannis, G.S., Poutahidis, T., Erdman, S.E., Kirsch, R., Riddell, R.H. and Diamandis, E.P. 2012. Cancer-associated fibroblasts drive the progression of metastasis through both paracrine and mechanical pressure on cancer tissue. *Mol Cancer Res.* **10**(11), pp.1403-1418.

Karahoca, M. and Momparler, R.L. 2013. Pharmacokinetic and pharmacodynamic analysis of 5-aza-2'-deoxycytidine (decitabine) in the design of its dose-schedule for cancer therapy. *Clin Epigenetics.* **5**(1), p3.

Kargi, A., Uysal, M., Bozcuk, H., Coskun, H.S., Savas, B. and Ozdogan, M. 2013. The importance of COX-2 expression as prognostic factor in early breast cancer. *J BUON.* **18**(3), pp.579-584.

Kastl, L., Brown, I. and Schofield, A.C. 2010. Effects of decitabine on the expression of selected endogenous control genes in human breast cancer cells. *Mol Cell Probes.* **24**(2), pp.87-92.

Kawamori, T., Uchiya, N., Nakatsugi, S., Watanabe, K., Ohuchida, S., Yamamoto, H., Maruyama, T., Kondo, K., Sugimura, T. and Wakabayashi, K. 2001. Chemopreventive effects of ONO-8711, a selective prostaglandin E receptor EP(1) antagonist, on breast cancer development. *Carcinogenesis.* **22**(12), pp.2001-2004.

Kim, H.S., Moon, H.G., Han, W., Yom, C.K., Kim, W.H., Kim, J.H. and Noh, D.Y. 2012. COX2 overexpression is a prognostic marker for Stage III breast cancer. *Breast Cancer Res Treat.* **132**(1), pp.51-59.

Kim, J., Yang, P., Suraokar, M., Sabichi, A.L., Llansa, N.D., Mendoza, G., Subbarayan, V., Logothetis, C.J., Newman, R.A., Lippman, S.M. and Menter, D.G. 2005. Suppression of prostate tumor cell growth by stromal cell prostaglandin D synthase-derived products. *Cancer Res.* **65**(14), pp.6189-6198.

Kim, J.E., Ahn, H.J., Ahn, J.H., Yoon, D.H., Kim, S.B., Jung, K.H., Gong, G.Y., Kim, M.J., Son, B.H. and Ahn, S.H. 2012. Impact of triple-negative breast cancer phenotype on prognosis in patients with stage I breast cancer. *J Breast Cancer.* **15**(2), pp.197-202.

Klein, T., Benders, J., Roth, F., Baudler, M., Siegle, I. and Komhoff, M. 2015. Expression of Prostacyclin-Synthase in Human Breast Cancer: Negative Prognostic Factor and Protection against Cell Death In Vitro. *Mediators Inflamm.* **2015**, p864136.

Kloten, V., Becker, B., Winner, K., Schrauder, M.G., Fasching, P.A., Anzeneder, T., Veeck, J., Hartmann, A., Knuchel, R. and Dahl, E. 2013. Promoter hypermethylation of the tumor-suppressor genes ITIH5, DKK3, and RASSF1A as novel biomarkers for blood-based breast cancer screening. *Breast Cancer Res.* **15**(1), pR4.

Koch, A., De Meyer, T., Jeschke, J. and Van Criekinge, W. 2015. MEXPRESS: visualizing expression, DNA methylation and clinical TCGA data. *BMC Genomics.* **16**, p636.

Kochel, T.J. and Fulton, A.M. 2015. Multiple drug resistance-associated protein 4 (MRP4), prostaglandin transporter (PGT), and 15-hydroxyprostaglandin dehydrogenase (15-PGDH) as determinants of PGE2 levels in cancer. *Prostaglandins Other Lipid Mediat.* **116-117**, pp.99-103.

Kochel, T.J., Goloubeva, O.G. and Fulton, A.M. 2016. Upregulation of Cyclooxygenase-2/Prostaglandin E2 (COX-2/PGE2) Pathway Member Multiple Drug Resistance-Associated Protein 4 (MRP4) and Downregulation of Prostaglandin Transporter (PGT) and 15-Prostaglandin Dehydrogenase (15-PGDH) in Triple-Negative Breast Cancer. *Breast Cancer (Auckl).* **10**, pp.61-70.

Kochel, T.J., Reader, J.C., Ma, X., Kundu, N. and Fulton, A.M. 2017. Multiple drug resistance-associated protein (MRP4) exports prostaglandin E2 (PGE2) and contributes to metastasis in basal/triple negative breast cancer. *Oncotarget.* **8**(4), pp.6540-6554.

Kock, A., Larsson, K., Bergqvist, F., Eissler, N., Elfman, L.H.M., Raouf, J., Korotkova, M., Johnsen, J.I., Jakobsson, P.J. and Kogner, P. 2018. Inhibition of Microsomal Prostaglandin E Synthase-1 in Cancer-Associated Fibroblasts Suppresses Neuroblastoma Tumor Growth. *EBioMedicine.* **32**, pp.84-92.

Krysan, K., Reckamp, K.L., Dalwadi, H., Sharma, S., Rozengurt, E., Dohadwala, M. and Dubinett, S.M. 2005. Prostaglandin E2 activates mitogen-activated protein kinase/Erk pathway signaling and cell proliferation in non-small cell lung cancer cells in an epidermal growth factor receptor-independent manner. *Cancer Res.* **65**(14), pp.6275-6281.

Kumar, S., Desmedt, C., Larsimont, D., Sotiriou, C. and Goormaghtigh, E. 2013. Change in the microenvironment of breast cancer studied by FTIR imaging. *Analyst.* **138**(14), pp.4058-4065.

Lamouille, S., Xu, J. and Derynck, R. 2014. Molecular mechanisms of epithelial-mesenchymal transition. *Nat Rev Mol Cell Biol.* **15**(3), pp.178-196.

Landskron, G., De la Fuente, M., Thuwajit, P., Thuwajit, C. and Hermoso, M.A. 2014. Chronic inflammation and cytokines in the tumor microenvironment. *J Immunol Res.* **2014**, p149185.

Lee, E.J., Choi, E.M., Kim, S.R., Park, J.H., Kim, H., Ha, K.S., Kim, Y.M., Kim, S.S., Choe, M., Kim, J.I. and Han, J.A. 2007. Cyclooxygenase-2 promotes cell proliferation, migration and invasion in U2OS human osteosarcoma cells. *Exp Mol Med.* **39**(4), pp.469-476.

Lee, H.Z., Kwitkowski, V.E., Del Valle, P.L., Ricci, M.S., Saber, H., Habtemariam, B.A., Bullock, J., Bloomquist, E., Li Shen, Y., Chen, X.H., Brown, J., Mehrotra, N., Dorff, S., Charlab, R., Kane, R.C., Kaminskas, E., Justice, R., Farrell, A.T. and Pazdur, R. 2015. FDA Approval: Belinostat for the Treatment of Patients with Relapsed or Refractory Peripheral T-cell Lymphoma. *Clin Cancer Res.* **21**(12), pp.2666-2670.

Lee, J. and Huang, S. 2013. Cancer Epigenetics: Mechanisms and Crosstalk of a HDAC Inhibitor, Vorinostat. *Chemotherapy (Los Angel).* **2**(111).

Lee, J.J., Natsuizaka, M., Ohashi, S., Wong, G.S., Takaoka, M., Michaylira, C.Z., Budo, D., Tobias, J.W., Kanai, M., Shirakawa, Y., Naomoto, Y., Klein-Szanto, A.J., Haase, V.H. and Nakagawa, H. 2010. Hypoxia activates the cyclooxygenase-2-prostaglandin E synthase axis. *Carcinogenesis.* **31**(3), pp.427-434.

Leek, R.D., Lewis, C.E., Whitehouse, R., Greenall, M., Clarke, J. and Harris, A.L. 1996. Association of macrophage infiltration with angiogenesis and prognosis in invasive breast carcinoma. *Cancer Res.* **56**(20), pp.4625-4629.

Lehtinen, L., Vainio, P., Wikman, H., Reemts, J., Hilvo, M., Issa, R., Pollari, S., Brandt, B., Oresic, M., Pantel, K., Kallioniemi, O. and Iljin, K. 2012. 15-Hydroxyprostaglandin dehydrogenase associates with poor prognosis in breast cancer, induces epithelial-mesenchymal transition, and promotes cell migration in cultured breast cancer cells. *J Pathol.* **226**(4), pp.674-686.

Lentacker, I., Geers, B., Demeester, J., De Smedt, S.C. and Sanders, N.N. 2010. Design and evaluation of doxorubicin-containing microbubbles for ultrasound-triggered doxorubicin delivery: cytotoxicity and mechanisms involved. *Mol Ther.* **18**(1), pp.101-108.

Leonard, G.D. and Swain, S.M. 2004. Ductal carcinoma in situ, complexities and challenges. *J Natl Cancer Inst.* **96**(12), pp.906-920.

Li, A.M., Tian, A.X., Zhang, R.X., Ge, J., Sun, X. and Cao, X.C. 2013. Protocadherin-7 induces bone metastasis of breast cancer. *Biochem Biophys Res Commun.* **436**(3), pp.486-490.

Li, E. and Zhang, Y. 2014. DNA methylation in mammals. *Cold Spring Harb Perspect Biol.* **6**(5), pa019133.

Li, H.Y., McSharry, M., Walker, D., Johnson, A., Kwak, J., Bullock, B., Neuwelt, A., Poczobutt, J.M., Sippel, T.R., Keith, R.L., Weiser-Evans, M.C.M., Clambey, E. and Nemenoff, R.A. 2018. Targeted overexpression of prostacyclin synthase inhibits lung tumor progression by recruiting CD4+ T lymphocytes in tumors that express MHC class II. *Oncoimmunology.* **7**(5), pe1423182.

Li, L., Yang, F., Wang, X., Hu, J., Yang, L., Tang, C., Wu, Y., Miao, K., Liu, R. and Shou, T. 2014. Effect of 15-hydroxyprostaglandin dehydrogenase gene on the proliferation of gastric cancer cell murine forestomach carcinoma. *Exp Ther Med.* **7**(1), pp.290-294.

Li, M., Xie, J., Cheng, L., Chang, B., Wang, Y., Lan, X., Zhang, D., Yin, Y. and Cheng, N. 2008. Suppression of invasive properties of colorectal carcinoma SW480 cells by 15-hydroxyprostaglandin dehydrogenase gene. *Cancer Invest.* **26**(9), pp.905-912.

Li, S., Xu, X., Jiang, M., Bi, Y., Xu, J. and Han, M. 2015. Lipopolysaccharide induces inflammation and facilitates lung metastasis in a breast cancer model via the prostaglandin E2-EP2 pathway. *Mol Med Rep.* **11**(6), pp.4454-4462.

Li, Y., Li, S., Sun, D., Song, L. and Liu, X. 2014. Expression of 15-hydroxyprostaglandin dehydrogenase and cyclooxygenase-2 in non-small cell lung cancer: Correlations with angiogenesis and prognosis. *Oncol Lett.* **8**(4), pp.1589-1594.

Lim, S.P., Wong, N.C., Suetani, R.J., Ho, K., Ng, J.L., Neilsen, P.M., Gill, P.G., Kumar, R. and Callen, D.F. 2012. Specific-site methylation of tumour suppressor ANKRD11 in breast cancer. *Eur J Cancer.* **48**(17), pp.3300-3309.

Liu, Z., Li, M., Jiang, Z. and Wang, X. 2018. A Comprehensive Immunologic Portrait of Triple-Negative Breast Cancer. *Transl Oncol.* **11**(2), pp.311-329.

Liu, Z., Wang, X., Lu, Y., Du, R., Luo, G., Wang, J., Zhai, H., Zhang, F., Wen, Q., Wu, K. and Fan, D. 2010. 15-Hydroxyprostaglandin dehydrogenase is a tumor suppressor of human gastric cancer. *Cancer Biol Ther.* **10**(8), pp.780-787.

Liu, Z., Wang, X., Lu, Y., Han, S., Zhang, F., Zhai, H., Lei, T., Liang, J., Wang, J., Wu, K. and Fan, D. 2008. Expression of 15-PGDH is downregulated by COX-2 in gastric cancer. *Carcinogenesis.* **29**(6), pp.1219-1227.

Liu, Z.J., Semenza, G.L. and Zhang, H.F. 2015. Hypoxia-inducible factor 1 and breast cancer metastasis. *J Zhejiang Univ Sci B.* **16**(1), pp.32-43.

Lodygin, D., Epanchintsev, A., Menssen, A., Diebold, J. and Hermeking, H. 2005. Functional epigenomics identifies genes frequently silenced in prostate cancer. *Cancer Res.* **65**(10), pp.4218-4227.

Lou, L.H., Jing, D.D., Lai, Y.X., Lu, Y.Y., Li, J.K. and Wu, K. 2012. 15-PGDH is reduced and induces apoptosis and cell cycle arrest in gastric carcinoma. *World J Gastroenterol.* **18**(10), pp.1028-1037.

Lu, L., Byrnes, K., Han, C., Wang, Y. and Wu, T. 2014. miR-21 targets 15-PGDH and promotes cholangiocarcinoma growth. *Mol Cancer Res.* **12**(6), pp.890-900.

Ma, C., Liu, Y., Wang, Y., Zhang, C., Yao, H., Ma, J., Zhang, L., Zhang, D., Shen, T. and Zhu, D. 2014. Hypoxia activates 15-PGDH and its metabolite 15-KETE to promote pulmonary artery endothelial cells proliferation via ERK1/2 signalling. *Br J Pharmacol.* **171**(14), pp.3352-3363.

Ma, X., Kundu, N., Rifat, S., Walser, T. and Fulton, A.M. 2006. Prostaglandin E receptor EP4 antagonism inhibits breast cancer metastasis. *Cancer Res.* **66**(6), pp.2923-2927.

Ma, X., Yang, Q., Wilson, K.T., Kundu, N., Meltzer, S.J. and Fulton, A.M. 2004. Promoter methylation regulates cyclooxygenase expression in breast cancer. *Breast Cancer Res.* **6**(4), pp.R316-321.

Mahmoud, S.M., Lee, A.H., Paish, E.C., Macmillan, R.D., Ellis, I.O. and Green, A.R. 2012. Tumour-infiltrating macrophages and clinical outcome in breast cancer. *J Clin Pathol.* **65**(2), pp.159-163.

Makki, J. 2015. Diversity of Breast Carcinoma: Histological Subtypes and Clinical Relevance. *Clin Med Insights Pathol.* **8**, pp.23-31.

Malachi, T., Chaimoff, C., Feller, N. and Halbrecht, I. 1981. Prostaglandin E2 and cyclic AMP in tumor and plasma of breast cancer patients. *J Cancer Res Clin Oncol.* **102**(1), pp.71-79.

Malik, P. and Cashen, A.F. 2014. Decitabine in the treatment of acute myeloid leukemia in elderly patients. *Cancer Manag Res.* **6**, pp.53-61.

Mann, B.S., Johnson, J.R., Cohen, M.H., Justice, R. and Pazdur, R. 2007. FDA approval summary: vorinostat for treatment of advanced primary cutaneous T-cell lymphoma. *Oncologist.* **12**(10), pp.1247-1252.

Mann, J.R., Backlund, M.G., Buchanan, F.G., Daikoku, T., Holla, V.R., Rosenberg, D.W., Dey, S.K. and DuBois, R.N. 2006. Repression of prostaglandin dehydrogenase by epidermal growth factor and snail increases prostaglandin E2 and promotes cancer progression. *Cancer Res.* **66**(13), pp.6649-6656.

Markosyan, N., Chen, E.P., Ndong, V.N., Yao, Y., Sterner, C.J., Chodosh, L.A., Lawson, J.A., Fitzgerald, G.A. and Smyth, E.M. 2011. Deletion of cyclooxygenase 2 in mouse mammary epithelial cells delays breast cancer onset through augmentation of type 1 immune responses in tumors. *Carcinogenesis.* **32**(10), pp.1441-1449.

Marks, P.A. and Dokmanovic, M. 2005. Histone deacetylase inhibitors: discovery and development as anticancer agents. *Expert Opin Investig Drugs.* **14**(12), pp.1497-1511.

Martin, L.A., Davies, G.L., Weigel, M.T., Betambeau, N., Hills, M.J., Salter, J., Walsh, G., A'Hern, R. and Dowsett, M. 2010. Pre-surgical study of the biological effects of the selective cyclo-oxygenase-2 inhibitor celecoxib in patients with primary breast cancer. *Breast Cancer Res Treat.* **123**(3), pp.829-836.

Mathsyaraja, H. and Ostrowski, M.C. 2012. Setting Snail2's pace during EMT. *Nat Cell Biol.* **14**(11), pp.1122-1123.

Maxwell, P.H., Dachs, G.U., Gleadle, J.M., Nicholls, L.G., Harris, A.L., Stratford, I.J., Hankinson, O., Pugh, C.W. and Ratcliffe, P.J. 1997. Hypoxia-inducible factor-1 modulates gene expression in solid tumors and influences both angiogenesis and tumor growth. *Proc Natl Acad Sci U S A.* **94**(15), pp.8104-8109.

Medrek, C., Ponten, F., Jirstrom, K. and Leandersson, K. 2012. The presence of tumor associated macrophages in tumor stroma as a prognostic marker for breast cancer patients. *BMC Cancer.* **12**, p306.

Mei, S., Qin, Q., Wu, Q., Sun, H., Zheng, R., Zang, C., Zhu, M., Wu, J., Shi, X., Taing, L., Liu, T., Brown, M., Meyer, C.A. and Liu, X.S. 2017. Cistrome Data Browser: a data portal for ChIP-Seq and chromatin accessibility data in human and mouse. *Nucleic Acids Res.* **45**(D1), pp.D658-D662.

Miki, Y., Swensen, J., Shattuck-Eidens, D., Futreal, P.A., Harshman, K., Tavtigian, S., Liu, Q., Cochran, C., Bennett, L.M., Ding, W. and et al. 1994. A strong candidate for the breast and ovarian cancer susceptibility gene BRCA1. *Science.* **266**(5182), pp.66-71.

Miller, S.B. 2006. Prostaglandins in health and disease: an overview. *Semin Arthritis Rheum.* **36**(1), pp.37-49.

Min, A., Im, S.A., Kim, D.K., Song, S.H., Kim, H.J., Lee, K.H., Kim, T.Y., Han, S.W., Oh, D.Y., Kim, T.Y., O'Connor, M.J. and Bang, Y.J. 2015. Histone deacetylase inhibitor, suberoylanilide hydroxamic acid (SAHA), enhances anti-tumor effects of the poly (ADP-ribose) polymerase (PARP) inhibitor olaparib in triple-negative breast cancer cells. *Breast Cancer Res.* **17**, p33.

Mirza, S., Sharma, G., Parshad, R., Gupta, S.D., Pandya, P. and Ralhan, R. 2013. Expression of DNA methyltransferases in breast cancer patients and to analyze the effect of natural compounds on DNA methyltransferases and associated proteins. *J Breast Cancer.* **16**(1), pp.23-31.

Mitchell, M.D., Goodwin, V., Mesnage, S. and Keelan, J.A. 2000. Cytokine-induced coordinate expression of enzymes of prostaglandin biosynthesis and metabolism: 15-hydroxyprostaglandin dehydrogenase. *Prostaglandins Leukot Essent Fatty Acids.* **62**(1), pp.1-5.

Miyaki, A., Yang, P., Tai, H.H., Subbaramaiah, K. and Dannenberg, A.J. 2009. Bile acids inhibit NAD+-dependent 15-hydroxyprostaglandin dehydrogenase transcription in colonocytes. *Am J Physiol Gastrointest Liver Physiol.* **297**(3), pp.G559-566.

Montani, M., Hermanns, T., Muntener, M., Wild, P., Sulser, T. and Kristiansen, G. 2013. Multidrug resistance protein 4 (MRP4) expression in prostate cancer is associated with androgen signaling and decreases with tumor progression. *Virchows Arch.* **462**(4), pp.437-443.

Murata, H., Tsuji, S., Tsujii, M., Sakaguchi, Y., Fu, H.Y., Kawano, S. and Hori, M. 2004. Promoter hypermethylation silences cyclooxygenase-2 (Cox-2) and regulates growth of human hepatocellular carcinoma cells. *Lab Invest.* **84**(8), pp.1050-1059.

Myung, S.J., Rerko, R.M., Yan, M., Platzer, P., Guda, K., Dotson, A., Lawrence, E., Dannenberg, A.J., Lovgren, A.K., Luo, G., Pretlow, T.P., Newman, R.A., Willis, J., Dawson, D. and Markowitz, S.D. 2006. 15-Hydroxyprostaglandin dehydrogenase is an in vivo suppressor of colon tumorigenesis. *Proc Natl Acad Sci U S A.* **103**(32), pp.12098-12102.

Na, H.K., Park, J.M., Lee, H.G., Lee, H.N., Myung, S.J. and Surh, Y.J. 2011. 15-Hydroxyprostaglandin dehydrogenase as a novel molecular target for cancer chemoprevention and therapy. *Biochem Pharmacol.* **82**(10), pp.1352-1360.

Nakanishi, M., Gokhale, V., Meuillet, E.J. and Rosenberg, D.W. 2010. mPGES-1 as a target for cancer suppression: A comprehensive invited review "Phospholipase A2 and lipid mediators". *Biochimie.* **92**(6), pp.660-664.

Nakanishi, M. and Rosenberg, D.W. 2013. Multifaceted roles of PGE2 in inflammation and cancer. *Semin Immunopathol.* **35**(2), pp.123-137.

Nakanishi, T., Ohno, Y., Aotani, R., Maruyama, S., Shimada, H., Kamo, S., Oshima, H., Oshima, M., Schuetz, J.D. and Tamai, I. 2017. A novel role for OATP2A1/SLCO2A1 in a murine model of colon cancer. *Sci Rep.* **7**(1), p16567.

Nalwoga, H., Ahmed, L., Arnes, J.B., Wabinga, H. and Akslen, L.A. 2016. Strong Expression of Hypoxia-Inducible Factor-1alpha (HIF-1alpha) Is Associated with Axl Expression and Features of Aggressive Tumors in African Breast Cancer. *PLoS One.* **11**(1), pe0146823.

Nandy, A., Jenatschke, S., Hartung, B., Milde-Langosch, K., Bamberger, A.M. and Gellersen, B. 2003. Genomic structure and transcriptional regulation of the human NAD+-dependent 15-hydroxyprostaglandin dehydrogenase gene. *J Mol Endocrinol.* **31**(1), pp.105-121.

Narisawa, T., Kusaka, H., Yamazaki, Y., Takahashi, M., Koyama, H., Koyama, K., Fukaura, Y. and Wakizaka, A. 1990. Relationship between blood plasma prostaglandin E2 and liver and lung metastases in colorectal cancer. *Dis Colon Rectum.* **33**(10), pp.840-845.

Narumiya, S. and FitzGerald, G.A. 2001. Genetic and pharmacological analysis of prostanoid receptor function. *J Clin Invest.* **108**(1), pp.25-30.

Natarajan, R. and Nadler, J. 1998. Role of lipoxygenases in breast cancer. *Front Biosci.* **3**, pp.E81-88.

Neve, R.M., Chin, K., Fridlyand, J., Yeh, J., Baehner, F.L., Fevr, T., Clark, L., Bayani, N., Coppe, J.P., Tong, F., Speed, T., Spellman, P.T., DeVries, S., Lapuk, A., Wang, N.J., Kuo, W.L., Stilwell, J.L, Pinkel, D., Albertson, D.G., Waldman, F.M., McCormick, F., Dickson, R.B., Johnson, M.D., Lippman, M., Ethier, S., Gazdar, A. and Gray, J.W. 2006. A collection of breast cancer cell lines for the study of functionally distinct cancer subtypes. *Cancer Cell.* **10**(6), pp.515-527.

Newbold, A., Matthews, G.M., Bots, M., Cluse, L.A., Clarke, C.J., Banks, K.M., Cullinane, C., Bolden, J.E., Christiansen, A.J., Dickins, R.A., Miccolo, C., Chiocca, S., Kral, A.M., Ozerova, N.D., Miller, T.A., Methot, J.L., Richon, V.M., Secrist, J.P., Minucci, S. and Johnstone, R.W. 2013. Molecular and biologic analysis of histone deacetylase inhibitors with diverse specificities. *Mol Cancer Ther.* **12**(12), pp.2709-2721.

Ngeow, J., Sesock, K. and Eng, C. 2017. Breast cancer risk and clinical implications for germline PTEN mutation carriers. *Breast Cancer Res Treat.* **165**(1), pp.1-8.

Nie, D., Guo, Y., Yang, D., Tang, Y., Chen, Y., Wang, M.T., Zacharek, A., Qiao, Y., Che, M. and Honn, K.V. 2008. Thromboxane A2 receptors in prostate carcinoma: expression and its role in regulating cell motility via small GTPase Rho. *Cancer Res.* **68**(1), pp.115-121.

Nikiforova, Z.N., Taipov, M.A., Kudryavtsev, I.A. and Shevchenko, V.E. 2015. Association of miR-21 and miR-155 with Regulation of 15-HPGD mRNA in Human Breast Cancer Cells. *Biochemistry Moscow-Supplement Series B-Biomedical Chemistry*. **9**(2), pp.159-165.

Nomura, T., Lu, R., Pucci, M.L. and Schuster, V.L. 2004. The two-step model of prostaglandin signal termination: in vitro reconstitution with the prostaglandin transporter and prostaglandin 15 dehydrogenase. *Mol Pharmacol.* **65**(4), pp.973-978.

Norris, M.D., Smith, J., Tanabe, K., Tobin, P., Flemming, C., Scheffer, G.L., Wielinga, P., Cohn, S.L., London, W.B., Marshall, G.M., Allen, J.D. and Haber, M. 2005. Expression of multidrug transporter MRP4/ABCC4 is a marker of poor prognosis in neuroblastoma and confers resistance to irinotecan in vitro. *Mol Cancer Ther.* **4**(4), pp.547-553.

O'Callaghan, G. and Houston, A. 2015. Prostaglandin E2 and the EP receptors in malignancy: possible therapeutic targets? *Br J Pharmacol.* **172**(22), pp.5239-5250.

Onitilo, A.A., Engel, J.M., Greenlee, R.T. and Mukesh, B.N. 2009. Breast cancer subtypes based on ER/PR and Her2 expression: comparison of clinicopathologic features and survival. *Clin Med Res.* **7**(1-2), pp.4-13.

Otto, T., Rembrink, K., Goepel, M., Meyer-Schwickerath, M. and Rubben, H. 1993. E-cadherin: a marker for differentiation and invasiveness in prostatic carcinoma. *Urol Res.* **21**(5), pp.359-362.

Pal, S.K., Lau, S.K., Kruper, L., Nwoye, U., Garberoglio, C., Gupta, R.K., Paz, B., Vora, L., Guzman, E., Artinyan, A. and Somlo, G. 2010. Papillary carcinoma of the breast: an overview. *Breast Cancer Res Treat.* **122**(3), pp.637-645.

Pan, M.R., Hou, M.F., Chang, H.C. and Hung, W.C. 2008. Cyclooxygenase-2 up-regulates CCR7 via EP2/EP4 receptor signaling pathways to enhance lymphatic invasion of breast cancer cells. *J Biol Chem.* **283**(17), pp.11155-11163.

Park, Y.S., Lee, J.H., Jung, D.B., Kim, H.B., Jung, J.H., Pak, S., Ryu, Y.M., Park, H.J., Park, Y.Y., Jung, H.Y. and Myung, S.J. 2018. MicroRNA-21 induces loss of 15-hydroxyprostaglandin dehydrogenase in early gastric tubular adenocarcinoma. *Sci Rep.* **8**(1), p17717.

Paul, A. and Paul, S. 2014. The breast cancer susceptibility genes (BRCA) in breast and ovarian cancers. *Front Biosci (Landmark Ed).* **19**, pp.605-618.

Peinado, H., Ballestar, E., Esteller, M. and Cano, A. 2004. Snail mediates E-cadherin repression by the recruitment of the Sin3A/histone deacetylase 1 (HDAC1)/HDAC2 complex. *Mol Cell Biol.* **24**(1), pp.306-319.

Perou, C.M., Sorlie, T., Eisen, M.B., van de Rijn, M., Jeffrey, S.S., Rees, C.A., Pollack, J.R., Ross, D.T., Johnsen, H., Akslen, L.A., Fluge, O., Pergamenschikov, A., Williams, C., Zhu, S.X., Lo nning, P.E., Borresen-Dale, A.L., Brown, P.O. and Botstein, D. 2000. Molecular portraits of human breast tumours. *Nature.* **406**(6797), pp.747-752.

Phan, N.L., Trinh, N.V. and Pham, P.V. 2016. Low concentrations of 5-aza-2'-deoxycytidine induce breast cancer stem cell differentiation by triggering tumor suppressor gene expression. *Onco Targets Ther.* **9**, pp.49-59.

Piepoli, A., Cotugno, R., Merla, G., Gentile, A., Augello, B., Quitadamo, M., Merla, A., Panza, A., Carella, M., Maglietta, R., D'Addabbo, A., Ancona, N., Fusilli, S., Perri, F. and Andriulli, A. 2009. Promoter methylation correlates with reduced NDRG2 expression in advanced colon tumour. *BMC Med Genomics.* **2**, p11.

Pirkmajer, S. and Chibalin, A.V. 2011. Serum starvation: caveat emptor. *Am J Physiol Cell Physiol.* **301**(2), pp.C272-279.

Poligone, B. and Baldwin, A.S. 2001. Positive and negative regulation of NF-kappaB by COX-2: roles of different prostaglandins. *J Biol Chem.* **276**(42), pp.38658-38664.

Pollard, J.W. 2004. Tumour-educated macrophages promote tumour progression and metastasis. *Nat Rev Cancer.* **4**(1), pp.71-78.

Qi, X., Wang, Y., Hou, J. and Huang, Y. 2017. A Single Nucleotide Polymorphism in HPGD Gene Is Associated with Prostate Cancer Risk. *J Cancer.* **8**(19), pp.4083-4086.

Qiao, H. and May, J.M. 2011. CpG methylation at the USF-binding site mediates cell-specific transcription of human ascorbate transporter SVCT2 exon 1a. *Biochem J.* **440**(1), pp.73-84.

Qualtrough, D., Kaidi, A., Chell, S., Jabbour, H.N., Williams, A.C. and Paraskeva, C. 2007. Prostaglandin F(2alpha) stimulates motility and invasion in colorectal tumor cells. *Int J Cancer.* **121**(4), pp.734-740.

Quidville, V., Segond, N., Lausson, S., Frenkian, M., Cohen, R. and Jullienne, A. 2006. 15-Hydroxyprostaglandin-dehydrogenase is involved in anti-proliferative effect of non-steroidal anti-inflammatory drugs COX-1 inhibitors on a human medullary thyroid carcinoma cell line. *Prostaglandins Other Lipid Mediat.* **81**(1-2), pp.14-30.

Quintas-Cardama, A., Santos, F.P. and Garcia-Manero, G. 2010. Therapy with azanucleosidesfor myelodysplastic syndromes. *Nat Rev Clin Oncol.* **7**(8), pp.433-444.

Quintas-Cardama, A., Santos, F.P. and Garcia-Manero, G. 2011. Histone deacetylase inhibitors for the treatment of myelodysplastic syndrome and acute myeloid leukemia. *Leukemia.* **25**(2), pp.226-235.

Rakha, E.A., Reis-Filho, J.S., Baehner, F., Dabbs, D.J., Decker, T., Eusebi, V., Fox, S.B., Ichihara, S., Jacquemier, J., Lakhani, S.R., Palacios, J., Richardson, A.L., Schnitt, S.J., Schmitt, F.C., Tan, P.H., Tse, G.M., Badve, S. and Ellis, I.O. 2010. Breast cancer prognostic classification in the molecular era: the role of histological grade. *Breast Cancer Res.* **12**(4), p207.

Ramalingam, S.S., Kummar, S., Sarantopoulos, J., Shibata, S., LoRusso, P., Yerk, M., Holleran, J., Lin, Y., Beumer, J.H., Harvey, R.D., Ivy, S.P., Belani, C.P. and Egorin, M.J. 2010. Phase I study of vorinostat in patients with advanced solid tumors and hepatic dysfunction: a National Cancer Institute Organ Dysfunction Working Group study. *J Clin Oncol.* **28**(29), pp.4507-4512.

Regulski, M., Regulska, K., Prukala, W., Piotrowska, H., Stanisz, B. and Murias, M. 2016. COX-2 inhibitors: a novel strategy in the management of breast cancer. *Drug Discov Today.* **21**(4), pp.598-615.

Ristimaki, A., Sivula, A., Lundin, J., Lundin, M., Salminen, T., Haglund, C., Joensuu, H. and Isola, J. 2002. Prognostic significance of elevated cyclooxygenase-2 expression in breast cancer. *Cancer Res.* **62**(3), pp.632-635.

Robertson, F.M., Mallery, S.R., Bergdall-Costell, V.K., Cheng, M., Pei, P., Prosperi, J.R. and Ferrari, M. 2007. Cyclooxygenase-2 directly induces MCF-7 breast tumor cells to develop into exponentially growing, highly angiogenic and regionally invasive human ductal carcinoma xenografts. *Anticancer Res.* **27**(2), pp.719-727.

Romero-Ramirez, L., Cao, H., Nelson, D., Hammond, E., Lee, A.H., Yoshida, H., Mori, K., Glimcher, L.H., Denko, N.C., Giaccia, A.J., Le, Q.T. and Koong, A.C. 2004. XBP1 is essential for survival under hypoxic conditions and is required for tumor growth. *Cancer Res.* **64**(17), pp.5943-5947.

Russel, F.G., Koenderink, J.B. and Masereeuw, R. 2008. Multidrug resistance protein 4 (MRP4/ABCC4): a versatile efflux transporter for drugs and signalling molecules. *Trends Pharmacol Sci.* **29**(4), pp.200-207.

Ryu, Y.M., Myung, S.J., Park, Y.S., Yang, D.H., Song, H.J., Jeong, J.Y., Lee, S.M., Song, M., Kim, D.H., Lee, H.J., Park, S.K., Fink, S.P., Markowitz, S.D., Jung, K.W., Kim, K.J., Ye, B.D., Byeon, J.S., Jung, H.Y., Yang, S.K. and Kim, J.H. 2013. Inhibition of 15-hydroxyprostaglandin dehydrogenase by Helicobacter pylori in human gastric carcinogenesis. *Cancer Prev Res (Phila).* **6**(4), pp.349-359.

Saba, H.I. 2007. Decitabine in the treatment of myelodysplastic syndromes. *Ther Clin Risk Manag.* **3**(5), pp.807-817.

Sales, K.J., Boddy, S.C. and Jabbour, H.N. 2008. F-prostanoid receptor alters adhesion, morphology and migration of endometrial adenocarcinoma cells. *Oncogene.* **27**(17), pp.2466-2477.

Sales, K.J., Boddy, S.C., Williams, A.R., Anderson, R.A. and Jabbour, H.N. 2007. F-prostanoid receptor regulation of fibroblast growth factor 2 signaling in endometrial adenocarcinoma cells. *Endocrinology.* **148**(8), pp.3635-3644.

Salmaninejad, A., Valilou, S.F., Shabgah, A.G., Aslani, S., Alimardani, M., Pasdar, A. and Sahebkar, A. 2019. PD-1/PD-L1 pathway: Basic biology and role in cancer immunotherapy. *J Cell Physiol.* **234**(10), pp.16824-16837.

Sasaki, T., Niizeki, H., Shimizu, A., Shiohama, A., Hirakiyama, A., Okuyama, T., Seki, A., Kabashima, K., Otsuka, A., Ishiko, A., Tanese, K., Miyakawa, S., Sakabe, J., Kuwahara, M., Amagai, M., Okano, H., Suematsu, M. and Kudoh, J. 2012. Identification of mutations in the prostaglandin transporter gene SLCO2A1 and its phenotype-genotype correlation in Japanese patients with pachydermoperiostosis. *J Dermatol Sci.* **68**(1), pp.36-44.

Sasaki, Y., Kamiyama, S., Kamiyama, A., Matsumoto, K., Akatsu, M., Nakatani, Y., Kuwata, H., Ishikawa, Y., Ishii, T., Yokoyama, C. and Hara, S. 2015. Genetic-deletion of Cyclooxygenase-2 Downstream Prostacyclin Synthase Suppresses Inflammatory Reactions but Facilitates Carcinogenesis, unlike Deletion of Microsomal Prostaglandin E Synthase-1. *Sci Rep.* **5**, p17376.

Schmelz, K., Sattler, N., Wagner, M., Lubbert, M., Dorken, B. and Tamm, I. 2005. Induction of gene expression by 5-Aza-2'-deoxycytidine in acute myeloid leukemia (AML) and myelodysplastic syndrome (MDS) but not epithelial cells by DNA-methylation-dependent and -independent mechanisms. *Leukemia.* **19**(1), pp.103-111.

Schneider, C.A., Rasband, W.S. and Eliceiri, K.W. 2012. NIH Image to ImageJ: 25 years of image analysis. *Nat Methods.* **9**(7), pp.671-675.

Schon, K. and Tischkowitz, M. 2018. Clinical implications of germline mutations in breast cancer: TP53. *Breast Cancer Res Treat.* **167**(2), pp.417-423.

Schuligoi, R., Schmidt, R., Geisslinger, G., Kollroser, M., Peskar, B.A. and Heinemann, A. 2007. PGD2 metabolism in plasma: kinetics and relationship with bioactivity on DP1 and CRTH2 receptors. *Biochem Pharmacol.* **74**(1), pp.107-117.

Seelan, R.S., Mukhopadhyay, P., Pisano, M.M. and Greene, R.M. 2018. Effects of 5-Aza-2'-deoxycytidine (decitabine) on gene expression. *Drug Metab Rev.* **50**(2), pp.193-207.

Seo, S.H., Kang, M.S., Kim, K.H., An, M.S., Ha, T.K., Bae, K.B., Oh, M.K., Choi, C.S., Oh, S.H. and Choi, Y.K. 2015. Correlation of 15-prostagladin dehydrogenase expression with clinicopathological factors and survival rate in gastric adenocarcinoma. *Int J Surg.* **13**, pp.96-101.

Seo, T., Tatsuguchi, A., Shinji, S., Yonezawa, M., Mitsui, K., Tanaka, S., Fujimori, S., Gudis, K., Fukuda, Y. and Sakamoto, C. 2009. Microsomal prostaglandin E synthase protein levels correlate with prognosis in colorectal cancer patients. *Virchows Arch.* **454**(6), pp.667-676.

Sewell-Loftin, M.K., Bayer, S.V.H., Crist, E., Hughes, T., Joison, S.M., Longmore, G.D. and George, S.C. 2017. Cancer-associated fibroblasts support vascular growth through mechanical force. *Sci Rep.* **7**(1), p12574.

Shah, S.P., Roth, A., Goya, R., Oloumi, A., Ha, G., Zhao, Y., Turashvili, G., Ding, J., Tse, K., Haffari, G., Bashashati, A., Prentice, L.M., Khattra, J., Burleigh, A., Yap, D., Bernard, V., McPherson, A., Shumansky, K., Crisan, A., Giuliany, R., Heravi-Moussavi, A., Rosner, J., Lai, D., Birol, I., Varhol, R., Tam, A., Dhalla, N., Zeng, T., Ma, K., Chan, S.K., Griffith, M., Moradian, A., Cheng, S.W., Morin, G.B., Watson, P., Gelmon, K., Chia, S., Chin, S.F., Curtis, C., Rueda, O.M., Pharoah, P.D., Damaraju, S., Mackey, J., Hoon, K., Harkins, T., Tadigotla, V., Sigaroudinia, M., Gascard, P., Tlsty, T., Costello, J.F., Meyer, I.M., Eaves, C.J., Wasserman, W.W., Jones, S., Huntsman, D., Hirst, M., Caldas, C., Marra, M.A. and Aparicio, S. 2012. The clonal and mutational evolution spectrum of primary triple-negative breast cancers. *Nature.* **486**(7403), pp.395-399.

Shahi, P., Slorach, E.M., Wang, C.Y., Chou, J., Lu, A., Ruderisch, A. and Werb, Z. 2015. The Transcriptional Repressor ZNF503/Zeppo2 Promotes Mammary Epithelial Cell Proliferation and Enhances Cell Invasion. *J Biol Chem.* **290**(6), pp.3803-3813.

Sheibanie, A.F., Khayrullina, T., Safadi, F.F. and Ganea, D. 2007a. Prostaglandin E2 exacerbates collagen-induced arthritis in mice through the inflammatory interleukin-23/interleukin-17 axis. *Arthritis Rheum.* **56**(8), pp.2608-2619.

Sheibanie, A.F., Yen, J.H., Khayrullina, T., Emig, F., Zhang, M., Tuma, R. and Ganea, D. 2007b. The proinflammatory effect of prostaglandin E2 in experimental inflammatory bowel disease is mediated through the IL-23-->IL-17 axis. *J Immunol.* **178**(12), pp.8138-8147.

Shekhar, M.P., Tait, L., Pauley, R.J., Wu, G.S., Santner, S.J., Nangia-Makker, P., Shekhar, V., Nassar, H., Visscher, D.W., Heppner, G.H. and Miller, F.R. 2008. Comedo-ductal carcinoma in situ: A paradoxical role for programmed cell death. *Cancer Biol Ther.* **7**(11), pp.1774-1782.

Sheng, H., Shao, J., Morrow, J.D., Beauchamp, R.D. and DuBois, R.N. 1998. Modulation of apoptosis and Bcl-2 expression by prostaglandin E2 in human colon cancer cells. *Cancer Res.* **58**(2), pp.362-366.

Shim, J.Y., An, H.J., Lee, Y.H., Kim, S.K., Lee, K.P. and Lee, K.S. 2003. Overexpression of cyclooxygenase-2 is associated with breast carcinoma and its poor prognostic factors. *Mod Pathol.* **16**(12), pp.1199-1204.

Simopoulos, A.P. 1999. Essential fatty acids in health and chronic disease. *Am J Clin Nutr.* **70**(3 Suppl), pp.560S-569S.

Simopoulos, A.P. 2016. An Increase in the Omega-6/Omega-3 Fatty Acid Ratio Increases the Risk for Obesity. *Nutrients.* **8**(3), p128.

Sinn, H.P. and Kreipe, H. 2013. A Brief Overview of the WHO Classification of Breast Tumors, 4th Edition, Focusing on Issues and Updates from the 3rd Edition. *Breast Care (Basel).* **8**(2), pp.149-154.

Siqueira, J.F., Jr., Fouad, A.F. and Rocas, I.N. 2012. Pyrosequencing as a tool for better understanding of human microbiomes. *J Oral Microbiol.* **4**.

Sobolewski, C., Cerella, C., Dicato, M., Ghibelli, L. and Diederich, M. 2010. The role of cyclooxygenase-2 in cell proliferation and cell death in human malignancies. *Int J Cell Biol.* **2010**, p215158.

Sola-Villa, D., Dilme, J.F., Rodriguez, C., Soto, B., Vila, L., Escudero, J.R., Martinez-Gonzalez, J. and Camacho, M. 2015. Expression and Cellular Localization of 15-Hydroxy-Prostaglandin-Dehydrogenase in Abdominal Aortic Aneurysm. *PLoS One.* **10**(8), pe0136201.

Song, C., Wang, L., Wu, X., Wang, K., Xie, D., Xiao, Q., Li, S., Jiang, K., Liao, L., Yates, J.R., 3rd, Lee, J.D. and Yang, Q. 2018. PML Recruits TET2 to Regulate DNA Modification and Cell Proliferation in Response to Chemotherapeutic Agent. *Cancer Res.* **78**(10), pp.2475-2489.

Soon, P.S., Kim, E., Pon, C.K., Gill, A.J., Moore, K., Spillane, A.J., Benn, D.E. and Baxter, R.C. 2013. Breast cancer-associated fibroblasts induce epithelial-to-mesenchymal transition in breast cancer cells. *Endocr Relat Cancer.* **20**(1), pp.1-12.

Sostres, C., Gargallo, C.J., Arroyo, M.T. and Lanas, A. 2010. Adverse effects of non-steroidal anti-inflammatory drugs (NSAIDs, aspirin and coxibs) on upper gastrointestinal tract. *Best Pract Res Clin Gastroenterol.* **24**(2), pp.121-132.

Spector, A.A. and Kim, H.Y. 2015. Cytochrome P450 epoxygenase pathway of polyunsaturated fatty acid metabolism. *Biochim Biophys Acta.* **1851**(4), pp.356-365.

Steele, V.E., Holmes, C.A., Hawk, E.T., Kopelovich, L., Lubet, R.A., Crowell, J.A., Sigman, C.C. and Kelloff, G.J. 2000. Potential use of lipoxygenase inhibitors for cancer chemoprevention. *Expert Opin Investig Drugs.* **9**(9), pp.2121-2138.

Stresemann, C. and Lyko, F. 2008. Modes of action of the DNA methyltransferase inhibitors azacytidine and decitabine. *Int J Cancer.* **123**(1), pp.8-13.

Su, S., Liu, Q., Chen, J., Chen, J., Chen, F., He, C., Huang, D., Wu, W., Lin, L., Huang, W., Zhang, J., Cui, X., Zheng, F., Li, H., Yao, H., Su, F. and Song, E. 2014. A positive feedback loop between mesenchymal-like cancer cells and macrophages is essential to breast cancer metastasis. *Cancer Cell.* **25**(5), pp.605-620.

Subik, K., Lee, J.F., Baxter, L., Strzepek, T., Costello, D., Crowley, P., Xing, L., Hung, M.C., Bonfiglio, T., Hicks, D.G. and Tang, P. 2010. The Expression Patterns of ER, PR, HER2, CK5/6, EGFR, Ki-67 and AR by Immunohistochemical Analysis in Breast Cancer Cell Lines. *Breast Cancer (Auckl).* **4**, pp.35-41.

Sugimoto, Y. and Narumiya, S. 2007. Prostaglandin E receptors. *J Biol Chem.* **282**(16), pp.11613-11617.

Synnott, N.C., Murray, A., McGowan, P.M., Kiely, M., Kiely, P.A., O'Donovan, N., O'Connor, D.P., Gallagher, W.M., Crown, J. and Duffy, M.J. 2017. Mutant p53: a novel target for the treatment of patients with triple-negative breast cancer? *Int J Cancer.* **140**(1), pp.234-246.

Tai, H.H., Chi, X. and Tong, M. 2011. Regulation of 15-hydroxyprostaglandin dehydrogenase (15-PGDH) by non-steroidal anti-inflammatory drugs (NSAIDs). *Prostaglandins Other Lipid Mediat.* **96**(1-4), pp.37-40.

Tai, H.H., Ensor, C.M., Tong, M., Zhou, H. and Yan, F. 2002. Prostaglandin catabolizing enzymes. *Prostaglandins Other Lipid Mediat.* **68-69**, pp.483-493.

Tai, H.H., Tong, M. and Ding, Y. 2007. 15-hydroxyprostaglandin dehydrogenase (15-PGDH) and lung cancer. *Prostaglandins Other Lipid Mediat.* **83**(3), pp.203-208.

Takai, E., Tsukimoto, M. and Kojima, S. 2013. TGF-beta1 downregulates COX-2 expression leading to decrease of PGE2 production in human lung cancer A549 cells, which is involved in fibrotic response to TGF-beta1. *PLoS One.* **8**(10), pe76346.

Takeda, S., Tanigawa, T., Watanabe, T., Tatsuwaki, H., Nadatani, Y., Otani, K., Nagami, Y., Tanaka, F., Kamata, N., Yamagami, H., Shiba, M., Tominaga, K., Fujiwara, Y., Muguruma, K., Ohira, M., Hirakawa, K. and Arakawa, T. 2016. Reduction of prostaglandin transporter predicts poor prognosis associated with angiogenesis in gastric adenocarcinoma. *J Gastroenterol Hepatol.* **31**(2), pp.376-383.

Tamura, K., Sakurai, T. and Kogo, H. 2006. Relationship between prostaglandin E2 and vascular endothelial growth factor (VEGF) in angiogenesis in human vascular endothelial cells. *Vascul Pharmacol.* **44**(6), pp.411-416.

Tanaka, K., Imoto, S., Wada, N., Sakemura, N. and Hasebe, K. 2008. Invasive apocrine carcinoma of the breast: clinicopathologic features of 57 patients. *Breast J.* **14**(2), pp.164-168.

Thiel, A., Ganesan, A., Mrena, J., Junnila, S., Nykanen, A., Hemmes, A., Tai, H.H., Monni, O., Kokkola, A., Haglund, C., Petrova, T.V. and Ristimaki, A. 2009. 15-hydroxyprostaglandin dehydrogenase is down-regulated in gastric cancer. *Clin Cancer Res.* **15**(14), pp.4572-4580.

Thill, M., Fischer, D., Hoellen, F., Kelling, K., Dittmer, C., Landt, S., Salehin, D., Diedrich, K., Friedrich, M. and Becker, S. 2010a. Prostaglandin metabolising enzymes and PGE2 are inversely correlated with vitamin D receptor and 25(OH)2D3 in breast cancer. *Anticancer Res.* **30**(5), pp.1673-1679.

Thill, M., Fischer, D., Kelling, K., Hoellen, F., Dittmer, C., Hornemann, A., Salehin, D., Diedrich, K., Friedrich, M. and Becker, S. 2010b. Expression of vitamin D receptor (VDR), cyclooxygenase-2 (COX-2) and 15-hydroxyprostaglandin dehydrogenase (15-PGDH) in benign and malignant ovarian tissue and 25-hydroxycholecalciferol (25(OH2)D3) and prostaglandin E2 (PGE2) serum level in ovarian cancer patients. *J Steroid Biochem Mol Biol.* **121**(1-2), pp.387-390.

Thompson, C.L., Fink, S.P., Lutterbaugh, J.D., Elston, R.C., Veigl, M.L., Markowitz, S.D. and Li, L. 2013. Genetic variation in 15-hydroxyprostaglandin dehydrogenase and colon cancer susceptibility. *PLoS One.* **8**(5), pe64122.

Tian, J., Hachim, M.Y., Hachim, I.Y., Dai, M., Lo, C., Raffa, F.A., Ali, S. and Lebrun, J.J. 2017. Cyclooxygenase-2 regulates TGFbeta-induced cancer stemness in triple-negative breast cancer. *Sci Rep.* **7**, p40258.

Timoshenko, A.V., Xu, G., Chakrabarti, S., Lala, P.K. and Chakraborty, C. 2003. Role of prostaglandin E2 receptors in migration of murine and human breast cancer cells. *Exp Cell Res.* **289**(2), pp.265-274.

Tokudome, S., Kuriki, K., Yokoyama, Y., Sasaki, M., Joh, T., Kamiya, T., Cheng, J., Ogawa, K., Shirai, T., Imaeda, N., Goto, C., Tokudome, Y., Ichikawa, H. and Okuyama, H. 2015. Dietary n-3/long-chain n-3 polyunsaturated fatty acids for prevention of sporadic colorectal tumors: a randomized controlled trial in polypectomized participants. *Prostaglandins Leukot Essent Fatty Acids.* **94**, pp.1-11.

Tomozawa, S., Tsuno, N.H., Sunami, E., Hatano, K., Kitayama, J., Osada, T., Saito, S., Tsuruo, T., Shibata, Y. and Nagawa, H. 2000. Cyclooxygenase-2 overexpression correlates with tumour recurrence, especially haematogenous metastasis, of colorectal cancer. *Br J Cancer.* **83**(3), pp.324-328.

Tong, M., Ding, Y. and Tai, H.H. 2006a. Histone deacetylase inhibitors and transforming growth factor-beta induce 15-hydroxyprostaglandin dehydrogenase expression in human lung adenocarcinoma cells. *Biochem Pharmacol.* **72**(6), pp.701-709.

Tong, M., Ding, Y. and Tai, H.H. 2006b. Reciprocal regulation of cyclooxygenase-2 and 15-hydroxyprostaglandin dehydrogenase expression in A549 human lung adenocarcinoma cells. *Carcinogenesis.* **27**(11), pp.2170-2179.

Tootle, T.L. 2013. Genetic insights into the in vivo functions of prostaglandin signaling. *Int J Biochem Cell Biol.* **45**(8), pp.1629-1632.

Tost, J. and Gut, I.G. 2007. DNA methylation analysis by pyrosequencing. *Nat Protoc.* **2**(9), pp.2265-2275.

Truong, D., Puleo, J., Llave, A., Mouneimne, G., Kamm, R.D. and Nikkhah, M. 2016. Breast Cancer Cell Invasion into a Three Dimensional Tumor-Stroma Microenvironment. *Sci Rep.* **6**, p34094.

Tryndyak, V.P., Kovalchuk, O. and Pogribny, I.P. 2006. Loss of DNA methylation and histone H4 lysine 20 trimethylation in human breast cancer cells is associated with aberrant expression of DNA methyltransferase 1, Suv4-20h2 histone methyltransferase and methyl-binding proteins. *Cancer Biol Ther.* **5**(1), pp.65-70.

Tseng-Rogenski, S., Gee, J., Ignatoski, K.W., Kunju, L.P., Bucheit, A., Kintner, H.J., Morris, D., Tallman, C., Evron, J., Wood, C.G., Grossman, H.B., Lee, C.T. and Liebert, M. 2010. Loss of 15-hydroxyprostaglandin dehydrogenase expression contributes to bladder cancer progression. *Am J Pathol.* **176**(3), pp.1462-1468.

Uhlen, M., Fagerberg, L., Hallstrom, B.M., Lindskog, C., Oksvold, P., Mardinoglu, A., Sivertsson, A., Kampf, C., Sjostedt, E., Asplund, A., Olsson, I., Edlund, K., Lundberg, E., Navani, S., Szigyarto, C.A., Odeberg, J., Djureinovic, D., Takanen, J.O., Hober, S., Alm, T., Edqvist, P.H., Berling, H., Tegel, H., Mulder, J., Rockberg, J., Nilsson, P., Schwenk, J.M., Hamsten, M., von Feilitzen, K., Forsberg, M., Persson, L., Johansson, F., Zwahlen, M., von Heijne, G., Nielsen, J. and Ponten, F. 2015. Proteomics. Tissue-based map of the human proteome. *Science.* **347**(6220), p1260419.

Uhlen, M., Zhang, C., Lee, S., Sjostedt, E., Fagerberg, L., Bidkhori, G., Benfeitas, R., Arif, M., Liu, Z., Edfors, F., Sanli, K., von Feilitzen, K., Oksvold, P., Lundberg, E., Hober, S., Nilsson, P., Mattsson, J., Schwenk, J.M., Brunnstrom, H., Glimelius, B., Sjoblom, T., Edqvist, P.H., Djureinovic, D., Micke, P., Lindskog, C., Mardinoglu, A. and Ponten, F. 2017. A pathology atlas of the human cancer transcriptome. *Science.* **357**(6352).

Uhr, K., Prager-van der Smissen, W.J., Heine, A.A., Ozturk, B., Smid, M., Gohlmann, H.W., Jager, A., Foekens, J.A. and Martens, J.W. 2015. Understanding drugs in breast cancer through drug sensitivity screening. *Springerplus.* **4**, p611.

Uppal, S., Diggle, C.P., Carr, I.M., Fishwick, C.W., Ahmed, M., Ibrahim, G.H., Helliwell, P.S., Latos-Bielenska, A., Phillips, S.E., Markham, A.F., Bennett, C.P. and Bonthron, D.T. 2008. Mutations in 15-hydroxyprostaglandin dehydrogenase cause primary hypertrophic osteoarthropathy. *Nat Genet.* **40**(6), pp.789-793.

VanderMolen, K.M., McCulloch, W., Pearce, C.J. and Oberlies, N.H. 2011. Romidepsin (Istodax, NSC 630176, FR901228, FK228, depsipeptide): a natural product recently approved for cutaneous T-cell lymphoma. *J Antibiot (Tokyo).* **64**(8), pp.525-531.

Vranic, S., Gatalica, Z. and Wang, Z.Y. 2011. Update on the molecular profile of the MDA-MB-453 cell line as a model for apocrine breast carcinoma studies. *Oncol Lett.* **2**(6), pp.1131-1137.

Walker, J.D., Sehgal, I. and Kousoulas, K.G. 2011. Oncolytic herpes simplex virus 1 encoding 15-prostaglandin dehydrogenase mitigates immune suppression and reduces ectopic primary and metastatic breast cancer in mice. *J Virol.* **85**(14), pp.7363-7371.

Wang, D., Buchanan, F.G., Wang, H., Dey, S.K. and DuBois, R.N. 2005. Prostaglandin E2 enhances intestinal adenoma growth via activation of the Ras-mitogen-activated protein kinase cascade. *Cancer Res.* **65**(5), pp.1822-1829.

Wang, D. and Dubois, R.N. 2010. Eicosanoids and cancer. *Nat Rev Cancer.* **10**(3), pp.181-193.

Wang, D. and DuBois, R.N. 2016. The Role of Prostaglandin E(2) in Tumor-Associated Immunosuppression. *Trends Mol Med.* **22**(1), pp.1-3.

Wang, D., Wang, H., Shi, Q., Katkuri, S., Walhi, W., Desvergne, B., Das, S.K., Dey, S.K. and DuBois, R.N. 2004. Prostaglandin E(2) promotes colorectal adenoma growth via transactivation of the nuclear peroxisome proliferator-activated receptor delta. *Cancer Cell.* **6**(3), pp.285-295.

Wang, H., Maurano, M.T., Qu, H., Varley, K.E., Gertz, J., Pauli, F., Lee, K., Canfield, T., Weaver, M., Sandstrom, R., Thurman, R.E., Kaul, R., Myers, R.M. and Stamatoyannopoulos, J.A. 2012.

Widespread plasticity in CTCF occupancy linked to DNA methylation. *Genome Res.* **22**(9), pp.1680-1688.

Wang, S.J., Saadi, W., Lin, F., Minh-Canh Nguyen, C. and Li Jeon, N. 2004. Differential effects of EGF gradient profiles on MDA-MB-231 breast cancer cell chemotaxis. *Exp Cell Res.* **300**(1), pp.180-189.

Wang, W., Hu, Y., Wang, X., Wang, Q. and Deng, H. 2018. ROS-Mediated 15-Hydroxyprostaglandin Dehydrogenase Degradation via Cysteine Oxidation Promotes NAD(+)-Mediated Epithelial-Mesenchymal Transition. *Cell Chem Biol.* **25**(3), pp.255-261 e254.

Wang, X., Li, G., Wang, A., Zhang, Z., Merchan, J.R. and Halmos, B. 2013. Combined histone deacetylase and cyclooxygenase inhibition achieves enhanced antiangiogenic effects in lung cancer cells. *Mol Carcinog.* **52**(3), pp.218-228.

Ward, R., Sims, A.H., Lee, A., Lo, C., Wynne, L., Yusuf, H., Gregson, H., Lisanti, M.P., Sotgia, F., Landberg, G. and Lamb, R. 2015. Monocytes and macrophages, implications for breast cancer migration and stem cell-like activity and treatment. *Oncotarget.* **6**(16), pp.14687-14699.

Weigelt, B., Geyer, F.C. and Reis-Filho, J.S. 2010. Histological types of breast cancer: how special are they? *Mol Oncol.* **4**(3), pp.192-208.

Wesola, M. and Jelen, M. 2017. The risk of breast cancer due to PALB2 gene mutations. *Adv Clin Exp Med.* **26**(2), pp.339-342.

Whitlock, E.P., Williams, S.B., Burda, B.U., Feightner, A. and Beil, T. 2015. Aspirin Use in Adults: Cancer, All-Cause Mortality, and Harms: A Systematic Evidence Review for the U.S. Preventive Services Task Force. Rockville (MD).

Williams, C. and Lin, C.Y. 2013. Oestrogen receptors in breast cancer: basic mechanisms and clinical implications. *Ecancermedicalscience.* **7**, p370.

Wlcek, K., Svoboda, M., Thalhammer, T., Sellner, F., Krupitza, G. and Jaeger, W. 2008. Altered expression of organic anion transporter polypeptide (OATP) genes in human breast carcinoma. *Cancer Biol Ther.* **7**(9), pp.1450-1455.

Wolf, I., O'Kelly, J., Rubinek, T., Tong, M., Nguyen, A., Lin, B.T., Tai, H.H., Karlan, B.Y. and Koeffler, H.P. 2006. 15-hydroxyprostaglandin dehydrogenase is a tumor suppressor of human breast cancer. *Cancer Res.* **66**(15), pp.7818-7823.

Wu, R., Liu, T., Yang, P., Liu, X., Liu, F., Wang, Y., Xiong, H., Yu, S., Huang, X. and Zhuang, L. 2017. Association of 15-hydroxyprostaglandin dehydrogenate and poor prognosis of obese breast cancer patients. *Oncotarget.* **8**(14), pp.22842-22853.

Wu, Y., Zhang, N. and Yang, Q. 2017. The prognosis of invasive micropapillary carcinoma compared with invasive ductal carcinoma in the breast: a meta-analysis. *BMC Cancer.* **17**(1), p839.

Wymann, M.P. and Schneiter, R. 2008. Lipid signalling in disease. *Nat Rev Mol Cell Biol.* **9**(2), pp.162-176.

Xu, F., Li, M., Zhang, C., Cui, J., Liu, J., Li, J. and Jiang, H. 2017. Clinicopathological and prognostic significance of COX-2 immunohistochemical expression in breast cancer: a meta-analysis. *Oncotarget.* **8**(4), pp.6003-6012.

Xun, C.Q., Tian, Z.G. and Tai, H.H. 1991. Stimulation of synthesis de novo of NAD(+)-dependent 15-hydroxyprostaglandin dehydrogenase in human promyelocytic leukaemia (HL-60) cells by phorbol ester. *Biochem J.* **279 (Pt 2)**, pp.553-558.

Yan, M., Rerko, R.M., Platzer, P., Dawson, D., Willis, J., Tong, M., Lawrence, E., Lutterbaugh, J., Lu, S., Willson, J.K., Luo, G., Hensold, J., Tai, H.H., Wilson, K. and Markowitz, S.D. 2004. 15-Hydroxyprostaglandin dehydrogenase, a COX-2 oncogene antagonist, is a TGF-beta-induced suppressor of human gastrointestinal cancers. *Proc Natl Acad Sci U S A.* **101**(50), pp.17468-17473.

Yang, L., Amann, J.M., Kikuchi, T., Porta, R., Guix, M., Gonzalez, A., Park, K.H., Billheimer, D., Arteaga, C.L., Tai, H.H., DuBois, R., Carbone, D.P. and Johnson, D.H. 2007. Inhibition of epidermal growth factor receptor signaling elevates 15-hydroxyprostaglandin dehydrogenase in non-small-cell lung cancer. *Cancer Res.* **67**(12), pp.5587-5593.

Yang, L., Huang, Y., Porta, R., Yanagisawa, K., Gonzalez, A., Segi, E., Johnson, D.H., Narumiya, S. and Carbone, D.P. 2006. Host and direct antitumor effects and profound reduction in tumor metastasis with selective EP4 receptor antagonism. *Cancer Res.* **66**(19), pp.9665-9672.

Yang, M., Li, Z., Ren, M., Li, S., Zhang, L., Zhang, X. and Liu, F. 2018. Stromal Infiltration of Tumor-Associated Macrophages Conferring Poor Prognosis of Patients with Basal-Like Breast Carcinoma. *J Cancer.* **9**(13), pp.2308-2316.

Yang, R., Pfutze, K., Zucknick, M., Sutter, C., Wappenschmidt, B., Marme, F., Qu, B., Cuk, K., Engel, C., Schott, S., Schneeweiss, A., Brenner, H., Claus, R., Plass, C., Bugert, P., Hoth, M., Sohn, C., Schmutzler, R., Bartram, C.R. and Burwinkel, B. 2015. DNA methylation array analyses identified breast cancer-associated HYAL2 methylation in peripheral blood. *Int J Cancer.* **136**(8), pp.1845-1855.

Yang, W., Soares, J., Greninger, P., Edelman, E.J., Lightfoot, H., Forbes, S., Bindal, N., Beare, D., Smith, J.A., Thompson, I.R., Ramaswamy, S., Futreal, P.A., Haber, D.A., Stratton, M.R., Benes, C., McDermott, U. and Garnett, M.J. 2013. Genomics of Drug Sensitivity in Cancer (GDSC): a resource for therapeutic biomarker discovery in cancer cells. *Nucleic Acids Res.* **41**(Database issue), pp.D955-961.

Yao, L., Chen, W., Song, K., Han, C., Gandhi, C.R., Lim, K. and Wu, T. 2017. 15-hydroxyprostaglandin dehydrogenase (15-PGDH) prevents lipopolysaccharide (LPS)-induced acute liver injury. *PLoS One.* **12**(4), pe0176106.

Yersal, O. and Barutca, S. 2014. Biological subtypes of breast cancer: Prognostic and therapeutic implications. *World J Clin Oncol.* **5**(3), pp.412-424.

Young, A.L., Chalmers, C.R., Hawcroft, G., Perry, S.L., Treanor, D., Toogood, G.J., Jones, P.F. and Hull, M.A. 2013. Regional differences in prostaglandin E(2) metabolism in human colorectal cancer liver metastases. *BMC Cancer.* **13**, p92.

Zanoaga, O., Jurj, A., Raduly, L., Cojocneanu-Petric, R., Fuentes-Mattei, E., Wu, O., Braicu, C., Gherman, C.D. and Berindan-Neagoe, I. 2018. Implications of dietary omega-3 and omega-6 polyunsaturated fatty acids in breast cancer. *Exp Ther Med.* **15**(2), pp.1167-1176.

Zhang, B., Ma, X., Li, Z., Gao, X., Wang, F., Liu, L., Shen, G., Sang, Y., Li, M., Li, Y., Zhao, J. and Wei, Y. 2013. Celecoxib enhances the efficacy of 15-hydroxyprostaglandin dehydrogenase gene therapy in treating murine breast cancer. *J Cancer Res Clin Oncol.* **139**(5), pp.797-807.

Zhang, G., Wang, Z., Qian, F., Zhao, C. and Sun, C. 2015. Silencing of the ABCC4 gene by RNA interference reverses multidrug resistance in human gastric cancer. *Oncol Rep.* **33**(3), pp.1147-1154.

Zhou, Q., Chaerkady, R., Shaw, P.G., Kensler, T.W., Pandey, A. and Davidson, N.E. 2010. Screening for therapeutic targets of vorinostat by SILAC-based proteomic analysis in human breast cancer cells. *Proteomics.* **10**(5), pp.1029-1039.

Zhou, X., Updegraff, B.L., Guo, Y., Peyton, M., Girard, L., Larsen, J.E., Xie, X.J., Zhou, Y., Hwang, T.H., Xie, Y., Rodriguez-Canales, J., Villalobos, P., Behrens, C., Wistuba, II, Minna, J.D. and O'Donnell, K.A. 2017. PROTOCADHERIN 7 Acts through SET and PP2A to Potentiate MAPK Signaling by EGFR and KRAS during Lung Tumorigenesis. *Cancer Res.* **77**(1), pp.187-197.

Zhu, Q., Liang, X., Dai, J. and Guan, X. 2015. Prostaglandin transporter, SLCO2A1, mediates the invasion and apoptosis of lung cancer cells via PI3K/AKT/mTOR pathway. *Int J Clin Exp Pathol.* **8**(8), pp.9175-9181.